Lawrence Berkeley National Laboratory

Recent Work

Title

A REVIEW OF NUCLEAR FISSION PART ONE-FISSION PHENOMENA AT LOW ENERGY

Permalink

https://escholarship.org/uc/item/18j6b3fx

Author

Hyde, Earl K.

Publication Date

1960

eScholarship.org Powered by the California Digital Library
University of California

UCRL-9036

UNIVERSITY OF CALIFORNIA

Ernest O. Lawrence Radiation Laboratory

TWO-WEEK LOAN COPY

This is a Library Circulating Copy
which may be borrowed for two weeks.
For a personal retention copy, call
Tech. Info. Division, Ext. 5545

BERKELEY, CALIFORNIA

DISCLAIMER

This document was prepared as an account of work sponsored by the United States Government. While this document is believed to contain correct information, neither the United States Government nor any agency thereof, nor the Regents of the University of California, nor any of their employees, makes any warranty, express or implied, or assumes any legal responsibility for the accuracy, completeness, or usefulness of any information, apparatus, product, or process disclosed, or represents that its use would not infringe privately owned rights. Reference herein to any specific commercial product, process, or service by its trade name, trademark, manufacturer, or otherwise, does not necessarily constitute or imply its endorsement, recommendation, or favoring by the United States Government or any agency thereof, or the Regents of the University of California. The views and opinions of authors expressed herein do not necessarily state or reflect those of the United States Government or any agency thereof or the Regents of the University of California.

UCRL-9036

UNIVERSITY OF CALIFORNIA
Lawrence Radiation Laboratory
Berkeley, California
Contract No. W-7405-eng-48

A REVIEW OF NUCLEAR FISSION
PART ONE - FISSION PHENOMENA AT LOW ENERGY

Earl K. Hyde

January 1960

A REVIEW OF NUCLEAR FISSION

PART ONE - FISSION PHENOMENA AT LOW ENERGY

Earl K. Hyde

January 1960

Author's note: This is a preliminary version of a review of nuclear fission. Part two which is entitled "A Fission Phenomena at Moderate and High Energy" will be issued separately. These are self-contained reports which will later be incorporated in a larger work covering many other aspects of the nuclear physics of the heaviest elements. This larger work is being prepared under the authorship of E. K. Hyde, I. Perlman and G. T. Seaborg. This material is being given limited circulation at this time in the hope that it will provide a useful review in its present form. The author would be grateful for comments, for notification of errors or for new data or information pertinent to the subject.

PART ONE - FISSION PHENOMENA AT LOW ENERGY

11.1 HISTORICAL ACCOUNT OF THE DISCOVERY OF FISSION

11.2 FISSION THEORY

- 11.2.1 The Liquid Drop Model of Fission

11.3 THE PROBABILITY OF FISSION

- 11.3.1 Empirical Relationships for Fission Activation Energy
- 11.3.2 Cross Sections for Fission with Thermal Neutrons
- 11.3.3 Fission Cross Section as a Function of Neutron Energy in the Thermal and Resonance Energy Region
- 11.3.4 Fission Thresholds by the (d,p) Method
- 11.3.5 Fission Cross Sections for Neutrons in the Mev Energy Range
- 11.3.6 Probability of Spontaneous Fission
- 11.3.7 Probability of Photofission and Fission Induced by Charged Particles. (A brief cross reference to Chapter 12)

11.4 DISTRIBUTION OF MASS IN FISSION

- 11.4.1 Introduction
- 11.4.2 Summary of Fission Yields
- 11.4.3 Closed Shell Effects and Fine Structure in the Mass Yield Curve
- 11.4.4 Distribution of Mass in Fission Induced by Neutrons of Resonance Energy
- 11.4.5 Fission Product Yields in Spontaneous Fission
- 11.4.6 Ternary Fission

11.5 DISTRIBUTION OF NUCLEAR CHARGE IN FISSION

11.6 KINETIC ENERGY OF THE FISSION FRAGMENTS

- 11.6.1 Ion Chamber Measurement of Fragment Energy Distribution in Slow Neutron Fission of U^{235}, U^{233} and Pu^{239}
- 11.6.2 Ion Chamber Measurements of Fragment Energy Distribution in Spontaneous Fission
- 11.6.3 Time-of-flight Measurements of Fission Fragment Velocities
- 11.6.4 Measurement of Fission Fragment Ranges
- 11.6.5 Calorimetric Measurement of the Energy Released in Fission

11.7 PROMPT NEUTRONS EMITTED IN FISSION
  11.7.1 Measurements of $\bar{\nu}$, the Average Number of Neutrons Emitted in Fission
  11.7.2 Measurements of P (ν)
  11.7.3 Measurements of P (ν) as a Function of Fission Mode
  11.7.4 The Energy Spectrum and Angular Distribution of the Prompt Neutrons from Fission
  11.7.5 Theoretical Calculations of Prompt-Neutron Multiplicities
11.8 DELAYED NEUTRONS IN FISSION
  11.8.1 Introduction and Résumé of Early Investigations
  11.8.2 Recent Results on Delayed-Neutron Periods and Their Abundances
  11.8.3 Radiochemical Identification of Delayed Neutron Precursors
  11.8.4 The Shell Model Interpretation of the Delayed-Neutron Emitters
11.9 GAMMA RAYS IN FISSION

PART ONE - FISSION PHENOMENA AT LOW ENERGY‡

11.1 HISTORICAL ACCOUNT OF THE DISCOVERY OF FISSION

After the neutron was discovered by CHADWICK[1] in 1932 and artificial radioactivity by I. CURIE and F. JOLIOT[2] in 1934, FERMI showed the effectiveness of paraffin-slowed neutrons in the preparation of artificial radioelements. He and his co-workers[3] at Rome exploited this technique very thoroughly by the systematic bombardment of all the easily-available chemical elements with the neutrons emitted by a radium-beryllium source. Quite naturally this study led to the search for transuranium elements by the bombardment of uranium with slow neutrons. FERMI and his collaborators[3,4] produced a 13 minute activity by bombardment of uranium and succeeded in separating it from elements 82 to 92 inclusive. This led them to the logical conjecture that this activity must be element 93, in view of the fact that it seemed to have the chemical properties at that time expected for this element (namely, properties like those of rhenium). The formation of element 93 would be expected from the capture of a neutron by uranium followed by beta decay. Continued work by the FERMI group and by other investigators, however, resulted in the discovery of numerous additional activities--far too many to explain without postulating a very unusual pattern of isomerism. Furthermore, the radiochemical properties of many of the new "transuranium" elements differed from those to be expected of such elements. In addition to the apparent transuranium elements, four radioactivities were found which were reported to be β- active isotopes of radium because they precipitated with barium compounds traditionally used as carriers for radium.

---

‡ Published literature to mid-1959 and selected literature to the end of 1959 was surveyed in the preparation of this review.

1. J. Chadwick, Proc. Roy. Soc. A136, 692 (1932).
2. I. Curie and F. Joliot, Comptes Rendus 198, 254 (1934).
3. E. Amaldi, O. D'Agostino, E. Fermi, B. Pontecorvo, F. Rasetti and E. Segre, Proc. Roy. Soc. A149, 522 (1935); A146, 483 (1934).
4. E. Fermi, Nature 133, 898 (1934).

The investigation of those confusing products of the irradiation of uranium with neutrons occupied the period from 1935-1939. The extent of the experimental work done on the "transuranium elements" during this period and the confusing difficulties in the way of their classification can be seen by consulting a review[5] published about one year before the discovery of fission.

The honor of proving that the new activities were not heavy element isotopes, but isotopes of medium-weight elements produced by an entirely unexpected nuclear phenomenon fell to the German radiochemists HAHN and STRASSMANN[6,7]. These two chemists as well as I. CURIE and P. SAVITCH[8], who were working simultaneously in France, were investigating the radiochemical properties of the new radium isotopes and finding surprising difficulty in separating them from inactive barium which had been added as a carrier element. The problem was solved by HAHN and STRASSMANN when they added ThX(Ra^{224}) or $MsTh_I$(Ra^{228}) to the mixture and carried out a partial separation of barium and radium by fractional crystallization of chloride, bromide and chromate salts. The unidentified activities isolated from neutron-bombarded uranium targets were observed to concentrate in the barium and to be separated from the ThX or $MsTh_I$ fraction. This proved that the unknown activities must be isotopes of barium and not of radium since other elements had been eliminated in the preliminary separation. In order to clinch the identification, radiochemical experiments were performed on the daughter activities of the strange "radium" isotopes. Previously the daughter activities had been believed to be isotopes of actinium. HAHN and STRASSMANN separated the daughter products with lanthanum carrier, then added $MsTh_2$(Ac^{228}) as an indicator for actinium. When a partial separation of lanthanum and actinium was carried out by fractional crystallization of lanthanum oxalate, it was observed that the identified daughter activities did not concentrate in the actinium fraction. The experiments described in HAHN and STRASSMANN's "second" paper[7] rank among the most careful umambiguous ever carried out in radiochemistry. The authors felt that

---

5. L. L. Quill, Chem. Reviews 23, 87-155 (1938).
6. O. Hahn and F. Strassmann, Naturwiss. 27, 11 (1939).
7. O. Hahn and F. Strassmann, Naturwiss. 27, 89 (1939).
8. I. Curie and P. Savitch, J. de Phys. [7] 8, 385 (1937); [7] 9, 355 (1938).

their proof had to be complete because the conclusion was so unexpected and so much at variance with previous experience in nuclear reactions. Thus, they had succeeded in proving that uranium, when bombarded with neutrons, undergoes an unusual nuclear rearrangement resulting in the formation of radioelements with about half the atomic number of uranium.

This was a sensational finding which was immediately given the correct interpretation by MEITNER and FRISCH[9] as the division of an excited uranium nucleus into two fragments of medium weight. The partner to barium in such a nuclear division would be krypton and radioactive isotopes of krypton were immediately found by HAHN and STRASSMANN.[7] HAHN and STRASSMANN'S results were soon confirmed by chemical and physical experiments in laboratories all over the world. More than one hundred papers were published on this subject within a year.

MEITNER and FRISCH[9] coined the expression nuclear fission (kernspaltung, la fission nucleaire) for this new phenomenon. From a consideration of the mass deficiencies of the elements in the periodic table these authors also immediately recognized that an exceptionally large amount of energy should be released in the reaction. A rough calculation indicated that about 200 Mev of energy should be released per fission, an amount 25 to 50 times greater than that released in alpha particle emission. FRISCH[10] first demonstrated this large energy release by recording the large pulses of ionization produced in a gas chamber by the recoil of the fission fragments. Almost simultaneously JOLIOT[11] also showed the large kinetic energy of the fragments by range measurements.

Quantitative measurements of this ionization gave the first evidence of the asymmetric nature of fission. JENTSCHKE and PRANKL[12] demonstrated the presence of a low energy group and a high energy group centered at about 60

---

[9] L. Meitner and O. R. Frisch, Nature 143, 239, 471 (1939).

[10] O. R. Frisch, Nature 143, 276 (1939).

[11] F. Joliot, Compt. rend. 208, 341, 647 (1939).

[12] W. Jentschke and F. Prankl, Naturwiss. 27, 134 (1939).

Mev and 100 Mev respectively. Detailed radiochemical investigations confirmed this by showing that the main yield of the fission products comes in two groups centering around mass numbers 95 and 138.

Uranium has a neutron-to-proton ratio of 1.55 whereas the stable isotopes of the elements in the fission product region have a neutron-to-proton ratio of 1.25 - 1.45. Hence, the fission products are neutron-rich and unstable towards β- emission. The initial excitation of the fragments is sufficiently great that neutron emission can compete with γ-emission as a de-excitation process. HAHN and STRASSMANN[7] noted the possibility that neutrons would be set free and such neutrons were soon observed by VON HALBAN, JOLIOT and KOWARSKI[13] in Paris, by ANDERSON, FERMI and HANSTEIN[14] in New York, and by others.

It was also soon found[15] that a small fraction of these neutrons were delayed in their emission and that the half-life periods for the emission of delayed neutrons ranged up to one minute. Since neutron emission is not slowed by potential barrier effects, these delayed neutrons were attributed to beta emitters which decay with an appreciable half-life to highly excited levels in daughter products which instantaneously emit neutrons.

The early measurements of the number of neutrons emitted at the instant of fission indicated that this number was certainly greater than one and probably in the range of 2 to 3. This fact made it possible to conceive of a chain reaction in which massive amounts of energy might be released. For this to be possible, it is necessary that more than one of the neutrons so released be absorbed by other uranium atoms to cause fission. This is a difficult problem since neutron losses can occur by complete escape from the reacting system or by (n,γ) reactions with U^{238} or in the moderating material. It is interesting to note that FLUGGE[16] in 1939 had already published an extensive review of the possibilities and problems of the release of large amounts of energy by the fission of uranium. FLUGGE calculated that one cubic meter of U_3O_8 might develop 10^{12} kilowatt hours in less than 0.01 seconds.

---

[13] H. von Halban, Jr., F. Joliot and L. Kowarski, Nature 143, 470 (1939); Nature 143, 680 (1939).

[14] H. L. Anderson, E. Fermi and H B. Hanstein, Phys. Rev. 55, 797 (1939).

[15] R. Roberts, R. Meyer and P. Wang, Phys. Rev. 55, 510 (1939).

[16] S. Flugge, Naturwiss. 27, 402 (1939).

It was natural that experimentalists should try to initiate the fission reaction by other means than neutron irradiation of uranium. It was soon found that fission could be initiated by bombardment with high energy photons, protons, deuterons, helium ions, etc. Thorium was not observed to fission with thermal neutrons, but if high energy neutrons or charged particles were used, fission did occur. It was even conceived that uranium might fission spontaneously without excitation from any external agent and this phenomenon was first demonstrated by PETRZHAK and FLEROV.[17]

The slow-neutron fissionability of uranium was first attributed to the rare isotope of mass number 235 by BOHR,[18] and within a year this was verified experimentally by studies of uranium isotopes separated in a mass spectrometer.[19,20]

BOHR and WHEELER[21] developed a theory of the fission process in 1939 based on a conception of the nucleus as a liquid drop; FRANKEL[22] independently proposed a similar theory. Their application of this theory did not explain the most striking feature of fission, namely, the asymmetry of the mass split, but it accounted satisfactorily for a number of features of the reaction. This theory is briefly reviewed in the next section. Many theoretical developments since 1939 have been based in some way on the BOHR-WHEELER treatment. No adequate theory of fission has ever been developed; the great variety of observations on this highly complex nuclear phenomenon which are detailed in the remainder of this chapter present a very formidable task for the theoretician.

---

17. K. A. Petrzhak and G. N. Flerov, Compt. rend. Acad. Sci. USSR 25, 500 (1940).
18. N. Bohr, Phys. Rev. 55, 418 (1939).
19. A. O. Nier et al., Phys. Rev. 57, 546, 748 (1940).
20. K. K. Kingdon et al., Phys. Rev. 57, 749 (1940).
21. N. Bohr and J. Wheeler, Phys. Rev. 56, 426 (1939).
22. J. Frankel, Phys. Rev. 55, 987 (1939); J. Phys. USSR 1, 125 (1939).

A rather complete historical account of the first year of work on uranium fission is given by TURNER.[23] This review is highly interesting reading and provides insight into the development of physics at the time of a fundamentally new discovery. HAHN[24] has written an informative popular account of his early experiments in the book "New Atoms".

In the remainder of this chapter, a brief review of fission theory is followed by a detailed review of the phenomena accompanying low energy fission. The description of high energy fission is deferred until the following chapter.

---

[23] L. A. Turner, "Nuclear Fission", Rev. Mod. Phys. 12, 1-29 (1940).

[24] O. Hahn, "New Atoms, Progress and Some Memories", Elsevier Publishing Co., New York (1950).

11.2 FISSION THEORY

11.2.1 *The liquid drop model of fission.*[‡] If we had a complete knowledge of nucleons and of internucleonic forces we could write down an exact nuclear Hamiltonian for the energy of the nucleus in the following form

$$H = \sum_{1}^{A} \frac{P_i^2}{2n} + 1/2 \sum_{i \neq J}^{A} V_{ij} + \text{E.M.} \qquad (11.1)$$

where P_i is the momentum of the ith particle, V_{ij} is the exact potential of the interaction of the ith and jth particle, and E.M. is a less important term which allows for the existence of the electromagnetic field; this last term can be relevant for fission if we consider gamma-induced fission.

A nuclear theory based on this exact Hamiltonian could in principle provide us with a complete explanation of all nuclear phenomena including fission, alpha emission, neutron and proton emission, gamma emission, etc. We do not know the form of V_{ij} in sufficient detail and if we did we would have very substantial difficulty in applying it in the case of a complex heavy nucleus. Hence it is necessary to replace the exact Hamiltonian with a much simpler one (that is to say we must construct a nuclear model) which we can solve and whose solutions hopefully will tell us something about the behavior of real nuclei. In the case of nuclear fission we consider an incompressible uniformly-charged drop to be in some important respects analogous to an atomic nucleus and substitute the study of the fission of such a drop for the study of the fission of a real nucleus. BOHR and KALCKAR[25,26] were among the first to propose the analogy of a nucleus to a liquid drop. Soon after HAHN and STRASSMANN'S proof of the presence of barium activities in neutron-irradiated uranium, MEITNER and FRISCH[27] suggested that medium-mass products might result from the division or fission of the nucleus in a process analogous to the division of a charged liquid drop. In 1939, BOHR and WHEELER[21] gave an extensive treatment of the theory of such a fission process in a paper which remained the cornerstone of fission theory for decades. FRANKEL[28] published a description of a liquid drop model of fission at about the same time.

[‡] The author wishes to express his great appreciation to Dr. W. J. Swiatecki who by his published works, lectures and private conversations on the division of an idealized charged liquid drop has influenced greatly the treatment of the subject in this chapter. Limitations of space in this brief survey of the present status of fission theory unfortunately do not permit us to treat adequately the detailed contributions of Dr. Swiatecki and of other authors.

If we are interested in the emission of single particles or in the motion and energy states of single particles within the nucleus, we use the independent particle model whose Hamiltonian is of the form

$$H_{\text{shell}} = \Sigma \frac{p^2}{2m} + \sum_{1}^{A} V\,(r_1) \qquad (11.2)$$

where V is the interaction of the particle i with a central potential defined by all the other nucleons. Or we can combine the shell model with the liquid drop model to form the unified model which can tell us something about single particle properties as well as about fission, α-emission and other collective properties. Because of the approximations in the liquid drop and shell models the unified model also is only an approximation to the exact Hamiltonian of Eq. (11.1) and the unified model is more difficult to work with than either of the two other models.

$$H_{\text{unified}} = H_{\text{LD}} + H_{\text{shell}} + H_{\text{interaction}}. \qquad (11.3)$$

The relationships of these various models is shown in Fig. 11.1.

These introductory remarks are meant as a reminder that the liquid drop model cannot be expected to provide us with anything like a complete description of fission phenomena. We now turn to a brief outline of liquid drop calculations of the 1939 period and recent developments dating largely from the late nineteen fifties.

---

25. N. Bohr, Nature 137, 344, 351 (1936).
26. N. Bohr and F. Kalckar, Dan. Mat. Fys. Medd. 14, No. 10 (1937).
27. L. Meitner and O. R. Frisch, Nature 143, 239 (1939).
28. J. Frankel, Phys. Rev. 55, 987 (1939); J. Phys. USSR 1, 125 (1939).

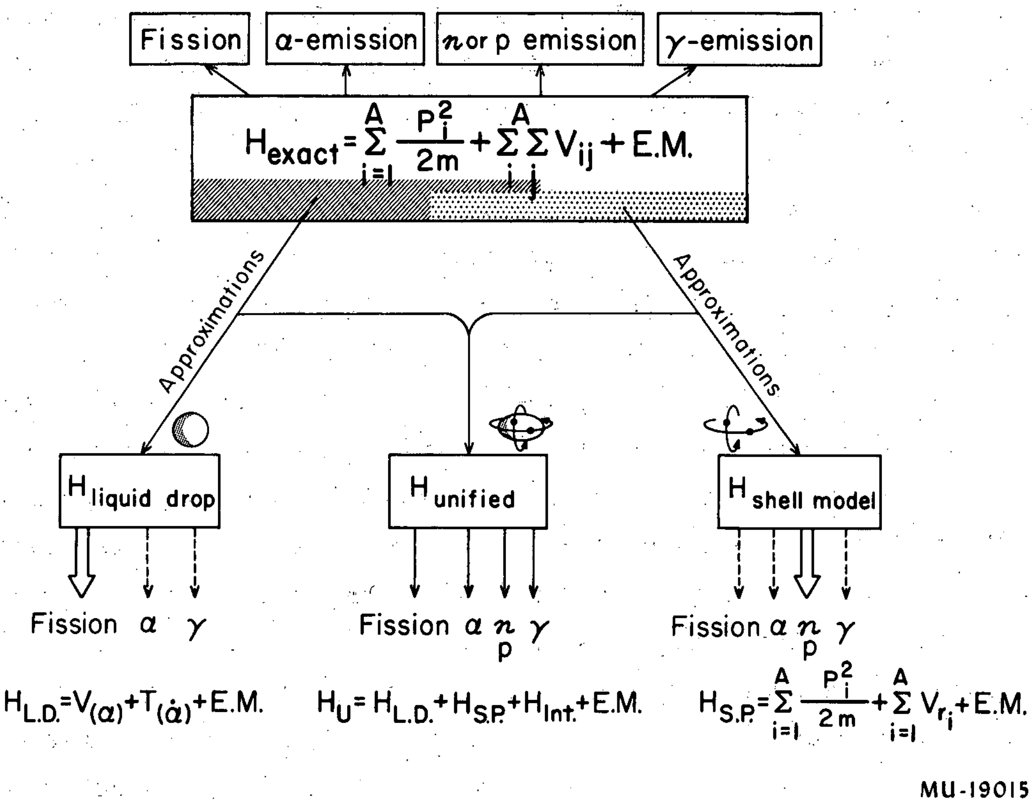
Fission
α-emission
n or p emission
γ-emission
$H_{exact} = \sum_{i=1}^{A} \frac{P_i^2}{2m} + \sum_{i}^{A}\sum_{j} V_{ij} + E.M.$
Approximations
Approximations
$H_{liquid\ drop}$
$H_{unified}$
$H_{shell\ model}$
Fission α γ
Fission α n p γ
Fission α n p γ
$H_{L.D.} = V(\alpha) + T(\dot{\alpha}) + E.M.$
$H_U = H_{L.D.} + H_{S.P.} + H_{Int.} + E.M.$
$H_{S.P.} = \sum_{i=1}^{A} \frac{P_i^2}{2m} + \sum_{i=1}^{A} V_{r_i} + E.M.$
MU-19015

Fig. 11.1. Schematic diagram showing relationship of exact nuclear Hamiltonian to three commonly used nuclear models.

One common reason for the choice of a model to replace an exact physical Hamiltonian is the relative ease with which solutions can be extracted from a model. However, we shall see that the liquid drop model is not an easy one to follow through with any mathematical rigor. Hence the exploitation of the model has often been done by approximate treatments of selected nuclear shapes and of motions believed to be the pertinent ones out of all those possible.

The rationale of the liquid drop model is somewhat as follows. The forces operating between the neutrons and protons in the nucleus are the short-range, charge-independent, nucleon-nucleon forces and the Coulomb repulsive forces of the protons. The shape assumed by the nucleus represents a balance between the nuclear forces, idealized as a surface tension, and the Coulombic repulsive forces. The strength of the surface tension can be estimated from the surface correction term in the empirical mass equations while the strength of the Coulomb forces can be calculated from the proton charge, the proton number, the assumed uniform volume distribution of protons within the nucleus and the dimensions of the nucleus. When excitation energy is added to the nucleus oscillations are set up within the drop. This increases the surface area of the drop and the resultant increase in surface energy tends to return the drop to its original shape. On the other hand the electrostatic forces tend to increase the distortion. If the electrostatic force becomes greater than the surface tension the deformation of the drop will grow and eventually the drop may divide into two or more fragments.

For most nuclei under moderate excitation the surface tension is far stronger than the Coulombic force so that any modest deviation from the most stable shape is soon overcome and the excitation energy is liberated by the emission of gamma rays or of single nucleons. Only the very heaviest elements have such a large protonic charge that relatively slight deformations of the nucleus can lead to fission.

AN ELEMENTARY CALCULATION OF A SPONTANEOUS FISSION LIMIT ON THE SYNTHESIS OF VERY HEAVY ELEMENTS

It is instructive in this connection to make an elementary calculation for a spherical nucleus given a small symmetrical distortion of the P_2 (cos Θ) type. The radius of the slightly distorted sphere is given by

$$R(\Theta) = R_o\,[\,1 + \alpha_2\,P_2\,(\cos\Theta)] \qquad (11.4)$$

where P_2 is a Legendre polynomial and α_2 is a coefficient. It is easily shown that

$$\text{surface energy} = E_s = E_s^o\,(1 + 2/5\,\alpha_2^2 + \text{higher powers of } \alpha_2) \qquad (11.5)$$

$$\text{electrostatic energy} = E_c = E_c^o\,(1 - 1/5\,\alpha_2^2 + \text{higher powers of } \alpha_2) \qquad (11.6)$$

where E_s^o and E_c^o refer to the undistorted sphere.
Hence the deformation energy, $\Delta V = V - V^{\text{sphere}} = (E_s - E_s^o) + (E_c - E_c^o)$, becomes

$$\Delta V = 1/5\,\alpha_2^2\,(2E_s^o - E_c^o) + \text{higher powers of } \alpha_2. \qquad (11.7)$$

For small distortions we can neglect the higher powers of α_2 and simply write

$$\Delta V = 1/5\,\alpha_2^2\,(2E_s^o - E_c^o). \qquad (11.8)$$

We can state then that a spherical charged drop is stable toward small distortions of the $\alpha_2 P_2$ (cos Θ) type if $2E_s^o > E_c^o$ and unstable if $2E_s^o < E_c^o$. If we consider a liquid drop on which the charge is gradually being raised, then at a certain critical value of the charge corresponding to $E_c^o = 2E_s^o$ the drop will become unstable and will divide spontaneously.

For the case of an idealized nucleus we can express this differently in terms of a fissionability parameter x introduced by BOHR and WHEELER[21] and defined as follows:

$$x = \frac{E_c^o}{2E_s^o} = 1/2\,\frac{\text{electrostatic energy for charged sphere}}{\text{surface energy of sphere}} \qquad (11.9)$$

From electrostatics, $E_c^o = 3/5\,\frac{Ze^2}{R_o}$. From an analysis of nuclear data one can set*

$$R_o = 1.216\,A^{1/3} \qquad (11.10)$$

---

* constants evaluated by A. E. S. Green, Phys. Rev. 95, 1006 (1954).

so that

$$E_c^o = \frac{0.7103\ Z^2}{A^{1/3}} \tag{11.11}$$

From geometry, E_s^o = area of sphere x surface tension Ω

$$= 4\pi\ R_o^2\ \Omega \tag{11.11a}$$

Substituting for R_o in Eq. (11.11a) and evaluating Ω from the semi-empirical mass equation* we get

$$E_s^o = 17.80\ A^{2/3} \tag{11.12}$$

Substituting these values for E_s^o and E_c^o back into Eq. (11.9) we find

$$x = \frac{0.7103\ Z^2/A^{1/3}}{2 \times 17.80\ A^{2/3}} = \frac{Z^2/A}{50.13} \tag{11.13}$$

Thus the ratio $E_c^o/2E_s^o$ is proportional to the combination Z^2/A.

$$(Z^2/A)_{\text{critical}} = 50.13. \tag{11.14}$$

A few Z^2/A and x values are given for representative nuclei in Table 11.1.

Equation (11.14) suggests that all nuclei of $Z > \sim 120$ will be characterized by the absence of a classical barrier toward spontaneous fission.

THE PRINCIPAL PARTS OF A COMPLETE THEORY

These simple considerations on the stability of a spherical drop against small distortions of the $\alpha_2 P_2$ (cos Θ) type must be replaced by much more complex calculations when larger distortions are considered, particularly when x is substantially less than 1.0.

The Hamiltonian of the liquid drop model takes the form

$$H = V(\alpha) + T(\dot{\alpha}) \tag{11.15}$$

where $V(\alpha)$ is the potential energy of the drop as a function of a set

---

*constants evaluated by A. E. S. Green, Phys. Rev. 95, 1006 (1954).

Table 11.1

Nucleus	Z^2/A	$x = \frac{Z^2/A}{50.13}$
Bi^{209}	32.96	0.6575
Th^{232}	34.91	0.6969
U^{235}	36.02	0.7185
U^{238}	35.56	0.7099
Fm^{254}	39.37	0.7854

of deformation variables α and T is the kinetic energy as a function of the time derivatives $\dot{\alpha}$ of the deformation variables.

To carry through any kind of a dynamical calculation of the motion of a liquid drop with this basic Hamiltonian, it is necessary to develop an adequate knowledge of the following matters.

(1) Mapping of the potential energy. It is necessary to prepare many-dimensional maps of the potential energy considered as a function of the deformation coordinates. These potential energy maps are quite strong functions of the fissionability parameter x. Since such mapping is a tedious and difficult undertaking, detailed calculations have been carried out chiefly for what are considered to be the relevant regions of the deformation space.

(2) Mapping of the kinetic energy $T(\dot{\alpha})$. Similarly, it is necessary to have an adequate knowledge of T as a function of the time derivatives $\dot{\alpha} = \frac{d\alpha}{dt}$ for types of motion likely to be of interest. This stage involves the calculation of inertia coefficients.

(3) Solution of the equations of motion. Once the potential and kinetic energy variation is known over all that deformation space which plays a significant part in the fission process, it is possible in principle to carry out a complete dynamical calculation starting from a given set of initial conditions. A collection of nuclei will, in general, exist in a wide variety of initial conditions so that a complete dynamical description of fission will involve the solution of a large number of equations of motion. These calculations must be properly quantized.

(4) Statistical mechanics of fission. For a proper calculation of such average quantities as fission rates, the kinetic energy and excitation energy distribution of the fragments, etc. enormous numbers of nuclei are involved and the powerful methods of statistical mechanics are required. We shall refer below to the application of the "transition state" method in its classical and quantized version to the estimation of the rate of fission. We shall also refer to a statistical theory of FONG.

We now take up each of these topics and describe the state of our present knowledge of them.

POTENTIAL ENERGY MAPPING

We turn our attention first to a discussion of the potential energy mapping. For distortions which are not too different from a sphere or spheroid it is convenient to express the drop shape by the following radius equation.

$$R\ (\theta) = \frac{R_o}{\lambda}\ 1 + \sum_{n=1} \alpha_n P_n\ (\cos\ \theta) \qquad (11.16)$$

where R_o is the radius of the undistorted spherical drop

P_n is the Legendre Polynomial of order n, and

λ is a scale factor required by the condition of constant volume.

An examination of the Legendre Polynomials shows that even values of n give shapes which are axially symmetric and symmetric toward reflection through the central plane perpendicular to the axis. Odd values of n give axial symmetry but do not give reflection symmetry.

The task then is to map V (α) or ΔV in the many-dimensional space of the α_n. In the consideration of various features of this mapping, it is convenient to consider schematic topographic maps in two dimensions of the α_n. For example V or ΔV may be shown as contour lines on an α_2 versus α_4 plot. For small or moderate distortions of the symmetric type, the α_2-α_4 mapping is the most important, although mapping covering α_6 and α_8 coordinates may contribute significantly. For a complete description we need a series of maps covering all the α_n dimensions including those of odd order. At the least, we need to apply some tests to satisfy ourselves that neglected degrees of freedom are unimportant.

Let us consider first some very general features of this mapping as given in Fig. 11.2 which is meant to represent roughly the potential energy mapping for a nucleus of rather high fissionability parameter x. The curved lines are contour lines giving the potential energy associated with various deformations specified by the α_2 and α_4 coefficients. These coefficients relate to the P_2 (cos θ) and P_4 (cos θ) terms of Eq. (11.16). Division into

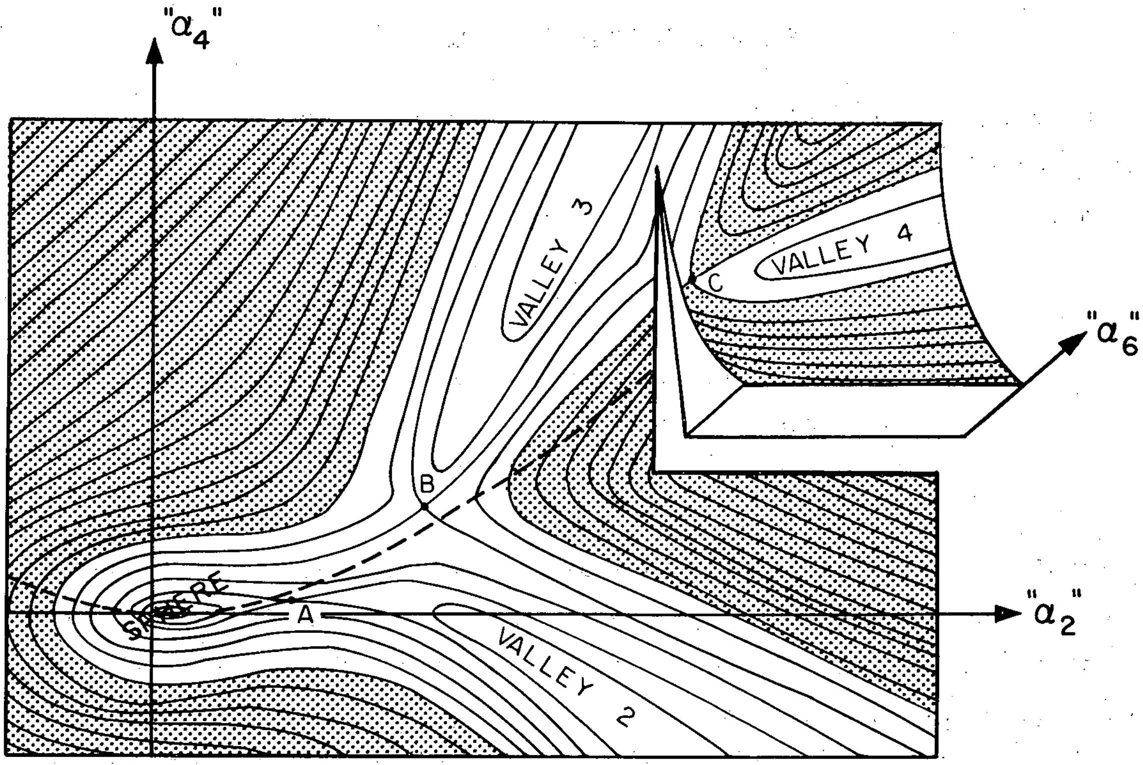

MU-15147

Fig. 11.2. A schematic map of several potential-energy valleys separated from one another and from the hollow around the spherical configuration by saddle points A,B,C. The reason for the name, "saddle point", is that the potential energy surface has the appearance of a saddle or a mountain pass. The map corresponds to the case when the energies of the saddle points are in the order $E(A) < E(B) < E(C)$. The dashed line represents the locus of spheroidal distortions. One or two-waisted figures (presumably associated with 2 or 3 fragment valleys) can be represented qualitatively in the α_2 α_4 plane but a three-waisted figure (associated with the 4-fragment valley) needs at least an α_6 coordinate in addition to describe it. The radius vector for the nucleus is given at any point in the diagram by

$$R = R_o/\lambda \; [1 + \Sigma \, \alpha_n \, P_n \, (\cos \theta)]$$

where λ is a normalizing constant.

4 fragments cannot be properly represented solely with α_2 and α_4 contributions so an α_6 coordinate is also suggested. The normal spherical nucleus sits in a potential energy hollow at the origin. The spherical drop is stable toward small distortions for x values < 1.0. Valleys 2, 3 and 4 are deep hollows representing the potential energy of the system when the nucleus has divided into 2, 3, or 4 fragments. Point A shows the location of the saddle point. This is the low point or pass in the potential energy ridge which separates the spherical drop from the two-fragment valley. The potential energy of point A is the minimum amount of energy or threshold energy required to cause a charged drop to divide. Point B is another pass or saddle point showing the least energy required to cause division into 3 fragments. Since B is shown higher than A division into two fragments is much more likely than division into three fragments even though the latter may cause a greater overall release of energy.

Figure 11.3 is a scale drawing of cross sections of the drop shapes corresponding to various amounts of $\alpha_2 P_2$ (cos θ) and $\alpha_4 P_4$ (cos θ) in the radius Eq. (11.16). This drawing is meant to serve as a guide to the shapes at the various points in subsequent figures which show potential energy contours on an α_2-α_4 coordinate system.

In Fig. 11.2 saddle point A is drawn at a lower elevation than saddle point B but other relationships can be imagined as shown in Fig. 11.4 where the three possibilities of $A = B$, $A > B$ and $A < B$ are sketched.

From the experimental fact that nuclear fission is almost exclusively binary in character it seems likely that the saddle point leading to 2-fragments lies lowest but this is a point which must be verified by quantitative calculations.

For purposes of orientation it also is important to know the total energy release for division in various possible ways. It is a simple matter to calculate the energy release for division of an idealized charged drop into 2, 3, 4 or more equal and completely-separated fragments. SWIATECKI[29] gives the following expression for division into n equal fragments.

---

[29] W. J. Swiatecki, "Deformation Energy of a Charged Drop", Paper P/651 in Vol. 15, Proceedings of the Second U. N. Conference on the Peaceful Uses of Atomic Energy, Geneva, 1958.

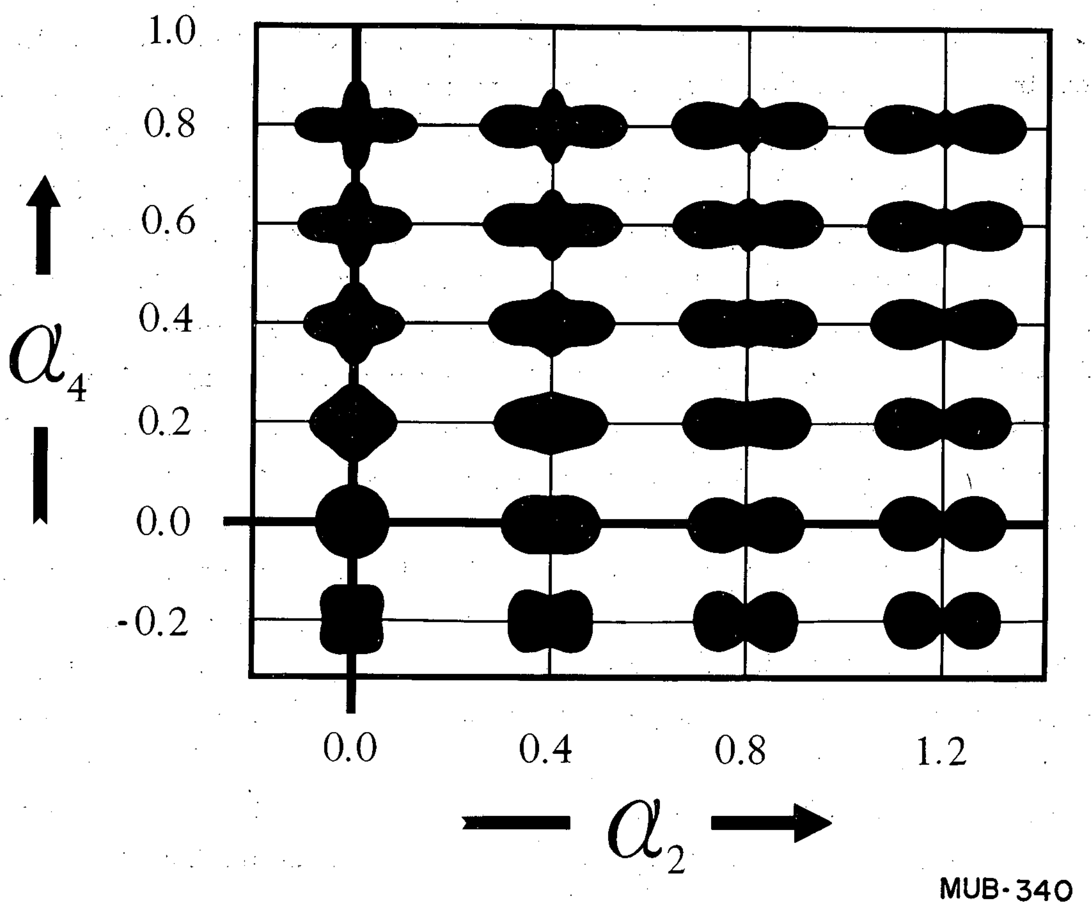
1.0
0.8
0.6
0.4
0.2
0.0
-0.2
α_4
0.0
0.4
0.8
1.2
α_2
MUB-340

Fig. 11.3. Cross sections of drop shapes corresponding to various locations on an α_2-α_4 map. Each shape should be visualized as a solid generated by revolving the two-dimensional figure around the horizontal axis. The radius for each shape is given by the expression

$$R = \frac{R_o}{\lambda}\left[1 + \alpha_2 P_2 (\cos\theta) + \alpha_4 P_4 (\cos\theta)\right]$$

where λ is a factor which normalizes the volume to a constant value.

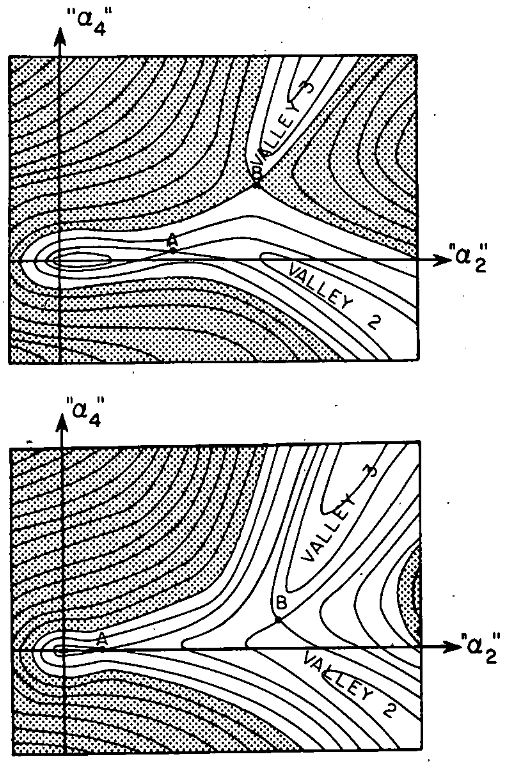

"α_4"
VALLEY 3
B
A
"α_2"
VALLEY 2
"α_4"
VALLEY 3
B
A
"α_2"
VALLEY 2
"α_4"
VALLEY 3
B
A
"α_2"
VALLEY 2

MU-15151

Fig. 11.4. Three maps showing schematically the relations between the two- and three- fragment valleys for different values of X. In (a) the threshold B is higher than A, $E(B) > E(A)$ and low-energy fission must proceed by way of the two-fragment valley. In (b) $E(B) = E(A)$ and in (c) $E(B) < E(A)$, and a competition between the two valleys would be involved. The true mapping for x values above a certain critical value of x may have considerably more structure in it between the saddle point A and the fragment valleys than is indicated here. See discussion of Fig. 11.9 below.

$$\Delta V_n = E_s^o \left\{ (n^{1/3} - 1) + 2x\left(\frac{1}{n^{2/3}} - 1 \right) \right\} \tag{11.17}$$

where E_s^o is, as above, the surface energy of the original drop,
ΔV_n is the total energy release, and
x is the fissionability parameter of Eq. (11.9).

Some calculations based on this equation are shown in Fig. 11.5. There are a number of interesting things to note about this figure. At x-values in the range 0.65 to 0.80 — which includes all the heavy nuclei from bismuth to fermium — there is no reason to limit consideration to division into two fragments since more energy is released in the formation of three, four and possibly five fragments. There is even less justification for this limitation in the study of heavier nuclei which may be made by reactions of artificial transmutation and whose x-values are closer to 1.0. At $x = 1.0$ division into as many as eight fragments releases more energy than a division into two. For such nuclei a division into four fragments is the most favored energetically. For this reason also, it may be incorrect to extrapolate trends in fission characteristics derived from an examination of experimental data in one region of x into a higher range of x-values. Vice versa it may be incorrect to use theoretical calculations based on the limit $x \to 1$ to interpret phenomena observed at $x = 0.7$-0.8. Therefore any adequate mapping of the potential and kinetic energy should give enough information about division in many possible ways to permit a proper judgment of the relative importance of the alternate modes of fission. It is also worth noting that while the shape of the nucleus at the traditional Bohr-Wheeler saddle point may be highly distorted from a spherical shape in the range of x-values corresponding to fissionable nuclei, nonetheless the nucleus does not appear to be "committed" to a division into a definite number of fragments at the moment it passes over the Bohr-Wheeler saddle in the potential energy surface. See Fig. 11.7.

Let us now list the chief mathematical techniques which have been used for quantitative calculations of the potential energy as a function of the deformation coordinates.

(1) Expansion about a sphere. A natural choice of parameters for expressing the shape of a drop slightly distorted from a sphere is a set of Legendre polynomials. The change in the surface and Coulombic energy terms

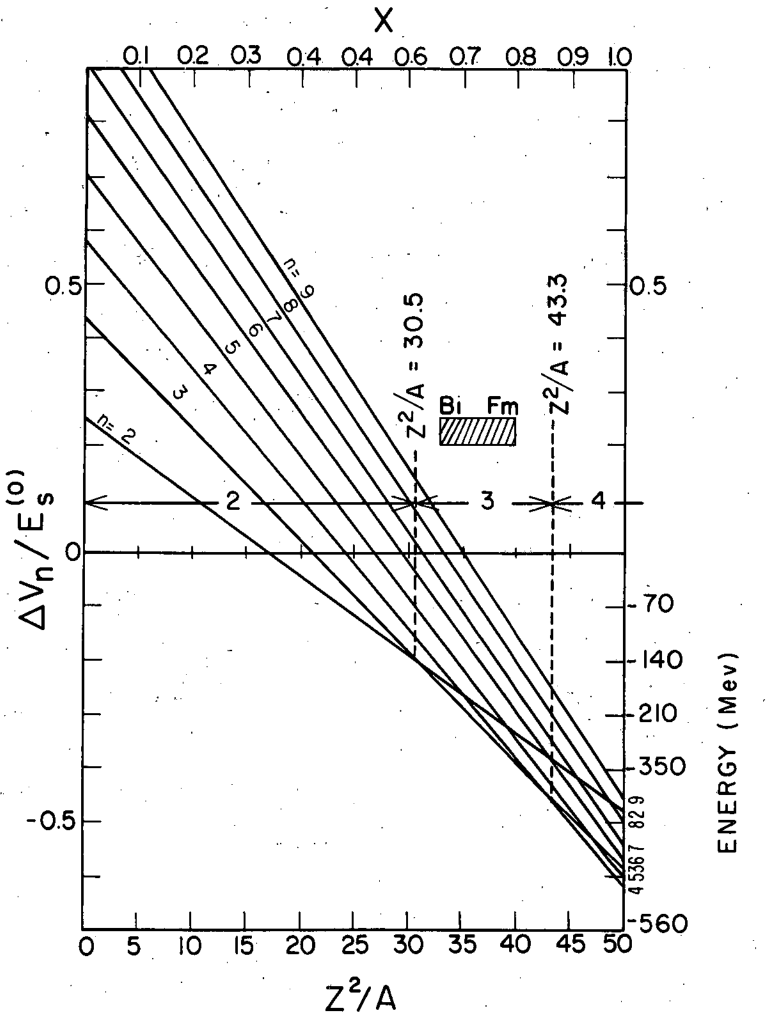

MU-15143

Fig. 11.5. The energy released in the division of an idealized charged liquid drop into n equal parts as a function of the fissionability parameter X. From SWIATECKI, reference 28.

upon distortion of the sphere to a new shape can be computed as a power series in the coefficients, α_n, of the Legendre Polynomials. This method was used by BOHR and WHEELER[21] in 1939 with the limitation that for computational simplicity the deformation coordinates were restricted to the P_2 and P_4 types and coefficients were evaluated only to the fourth order in α_2 and the second order in α_4. A further restriction was that the fissionability parameter was limited to values not far below 1.0. PRESENT and KNIPP[29a] extended this treatment somewhat and added $\alpha_3 P_3$ and $\alpha_5 P_5$ odd terms. REINES, PRESENT and KNIPP[30] extended the calculations sufficiently to cover saddle point shapes for $1.0 \geq x \geq 0.8$. SWIATECKI'S Geneva paper[28] should be consulted for a complete development and tabulation of coefficients with sufficient completeness to give the conventional threshold energy to sixth order in the quantity $(1-X)$.

(2) Machine calculations. In principle, calculations made on modern high speed computers are the most powerful but only limited calculations have been published. FRANKEL and METROPOLIS[31] introduced this method in the year 1947 in some published calculations which used the method of expansion about the spherical shape. A power series in Legendre Polynomials including terms as high as P_{10} was used over a range of X values of $1 \geq x \geq 0.65$. In principle the computor method is not restricted to Legendre expansions and more sppropriate coordinate sets could be used particularly for nuclear shapes which differ greatly from a sphere or spheroid.

(3) Expansion around a spheroidal shape. Method 1 becomes less and less accurate as the drop shape departs more and more from that of a sphere. If the shape does not differ too much from that of a spheroid, it is possible to express the deviation in surface energy or coulombic energy of a deformed drop as a power series in the deviations from the spheroidal shape. This is a sensible approach to use because it is not difficult to make exact calculations of electrostatic and surface energy for spheroidal shapes. A spheroid can be represented by a series

---

[29a] R. D. Present and J. K. Knipp, Phys. Rev. 57, 751, 1188 (1940).

[30] R. D. Present, F. Reines and J. K. Knipp, Phys. Rev. 70, 557 (1946).

[31] S. Frankel and N. Metropolis, Phys. Rev. 72, 914 (1947).

$$R\ (\theta) = \frac{Ro}{\lambda} \left[1 + \sum_{2}^{\infty} \alpha_n P_n \right] \qquad (11.18)$$

where the n values must be even. R (θ) is the radius vector from the origin to any point on the surface as a function of the angle between the radius vector and the main axis of the spheroid. λ is a constant which maintains constancy of volume. The values of the coefficients will vary with the eccentricity. Some values of the α_n for definite choices of major and minor axes are the following:

$$\begin{array}{ll} c/a = 1.43 & 1+0.2318\ P_2 + 0.0418\ P_4 + 0.0072\ P_6 + \ldots \\ c/a = 1.81 & 1+0.3749\ P_2 + 0.1104\ P_4 + 0.0378\ P_6 + \ldots \\ c/a = 2.40 & 1+0.5315\ P_2 + 0.2233\ P_4 + 0.0925\ P_6 + \ldots \end{array} \qquad (11.19)$$

Here c and a are the lengths of the major and minor axes. If we ignore the smaller contributions of the P_6 and higher terms and plot the α_2 and α_4 coefficients on an $\alpha_2\ \alpha_4$ chart we can determine a line of spheroids. (See Fig. 11.6)

We now want to consider some deformed shape which is nearly but not quite a spheroid. On an $\alpha_2\ \alpha_4$ map such a deformed shape would fall in the shaded area of Fig. 11.6. It is for such a drop shape that it is appropriate to express the deviation in surface and Coulombic energy as a power series in the deviation from a spheroidal shape. The appropriate coordinate system for these expansions will be a spheroidal coordinate system. Formulas have been developed for such expansions among others by NOSSOFF,[32] by BUSINARO and GALLONE,[33] and by SWIATECKI;[29] these references should be consulted for details. The expressions for the case of expansion about a spheroid must reduce to those for expansion about a sphere when the eccentricity is reduced to zero.

(4) Calculation of shapes far removed from a spheroid. The calculation of surface and coulombic energy terms for highly deformed shapes may be tedious

---

32. V. G. Nossoff report P/653 in Vol. 2, p. 205, Proceedings of the 1955 U.N. International Conference on the Peaceful Uses of Atomic Energy, 1956.

33. U. L. Businaro and S. Gallone, Nuovo Cimento 1, 629, 1277 (1955).

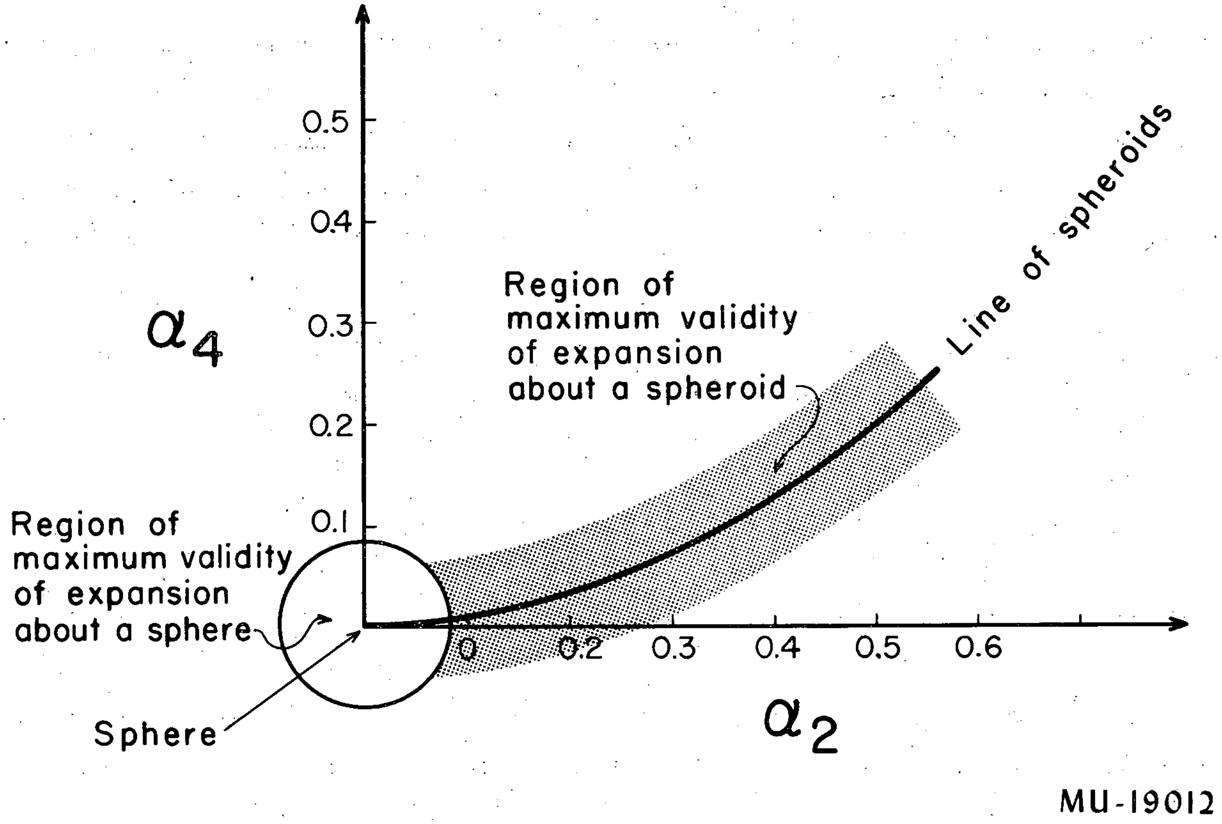
0.5
0.4
0.3
0.2
0.1
α_4
Region of maximum validity of expansion about a spheroid
Line of spheroids
Region of maximum validity of expansion about a sphere
Sphere
0
0.2
0.3
0.4
0.5
0.6
α_2
MU-19012

Fig. 11.6. Schematic diagram in $\alpha_2\alpha_4$ deformation space showing the location of the "line-of-spheroids".

and approximate when performed by the methods listed above. For certain types of axially symmetric shapes, the Legendre Polynomial expansion may be inapplicable. This is true, for example, for any shape in which some radius vectors cut the surface more than once. For highly regular shapes the choice of a suitable coordinate system may result in an easy analytical solution. For other shapes it may prove useful to obtain rough answers by approximating the shape with a combination of simple geometrical shapes for which the surface and Coulombic repulsion energies can be quickly computed. Examples of this approach are given by SWIATECKI.[29,34]

Let us now consider some of the results obtained from these four computational methods. In the range of x values from 0.8 to 1.0 the potential energy is known quite well in the α_2 α_4 deformation coordinates out to the point of unstable equilibrium known as the saddle point. We shall refer to this saddle point as the "BOHR-WHEELER saddle point" or as the "conventional saddle point". Formulae have been developed for the energy and shape of the saddle point configuration as a function of x. The saddle point energy is given by the following sixth-order expression.[29]

$$\left(\frac{\Delta V}{E_s^0}\right)_{S.P.} = \underbrace{0.7259(1-x)^3-0.3302(1-x)^4}_{\text{original Bohr-Wheeler expression}} + \underbrace{1.9208(1-x)^5-0.2125(1-x)^6+\dots}_{\text{additional terms}} \qquad (11.20)$$

This equation agrees with the FRANKEL and METROPOLIS[9] calculations and with the calculations based on a spheroid[29,32,33] to within one percent for x-values above 0.74.

The saddle point energy is often considered to be the threshold energy for fission and by substituting into Eq. (11.20) x-values and surface tension values evaluated for real nuclei several authors have calculated fission threshold energies for comparison with experimental data. The agreement is poor. An

---

[34] W. J. Swiatecki, unpublished results, 1959.

idea of the extent of the disagreement can be obtained from Table 11.2 from which it is apparent that the observed thresholds of real nuclei are lower and have a much weaker variation with x than do the calculated values. It is true that the calculated values are classical thresholds and hence subject to some correction for quantum-mechanical barrier-penetration but this correction cannot be enough to affect the results substantially.

The configuration of the conventional saddle point is given quite well down to $x = 0.74$ by the expression

$$1 + \alpha_2 P_2 + \alpha_4 P_4 + \alpha_6 P_6 \qquad (11.21)$$

where $\alpha_2 = 2.3333\ (1-x) - 1.2262\ (1-x)^2 + 9.500\ (1-x)^3 - 8.0509\ (1-x)^4 + \ldots$

$\alpha_4 = 1.9765\ (1-x)^2 - 1.6950\ (1-x)^3 + 17.7419\ (1-x)^4 + \ldots$

$\alpha_6 = -0.9500\ (1-x)^3 + \ldots$

Table 11.3 lists some explicit values for the α coefficients for high x values. These coordinates correspond to cylinder-like shapes as can be seen in Fig. 11.7.

At the opposite extreme of $x = 0$ (i.e. of an unchanged drop) the saddle point configuration consists of 2 equal spherical fragments in contact. Or, to be more general, as $x \to 0$ there are several discrete families of equilibrium configuration corresponding to strings of 2, 3, 4 .... n equal spherical fragments in contact.

The fate of the Bohr-Wheeler family of cylinder-like shapes has never been traced down to small values of x, but it has usually been assumed that below $X = 0.75$ the cylinder with rounded ends develops an equatorial waist, and gradually goes over into the n2 family, i.e. into the configuration of 2 spherical fragments connected by a neck.

This smooth transition can be represented by the diagrams of Fig. 11.8 which show qualitatively how the potential energy of the conventional Bohr-Wheeler family was expected to join with the potential energy of the family of 2 spherical fragments joined by a small neck. Also shown is the supposed transition in the shape of the saddle point; the magnitude of the major axis of the saddle point shape is used as a measure of its deformation.

In 1959, W. J. SWIATECKI[34] performed some new calculations and reexamined all previous quantitative calculations in an attempt to trace the behavior of the conventional saddle point, its shape and its energy, as a

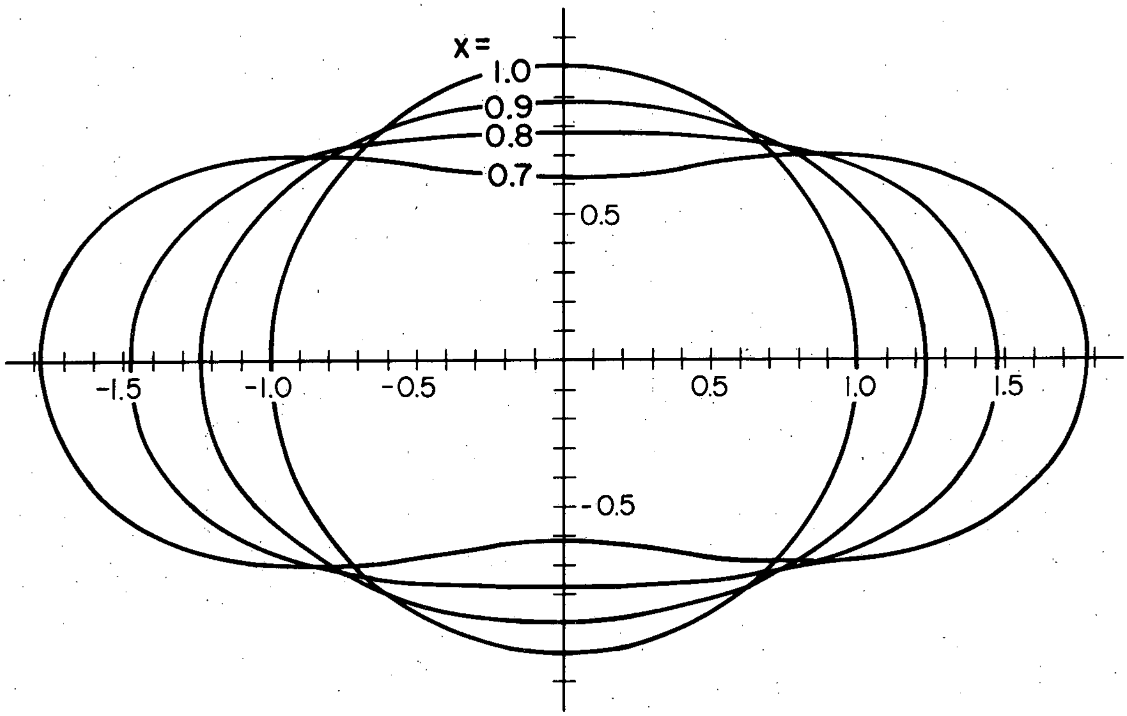

MU-19016

Fig. 11.7. Saddle point shapes of conventional Bohr-Wheeler saddle for X = 1.0, 0.9, 0.8 and 0.7

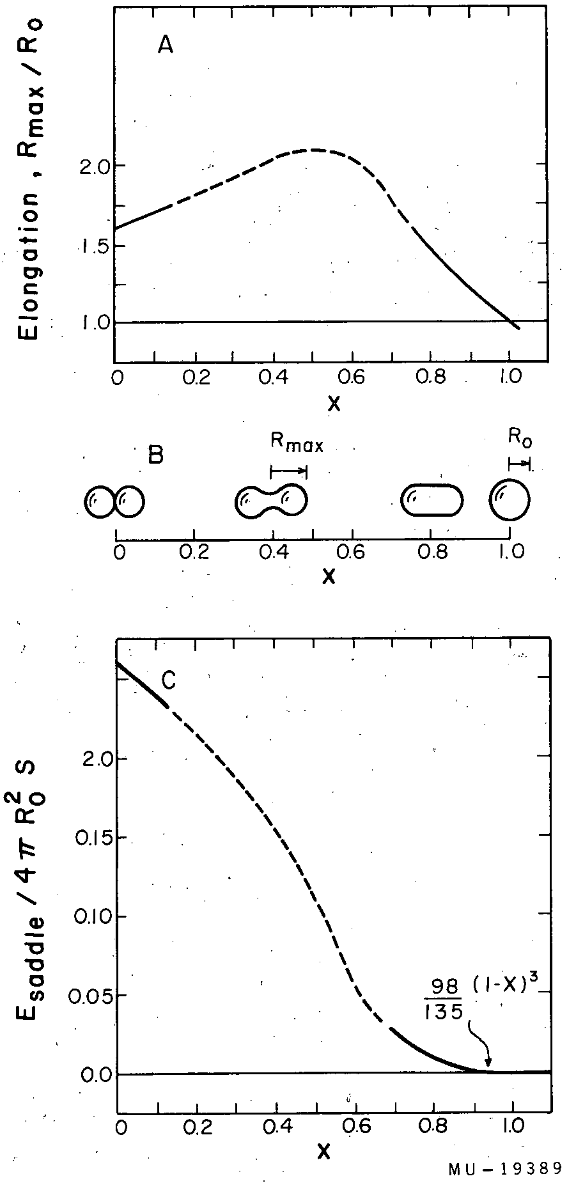

Fig. 11.8. Conventional view of the smooth transition of saddle point energy and shape from the Bohr-Wheeler family at values of the fissionability parameter, x, close to one to the two-fragment family approaching tangent spheres as x —> 0. x is defined as $Z^2/A \div (Z^2/A)_{critical}$. In part A the magnitude of the major axis is taken as a measure of the saddle point shape. The dotted portion of parts (A) and (C) is an interpolation.

Table 11.2

Comparison of Observed Thresholds with Liquid Drop Calculations

Nuclide	Z^2/A	x	$E_{Thres.}$ (Mev)	E_{obs}* (Mev)
Th^{232}	34.914	0.6969	15.08	5.95
Th^{233}	34.764	0.6939	15.58	6.44
Pa^{232}	35.694	0.7125	12.68	6.18
U^{233}	36.326	0.7251	10.96	5.49
U^{235}	36.017	0.7189	11.79	5.75
U^{237}	35.713	0.7129	12.63	6.40
U^{238}	35.563	0.7099	13.06	5.80
U^{239}	35.414	0.7069	13.51	6.15
Np^{237}	36.494	0.7285	10.53	5.49
Np^{238}	36.340	0.7254	10.92	6.04
Pu^{239}	36.971	0.7380	9.39	5.48

*These data are taken from excitation functions for photofission and neutron induced fission with the threshold estimated (rather subjectively) as the energy at which barrier penetration fission gives way to over-the-barrier fission.

Table 11.3

Fissionability parameter x	Potential energy of traditional Bohr-Wheeler saddle point $\left(\frac{\Delta V}{E_s^o}\right)_{sp}$	Shape parameters of Bohr-Wheeler saddle point		
		α_2	α_4	α_6
1.0	0	0	0	0
0.95	0.00008927	0.11474	0.0048403	-0.0001188
0.90	0.0007119	0.22976	0.019844	-0.0009500
0.85	0.002426	0.35039	0.047732	-0.003206
0.80	0.005880	0.48073	0.093887	-0.007600
0.75	0.01188	0.62368	0.16635	-0.01484

Calculated from Eqs. (11.20) and (11.21).

function of the relative charge on the drop between the two limits $x \rightarrow 0$ and $x \rightarrow 1$ of the fissionability parameter x. These studies suggested that the conventional family of saddle point shapes behaved in a very different way from what was the accepted picture. SWIATECKI[34] found evidence to support the hypothesis that, when the charge on the drop exceeds a certain critical value, the disintegration of a liquid drop may become a two-stage process which may be written as

sphere $\xrightarrow{\text{saddle}}$ intermediate $\xrightarrow{\text{saddle}}$ two fragments
stage with
cylinder-like
drop shape

This situation is to be contrasted with the older view that fission is a one-stage process for all values of X.

sphere $\xrightarrow{\text{saddle}}$ two fragments.

According to the tentative newer picture the potential energy map illustrated schematically in Fig. 11.2 or in Fig. 11.4 is valid only below a certain critical value of the fissionability parameter X. Above the critical value these figures must be replaced by diagrams such as that shown in Fig. 11.9. Part (a) shows the map for $x < x_{\text{critical}}$. This map is similar to the conventional diagram such as that shown earlier as Fig, 11.2. Part (b) and (c) show the diagram for $x = x_{\text{critical}}$ and $x > x_{\text{critical}}$.

In all three cases the origin, which corresponds to a spherical nucleus, is a local minimum indicating that the sphere is stable toward small deformations, (for any value of $x < 1.0$). For the cases of $x > x_{\text{critical}}$ there exists A, the conventional Bohr-Wheeler saddle point or pass, indicating a point of unstable equilibrium toward further deformation. The important new feature is the appearance of a hollow between the Bohr-Wheeler saddle point and a second saddle point B which leads to the two-fragment valley. The bottom of this hollow corresponds to an elongated drop, a cylinder-like shape with rounded ends, which is stable toward all small changes in shape, or at least to all axially symmetric changes in shape.

As x gets larger and larger with respect to x_{critical} the shape corresponding to the stable hollow becomes more and more elongated, i.e. moves further out to the right on the α_2 α_4 map, and the depth of the hollow increases. The potential energy changes are illustrated by the sketches in Fig. 11.10 which show plots of the potential energy taken along the dotted lines in Fig. 11.9. For x greater than x_{critical} (but less than 1.0) the first maximum in Fig. 11.10 corresponds to a member on the traditional Bohr-Wheeler family (a saddle point in Fig. 11.9). The minimum corresponds to a new group of equilibrium shapes (a potential energy hollow in Fig. 11.9). For $x < x_{\text{critical}}$ no Bohr-Wheeler shape exists. This disappearance comes about when the maximum (saddle) and minimum (hollow) come together and annihilate in a point of inflection at $x = x_{\text{critical}}$ in Fig. 11.10. The last maximum in Fig. 11.10 which corresponds to the saddle shape at the head of the 2 fragment valley may be unrelated to the Bohr-Wheeler shapes.

According to SWIATECKI'S[34] hypothesis the diagrams given in Fig. 11.8 summarizing the conventional view on the gradual transition of the Bohr-Wheeler family of equilibrium saddle shapes into the two-fragment family as x decreases from 1 to zero must be incorrect. According to the newer picture the equilibrium shapes (Bohr-Wheeler family) which tend toward the sphere for x → 1 does not undergo a smooth transition into the family of equilibrium shapes which tends toward two spheres in contact for x → 0. In fact it is possible that these two families of equilibrium shapes are unrelated. We must consider a new set of drawings to replace those of Fig. 11.8. We show a possible new set as Fig. 11.11.

In the top part of the figure curve d we see that the Bohr-Wheeler family, which starts as a sphere at x = 1 does not tend to two spheres in contact as x is decreased but instead this family goes "round a bend" which means that for x less than a certain critical value of x the Bohr-Wheeler family ceases to exist whereas for $x > x_{\text{critical}}$ two members of the family exist simultaneously. The first member of the family is the conventional Bohr-Wheeler family corresponding to a saddle point shape of unstable equilibrium; the second member of the family is a shape of stable equilibrium corresponding to the bottom of the hollow in Fig. 11.9. SWIATECKI refers to it as the second branch of the Bohr-Wheeler family. This second Bohr-Wheeler shape is more elongated than the first. The point where the two branches of the family meet (at $x = x_{\text{critical}}$) is called the "point of bifurcation" of the family. Various estimates of potential energy

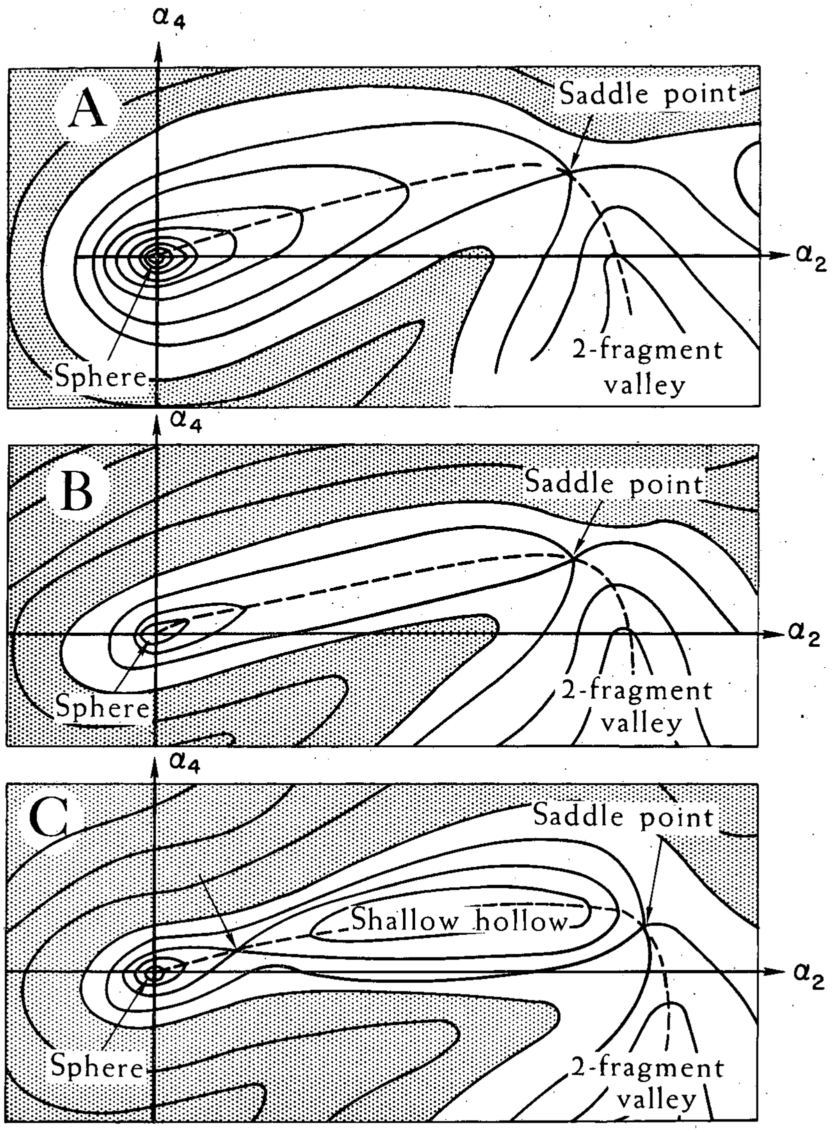
α_4
A
Saddle point
α_2
Sphere
2-fragment valley
α_4
B
Saddle point
α_2
Sphere
2-fragment valley
α_4
C
Saddle point
Shallow hollow
α_2
Sphere
2-fragment valley

MU-19390

Fig. 11.9. Possible schematic views of the potential energy map in the $\alpha_2 \cdot \alpha_4$ deformation plane as visualized by SWIATECKI.[34] These views correspond to case (d) in Fig. 11.11(A). α_2 and α_4 refer to the coefficients of Legendre polynomials in the radius expression, $\underline{R} = \frac{R_0}{\lambda}[1 + \alpha_2 P_2 (\cos \Theta) + \alpha_4 P_4 (\cos \Theta)]$. Three cases corresponding to different values of the fissionability parameter, $x = Z^2/A \,/\, [Z^2/A]_{critical}$ are shown. In (A) $x < x_{critical}$, in (B) $x = x_{critical}$ and in (C) $x > x_{critical}$. The important new feature above $x_{critical}$ is the occurrence of a hollow containing elongated cylinder-like shapes which are stable toward all small changes in deformation of the P_2 or P_4 type. A second saddle point must be passed to get to the two-fragment valley. This saddle point is shown here lying higher than the first; at a higher value of x it might lie lower.

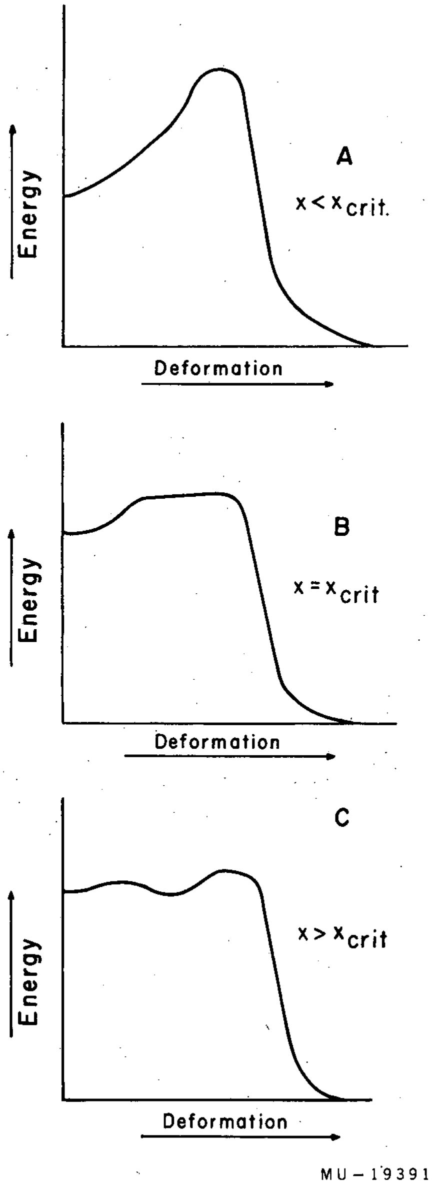

Fig. 11.10. Potential energy of a charged drop as a function of deformation measured along the dotted paths in Fig. 11.9A, B and C. These curves assume case (d) in Fig. 11.11(A) to be correct. Under this assumption there is a critical value of x above which a double hump occurs in the potential energy curve as shown here in (C). If similar potential energy curves were drawn corresponding to cases (b) and (c) in Fig. 11.11(A) the chief difference would be the elimination of the shallow dip for $x > x_{crit}$. The potential energy curves would still have the general feature of a thick barrier with a rather flat top.

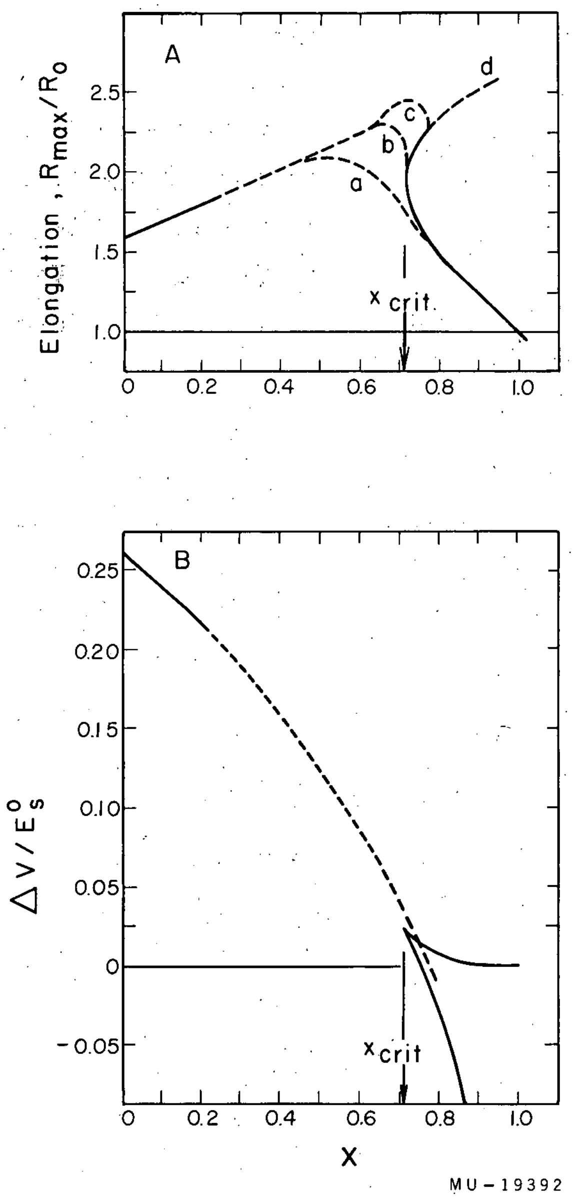

Fig. 11.11. Changes in shape and in potential energy of equilibrium shapes of a charged liquid drop as a function of the parameter x. Curve (a) is identical with (A) of Fig. 11.8 and shows the conventional interpolation between the Bohr-Wheeler saddle shapes at x -> 1 and the 2 fragment family at x -> 0. Curves (b), (c) and (d) are possible interpolations suggested by SWIATECKI.[34] Several lines of evidence suggest that (b), (c) and (d) are more nearly correct than is (a). All three have the common feature that the charged drop suddenly becomes soft toward deformation into greatly elongated shapes over a narrow range of x-values. Curve (d) is an extreme possibility according to which there is a "turning back" of the Bohr-Wheeler family; in this case there may exist no smooth transition to the two-fragment family. In the bottom half of the figure (part B) the potential energy of the equilibrium shapes is shown for case (d).

for deformed shapes establish quite clearly that a rapid change does occur in the shapes of the Bohr-Wheeler family at a critical range of x-values, but more detailed calculations are required before the exact fate of the Bohr-Wheeler family below this critical range of x can be settled. Various possibilities are shown as curves (b), (c) and (d) in Fig. 11.11A. Case (d) is the extreme case of a "turning back" with its implication of double-barrier fission. Cases (b) and (c) show a smooth transition of Bohr-Wheeler shapes into equilibrium shapes of the two-fragment family but with a very rapid transition in a narrow range of x. Many of the physical implications are the same as for case (d). The barrier to fission is not double but it is very broad which should drastically affect barrier penetrability.

The value of the critical value of x is naturally of great interest. From his examination of the quantitative data SWIATECKI[34] concluded that x_{critical} for an idealized liquid drop is about 0.73. Since this falls within the range of x-values of known heavy nuclei (see Table 11.1) the possibility exists that more than one type of fission may be of significance in real nuclei.

In the case of hypothetical "turning back" of the Bohr-Wheeler family a crucial question concerning the equilibrium family of very elongated shapes is whether these shapes are stable toward types of deformation other than those which were considered in the calculations which led to the possible existence of this second branch.

The types of quantitative and semi-quantitative estimates which led SWIATECKI[34] to postulate the "turning back" of the Bohr-Wheeler family and the occurrence of stable shapes of considerable elongation were not extensive enough to settle the question whether these elongated "stable" shapes are really stable toward various simple types of surface rippling resulting in the waist formation and ultimately to division into several fragments.

The newer view of the potential energy mapping has many interesting implications particularly if the new second branch of the Bohr-Wheeler family proves to be stable for all types of surface rippling. The conventional view of fission thresholds must be re-examined since there is no reason to expect that they should necessarily be identified with the energy of the first Bohr-Wheeler saddle point. Estimates of spontaneous fission half lives based on estimates of quantum-mechanical tunneling of a potential energy barrier are fundamentally incorrect if, in fact, two barriers rather than one are significant. Furthermore, the question of the ultimate limits of the periodic system of elements must be reopened. In the conventional view, as Z^2/A approaches a critical value of ~50 corresponding to $x = 1$ the nucleus loses all stability toward fission. In the later view even when x is greater than 1, there may exist long cylindrical shapes which are stable (at least for slight excitation) against fission. The half lives for such nuclei might still be quite short because of the thinness or lowness of the barrier toward various types of decay, but at the present time there is no estimate of the important quantities.

Returning now to the question of possible instabilities toward asymmetric types of deformation, we can cite a few publications in which some attention is paid to deformations of the $\alpha_3 P_3$ (cos Θ) and $\alpha_5 P_5$ (cos Θ) type. Most of these have been concerned with possible instabilities in the region of the conventional Bohr-Wheeler saddle point configuration. From the few explorations which have been made of possible instabilities toward asymmetric shapes, it has been found that spherical shapes or nearly-spherical shapes are stable toward any distortions of the odd-P_n type. This stiffness toward asymmetry reduces rapidly as we move away from the sphere in the α_2-α_4 plane. However, the conventional Bohr-Wheeler saddle point shape, when x is 0.8 or higher, appears to be stable to asymmetric distortions. The calculations of

BUSINARO and GALLONE[33] indicate that a strong instability toward asymmetric shapes may set in beyond the Bohr-Wheeler saddle point for x values of interest in the heavy element region. HILL and WHEELER[35] have suggested on dynamical considerations that asymmetrical components of nuclear motion might become amplified when the inversion point is passed and this might be crucial for the ultimate production of asymmetric division of mass.

SWIATECKI[29] has pointed out that an unequal division of mass could also come about in the case of a symmetric saddle point shape with instability toward division into three equal fragments. If, in the course of descent into some 3-fragment valley, one end of the elongated drop necked down in advance of the other, it might happen that one third of the drop would be severed, leaving the remainder of the drop as a system with a smaller ratio of electrostatic to surface energy which might fail to complete division, thus remaining as a single relatively large fragment.

It must be stated that there is no clear indication from the shapes and energies of saddle point configurations or from the topography of the potential energy maps of any fundamental explanation of the uneven mass split in nuclear fission. It is not correct, however, to state that the liquid drop model predicts symmetric fission.

KINETIC ENERGY MAPPING AND SOLUTION OF THE EQUATIONS OF MOTION

We turn now to a brief discussion of the kinetic energy of the motions of a liquid drop as a function of the shape of the drop. We shall find that our knowledge of the kinetic energy map is considerably less than that of the potential energy.

If we restrict ourselves first to the case of small vibrations about a spherical shape, we can develop satisfactory expressions for the kinetic energy. As before, we consider an arbitrary shape (except for a restriction to axial symmetry) which is changing with time according to the expression,

$$R = \frac{R_o}{2} \left[1 + \sum_{2}^{\infty} \alpha_n (t) P_n (\cos \theta) \right] \qquad (11.22)$$

---

[35] D. L. Hill and J. A. Wheeler, Phys. Rev. 89, 1102 (1953).

The instantaneous rates of change of the α_n are given by $\frac{\partial \alpha_n}{d\,t} = \dot{\alpha}_n$. The deformation of the surface pushes around the fluid of which the drop is composed and this motion gives rise to a kinetic energy. For small values of the α_n this kinetic energy is given by

$$T(\dot{\alpha}) = \frac{1}{2} \sum_{2}^{\infty} B_n \, (\dot{\alpha}_n)^2 \qquad (11.23)$$

where
$$B_n = \left\{ \frac{4\pi}{5} \, \rho \, R_o^{\,5} \cdot \frac{1}{n} \right\} \frac{5}{2n+1} \qquad (11.24)$$

ρ = mass density

or, equivalently where

$$B_n = \frac{3}{5n\,(2n+1)} \, AM \, R_o^{\,2} \qquad (11.25)$$

A = mass number

M = nucleon mass and

R_o = nuclear radius of the spherical nucleus.

In the same deformation region, restricted to small distortions from a spherical shape, the potential energy can be approximated by the expression

$$\Delta V\ (\alpha) = V\ (\alpha) - V\ (\text{sphere}) = \frac{1}{2} \sum_{n=2}^{\infty} C_n \, \alpha_n^{\,2} \qquad (11.26)$$

where

$$C_n = \left\{ 4\pi \, R_o^2 \, S \cdot \frac{1}{5} \, (n-1)(n+2) - \frac{3}{5} \, \frac{(Ze)^2}{R_o} \cdot 2 \cdot \frac{n-1}{2n+1} \right\} \frac{5}{2n+1} \qquad (11.27)$$

We can proceed directly to a solution of the equations of motion for this special case which is simply a small general vibration of the drop about the spherical shape.

The Hamiltonian (total energy) is

$$H = \sum_{2}^{\infty} \frac{1}{2} C_n \, \alpha_n^{\,2} + \sum_{2}^{\infty} \frac{1}{2} B_n \, (\dot{\alpha}_n)^2 \qquad (11.28)$$

$$= \sum_{n=2}^{\infty} \left(\frac{1}{2} C \, \alpha^2 + \frac{1}{2} B \, \dot{\alpha}^2 \right)_n$$

This represents the superposition of independent oscillators each with a stiffness C_n and an inertia B_n. These oscillators may be treated separately leading to harmonic oscillator amplitude expressions for each mode of motion

$$\alpha_n(t) = (\text{Constant})_n \cos(\omega_n t + \delta_n) \qquad (11.29)$$

Where δ_n is a phase factor and ω_n, the angular frequency, is given by the well-known formula

$$\omega_n = \sqrt{\frac{\text{stiffness}}{\text{inertia}}} = \sqrt{\frac{C_n}{B_n}} \qquad (11.30)$$

Figure 11.12 shows the calculated excitation energy for the first three modes of vibration as a function of mass number.

A consideration of these vibrational oscillations does not tell us directly anything about the division of a charged drop, but does help to evaluate the appropriateness of the liquid drop model. For example, one can calculate the period of oscillation and compare it to a typical period for single particle motion. In the liquid drop model the motions of the individual particles are disregarded but in a real nucleus this comparison is of fundamental importance when the internal degrees of freedom are included. A rough calculation shows that the α_2 vibration in U^{238} might be expected to have a period of 32×10^{-22} seconds whereas a representative nucleon might take $\sim 5 \times 10^{-22}$ seconds to cross the nucleus and return.

In our survey of the kinetic energy mapping, let us now go over to the opposite extreme and write down a kinetic energy expression for the separating fragments. For two fragments this is simply

$$\text{K.E.} = \frac{1}{2} M_1 v_1^2 + \frac{1}{2} M_2 v_2^2 + \text{correction}. \qquad (11.31)$$

The first two terms give simply the kinetic energy of the center-of-mass motion of the fragments. The correction term refers to any vibrational excitation which the fragments may have. If this is small, we can again use the formula

$$T(\dot{\alpha}) = \frac{1}{2} \sum_{2}^{\infty} B_n (\dot{\alpha}_n)^2 \qquad (11.32)$$

but with the B_n's appropriate to the fragments instead of the original drop.

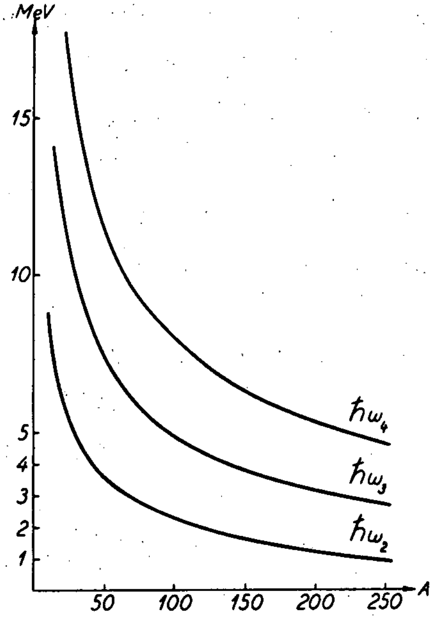

MU-18883

Fig. 11.12. The quantum energies $\hbar\omega_n$ for the nuclear shape oscillations of multipole orders n = 2, 3, and 4 as a function of mass number A. The nucleus is approximated by a charged incompressible drop with a surface tension evaluated from empirical mass curves. Oscillation energies of real nuclei are expected to depend also on nucleonic assignments but the effects of individual particle orbitals are disregarded in the above calculation. Figure reproduced from A. Bohr and B. R. Mottelson, Dan. Mat. Fys. Medd. 27, No. 16, 1953.

The kinetic energy map for deformations in the saddle point region and in the regions connecting the saddle point region with the spherical nucleus on the one hand and with the separating fragments on the other is simply not known. And without this kinetic energy mapping it is not possible to solve the equations of motion and carry through a complete dynamical calculation of a dividing drop.

Some dynamical calculations have been carried through in a few special cases by D. L. HILL and his associates[36] at Los Alamos. One interesting calculation reported by HILL was the complete case history of a U^{235} nucleus (idealized as a liquid drop) caused to fission by giving the initial spherical nucleus a "blow" of 50 Mev concentrated in the P_2 mode of motion. This initial condition set the original values for the shape and velocity of the surface. The motion was then followed step by step on an electronic computor. Twenty "pictures" were taken of the nucleus in the course of the division. The results are displayed in Fig. 11.13.

This figure is not to be construed as a picture of a real nucleus undergoing fission since the initial excitation is artificially restricted to the P_2 mode and asymmetric modes of oscillation are not included in the calculation.

STATISTICAL MECHANICS OF FISSION

We have seen that the equations of motion have been followed through a complete fission event in only one or two special cases where rather arbitrary limiting assumptions had to be made to reduce the calculation to tractability. Since an ensemble of fissionable nuclei will naturally exist in a great variety of initial conditions we know that a comprehensive calculation of the dynamics of such an ensemble would be a formidable task. We can, however, appeal to statistical mechanics to provide some notion about the average results of a large number of divisions. If we make a number of reasonable assumptions we can calculate a rate of fission for a collection of nuclei. In payment for this simplicity we will forego any chance to know the details of the sequence of events leading to the saddle point and beyond.

First, let us discuss a classical statistical mechanism of fission and then consider the modifications which quantization introduces. The statistical mechanical analysis of fission is closely analogous to the statistical mechanical

---

[36] D. L. Hill, "The Dynamics of Nuclear Fission," Paper P/660 in Vol. 15, Proceedings of the Second Geneva Conference on the Peaceful Uses of Atomic Energy, Geneva, 1958; and unpublished results.

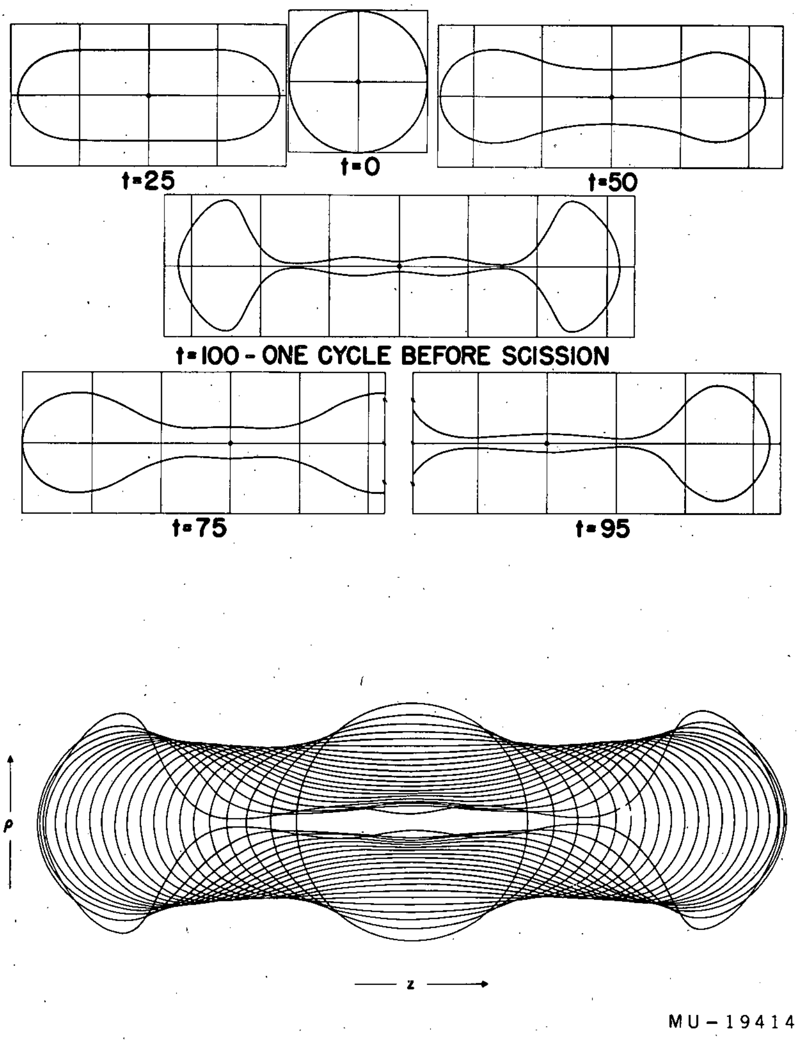
t=25
t=0
t=50
t=100 - ONE CYCLE BEFORE SCISSION
t=75
t=95
ρ
z
MU-19414

Fig. 11.13. Successive forms taken by the surface of a heavy nucleus idealized as a spherical liquid drop for motion initiated with a purely symmetric velocity distribution. Twenty stages of time integration were used to pass between each of the successive shapes shown in the composite figure. For clarity representative shapes from this composite figure have also been shown separately. From D. L. Hill, reference 36.

analysis of the division of a molecule. In particular many of the ideas applied in the "transition state" analysis[37] of the chemical reaction system

$$\begin{gathered} H + H_2 \rightarrow H_2 + H \\ \text{plus} \\ H + H_2 \rightarrow H + H + H \end{gathered} \qquad (11.33)$$

can be taken over directly to the fission case.

In our fission example we imagine that the potential energy surface in $\alpha_2 - \alpha_4$ coordinate system has the appearance of Fig. 11.14.. (We could show additional coordinates but it would not change the following descriptive remarks). We assume that there is a single saddle point (or at any rate one saddle point which dominates the fission process). We imagine a very large number of particles all initially in the hollow surrounding $\alpha_2 = 0$, $\alpha_4 = 0$ and ask what the average lifetime of this sytem, or, equivalently, what is the average rate of diffusion of representative points out of the hollow and over the saddle point. First we give the system a certain total amount of energy E and assume thermodynamic equilibrium between all the possible degrees of freedom which we designate by N.

The equation $\frac{E}{N} = kT$ defines a temperature which does not refer to thermal motion of the nucleons but to motions of the surface.

From the Boltzmann distribution law we know that the probability of finding the system in a state in which a certain degree of freedom has a value ϵ goes down exponentially according to

$$\begin{aligned} \text{probability density} &= \text{Constant} \cdot e^{-\frac{\epsilon}{kT}} \\ &= \text{Constant}\ e^{-\frac{\text{Pot.En.}}{kT}}\ e^{-\frac{\text{Kin.En.}}{kT}} \end{aligned} \qquad (11.34)$$

From this expression we learn that most of the representative points are concentrated near the bottom of the hollow where the potential energy is lowest and that this density thins out exponentially toward the higher energy regions of the saddle point. The fall-off in density is rapid if the "temperature " is small, and low if the "temperature" is high. We also learn that the kinetic

---

[37] Glasstone, Laidler and Eyring, "The Theory of Rate Processes", McGraw-Hill Book Co., Inc., New York, 1941.

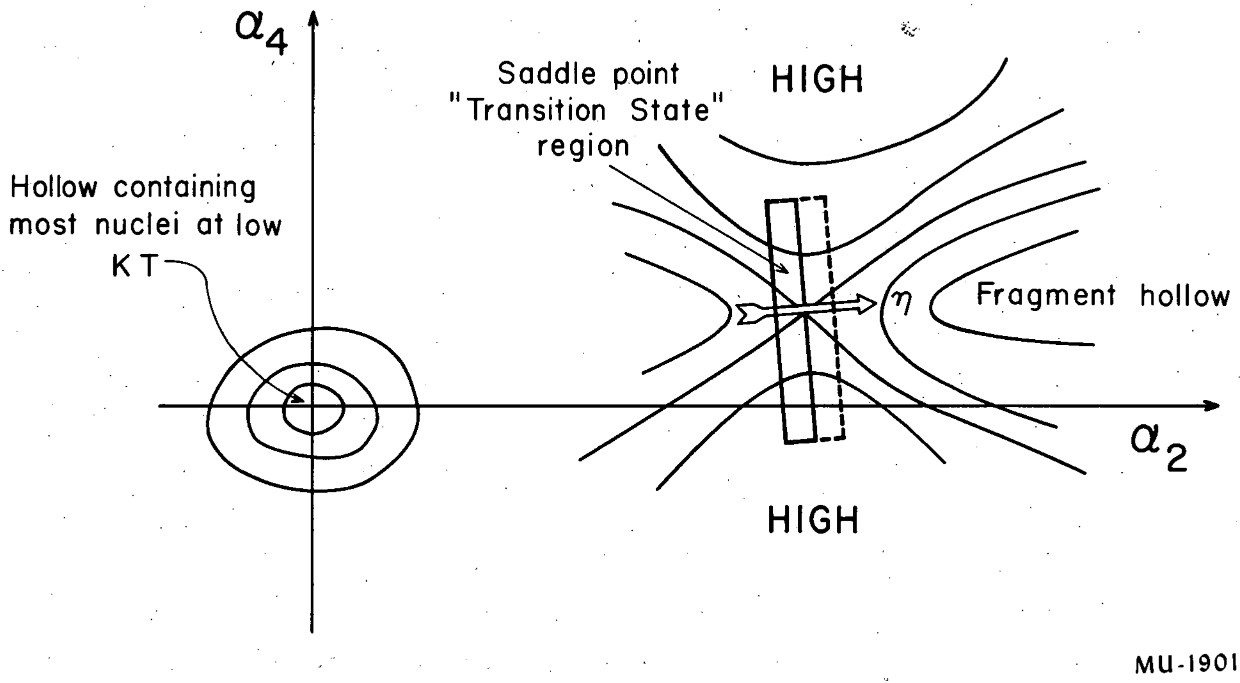
α_4
α_2
Hollow containing most nuclei at low KT
Saddle point "Transition State" region
HIGH
HIGH
η
Fragment hollow
MU-19013

Fig. 11.14. Potential energy map in α_2,α_4 space for a charged incompressible liquid drop. The map is assumed to be known in neighborhood of $\alpha_2 = \alpha_4 = 0$ and in the saddle point region but in no other region. In the transition states analysis a slab of phase space near the saddle point moving in the fission direction η plays a central role.

energy distribution for those few points which do lie in the saddle point region also follows a law of exponential fall-off with low kinetic energy the most probable.

We then have a simple way to estimate the density and kinetic energy distributions of particles in the saddle point region. In the transition state method, indicated schematically in Fig. 11.14, we consider a slab lying near the pass and at right angles to the direction η of the pass. We calculate all the points within this slab moving in the direction of the fragment valley. If the average velocity of these points in the direction η is $\bar{v}_n$ the slab will shift a distance $\bar{v}_n$ t in time, t, and we then know the rate at which our system points are going over the pass. SWIATECKI[38] formulated a simple analogy which may make the nature of this calculation more easily visualized. Consider a huge crater hundreds of miles high with gas at a certain temperature T trapped in the crater by the earth's gravitational field. Suppose that the space outside the crater is a high vacuum. Suppose further the crater has a small lip at the top. Our problem then is to calculate the rate at which the gas atoms leak out through the lip. This rate will depend on the Boltzmann law, the temperature of the gas, the height and breadth of the lip.

From a simple straightforward development which we do not go through here it is possible to derive a rate equation for fission of the general form

$$\text{Rate of fission} = Ae^{-E_{th}/kT}$$

where E_{th} is the fission threshold energy and A is a frequency factor. This equation is exactly analogous to the well-known formula for the rate of a chemical reaction. The analogous quantities and concepts in the two cases are

Chemical Reaction		Fission
Activation energy	→	threshold energy
Reaction rate	→	fission width
Adiabatic hypothesis	→	disregard of internal degrees of freedom

The fission threshold energy is just the potential energy of the nucleus in the deformed configuration of the saddle point. The frequency factor A can be approximated in the case of kT small by an expression of the type

---

[38] W. J. Swiatecki, private communication.

$$A \sim \sqrt{\left(\frac{C_2}{M^*}\right)\left(\frac{C_4}{C_4'}\right)\left(\frac{C_6}{C_6'}\right)} \cdots \qquad (11.35)$$

where the C_n's are elastic constants of the type $\frac{\partial^2 V}{\partial \alpha_n^2}$.

The unprimed constants refer to the spherical nucleus and the primed constants to the saddle point shape. In order to evaluate them it is necessary to know the contours of the potential surface in these two regions, but in no others. The C' constants give the dimensions of the lip through which the "gas" is leaking. With the exception of C_2 the elastic constants are paired off - one for the ground state and one for the saddle point. The M^* is an effective mass for motion in the α_2 mode.

If we were making an order of magnitude estimate we would guess that the ratios of the elastic constants C_n/C_n', would be about one so that the frequency factor A would simplify even further to

$$A \sim \sqrt{\frac{C_2}{M^*}} \sim \sqrt{\frac{\text{stiffness in a direction roughly toward the saddle point}}{\text{an effective mass, i.e. an inertia coefficient for motion across S.P}}} \qquad (11.36)$$

In this approximation, A is a frequency of magnitude $\sim 10^{-21}$ seconds. This leads to a crude rate formula

$$\text{Rate} \sim 10^{21} \text{ sec. } e^{-E_{th}/kT}$$

which provides a rough estimate of the rate of division of a charged liquid drop when the excitation energy is limited by

$$E_{th} \ll E \ll NE_{th}.$$

From present knowledge of the potential energy mapping in the ground state and saddle point region it should be possible to evaluate the elastic constants C_n as well as the threshold energy and thus derive a somewhat better estimate of the frequency factor than the 10^{-21} second estimate given above but there are no published estimates of this. Therefore, our statements here are meant only as a suggestion of the general nature of the calculation of "over-the-barrier" division of a liquid drop by classical statistical mechanics.

It is clear that a correct statistical mechanical calculation would have to be quantized and that the influence of internal degrees of freedom (in the case of real nuclei) would have to be included. We now explore a few general features of the quantization.

In their 1939 paper BOHR and WHEELER[39] outlined a general approach to a quantum, statistical-mechanical calculation of the rate of fission.

Consider the sketch in Fig. 11.15 which shows the potential barrier to fission along a fission dimension in deformation space. (For heavy nuclei with x close to 1 this fission dimension will be chiefly α_2). We consider a collection of nuclei all excited to an energy interval of E to E + dE. The number of energy levels in this interval is $\rho(E)dE$ and we consider every level to be filled. But we wish to apply the "transition state" technique which focuses attention on those nuclei which have a deformation close to the saddle point shape. BOHR and WHEELER[39] then suggest that we divide the total excitation energy E into two parts. The first consists of the potential and kinetic energy, $E_f + K$, associated with the transition state, i.e. with motion in the "fission dimension". The second consists of the energy ϵ arising from the excitation of all degrees of freedom other than that leading to fission. It is clear that

$$\epsilon = E - E_f - K \qquad (11.37)$$

We define a level density $\rho^*(E - E_f - K)$ which gives the density of levels of the transition state excited in all the non-fission degrees of fission to the energy interval ϵ to $\epsilon + d\epsilon$. The level density expression $\rho^*(E - E_f - K)$ can be integrated over all possible values of the kinetic energy K to yield the total number of nuclei with the transition state region. But the only transition state nuclei which slide over the potential energy hump and get irrevocably committed to fission are those which have a component of velocity v outward in the fission direction and we must take account of this. From such considerations BOHR and WHEELER[39] derive the following expression for the fission rate

$$\text{Fission rate} = dE \int_K \rho^*(E - E_f - K)\, V \frac{dp}{h}$$

---

[39] N. Bohr and J. A. Wheeler, Phys. Rev. 56, 426 (1939).

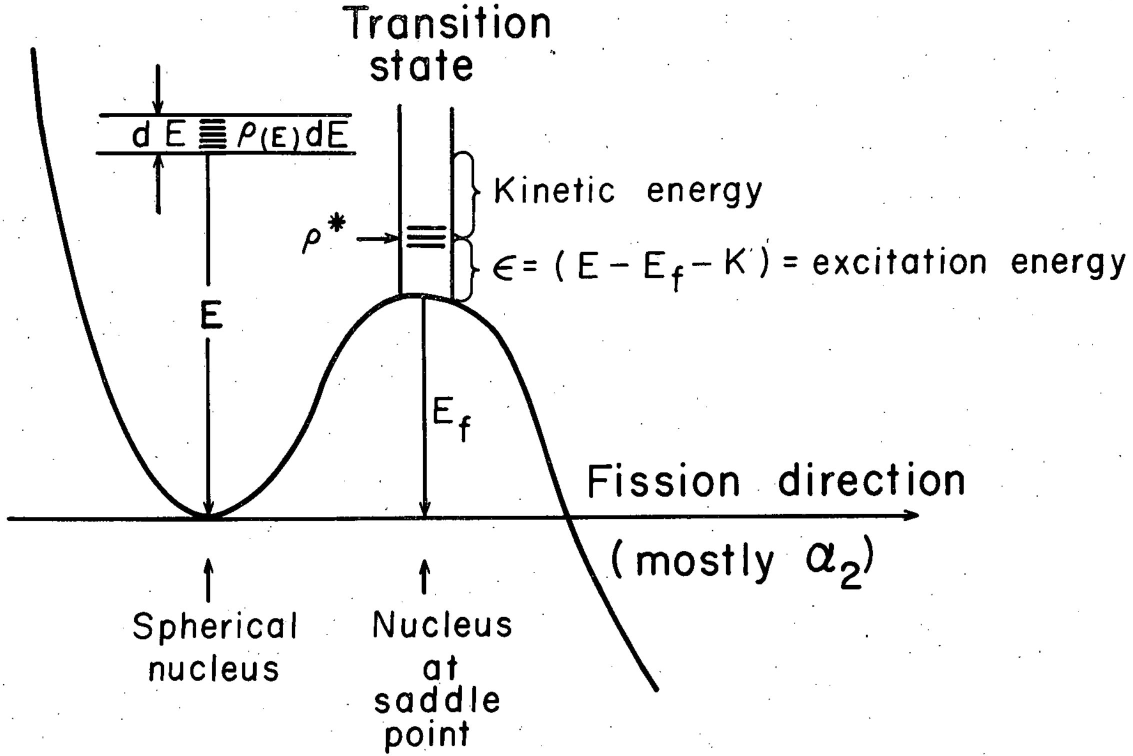
Transition state
dE ≡ ρ(E)dE
Kinetic energy
ρ*
ϵ = (E − E_f − K) = excitation energy
E
E_f
Fission direction
(mostly α_2)
Spherical nucleus
Nucleus at saddle point

MU-19393

Fig. 11.15. Transition state statistical analysis of the rate of fission according to the qualitative development of BOHR and WHEELER.[39]

where the terms dE, ρ^*, E, E_K and K are defined above. V is the outward velocity in the fission direction, dp is the momentum interval, and dK = vdp.

In order to apply this equation we must have some way of getting the level density ρ^* for excited transition state nuclei. There is no serious published literature which carries this statistical treatment beyond the qualitative development of BOHR and WHEELER. A more complete treatment would include the competition for de-excitation of the nucleus by neutron emission when the total energy exceeds the neutron binding energy. This is not a factor in the liquid drop "model" but is an important effect for nuclei. BOHR and WHEELER also outline a statistical treatment for decay by neutron emission.

If the total energy of the system is reduced to some value very close to or less than the fission barrier energy the rate of fission will decrease markedly. In the classical case the fission rate becomes zero when the excitation energy is less than the fission barrier but in quantum mechanics there is a finite chance of barrier penetration. This leaking is responsible for the occurrence of spontaneous fission. Figure 11.16 shows a schematic representation of penetration of the fission barrier for a single nucleus in a specific initial quantum state. The situation is qualitatively very similar to the spontaneous emission of an alpha particle from a heavy element and, as in the alpha case, we can distinguish three regions within which the nature of the wave function will be different. It is important to recognize, however, that the wave function in the fission decay picture is not a wave function for a particle penetrating a barrier but for the motion of a surface going through a potential energy maximum in deformation space.

The first potential energy region corresponds to small vibrations of the nucleus around a spherical shape which is stable toward these small distortions. The potential curve is roughly parabolic and the wave functions of the system are very similar to harmonic oscillar wave functions. A complete treatment would also include supplementary wave functions to describe possible rotations of the drop.

In the ground state there will remain some residual zero point energy of vibration. In Fig. 11.16 the wave function shown is for a nucleus excited above the ground state to some oscillator quantum state located below the barrier.

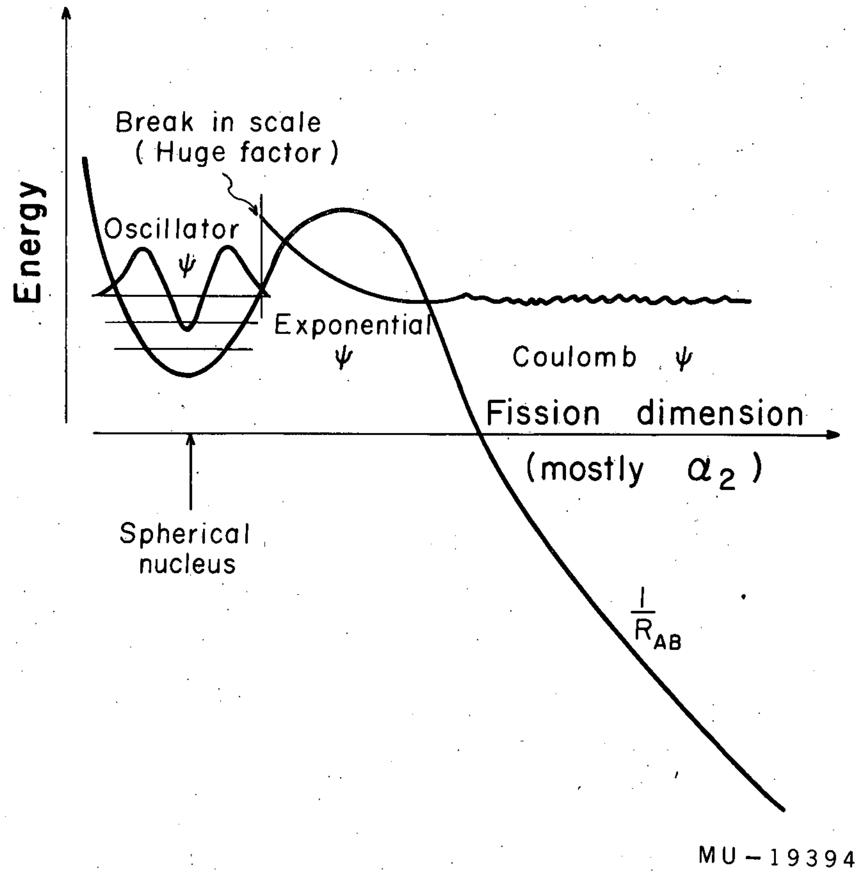
Energy
Break in scale
(Huge factor)
Oscillator
ψ
Exponential
ψ
Coulomb ψ
Fission dimension
(mostly α_2)
Spherical nucleus
$\frac{1}{R_{AB}}$
MU-19394

Fig. 11.16. Schematic drawing indicating quantum mechanical penetration of a fission barrier by a nucleus excited to less than the barrier energy.

In a calculation of spontaneous fission the proper wave function would be that for the ground state.

In the barrier region the wave function of the surface motion is an exponential function decreasing outward. For low-lying states of nuclei the wave function in the barrier region will be very small. Beyond the barrier the potential energy is governed by the Coulomb repulsion of two charged fragments. At great distances the potential energy curve has a $\frac{1}{R_{AB}}$ dependence where R_{AB} is the distance of separation of the fragment centers. The wave function in this region rapidly reduces to a pure Coulombic wave function.

The mathematical techniques for solving this barrier penetration problem would be patterned closely after those used in the alpha decay problem. Order-of-magnitude estimates using a rough barrier penetration equation show that the enormously long spontaneous fission half lives of such elements as uranium and thorium are quite understandable. In a quantitative sense, however, these rough estimates of spontaneous fission half-lives are still very crude. FOLAND and PRESENT[39a] have carried through a barrier penetration calculation for spontaneous fission using a hydrodynamic model assuming irrotational flow. They made a comparison of their equations with experimental data on the isotopes of fermium. WHEELER[39b] has also discussed the fission barrier penetration problem.

It must also be noted that the views of SWIATECKI concerning the two branched nature of the BOHR-WHEELER family of equilibrium shapes which we discussed above have very important implications for a quantum mechanical calculation of spontaneous fission rates. Above a critical value of x the fission process may become:

$$\text{sphere} \xrightarrow{\text{barrier}} \text{elongated shape} \xrightarrow{\text{barrier}} \text{2 fragments.}$$

It is necessary to consider the penetration of the system through two barriers instead of one. It is important to have some way of estimating the height and the thickness of both of these barriers.

[39a] W. D. Foland and R. D. Present, Phys. Rev. 113, 613 (1959).

[39b] J. A. Wheeler in the book "Niels Bohr and the Development of Physics"

FONG'S STATISTICAL TREATMENT OF FISSION

In the mid nineteen-fifties FONG[40] developed a statistical mechanical treatment of nuclear fission which differs in one important respect from the one we have discussed above. FONG[40] focuses attention on the nucleus just at the critical moment of scission into two fragments rather than at the moment of crossing the saddle point. He argues that the fission process is sufficiently slow that a nucleon might cross the nucleus many times as the nucleus moves from saddle point to scission. Therefore it is possible that an instantaneous statistical equilibrium will be established at any instant of the process from saddle point to separation. If this is true the crucial statistical quantities may be the relative densities of quantum states of the nuclear configurations corresponding to different fission modes just at the moment when statistical equilibrium is last established, presumably the moment just before separation.

For convenience of calculation FONG approximates the configuration at this critical moment by two deformed fragments in contact and for further computational simplicity assumes deformation of the P_3 (cos Θ) type ,only where P_3 is a Legendre Polynomial. This particular choice was made because it reproduces most closely our intuitive feeling of the dominant shape of the just-formed fission fragments. The density of quantum states obviously depends upon the excitation energies of the two fragments at the critical moment; hence it is important to estimate the excitation energy carefully. Larger excitation energy corresponds to a large density of quantum states and thus to larger relative probability. The density of excitation states of a nucleus was taken from the general statistical model of the nucleus to be

$$W_o(E) = c_{\exp} \, 2\sqrt{aE}$$

where a and c are empirical parameters evaluated from other data and E is the excitation energy. Since this level density expression is a rapidly increasing function of the excitation energy, a small change in the latter may result in a large change of the relative probability. In the statistical theory of FONG the basic reason for the favoring of asymmetric modes of fission is that asymmetric fission is believed to have an excitation energy larger by some 5 Mev than does symmetric fission. For the basic calculation of the total energy release in fission FONG derived his own semi-empirical equation for the masses of the primary fragments in various modes of fission. This mass equation, unlike the older equation of BOHR and WHEELER[39] made allowance for shell effects in the mass surface. Hence, in a sense, the occurrence of asymmetric fission is related to the shell model of the nucleus, a suggestion which has been made also by other authors.[41-43]

---

[40] P. Fong, Phys. Rev. 102, 434 (1956).

The total energy release has to be divided between internal excitation energy and deformation energy of the fragments, the energy of Coulombic repulsion, and the energy of translation. The internal excitation energy which is of crucial importance in determining relative probability of fission modes according to this theory depends on the mass numbers, the charge numbers and the deformation shapes of the fragments. FONG performed suitable integrations over these variables and was able to calculate a number of features of the fission reaction such as the mass distribution curve, the charge distribution curve, the kinetic energy distribution, etc. In particular, the calculations were able to reproduce the mass distribution curve for U^{235} very well. However, PERRING and STOREY[44] were not able to obtain a fit to the Pu^{239} fission yield data using FONG'S theory although FONG[45] was later able to secure a better fit by a revised choice of parameters in his mass equations.

A number of objections have been raised to this purely statistical theory of fission. It places the entire emphasis on equilibrium level densities just at the point of fission and takes no account of quantum state transition channels of the fissioning nucleus at the top of the fission barrier at the saddle point. It uses a simplified model of fragment deformation energy; presumably one should use Nilsson-type calculations of deformation energy for all possible modes of deformation. The level density distribution which is

---

41. M. G. Mayer, Phys. Rev. 74, 235 (1948).
42. L. Meitner, Nature 165, 561 (1950).
43. D. Curie, Compt. rend. 235, 1286 (1952); 237, 1401 (1953).
44. J. K. Perring and J. S. Storey, Phys. Rev. 98, 1525 (1955).
45. P. Fong, Phys. Rev. (Letter to Editor on Pu^{239} fission).

crucial to the theory is not based directly on experimental information and may not be correct for fission fragments close to the magic numbers. Also, it is not certain that the level density formula is correctly chosen for deformed fragments. NEWTON[46,47] has developed a level spacing formula which reproduced shell effects on the spacing of nuclear levels when nuclear excitation is greater than one Mev. If this formula is substituted for the level density formula used by FONG in his statistical model of fission the agreement with experimental mass yield curves and other characteristics is no longer good. Furthermore, STEIN and WHETSTONE[48] in a study of the prompt neutrons emitted from the spontaneously fissioning nucleus Cf^{252} did not find a variation in the number of neutrons emitted as a function of the mass ratio of the fragments which the theory predicts.

A more careful consideration will have to be given to the potential and kinetic energy mapping of a deformed liquid drop and of the dynamics of division before it will be possible to judge whether the fundamental assumptions of FONG'S treatment are valid.

EFFECT OF ANGULAR MOMENTUM

In the treatment of the liquid drop model as reviewed here nothing has been said concerning the influence of angular momentum. This neglect is justified in the case of spontaneous fission or of fission induced by capture of slow neutrons. However, when fission is induced by particles of high energy the angular momentum may be quite high and may play an important role. This is particularly true in the bombardment of heavy element targets with heavy ions when the angular momentum of the compound system may range from 50 to 130 units or more.

---

[46] T. D. Newton, Shell Effects on the Spacing of Nuclear [illegible] Levels, Can. J. Phys. 34, 804 (1956).

[47] See T. D. Newton, Paper D1, Proceedings of the Symposium on the Physics of Fission, held at Chalk River, Ontario, May 14-18, 1956 report CRP-642-A. Atomic Energy of Canada Limited, Chalk River, Ontario, Canada.

[48] W. E. Stein and S. L. Whetstone, Jr., Phys. Rev. 110, 476 (1958).

PIK-PICHAK[49] considered the influence of angular momentum on fission barrier height and cross-section. He assumed the validity of the liquid drop model and further assumed that moment of inertia of the rotating drop was equivalent to that of a rigid body.

The change in total energy of the drop as the spherical drop is deformed contains a surface energy and a coulombic energy term as before but, in addition, there is a term for the shift in rotational energy as the shape of the drop is changed.

$$\Delta E_{\text{Total}} = \Delta E_s + \Delta E_q + \Delta E_{\text{Rot}}$$

For a given value of angular momentum the potential energy mapping as a function of the deformation coordinates can be calculated and the saddle points corresponding to points of unstable equilibrium again computed. PIK-PICHAK[49] shows that the energy of the saddle point is definitely lowered by the angular momentum and that fission probability is greatly increased. Thus, angular momentum must rank with nuclear charge as an important factor pushing toward nuclear fission.

For each value of the fissionability parameter, $x = (Z^2/A)/(Z^2/A)_{\text{crit}}$, there is a critical value of the ratio, $\frac{E_{\text{Rot}}}{E_s}$, which establishes a limit above which the spherical charged drop is no longer a configuration of stability. In the conventional picture of the liquid drop model all such nuclei would fission instantly.

Some detailed calculations of the influence of angular momentum on saddle point energies and other characteristics of fission are being computed by HISKES.[50]

11.2.2 The Unified Model and Fission Theory. According to the unified model of A. BOHR,[51] some fission phenomena are expected to be correlated with the properties of particular quantum states at the saddle point. As the excited nucleus approaches the saddle point its excitation energy is converted into potential energy of deformation, with the result that at the saddle point the nucleus is "cold". Only a few widely spaced levels will be available to the nucleus and the spins and parities of these levels will probably have a marked effect on the mode of fission. It is thought that the spectrum of low-lying levels at the saddle point will resemble that [illegible] of the levels of the nucleus near its ground state configuration. In Chapter 9 it is shown that the low-lying states of even-even compound nuclei consist of a series of rotational levels (0+, 2+, 4+, 6+, etc.) based on a 0+ ground state and a series of negative parity states (1-, 3-, 5-, ...). The negative parity states are believed to represent a rotational set of levels based on a 1- base state which itself represents a deformation of the nucleus into an asymmetric shape.

---

[49] G. A. Pik-Pichak, Soviet Physics JETP 1, 238 (1958).

[50] J. Hiskes, unpublished results, Lawrence Radiation Laboratory, Berkeley, California, 1959-1960.

[51] A. Bohr, Paper No. P/911, "Proceedings of the International Conference on the Peaceful Uses of Atomic Energy", Vol. , United Nations, New York (1956).

If the low-lying levels of an even-even nucleus deformed to the saddle point configuration are similar to the low-lying levels for the undeformed nucleus then the 1- negative parity state may play an important role in the fission of nuclei which are excited to some energy close to the fission threshold. These ideas are given schematically in Fig. 11.17. Asymmetry in fission can possibly be related to the occurrence of these negative parity states. The angular distribution of the fragments may also be related to a fission process dominated by the passage of the nucleus through a 1- fission channel state. This is discussed more fully in Section 12.1.6 of the next chapter.

At high excitation energy when the potential energy requirements of the deformation at the saddle point removes only part of the initial energy of excitation many alternate levels become available as fission channels. Then fission becomes more symmetric and angular anisotropy effects are washed out.

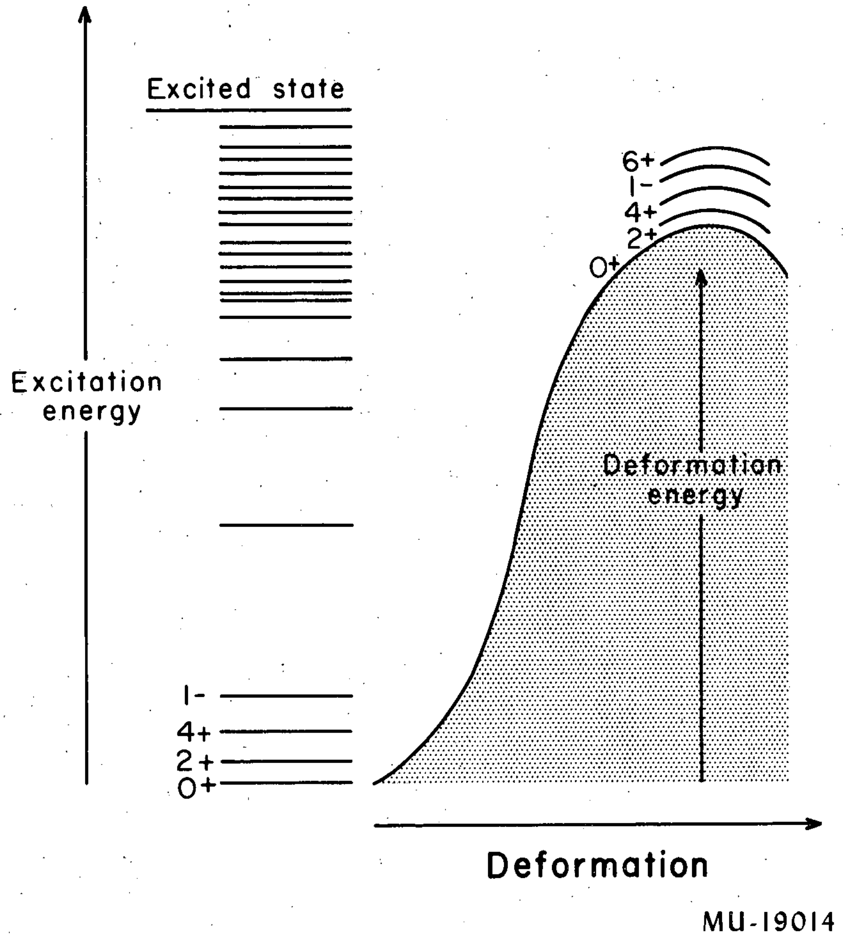
Excited state
Excitation energy
1-
4+
2+
0+
6+
1-
4+
2+
0+
Deformation energy
Deformation
MU-19014

Fig. 11.17. Schematic view of A. Bohr's suggestion that a nucleus caused to fission by neutron capture may use up most of its excitation energy in deformation leaving only a few possible quantum states (channels) available. These states may resemble the low-lying states of the unexcited compound nucleus.

11.3 THE PROBABILITY OF FISSION

11.3.1 Empirical Relationships for Fission Activation Energy. The theory of BOHR AND WHEELER[52] predicts a variation of fission-barrier or critical deformation energy for fission which has a strong dependence on Z^2/A. For this reason the quantity Z^2/A has come to be regarded as an important fissionability parameter. However, fission thresholds obtained from photofission and neutron-fission cross section measurements show that the apparent fission threshold does not depend so strongly on Z and A as the theory predicts.

Some years ago SEABORG[53] made an attempt to calculate the slow neutron fission threshold, or barrier, E_b, from an empirical equation for spontaneous fission half lives determined from the characteristics of a line like that shown in Figure 11.30 below. He noted that the general trend in the rate of spontaneous fission of even-even nuclei could be reproduced by the expression

$$T = 10^{-21} \times 10^{178 - 3.75\, Z^2/A} \qquad (11.38)$$

It is known that spontaneous fission is a quantum-mechanical barrier penetration process and that the half-life must be a sensitive function of the fission barrier height. In particular, FRANKEL AND METROPOLIS[54] derived the relationship

$$T = 10^{-21} \times 10^{7.85\ E_b} \text{ seconds} \qquad (11.39)$$

where the fission barrier, E_b, is in Mev. SEABORG[53] assumed the essential correctness of the form of equation 11.39 and used both equations to obtain

$$E_b = (19.0 - 0.36\, Z^2/A) \qquad (11.40)$$

This equation is applicable only to compound nuclei of the even-even type over a limited range of Z^2/A because the equation 11.38 upon which it is based applies only to this nuclear type. In section 11.3.6 below it is shown that the rate of spontaneous fission of even-odd and odd-even nuclides is less by an average factor of about 10^3, and the rate of spontaneous fission of odd-odd nuclides is less by a factor of about 10^5. Therefore, fission barriers might be effectively higher by about 0.4 and 0.7 Mev, respectively, on the basis that each factor of ten increase in half life corresponds to an increase of about 0.13 Mev in barrier height. Thus the empirical relationship becomes

---

[52] N. Bohr and J. A. Wheeler, Phys. Rev. 56, 426 (1939)

[53] G. T. Seaborg, Phys. Rev. 88, 1429 (1952)

[54] Frankel and Metropolis, Phys. Rev. 72, 914 (1947)

$$\begin{aligned} E_b &= (19.0 + 0.36\, Z^2/A + \epsilon\,)\text{Mev} \\ \text{where } \epsilon &= 0 \text{ for even-even,} \\ \epsilon &= 0.4 \text{ for even-odd and,} \\ \epsilon &= 0.7 \text{ for odd-odd nuclides.} \end{aligned} \qquad (11.41)$$

Since a measurable amount of induced fission can occur at an excitation energy less than the top of the barrier at a point when the time for fission becomes comparable with the time for gamma emission -- that is, in a time of about 10^{-14} seconds -- the required energy of activation, E_a, is less than the barrier height E_b which represents a hypothetical fission time of some 10^{-21} seconds. Thus if we use the relationship that each factor of ten in rate corresponds to some 0.13 Mev of energy, it follows that E_a is, in general, some 0.9 Mev less than E_b.

When the energy difference B_n (neutron binding energy) minus E_a (calculated activation energy) is tabulated as in Table 11.4 there results a correlation with slow-neutron fission which is surprisingly good. The nuclides which show a positive energy difference (B_n minus E_a) have a fission cross section greater than about one barn, and the nuclides with a negative (B_n minus E_a) energy difference have fission cross sections below this arbitrary line of demarcation of non-fissile and fissile nuclides. When the value of E_a exceeds the neutron binding energy, B_n, leading to a negative value for (B_n minus E_a) in Table I, this difference should be equal to the neutron energy threshold for fission. From the table, the following nuclides should have the indicated thresholds for neutron-induced fission: Th^{232} (0.9 Mev), Pa^{231} (0.4 Mev), U^{234} (0.3 Mev), U^{236} (0.3 Mev), U^{238} (0.9 Mev), and Np^{237} (0.3 Mev). Fission thresholds are not sharp i.e. are not true thresholds owing to the barrier penetration nature of the fission process and therefore experimentally determined thresholds depend somewhat on the sensitivity of the measuring technique. The following

Table 11.4 Correlation of slow neutron fissionability with activation energy for fission and corresponding neutron binding energy≠

Nuclide	E_b* (Mev	E_a** (Mev)	B_n*** (Mev)	B_n-E_a (Mev)	Slow neutron fissionability****
Ra^{226}	7.1	6.2	4.5	-1.7	-
Ra^{228}	7.2	6.3	4.7	-1.6	-
Ac^{227}	7.2	6.3	5.0	-1.3	-
Th^{227}	6.2	5.3	7.1	1.8	+
Th^{228}	6.7	5.8	5.3	-0.5	-
Th^{229}	6.3	5.4	6.8	1.4	+
Th^{239}	6.8	5.9	5.0	-0.9	-
Th^{232}	6.9	6.0	4.9	-1.1	-
Th^{233}	6.5	5.6	6.1	0.5	+
Th^{234}	7.0	6.1	4.6	-1.5	-
Pa^{230}	6.5	5.6	6.7	1.1	+
Pa^{231}	6.8	5.9	5.7	-0.2	-
Pa^{232}	6.6	5.7	6.5	0.8	+
Pa^{233}	7.0	6.1	5.2	-0.9	-
U^{230}	6.2	5.3	5.9	0.6	+
U^{231}	5.9	5.0	7.3	2.3	+
U^{232}	6.3	5.4	5.8	0.4	+
U^{233}	6.0	5.1	6.8	1.7	+
U^{234}	6.4	5.5	5.2	-0.3	-
U^{235}	6.1	5.2	6.5	1.3	+
U^{236}	6.5	5.6	5.3	-0.3	-
U^{238}	6.6	5.7	4.8	-0.9	-
U^{239}	6.3	5.4	5.9	0.5	+
Np^{234}	6.1	5.2	6.9	1.7	+
Np^{236}	6.2	5.3	6.7	1.4	+
Np^{237}	6.6	5.7	5.5	-0.2	-
Np^{238}	6.4	5.5	6.1	0.6	+
Np^{239}	6.7	5.8	5.1	-0.7	-
Pu^{236}	6.0	5.1	6.0	0.9	+
Pu^{238}	6.1	5.2	5.6	0.4	+
Pu^{239}	5.7	4.8	6.4	1.6	+

Table 11.4 (cont'd.)

Nuclide	E_b* (Mev)	E_a** (Mev)	B_n*** (Mev)	$B_n - E_a$ (Mev)	Slow neutron fission-ability****
Pu^{240}	6.2	5.3	5.4	0.1	+
Pu^{241}	5.9	5.0	6.3	1.3	+
Pu^{242}	6.3	5.4	5.0	-0.4	-
Am^{241}	6.3	5.4	5.6	0.2	+
Am^{242m}	6.0	5.1	6.2	1.1	+
Am^{242}	6.0	5.1	6.2	1.1	+
Am^{243}	6.4	5.5	5.2	-0.3	-
Cm^{242}	5.8	4.9	5.6	0.7	?
Cm^{243}	5.4	4.5	6.7	2.2	+
Cm^{244}	5.9	5.0	5.7	0.7	?
Cm^{245}	5.5	4.6	6.4	1.8	+
Cf^{249}	5.2	4.3	6.6	2.3	+
E^{254}	5.6	4.7	6.0	1.3	+

≠ This table reproduced from R. Vandenbosch and G. T. Seaborg, Phys. Rev. 110, 507 (1958).

* Potential barrier for fission calculated from equation 11.41.

** Activation energy for fission taken to be 0.9 Mev less than E_b.

*** Neutron binding energy for nuclide with mass number A + 1.

**** The + denotes that the cross section for fission is greater than about 1 barn;
The - denotes that the cross section for fission is less than about 1 barn.

approximate thresholds have been experimentally determined: Th^{232} (1.1 Mev), Pa^{231} (0.4 Mev), U^{234} (0.3 Mev), U^{236} (0.6 Mev) U^{238} (0.9 Mev), and Np^{237} (0.3 Mev). It can be seen that the agreement between the predicted and the experimentally determined threshold values is good.

It is possible to compare predicted and measured values even in those cases in which the threshold falls below the neutron binding energy. NORTHRUP, STOKES AND BOYER[55] have developed an experimental technique, based on the (d,p) reaction, for adding a neutron to a nucleus without exciting the new nucleus to the neutron binding energy. Fission thresholds were obtained by measuring the energy spectrum of protons in coincidence with fission events induced by deuterons of known energy. More details are given in section 11.3.4 below. The results indicate that detectable fission occurs in U^{235}, Pu^{239} and U^{233} at neutron energies with "negative" energies of 1.5, 2.0 and 2.0 respectively,[≠] in rough agreement with the values listed in Table 11.4.

11.3.2 Cross Section for Fission with Thermal Neutrons. The three nuclides U^{235}, U^{233} and Pu^{239} stand out in importance from all other heavy element nuclides because of their fission characteristics and availability. Their importance in nuclear reactor and nuclear weapons stems from the facts that they are readily induced to fission by slow neutrons, that they are sufficiently long-lived and can be produced and isolated in large quantities. In this book we shall not be concerned with the technological uses of these nuclides. Table 11.5 lists the "international" values for the fission cross-sections for the "big three".[*] HUGHES AND SCHWARTZ[56] reviewed all data reported to May 1958 and derived the values given in this table for neutrons of 2200 meters per second velocity. Because the cross sections and associated quantities are energy dependent, a slightly different set of values is required if a Maxwellian neutron energy distribution at room temperature is considered. Some recent cross section measurements are not in agreement with these "world consistent set" values and it may be necessary eventually to revise the values upward.

---

55. J. A. Northrop, R. H. Stokes and K. Boyer, Phys. Rev. 115, 1277 (1959).

56. D. N. Hughes and R. B. Schwartz, "Neutron Cross Sections", Brookhaven National Laboratory Report BNL-325, Second Edition, Sup. of Documents, U.S. Gov't Printing Office, Washington, D. C. (July 1958).

[≠] The threshold values deduced by Northrup, Stokes and Boyer from their curves are -0.60, -1.60 and -1.47 but these threshold are defined in a way less suitable for comparison with the "calculated" values of Table 11.4.

[*] Note added in proof, Table 11.5 as shown is taken from the later publication of Hughes, Nucleonics 17, No. 11, 132, 1959, rather than from reference 56.

Table 11.5 World Values of 2200 m/s Cross Sections of Fissionable Isotopes

	World Weighted Averages	World Consistent Set
	Uranium-233	
σ_{abs} (barns)	580 ± 4	578 ± 4
σ_F (barns)	523 ± 3	525 ± 4
α	0.099 ± 0.003	0.101 ± 0.004
η	2.29 ± 0.01	2.28 ± 0.02
ν	2.50 ± 0.02	2.51 ± 0.02
	Uranium-235	
σ_{abs} (barns)	683 ± 3	683 ± 3
σ_F (barns)	582 ± 4	582 ± 4
α	0.179 ± 0.009	0.174 ± 0.010
η	2.07 ± 0.01	2.07 ± 0.01
ν	2.43 ± 0.02	2.43 ± 0.02
	Plutonium-239	
σ_{abs} (barns)	1,028 ± 8	1,028 ± 8
σ_F (barns)	742 ± 4	742 ± 4
α	0.38 ± 0.02	0.39 ± 0.03
η	2.08 ± 0.02	2.08 ± 0.02
ν	2.89 ± 0.03	2.89 ± 0.03

σ_{abs} is the absorption cross section; σ_F is the fission cross section;

α is the ratio of radiative capture to fission;

η is the average number of neutrons emitted per neutron absorbed;

ν is the average number of neutrons emitted per fission event.

From D. J. Hughes, Nucleonic 17, No. 11, 132, 1959. See also Hughes, B. A. Magurno, M. K. Brussel, BNL-325 (II), Supplement 1, 1959.

and it may prove necessary eventually to revise the values upward.*

The cross sections for radiative capture of a neutron or for fission induced by neutron capture have been measured for many other heavy element nuclides and these are listed in Table 11.6. Most of these were measured by a comparison method using U^{235} or Pu^{239} as a reference standard in a Maxwellian distribution of neutrons from a "thermal column" of a reactor. Many of these nuclides have higher fission probabilities than do the "big three"; however, the half lives, the methods of production and other properties are not favorable for engineering uses.

An examination of the results shown in Table 11.6 reveals that a large percentage of those nuclides which undergo slow-neutron fission contain an odd number of neutrons. This is understandable when one considers that the compound nucleus in such cases is excited to a greater extent because of the energy released in the pairing of neutrons when the incoming neutron is absorbed. BOHR[57] pointed out very soon after the discovery of uranium fission that most of the fission in natural uranium was due to the odd-neutron isotope, U^{235}.

HUIZENGA AND DUFFIELD[58,59] called attention to an interesting correlation involving the ratio of fission to capture. The ratio of thermal neutron fission cross section to the thermal neutron capture cross section can be expressed as:

$$\frac{\sigma_f}{\sigma_c} = \frac{\Gamma_f}{\Gamma_c}$$

where $\Gamma_f/\hbar$ is the probability per unit time that the compound nucleus loses its

---

* For example, Bollinger, et al. obtained the value of 606 ± 6 barns for the fission cross section of U^{235} with 0.025 Mev neutrons using a new and very elegant method for making a direct absolute fission cross section measurement. Bull. Amer. Phys. Soc. Ser. II 2, 196 (1957); a program for the more accurate measurement of η in U^{233} was started in the AEC national laboratories in 1959. This may result in a revision of this important constant.

57. N. Bohr, Phys. Rev. 55, 418 (1939)

58. J. R Huizenga and R. B. Duffield, Phys. Rev. 88, 959 (1952)

59. J. R. Huizenga, Paper No.26, "Proceedings of the International Conference on the Peaceful Uses of Atomic Energy", Vol 2, United Nations, N.Y. (1956) p.208.

Table 11.6 Thermal Neutron Fission Cross Sections

Isotope	σ_f (barns)	Reference	$\sigma_{capture}$ (barns) Pile neutrons≠
Ra^{223}	< 100	1	125 ± 15
Ra^{226}	$< 1.1 \times 10^{-4}$	2	18
	< 0.05	3	
Ra^{228}	< 2	1	36 ± 5
Ac^{227}	< 2	1	495 ± 35
Th^{227}	1500 ± 1000	4	
Th^{228}	≤ 0.3	5	123 ± 15
Th^{229}	45 ± 11	5	
Th^{230}	< 0.001	6	26 ± 2
Th^{232}	< 0.0002	6	7.57 ± 0.17
Th^{232}	$\leq 4 \times 10^{-5}$	40	
Th^{233}	15 ± 2	7	1400 ± 200
Th^{234}	< 0.01	4	1.8 ± 0.5
Pa^{230}	1500 ± 250	8	
Pa^{231}	0.010 ± 0.005	6	293 ± 44
Pa^{232}	700 ± 100	8	760 ± 100
Pa^{233}	< 0.1	9	140 ± 20
Pa^{234}(1.18 m)	< 500	4	
Pa^{234}(6.7 h)	< 5000	4	
U^{230}	25 ± 10	4	
U^{231}	400 ± 300	4	
U^{232}	80 ± 15	10	300 ± 200
U^{233}	532 ± 6	11	56 ± 2
U^{234}	≤ 0.65	12	72 ± 10
U^{235}	582 ± 10	11	112 ± 10
U^{236}	--	--	24.6 ± 6
U^{238}	< 0.5	13	2.76 ± 0.06
U^{239}	12	14	22
Np^{234}	900 ± 300	15	
Np^{236}(5000 y)	2800 ± 800	16	
Np^{237}	0.019 ± 0.003	17	169 ± 6

Table 11.6 (cont'd)

Isotope	σ_f (barns)	Reference	$\sigma_{capture}$ (barns) Pile neutrons≠
Np^{238}	1600 ± 100	18	[illegible]
Np^{239}	< 3	19	60 ± 10
Pu^{236}	170 ± 35	36	
Pu^{237}	2500 ± 500	36	
Pu^{238}	18.2 ± 0.5	20	489 ± 3
	18.4 ± 0.9	33	
	16.5 ± 0.5*	35	
Pu^{239}	738 ± 9	11	287 ± 13
Pu^{240}	-0.8 ± 0.7**	21	530 ± 50
	~0.05	38	250 ± 40
	0.03 ± 0.045	39	
Pu^{241}	1060 ± 210***	22	390 ± 80
	950 ± 50	23,24	
Pu^{242}	< 0.3	35	18.6 ± 0.8
	0	34	
Pu^{243}			170 ± 90
Pu^{244}			1.5 ± 0.3
Pu^{245}			260 ± 145
Am^{241}	3.13 ± 0.15	33	700 ± 200
	3.0 ± 0.2	26,27	
Am^{242m}	3000	28	
	2500*	35	
	2000*	29	
Am^{242}	6000	29	5500
	6390 ± 500	33	
	4600*	35	
Am^{243}	< 0.072	33	133.8 ± 0.8
	< 0.05	35	
Cm^{242}	< 5*	27	25
Cm^{243}	490 ± 70	30	250 ± 150
	690 ± 50	33	

Table 11.6 (cont'd.)

Isotope	σ_f (barns)	Reference	$\sigma_{capture}$ (barns) Pile neutrons≠
Cm^{244}			25 ± 10
Cm^{245}	1880 ± 150	33	200 ± 100
	1800 ± 300	31	
Cm^{246}			15 ± 10
Cm^{247}			180
Cm^{248}			2.2 ± 0.7
Bk^{249}			1100 ± 300
Bk^{250}			350
Cf^{249}	630*	32	270 ± 100
Cf^{250}			1500
Cf^{251}			3000
Cf^{252}			30
Cf^{254}			< 2
E^{253}			$\longrightarrow E^{254m}$ 240
			$\longrightarrow E^{254}$ 7
E^{254}	2000*	30	40
	~2700*	35	
E^{255}			~40

≠ Values of $\sigma_{capture}$ are reprinted from Table in Chap. 2 where the references on which they are based are listed.

* Measurement made in pile neutron flux.

** Pu^{240} is of special importance in reactors. In a pile neutron flux it is important to consider the sharp resonance at 1 electron volt. See for example reference 37 and 38.

*** Pu^{241} has an important low-lying resonance at 0.252 ev.

References to Table 11.6

1. S. Peterson and A. Ghiorso, Paper 19.4 "The Transuranium Elements," Vol. 14B National Nuclear Energy Series, McGraw-Hill Book Co., New York, 1949.
2. D. P. Ames and A. Ghiorso, Paper 19.5 "The Transuranium Elements," Vol. 14B National Nuclear Energy Series, McGraw-Hill Book Co., New York, 1949.
3. B. Pontecorvo and D. West, reported in MP-210 (Dec. 1, 1945).
4. D. J. Hughes and J. A. Harvey, "Neutron Cross Sections," Brookhaven National Laboratory Report BNL-325, July 1955.
5. M. H. Studier, A. Ghiorso and F. Hagemann, unpublished data, 1946.
6. A. Ghiorso and Q. Van Winkle, Paper 9.12 of National Nuclear Energy Series, Div. IV, Vol. 17B, AEC Technical Information Service , TID-5223 Pt.2, Oak Ridge, Tenn. (1952).
7. D. J. Hughes and R. B. Schwartz, "Neutron Cross Sections," Brookhaven National Laboratory Report BNL-325, Supplement No. 1 (Jan. 1, 1957).
8. A. Ghiorso, M. H. Studier, and E. K. Hyde, unpublished data ( )
9. F. Hagemann, M. H. Studier and A. Ghiorso, Paper 9.4 of National Nuclear Energy Series, Division IV, Vol. 17B, AEC Technical Information Service, TID-5223 Pt.2, Oak Ridge, Tenn. (1952).
10. R. Elson, W. C. Bentley, A. Ghiorso and Q. Van Winkle, Phys. Rev. 89, 320 (1953).
11. "World Consistent Values" reported in "Neutron Cross Sections", Supplement No. 1 (Jan. 1, 1957).
12. C. Osborne, I. Floyd and I. Coveyou, Report MON-P-178 (1946).
13. R. L. Macklin and J. H. Lykins, J. Chem. Phys. 19, 844 (1951).
14. P.R. Fields, G. L. Pyle, and W. C. Bentley, Nucl. Sci. Eng. 2, 33 (1957).
15. E. K. Hyde, W. C. Bentley and F. Hagemann, Argonne National Laboratory Report ANL-4152 (May 1948).
16. M. H. Studier, J. E. Gindler and C. M. Stevens, Phys. Rev. 97, 88 (1955)
17. A. Ghiorso, D. W. Osborne and L.B. Magnusson, Paper 22.26 "The Transuranium Elements", Vol. 14B, National Nuclear Energy Series, McGraw-Hill Book Co., New York, 1949.
18. M. H. Studier, H. H. Hopkins, Jr., A. Ghiorso, and W. C. Bentley, Report CF-3762 (1947).
19. J. J. Floyd, H. Z. Schofield, J. Halperin, and L. B. Borst, Report MON-P-85 (March 31, 1956).

20. G. Reed, Jr., W. M. Manning, and W. C. Bentley, Argonne National Laboratory Report ANL-4112 (March 1, 1948).
21. C. B. Bigham, Can. J. Physics 36, 503 (1958).
22. P. R. Fields, G. L. Pyle, M. G. Inghram, H. Diamond, M. H. Studier and W.M. Manning, Nucl. Sci. Eng. 1, 62 (1956).
23. J. F. Raffle and B. T. Price, Paper P/422, Vol. 4, Proceedings of the International Conference on the Peaceful Uses of Atomic Energy, United Nations, New York, 1956.
24. Adamchuk et al., Paper P/645, Vol. 4, Proceedings of the International Conference on Peaceful Uses of Atomic Energy, United Nations, New York, 1956.
25. W. C. Bentley, et al., Paper P/809, Vol. 7, Proceedings of the International Conference on Peaceful Uses of Atomic Energy, United Nations, New York, 1956.
26. B. B. Cunningham and A. Ghiorso, Phys. Rev. 82, 558 (1951).
27. G. C. Hanna, B. G. Harvey, N. Moss, and P.R. Tunnicliffe, Phys. Rev. 81, 893, (1951).
28. G. Higgins and W. W. T. Crane, Phys. Rev. 94, 735 (1954).
29. K. Street, Jr., A. Ghiorso, and S. G. Thompson, Phys. Rev. 85, 135 (1952).
30. S. G. Thompson et al., unpublished results, University of California Radiation Laboratory, Berkeley, California, 1955.
31. P. R. Fields, et al., Phys. Rev. 102, 180 (1956).
32. B. G. Harvey, H. P. Robinson, S. G. Thompson, A. Ghiorso, and G. R. Choppin, Phys. Rev. 95, 581 (1954).
33. E. K. Hulet et al., Phys. Rev. 107, 1294 (1957).
34. Butler, Lounsbury and Merritt, Can. J. Phys. 35, 147 (1957).
35. J. P. Butler et al., "Review of the Joint AECL-KAPL Studies of the Transuranium Elements", report KAPL-1781, July ,1957 (unpublished).
36. J. Gindler, J. Gray and J. Huizenga, Phys. Rev. 115, 1271 (1959).
37. R. L. Crowther and J. W. Weil, Nuc. Sci. and Eng. 3, 747 (1958)
38. Leonard, Seppi, Friesin, and Kinderman, Bull. Amer. Phys. Soc. Ser. II, 1 248, (1958).
39. R. P. Schuman, Knolls Atomic Power Lab. Report, KAPL-1781, quoted in ref. 21.
40. G. N. Flerov, 1959.

excitation by fission and $\Gamma_c/\hbar$ is the probability per unit time that the compound nucleus loses its excitation by gamma ray emission. If Γ_c is a very slowly changing function of the nuclear excitation energy in the region under consideration (5 to 7 Mev) and if Γ_f has a sensitive dependence on nuclear excitation energy in the above energy range, then a correlation of σ_f/σ_c with the energy difference $B_n - E_a$ would be expected. Here B_n is the neutron binding energy and E_a is the activation energy for fission. Of course, nuclear type may influence the σ_f/σ_c ratio to some degree, but it is not possible to take this into account in a quantitative manner. For example, the probability for gamma ray emission may be less for the intermediate fissioning nuclei of the even-even type because of larger level spacing, which means that fission is relatively favored and would occur at lower excitation relative to the barrier height. Values of $B_n - E_a$ can be taken from Table 11.4. Some values of σ_f/σ_c are plotted in Figure 11.18 against the energy difference $B_n - E_a$. It can be seen that the ratio σ_f/σ_c decreases sharply and rather smoothly with decreasing value of $B_n - E_a$. This correlation is useful in predicting the fission cross section for nuclides for which this quantity has not been measured or is difficult to measure. Nuclides such as Pa^{231} and Np^{237}, for example, are on the borderline of thermal neutron fissionability. In the next chapter we shall be concerned with fission probability of nuclei excited to higher energy and there it will be regarded as a matter of some interest to explore the somewhat related ratio $\sigma_F/\sigma_n = \Gamma_F/\Gamma_n$ as a function of nuclear type and excitation energy. See section 12.1.4.

11.3.3 *Fission Cross Section as a Function of Neutron Energy in the Thermal and Resonance Energy Region.* The variation in fissionability of the heavy element nuclides as a function of neutron energy is a matter of the utmost practical importance in reactor calculations and design and is of great fundamental interest as well for an understanding of the nature of the fission reaction. For this reason very detailed studies have been made of the isotopes of thorium, uranium and plutonium with by far the greatest effort being devoted to U^{235} and Pu^{239}. These studies, which are still in progress in many laboratories all over the world, consist in the measurement of scattering cross-sections, total absorption cross sections, fission cross sections and related quantities such as α (ratio of radiative capture to fission), and $\bar{\nu}$ average number of neutrons per fission, as a function of neutron energy. A great deal

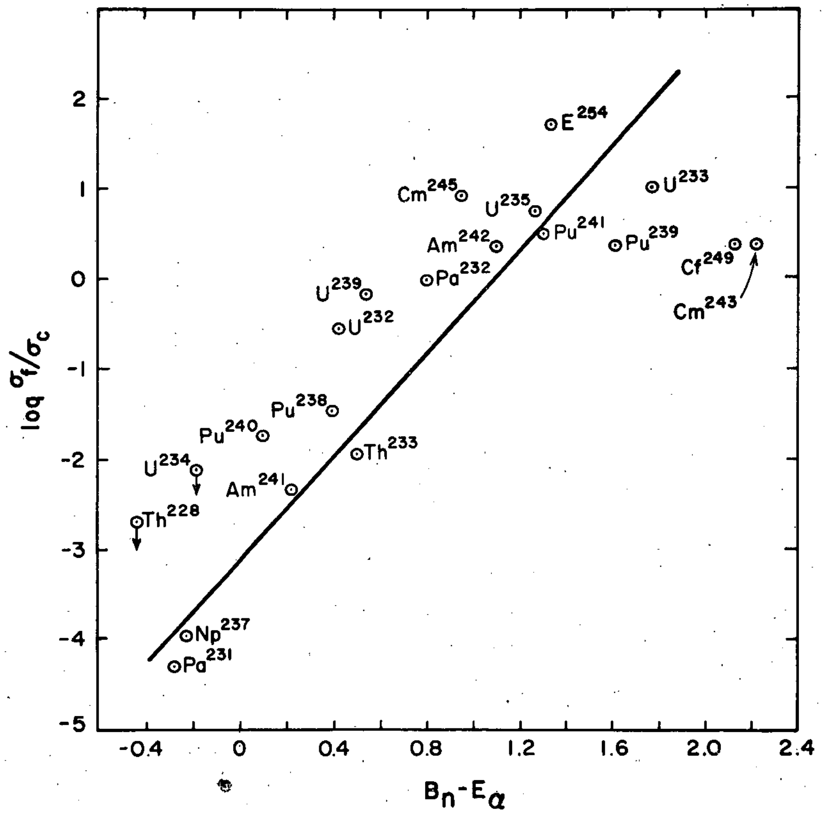

MU-19426

Fig. 11.18. Correlation of the ratio σ_f/σ_c with the energy difference B_n-E_a taken from Table 11.4.

of effort has gone into the development of monoenergetic beams of neutrons using time-of-flight techniques or crystal spectrometers. Accelerators and reactors have been used as sources of intense beams of neutrons. We have space to sketch in only a few of the results. Those requiring a more complete discussion of experimental techniques, results and interpretations can consult other references.[60-65]

Consider first Figure 11.19 which shows the fission cross-sections for U^{235} and Pu^{239} as a function of neutron energy. For U^{235} in the region from 0 to 0.2 electron volts the curve follows roughly the $1/\nu$ law. Above 0.2 electron volts there are many sharp peaks or "resonances" which reflect the capture of

---

60. D. J. Hughes, Pile Neutron Research, Cambridge, Mass.; Addison-Wesley, 1953.
61. D. J. Hughes and R. B. Schwartz, "Neutron Cross Sections" Report BNL-325, Second Edition (1958). For sale by Superintendent of Documents, U.S. Government Printing Office, Washington 25, D. C.
62. Vol.4 "Cross Sections Important to Reactor Design," Proceedings of the International Conference on the Peaceful Uses of Atomic Energy, U.N. New York, 1956. Vol. 15 "Physics in Nuclear Energy", Proceedings of the Second U.N. International Conference on the Peaceful Uses of Atomic Energy, Geneva, 1958.
63. Progress in Nuclear Energy, Series I, Physics and Mathematics, Vol. 1, Charpie, Horowitz, Hughes, and Littler, editors, McGraw-Hill Book Co., New York, 1956.
64. Conference on Neutron Physics by Time-of-Flight, held at Gatlinburg, Tenn., Nov. 1 and 2, 1956, Oak Ridge National Laboratory Report, ORNL-2309, July 1957.
65. Proceedings of the International Conference on the Neutron Interactions with the Nucleus, held at Columbia University, New York, Sept. 9-13, 1957. Report TID-7547. Available for $3.25 from Office of Technical Services Department of Commerce, Washington 25, D. C.

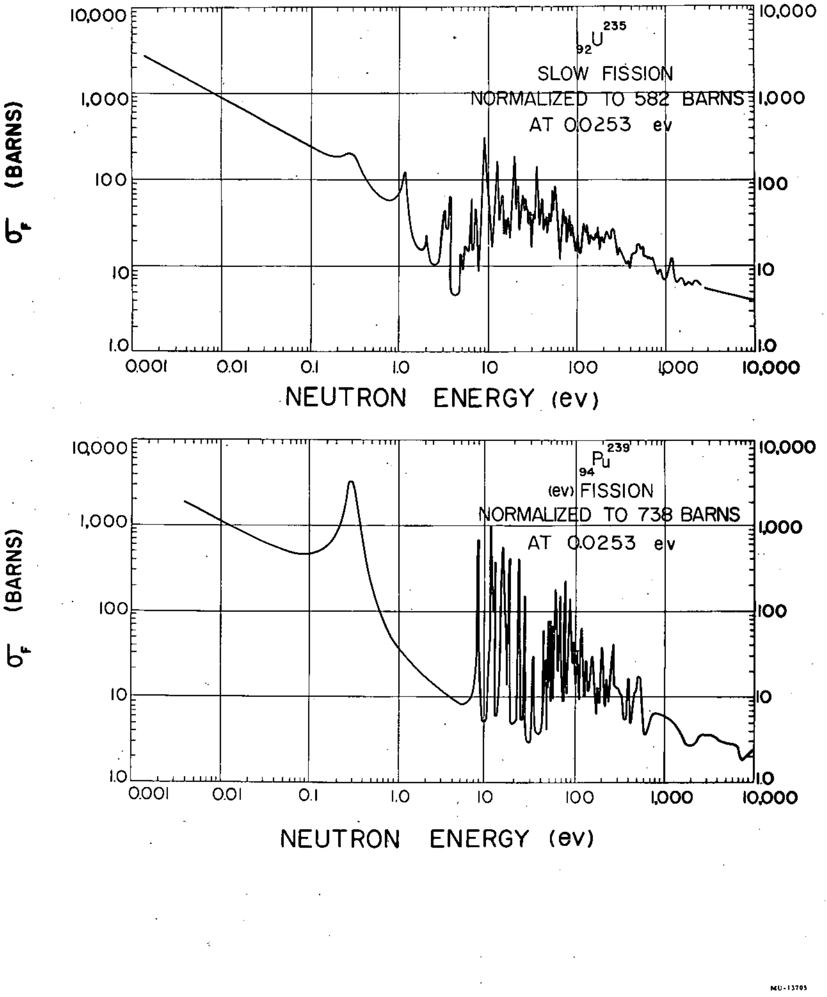

Fig. 11.19. Fission cross section as a function of neutron energy for U^{235} and Pu^{239}.

of a neutron with kinetic energy such that the binding energy plus the kinetic energy of the neutron is precisely equal to the energy of some quantum state in the excited nucleus. These resonances correspond to energy levels about 6 Mev above the ground level in the compound nucleus system. In the region of 0.2 ev to about 60 ev there are many dozens of sharp resonances with an average spacing between resonances of about 1 electron volt, a very small value. On the scale of this figure the curve can only indicate the complexity of the resonance structure. The extremely detailed experimental data on the individual resonances can be represented adequately only on a series of curves showing narrow cuts of the energy spectrum. We show here only one example of such plots (figure 11.20) since it is beyond the scope of our review to present a critical account of this specialized field of neutron physics. The total absorption cross-section curves are similar to the fission curves shown here; the same resonances appear in both capture and fission. However, the value of α, the ratio of capture to fission, is not the same for all resonances as can be seen in Figure 11.20. As stated above, the resonances observed in these studies correspond to energy levels about 6.4 Mev above ground level in the U^{236} compound nucleus because of the binding energy of the captured neutron.

The discovery of the sharp resonances in the fission cross-section curve and the large competition of radiative capture with fission was a surprise to most physicists at the time it was first discovered. It had been thought that the fissionable nuclides would have such large fission widths after capture of neutrons in the low and intermediate energy ranges that all resonance structure would be washed out. (See for example the discussion of BOHR AND WHEELER[52] in their 1939 paper.) The explanation of the sharp resonance structure is that the number of saddle point channels available for fission from any one resonance state is a number close to one. If a large number of channels were open for fission in a nucleus excited to a typical slow neutron resonance state then the resonance levels would become unresolved. This is presumably what happens at higher excitation energies.

The high value of α for some of the resonances, particularly for Pu^{239}, means that a large loss of neutrons by parasitic capture in the fuel can occur in a nuclear reactor unless the neutrons are very rapidly decelerated through the resonance region. This resonance radiative capture is particularly harmful in the case of breeder reactor. The fission cross section for Pu^{239} as a function

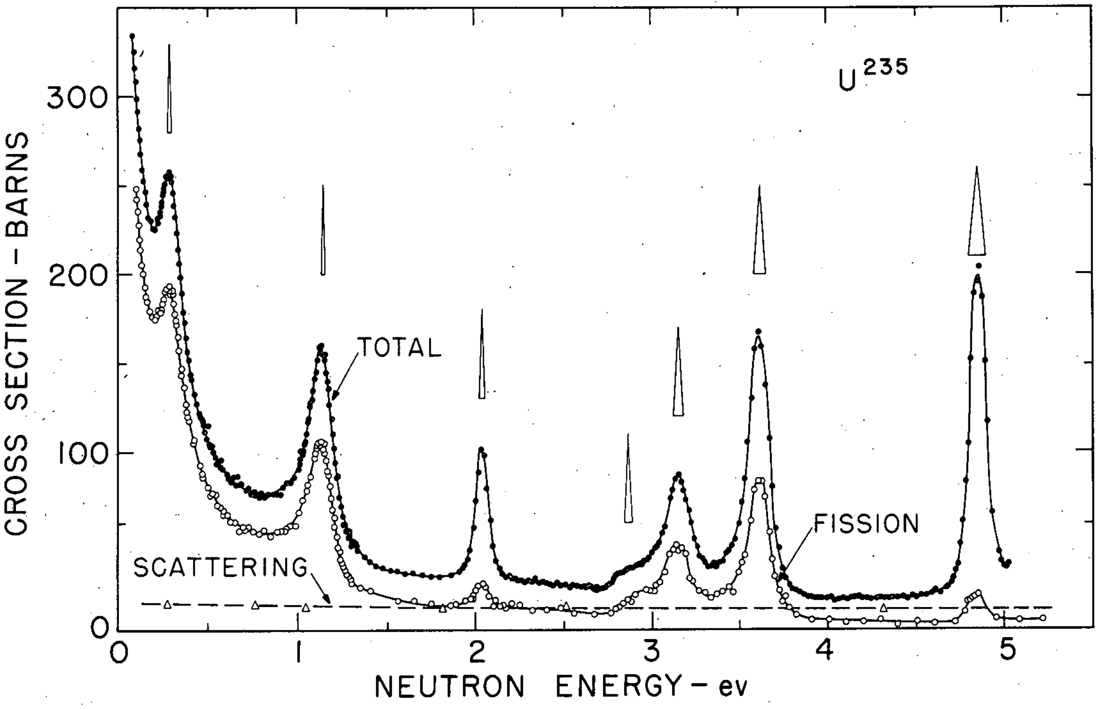

MU-18711

Fig. 11.20. Resonance structure in the interaction of neutrons with U^{235} in the energy range from 0.1 to 5 ev. The observed total cross section, fission cross section and scattering cross section are displayed. Note the identity of (n,γ) and fission resonances and the differing values of α from resonance to resonance. Figure from Shore and Sailor.[69]

of neutron energy (Figure 11.19) shows that a very important resonance occurs at the low neutron energy 0.296 electron volts. Since the value of α for this resonance is quite high, 0.69, it is particularly important in reactor design.

The analysis of the resonance peaks observed in capture and fission, is often carried out with the Breit-Wigner single level formula derived for a stationary nucleus and for a resonance isolated from its neighbors. The Breit-Wigner formula is

$$\sigma_{\text{fission}} = 4\pi\lambda\lambda^{o} \frac{g \; \Gamma_n \; \Gamma_f}{4(E-E_o)^2 + \Gamma^2} \qquad (11.42)$$

where

λ is the wave length of the neutrons

λ^{o} is the wave length of the neutrons at resonance

Γ, the total width of the level, is the sum of the neutron width Γ_n, the radiation width Γ_γ and the fission width Γ_f

E is the neutron energy and E_o refers to the neutron energy at exact resonance

g is a statistical weight factor given by $g = 1/2 \; 1 \pm \frac{1}{2I+1}$

I = spin of the target nucleus

It can be seen that the shape of the resonance is symmetrical with a maximum at the resonance energy. The quantities E_o, g, Γ_n, Γ_γ and Γ_f completely define a resonance; if these parameters are known for each resonance and if the effective nuclear radius is known, then the cross section can be accurately computed at any energy. The need for data of this type for reactor design has made the accurate analysis of the resonances of considerable importance. Several of the references[61-63] cited in this chapter give tables of such parameters. These tables are under continual revision as more resonance peaks are resolved.

In the neutron capture resonance spectrum many of the individual resonances have the expected symmetrical shape but in the fission spectrum many of the resonances have an asymmetric shape deviating markedly from the prediction of the single-level Breit-Wigner formula.[66-69] These observed asymmetries can be explained in two ways: (1) they are caused by small unresolved levels near the prominent ones; or (2) they are caused by interference between the resonance levels. An increasing amount of recent experimental evidence points toward interference as being the more frequent cause. If this is truly the case, then one should use a multilevel Breit-Wigner formula to describe the fission resonances. The size distribution of the reduced widths of a large number of levels gives supporting evidence for this and provides some information about the number of channels open to fission. Analysis of these distributions indicates that slow neutron fission may involve a small number of fission channels.[70] The experimental data favoring a multi-level Breit-Wigner analysis are presented by several authors, particularly V. L. Sailor.[66,67,69] A multi-level dispersion formula has been derived in published theoretical papers to account for the experimental data. REICH AND MOORE[71] derive a formula which is valid for the case of a single fission channel which SHORE AND SAILOR[69] apply quite successfully to the resonance structure of U^{235}. VOGT[72] derives a multichannel, few-level, dispersion formula which also accounts reasonably successfully for the experimental data.

One difficulty in the interpretation of resonance structure is the lack of an experimental method for the determination of the angular momentum quantum number for each resonance level.

The analysis of fission resonances in terms of a multilevel Breit-Wigner

---

66. V. L. Sailor, International Conference on the Peaceful Uses of Atomic Energy, Geneva, 1955, United Nations, New York 1956, Vol. IV, p.199.
67. F. J. Shore and V. L. Sailor, Proceedings of the International Conference on the Neutron Interactions with the Nucleus held at Columbia Univ. Sept. 9-13, 1957, document TID-7547, p.107-111.
68. J. E. Evans and R. G Fluharty, ibid, pp.98-104; see also Fluharty, Moore and Evans, Paper P/645 Vol 15, Proceedings of the Second United Nations International Conference on the Peaceful Uses of Atomic Energy, September, 1958.
69. F. J. Shore and V. L. Sailor, Phys. Rev. 112, 191 (1958); See also paper P/648, Vol. 15, Proceedings of Second United Nations International Conference on the Peaceful Uses of Atomic Energy, September, 1958.
70. C. E. Portor and R. G Thomas, Phys. Rev. 104, 483 (1956)
71. C. W. Reich and M. S. Moore, Phys. Rev. 111, 929 (1958)
72. E. Vogt, Phys. Rev. 112, 203 (1958).

formula has interesting theoretical consequences since it strongly suggests that slow-neutron fission is a process defined by one, or at most, a few reaction channels. This seems strange at first consideration because it seems natural to assume that each pair of fission fragments in each possible state of excitation constitutes a separate fission exit channel. The broad distribution of fission fragment masses and energies would on this picture imply a large number of channels. This anomaly can be removed in the model of the fission process briefly outlined by A. BOHR[73] at the 1955 Geneva Conference which is mentioned in Section 11.2.2. The essence of this theory is that the nucleus on its way to fission must pass through a transition state in which almost all of the excitation energy of the compound nucleus has been converted to potential energy of deformation. At this transition state the nucleus is relatively "cold" and only a few well defined quantum states will be available to it. These states may resemble the low-lying states found near the ground state for heavy nuclei which already at the ground state have considerable deformation. Thus, the original compound nucleus, although it could be formed by capture of the neutrons into numerous levels, could pass through only those very few available transition states with the proper total angular momentum and parity. The term "fission channel" would be associated with these transition states. Each of the transition states or fission channels can subsequently lead to the formation of a whole spectrum of fission fragments.

11.3.4 Fission Threshold Measurements by the (d,p) Fission Method.

It is not possible to investigate the threshold energy region for a compound nucleus formed by the capture of a slow neutron if this nucleus is already excited above the fission threshold when the neutron is absorbed. At the Los Alamos Scientific Laboratory STOKES, NORTHRUP AND BOYER[74,75] have developed a clever experimental technique for the measurement of fission cross sections of nuclei excited to a definite value below the neutron binding energy. The Z^A (d,p) Z^{A+1} reaction is used to produce the compound nucleus Z^{A+1} + 1 in an excited state. As in the case of neutron bombardment compound nuclei can achieve excitations greater than the neutron binding energy, ϵ_n (region B of figure 11.21); the compound nucleus is, however, not limited to this region of excitation as it is in the case of slow neutron capture, but in addition can achieve any excitation from zero up to ϵ_n (region A of figure 11.21). This region A where the absorbed neutron has "negative" kinetic energy is most interesting because the probability for fission is not obscured by neutron re-emission and because the fission thresholds of many fissioning nuclei may appear here.

---

[73] A. Bohr, Proceedings of the United Nations Conference on the Peaceful Uses of Atomic Energy, Geneva, 1955. United Nations, New York, 1956. Vol. 2 p. 151.

[74] R. H. Stokes, J. A. Northrup and K. Boyer, Paper P/659 in the Proceedings of the Second United Nations International Conference on the Peaceful Uses of Atomic Energy.

[75] J. A. Northrup, R. H. Stokes and K. Boyer, Phys. Rev. 115, 1277 (1959).

It should be noted that fission induced by capture of neutrons by deuteron stripping differs from fission induced by slow neutron capture in that angular momentum greater than zero may be brought into the nucleus in the first case. This angular momentum may have a noticeable effect on the fission process.

The experiment consists in the bombardment of suitable targets with 14 Mev deuterons in the external beam of a cyclotron and the simultaneous measurement of fission fragments and of protons with a known energy. A schematic diagram of the apparatus[76] is shown in Figure 11.22. The fission detector is a shallow proportional counter operating at reduced gas pressure. This counter detects fragments in a cone with a 50° half angle centered at a 90° scattering angle. The ΔE counter is an ion chamber which is used to measure the rate of energy loss of light charged particles. After passing through the ΔE counter these particles are stopped in a small crystal of NaI and give up the remainder of their kinetic energy, E. The NaI crystal is connected to a light pipe and photomultiplier tube and finally to a 100 channel analyzer which determines the quantity E by measuring the size of the pulse from the photomultiplier.

The purpose of measuring both ΔE and E for the light charged particles is that discrimination of protons from other particles, chiefly deuterons and tritons, can be achieved by forming the products, $\Delta E \times E$. From a theoretical consideration of the ways in which such charged particles as protons, deuterons and tritons give up their energy in passing through matter, it is found that the mass of a charged particle is nearly proportional, over a relatively large energy range, to the product of its initial rate of energy loss multiplied by its total energy. In the experiment of STOKES, NORTHRUP AND BOYER[74,75] the ΔE

---

[76] Details of the apparatus are given in Reviews of Scientific Instruments, 29 61 (1958).

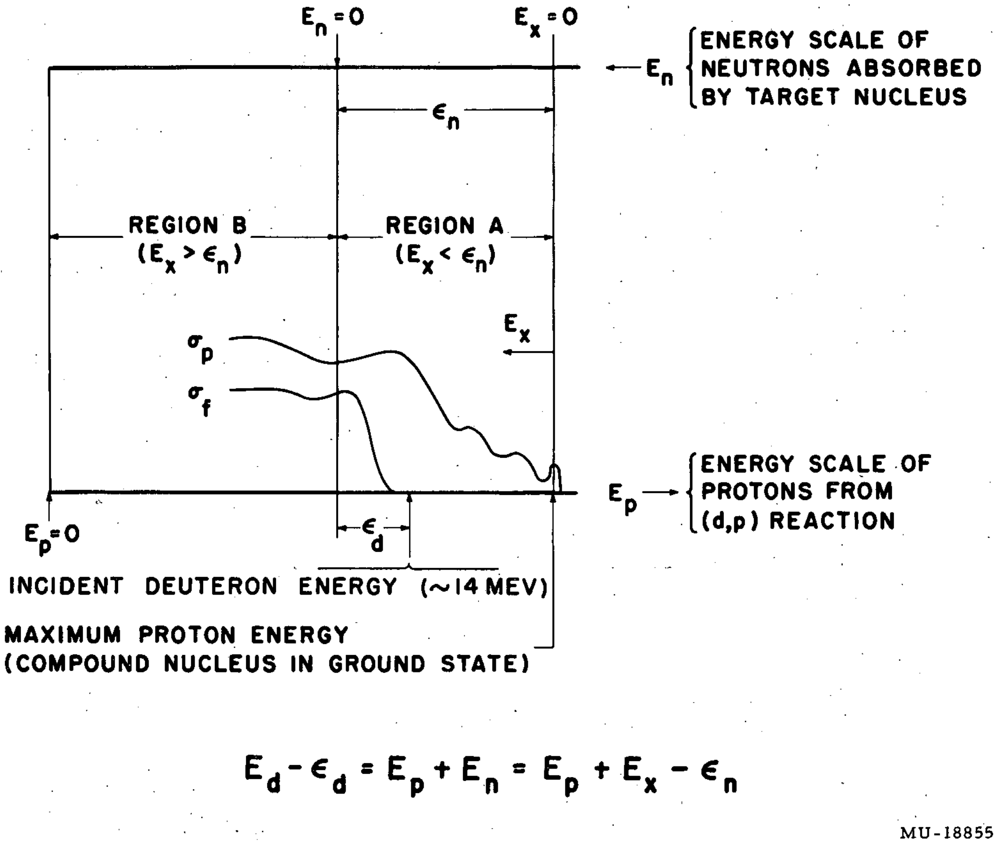
$E_n = 0$
$E_x = 0$
$\leftarrow E_n$
ENERGY SCALE OF NEUTRONS ABSORBED BY TARGET NUCLEUS
ϵ_n
REGION B ($E_x > \epsilon_n$)
REGION A ($E_x < \epsilon_n$)
E_x
σ_p
σ_f
$E_p \rightarrow$
ENERGY SCALE OF PROTONS FROM (d,p) REACTION
$E_p = 0$
ϵ_d
INCIDENT DEUTERON ENERGY (~14 MEV)
MAXIMUM PROTON ENERGY (COMPOUND NUCLEUS IN GROUND STATE)
$E_d - \epsilon_d = E_p + E_n = E_p + E_x - \epsilon_n$
MU-18855

Fig. 11.21. Energy relations for the (d,p) reaction on heavy elements. (Center-of mass-motion is neglected). E_d and ϵ_d are the kinetic and binding energy of the deuteron respectively. E_p is the kinetic energy of the outgoing proton and E_n is the equivalent kinetic energy of the incoming neutron. ϵ_n is the neutron binding energy and E_x is the excitation above the ground state, both for the compound nucleus. σ_p and σ_f are representative cross sections of the (d,p) reaction and this reaction followed by fission of the compound nucleus. The experiment is mainly concerned with region A where the captured neutron from the (d,p) reaction is bound. Figure from Stokes, Northrup and Boyer, Phys. Rev. 115, 1277 (1959).

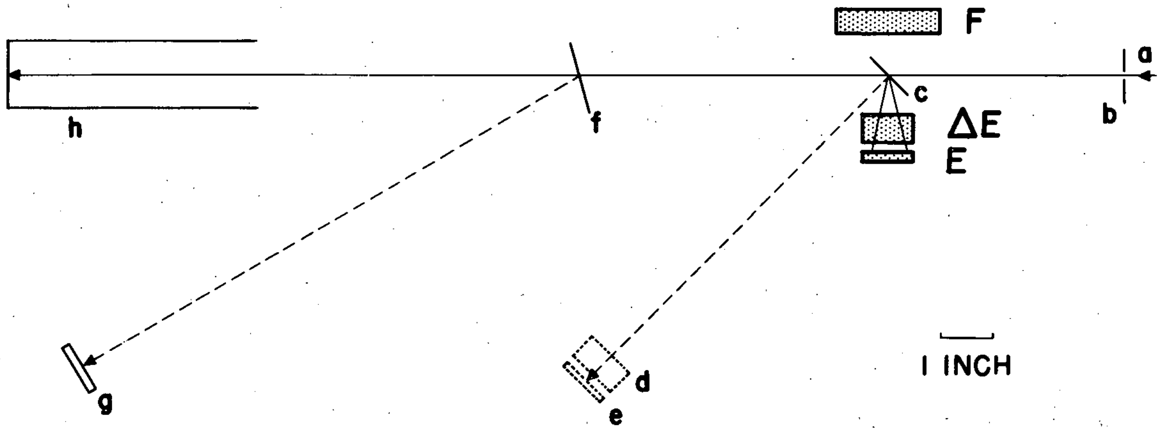

MU-18859

Fig. 11.22 Schematic drawing of the experimental apparatus used in the study of (d,p) fission with all counter sizes and distances drawn to scale. The main counters used in the proton-fission coincidence measurements are the following: F, fission proportional counter; ΔE, a thin transmission ion chamber; E, a NaI(Tl) spectrometer. The auxiliary components shown are these: (a) deuteron-beam path; (b) final gold collimator having a 1/16-in. aperture; (c) fissile target; (d) and (e) the alternate positions of the ΔE and E counters respectively during the E_d = 7-Mev runs; (f) 2-mg/cm^2 gold scattering foil; (g) NaI(Tl) counter used as the beam-energy monitor; and (h) Faraday cup. Figure from Stokes, Northrup and Boyer, Phys. Rev. 115, 1277, (1959).

counter takes out a sizable chunk of the initial energy so that $\Delta E \times E$ is not quite the proper product for use in mass identification. Instead, they use the expression, $(E + E_o + 1/2\ \Delta E)\ \Delta E$, where E_o is a constant, and achieve very clean discrimination of protons, deuterons and tritons. A high speed computor circuit utilizes coincident ΔE and E pulses to perform the required arithmetical operations. The output of the computor circuit is put through a simple discriminator which passes only those pulses identified as proton pulses. The 100 channel analyzer is used to measure the energy of any particle which has been identified as a proton. By a suitable arrangement of coincidence circuits it can also be used to measure the energy of any particle identified as a proton which is coincident in time with a fission event. By analyzing many (d,p) reaction events in this manner, curves are obtained showing the total (d,p) probability and the (d,p-fission) probability as a function of the energy of the protons. Data for the target nucleus Pu^{239} is shown in figure 11.23. The top spectrum is the fission-coincident proton energy spectrum corrected for chance rate. Below this is the total (d,p) proton energy spectrum corrected for light element contamination. It is instructive to plot the quotient of these two spectra and this is done in figure 11.24 not only for Pu^{239} but also for U^{233}, U^{235} and U^{238} targets. These curves are normalized according to the known solid angle of the fission counter assuming an isotropic fragment distribution. In figure 11.24 the energy scale has been reversed from the previous two figures to correspond to neutron energy increasing to the right.

The case of U^{238} is included since the fission threshold in this case falls in the region of positive neutron energies and a comparison can be made with the measurements made by more usual experimental methods. The agreement in this case with the fission excitation function of LAMPHERE[77] is satisfactory. The other three cases are quite interesting in showing fission thresholds in the region of "negative" neutron energies. There appears to be considerable structure corresponding to more than one distinct threshold in the case of Pu^{239} and U^{233}. STOKES, NORTHRUP AND BOYER[74,75] suggest an interpretation of these multiple thresholds in terms of A.BOHR'S[73] picture of the fission process as the passage of a deformed nucleus through a limited number of transi-

---

77. R. W. Lamphere, Phys. Rev. 104, 1654 (1956)

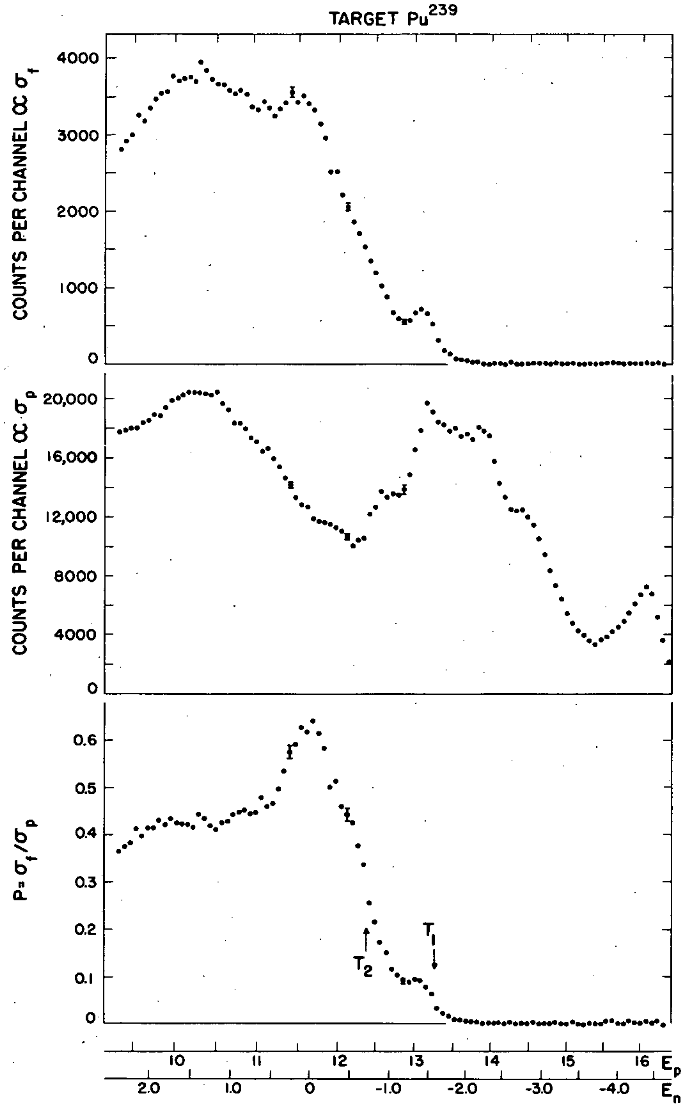

MU-18856

Fig. 11.23. Data obtained by Stokes, Northrup and Boyer for a Pu^{239} target in their (d,p-fission) experiment. The top curve is the energy spectrum of protons in coincidence with fissions (corrected for the chance rate) designated as σ_f. In the middle, σ_p is the total Pu^{239}(d,p)Pu^{240} proton spectrum corrected for light-element contaminants and the target backing material. At the bottom $P = \sigma_f/\sigma_p$ is the ratio of the top two curves and represents, at least in the bound-neutron region, the probability of fission decay of the compound nucleus. Representative statistical errors are shown. Figure from Stokes, Northrup and Boyer, Phys. Rev. 115, 1277 (1959).

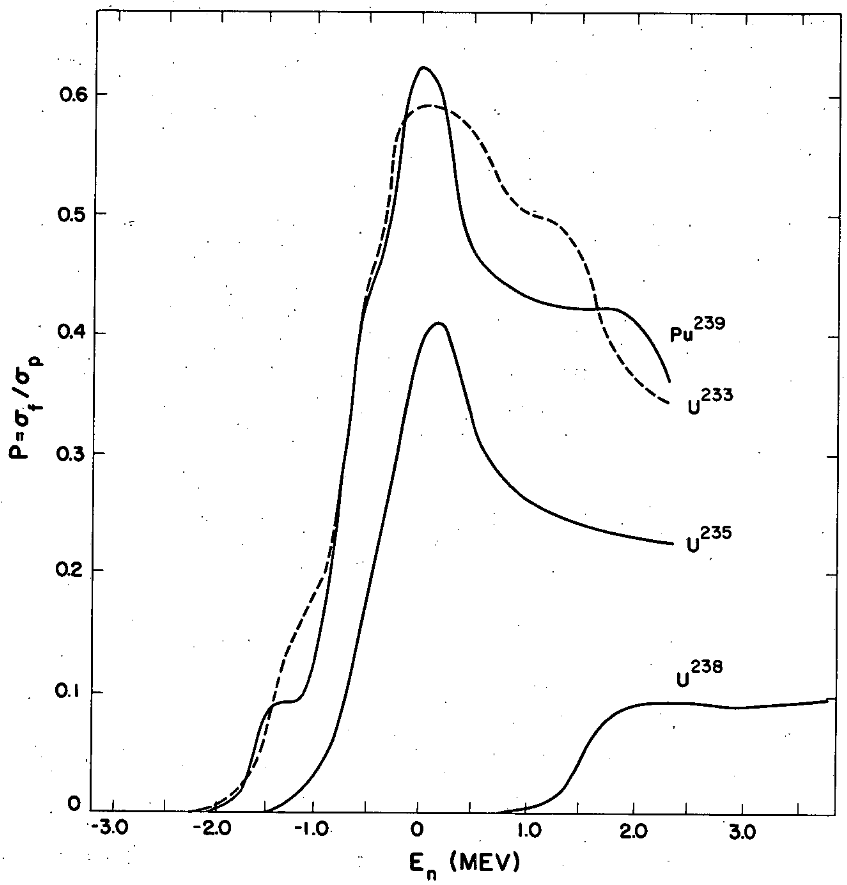

MU-18857

Fig. 11.24. The probability for fission, P, as a function of neutron energy as measured by the d,p-fission experiment showing the curves of four target nuclides in their proper relative position. Figure from Stokes, Northrup, and Boyer, Phys. Rev. 115,(1277 (1959).

tion states resembling the low energy states of non-spherical nuclei.

Two interesting comments can be made about the (dp - fission) experiment. It was found that when uranium targets are bombarded with deuterons, most of the total fission cross section results from compound nucleus formation and only a small fraction comes from the (d,p) reaction followed by fission. This conclusion agrees with that made by SUGIHARA AND COWORKERS[78] in a radiochemical analysis of fission product distributions. It was also found, as is evident from a glance at figure 11.24, that only a fraction of excited nuclei formed by the (d,p) reaction decayed by fission.

11.3.5 Cross-sections for Fission Induced by Neutrons in the Mev Range of Energy. We have seen that neutrons of thermal energy or of energy slightly above thermal in the so-called resonance region can induce fission when the excitation energy of the compound nucleus is above the fission threshold. With higher energy neutrons it is possible to induce fission in any heavy element nucleus. It is of interest to note how the cross section changes as the neutron energy rises through the Mev range of energies. We can roughly classify heavy element nuclides in three classes as shown schematically in figure 11.25.

In Category A we consider nuclides which have a fission threshold above thermal energies and a sharp rise in cross section to a value which is a sizable fraction of the geometrical cross section. The curve then flattens out over a several Mev range until a new rise sets in at about 5 to 7 Mev. This second rise is attributable to the fact that the excitation energy is high enough to permit evaporation of one neutron without reducing the excitation energy of the residual nucleus below the fission threshold; in this case, the system gets a second chance to undergo fission; (n,nf) reaction. An excellent example of this behavior is the U^{238} case shown in figures 11.26 and 11.27.

This type of fission excitation was predicted by BOHR[79] in 1940. Other isotopes for which experimental data are available[80-81] indicating an excitation curve of this general shape are Pa^{231}, U^{234}, U^{236}, Np^{237}, Pu^{240} and Am^{241}.

---

[78] T. T. Sugihara et. al., Phys. Rev. 108, 1264 (1957).

[79] N. Bohr, Phys. Rev. 58, 864 (1940)

[80] R. W. Lamphere, Phys. Rev. 104, 1654 (1956)

[81] R. K. Smith, R. L. Henkel and R. A. Nobles, Bull. Am. Phys. Soc. II, 2 196 (1957) and unpublished results, Los Alamos Scientific Laboratory.

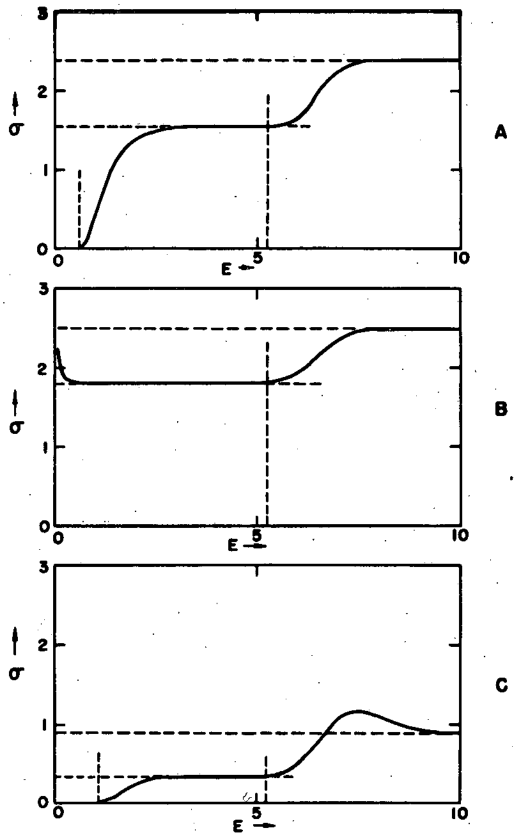

MU-18983

Fig. 11.25. Schematic behavior of neutron-induced fission cross sections. Cross-section in barns as function of neutron energy in Mev. (After J. D. Jackson).

Category A. Targets with finite fission threshold.

Category B. Targets which fission with thermal neutrons. The scale is too compressed to allow proper display of the curve in the thermal and low-energy resonance region.

Category C. Targets with finite fission threshold but with only moderate fissionability.

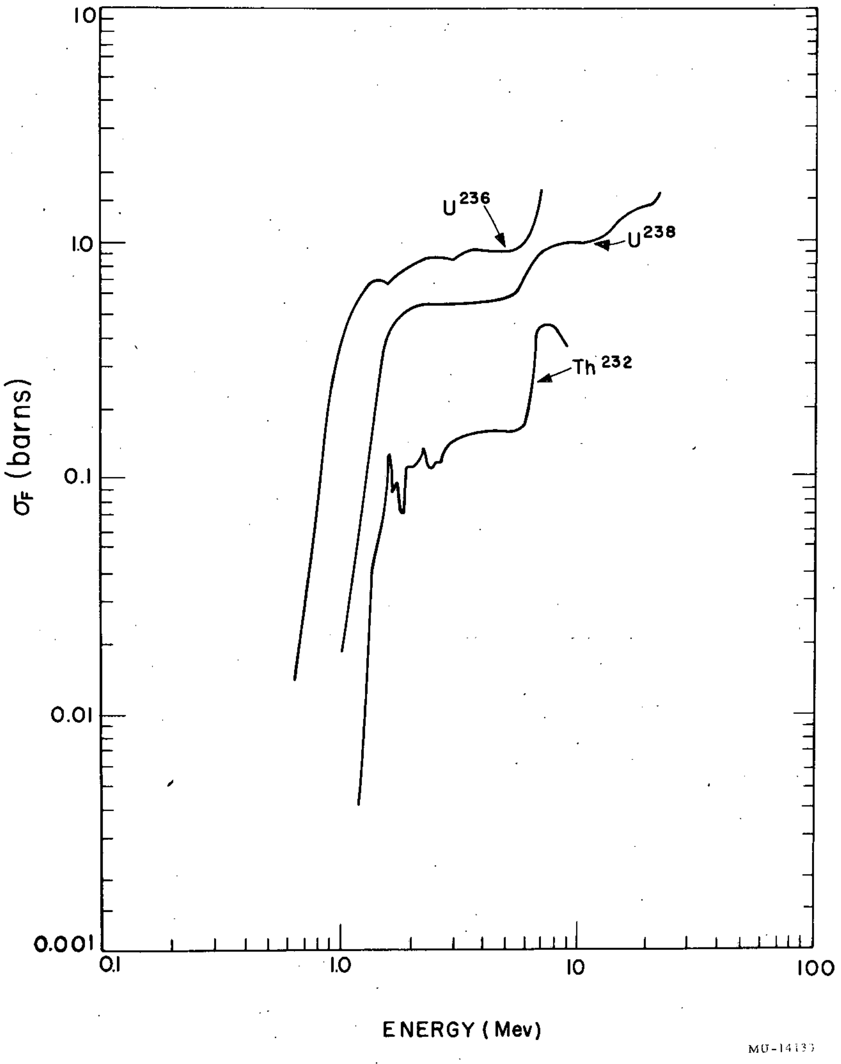

Fig. 11.26. Variation of fission cross section with neutron energy for Th^{232}, U^{236} and U^{238}.

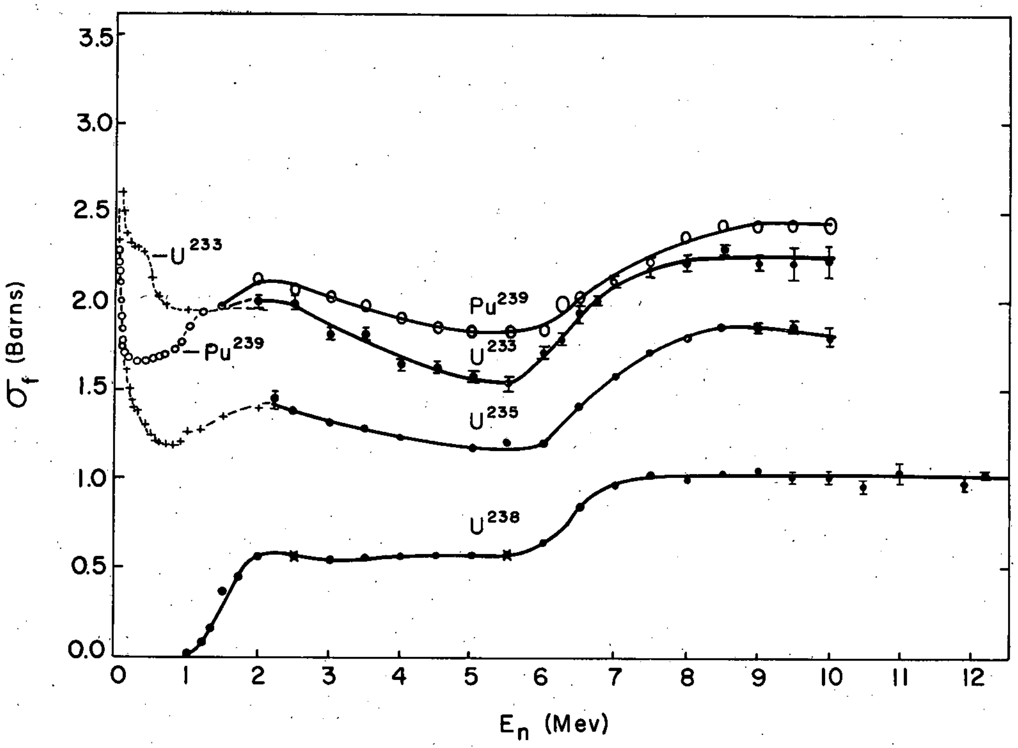

MU-13712

Fig. 11.27. Variation of fission cross section with fast neutron energy for U^{238}, U^{233}, U^{235} and Pu^{239}. Data from Smith, Nobles and Henkel.[81]

Curves are given in reference 61.

The measurements on U^{238} have been extended to neutron energies as high as 22 Mev as shown in figure 11.28, taken from a publication of HEMMENDINGER[82]. This figure is interesting because it shows a threshold for the (n,nf) reaction at 6 Mev, one for the (n,2nf) reaction near 13 Mev and a hint of one for the (n,3nf) process near 19 Mev.

The curve for the Th^{232} has several of the features expected for a nuclide in Category A (threshold value above thermal region, a rise at 6 Mev when "second-chance" fission sets in, etc.) but it also has some very special features. This curve, shown in figure 11.19 has pronounced structure in the 1.5 - 3.0 Mev range. This structure may be associated with the excitation of a few fission channels. This interpretation is in agreement with the violent shifts in the anisotropy of the fission fragments which have been found to occur as the neutron energy is changed across this energy region. See the discussion of section 12.1.6 in the next chapter.

Returning now to figure 11.25, we can discuss Category B which includes nuclides which have high cross sections for fission with thermal neutrons. In the Mev range of energies the fission cross section drops to something of the order of one barn, stays almost constant over a range of several Mev and rises again to a new plateau when the neutron energy is 6-8 Mev. We show the data of SMITH, HENKEL AND NOBLES[26] in figure 11.27 for U^{233}, U^{235} and Pu^{239} which are representative of Category B.

Category C represents nuclides of low fissionability with fission thresholds above the thermal region. We have no good experimental curve to show as an example. The plateau following the initial rise lies at a small fraction of the geometrical cross section. The peak in the region of the second plateau is expected because there should be a range of energies in which neutron emission will leave the intermediate nucleus with sufficient energy to fission, but not enough to emit a second neutron. When somewhat higher energies are reached, the emission of a second neutron becomes possible and since this is a more probable process for this class of nuclides, the observed fission cross-section decreases.

---

82. A. Hemmendinger, Paper P/663 Volume 15, Proceedings of the Second United Nations International Conference on the Peaceful Uses of Atomic Energy, 1958.

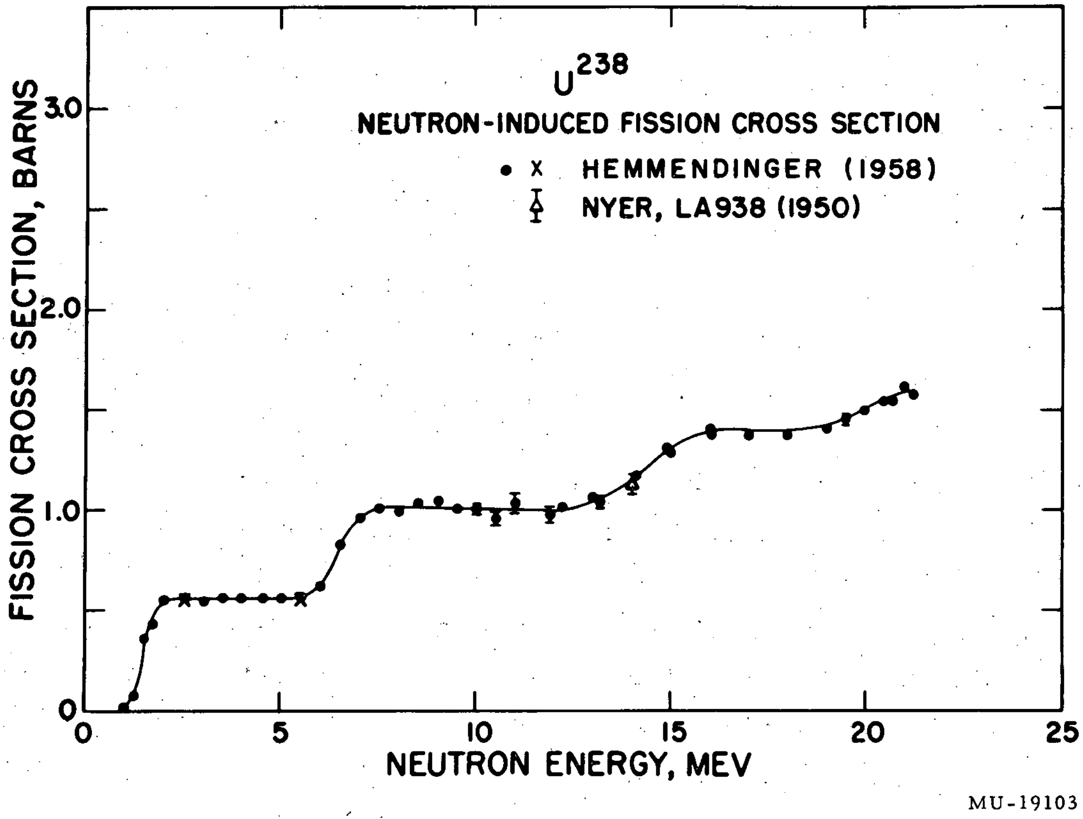

Fig. 11.28. Variation of fission cross section for U^{238} for neutrons ranging in energy from 1 to 22 Mev. From Hemmendinger, reference 82.

An interesting empirical correlation of fission cross sections for neutrons with energy falling about in the middle of the first plateau was proposed by HENKEL AND BARSCHALL[83]. They plotted the fission cross section for fission induced by 3 Mev neutrons against $Z^{4/3}/A$ and found the linear relationship shown in figure 11.29. This correlation is useful for predicting cross sections. There is no presently known theoretical reason for the special significance of the quantity $Z^{4/3}/A$.

11.3.6 Probability of Spontaneous Fission

HALF LIFE MEASUREMENTS

Spontaneous fission is generally observed for the even-even nuclides in the region of thorium and higher elements. Spontaneous fission is very strongly dependent on the atomic number. The rate is vanishingly small in Th^{232} but increases rapidly with increase of atomic number until at element 100 the rate for some isotopes becomes comparable to that for other modes of decay.

LIBBY[84] made the first reported attempt to discover spontaneous fission in uranium but failed to find it because of the low specific activity for the effect. PETRZHAK AND FLEROV[85] made the first positive demonstration of spontaneous fission; they made their discovery with the element uranium. SEGRE[86] described measurements made by himself and his coworkers at Los Alamos during World War II on the following nuclides: Th^{230}, Th^{232}, Pa^{231}, U^{233}, U^{234}, U^{235}, U^{238}, Np^{237}, Pu^{238}, Pu^{239}, and Am^{241}. In principle, the experiments consisted of putting a thin layer of the material to be investigated into an ionization chamber connected to suitable amplifying and recording circuits. These nuclides have such long half-lives for spontaneous fission that close attention must be given to discrimination against pulses from the manyfold more numerous alpha particles, from background effects, and from possible fission induced by stray neutrons.

---

[83] Henkel and Barschall, private communication from R. H. Stokes; See also Allen and Henkel, Progr. Nucl. Energy, [illegible] Series I, Vol II. 38 (1958)

[84] W. F. Libby, Phys. Rev. 55, 1269 (1939)

[85] K. A. Petrzhak and G. N. Flerov, Compt. Rendu. Acad. Sci. USSR 28, 500 (1940), J. Phys. USSR 3, 275 (1940).

[86] E. Segre, Phys. Rev. 86, 21 (1952).

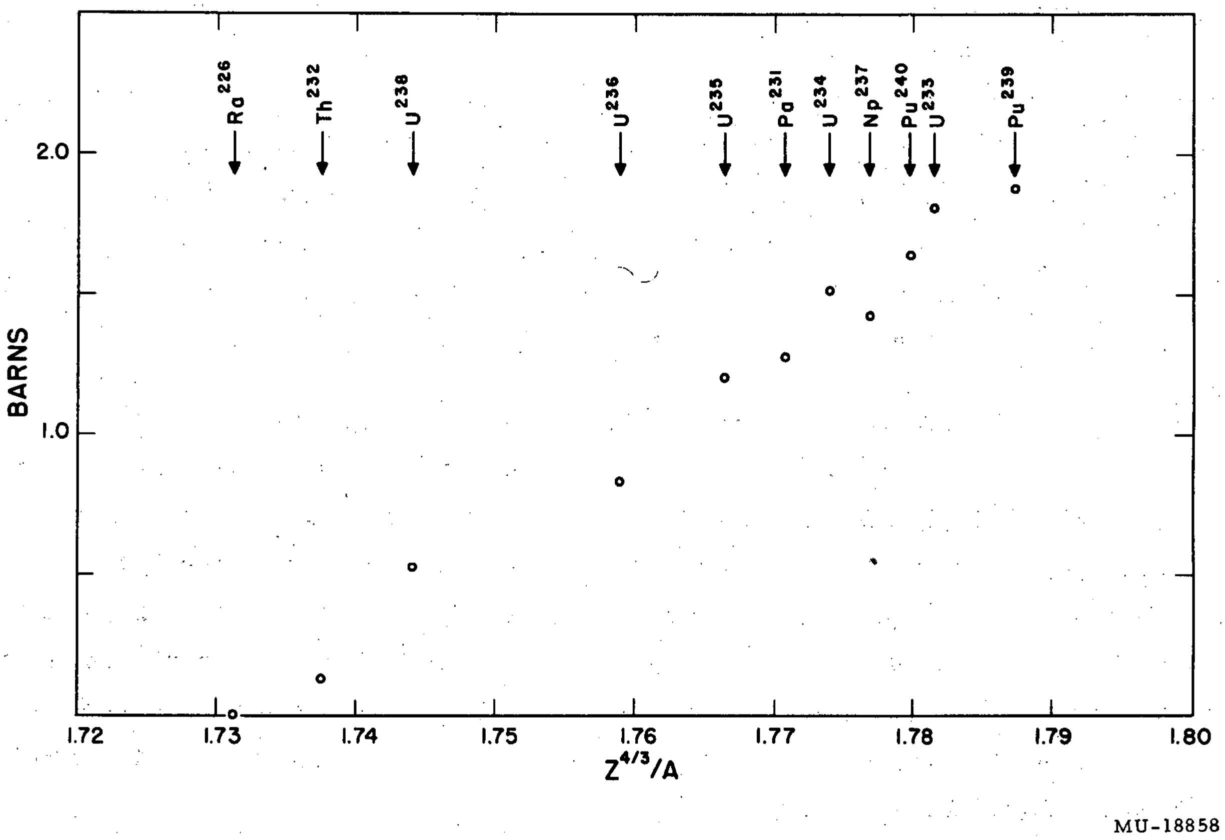

Fig. 11.29. Empirical correlation of fission cross section with $Z^{4/3}/A$ for fission induced with 3 Mev neutrons. Henkel and Barschall.[83]

Self absorption losses can be severe. These difficulties are greatly reduced as higher elements are studied. In particular, the study of spontaneous fission in californium and fermium is comparatively easy. For example, Cf^{252} and Fm^{254} have spontaneous fission decay rates which are a few percent of the alpha decay rate while Fm^{256} and Cf^{254} decay primarily by spontaneous fission. For such nuclides the measurement of spontaneous fission rates is a convenient routine method of detection and measurement. Spontaneous fission can also be detected and subjected to quantitative measurement by radiochemical analysis of fission products, a subject which is reviewed in section 11.4.4 later in this chapter.

Table 11.7 lists the known data on spontaneous fission half-lives together with references to the original data.

CORRELATIONS OF SPONTANEOUS FISSION DECAY RATES

The data on spontaneous fission can be treated graphically in a number of ways. WHITEHOUSE AND GALBRAITH[87] and G. T. SEABORG[88] independently made the interesting observation that in the case of even-even nuclides the half-life for spontaneous fission seems to decrease exponentially with increasing Z^2/A while nuclides with an odd number of nucleons (protons or neutrons or both) decay at a much slower rate. Thus a plot of the logarithm of the partial spontaneous fission half-life, T, against Z^2/A resulted in a fairly good straight line for the limited data available at the time.

$$T = 10^{-21} \times 10^{178 - 3.75\, Z^2/A} \text{ seconds.} \qquad (11.43)$$

When more data were accumulated, it became apparent that although the parameter Z^2/A accounted broadly in this manner for the variation in half-life over a range of Z values, for a given value of Z this parameter did not account for the variation of half life with A. Thus HUIZENGA[89] pointed out that for a given value of Z the half life goes through a maximum as A varies. In addition, there is a dramatic increase in the decay rate for nuclides with more than 152 neutrons as pointed out by GHIORSO[90]. A plot of the logarithm of the half-life versus

---

[87] W. J. Whitehouse and W. Galbraith, Nature, 169, 494 (1952)

[88] G. T. Seaborg, Phys. Rev. 85, 157 (1952)

[89] J. R. Huizenga, Phys. Rev. 94, 158 (1954)

[90] A. Ghiorso, Spontaneous Fission Correlations", Paper P/718, Proceedings of the International Conference on the Peaceful Uses of Atomic Energy, Vol. 7, United Nations, New York, 1956.

Table 11.7 Half Lives for Spontaneous Fission

Isotope	Half Life	Reference
Th^{230}	$\geq 1.5 \times 10^{17}$ y	E. Segre, Phys. Rev. 86,21 (1952)
Th^{232}	$> 10^{20}$ y	A. V. Podgurskaya et al., Zhur. Eksptl. i Teoret. Fiz. 28, 503 (1955)
	$> 10^{21}$ y	G. N. Flerov
U^{232}	$(8 \pm 5.5) \times 10^{13}$ y	A. H. Jaffey and A. Hirsch, unpublished work (1951).
U^{234}	1.6×10^{16} y	A. Ghiorso et al., Phys. Rev. 87, 163 (1952).
U^{235}	1.8×10^{17} y	E. Segre, Phys. Rev. 86, 21 (1952)
U^{236}	2×10^{16} y	A. H. Jaffey and A. Hirsch, unpublished data (1949)
U^{238}	8.04×10^{15} y	E. Segre, Phys. Rev. 86, 21 (1952)
U^{238}	$(5.9 \pm 0.14) \times 10^{15}$ y	P. K. Kuroda and R. R. Edwards, J. Inorg. Nucl. Chem. 3, 345 (1957)
U^{238}	$(1.3 \pm 0.2) \times 10^{16}$ y	N. A. Perfilov, J. Exp. Theor. Phys., USSR 17, 476 (1947)
Pu^{236}	3.5×10^{9} y	A. Ghiorso et al., Phys. Rev. 87, 163 (1952)
Pu^{238}	4.9×10^{10} y	A. H. Jaffey and A. Hirsch, unpublished data (1947)
Pu^{239}	5.5×10^{15} y	E. Segre, Phys. Rev. 86, 21 (1952)
Pu^{240}	1.2×10^{11} y	O. Chamberlain et al., Phys. Rev. 94 156 (1954)
	1.32×10^{11} y	E. M. Kinderman, Atomic Energy Commission Declassified Report HW-27660, April 1953
Pu^{242}	$(7.06 \pm 0.19) \times 10^{10}$ y	J. Mech et al., Phys. Rev. 103, 340 (1956)
	8.5×10^{10} y	Jones et al., Knolls Atomic Power Laboratory Report, KAPL-1378 (1955)
	$(6.64 \pm 0.10) \times 10^{10}$ y	J. P. Butler, Lounsbury and Merritt, Can. J. Phys. 34, 253 (1956)

Table 11.7 (cont'd)

Pu^{244}	$(2.5 \pm 0.8) \times 10^{10}$ y	P.R. Fields et al., Phys. Rev. 100, 172 (1955)
Cm^{240}	1.9×10^{6} y	A. Ghiorso et al., Phys. Rev. 87, 163 (1952)
Cm^{242}	7.2×10^{6} y	A. Ghiorso and H. P. Robinson, unpublished results (1947); G.C. Hanna et al., Phys. Rev. 81, 466, (1951)
Cm^{244}	1.4×10^{7} y	A. Ghiorso et al., Phys. Rev. 87, 163 (1952)
Cm^{246}	$(2 \pm 0.8) \times 10^{7}$ y	S. Fried, J. Inorg. Nuc. Chem. 2, 415 (1956)
Cm^{248}	$(4.6 \pm 0.5) \times 10^{6}$ y	J.P. Butler, T. A. Eastwood, H.G. Jackson and R.P. Schuman, Phys. Rev. 103, 965 (1956)
Cm^{250}	$\sim 2 \times 10^{4}$ y	J. Huizenga and H. Diamond, Phys. Rev. 107, 1087 (1957)
Bk^{249}	6×10^{8} y	A. Ghiorso et al., unpublished results (1955).
	$>2 \times 10^{8}$ y	L.B. Magnusson et al., Phys. Rev. 96, 1576 (1955)
	$> 1.4 \times 10^{9}$ y	T.A. Eastwood et al., Phys. Rev. 107 1635 (1957)
Cf^{246}	$(2.1 \pm 0.3) \times 10^{3}$ y	E. K. Hulet et al., Phys. Rev. 89, 878 (1953)
Cf^{248}	7×10^{3} y	E. K. Hulet, Ph.D. Thesis, University of California Unclassified Report UCRL-2283 (August 1953)
	$>1.5 \times 10^{4}$ y	E.K. Hulet, Unpublished results
Cf^{249}	1.5×10^{9} y	A. Ghiorso et al., Unpublished results (1954)
	$> 4.5 \times 10^{8}$ y	T.A. Eastwood et al., Phys. Rev. 107 1635 (1957)
Cf^{250}	$(1.5 \pm 0.5) \times 10^{4}$ y	A. Ghiorso et al., Phys. Rev. 94, 1081 (1954); P.R. Fields et al., Nature 174 265 (1954); L.B. Magnusson et al., Phys. Rev. 96, 1576 (1954)
Cf^{252}	66 ± 10 y	L.B. Magnusson et al., Phys. Rev. 96, 1576 (1954); A. Ghiorso et al., Phys. Rev. 94, 1081 (1954)

Table 11.7 (cont'd)

	82 ± 6 y	T. A. Eastwood *et al.*, Phys. Rev. **107**, 1635 (1957)
Cf^{254}	56.2 ± 0.7 d	J. R. Huizenga and H. Diamond, Phys. Rev. **107**, 1087 (1957)
	85 ± 15 d	B. G. Harvey *et al.*, Phys. Rev. **99**, 337 (1955)
	55 d	P.R. Fields *et al.*, Phys. Rev. **102**, 180 (1956)
	60 ± 12 d	W.C. Bentley *et al.*, Vol 7, p.261, Proceedings of the International Conference on the Peaceful Uses of Atomic Energy, Geneva 1955, United Nations, New York, 1956
E^{253}	3×10^5 y	P.R. Fields *et al.*, Phys. Rev. **94**, 209 (1954); A. Ghiorso *et al.*, unpublished results (1954)
	$(7 \pm 3) \times 10^5$ y	Jones *et al.*, Phys. Rev. **102**, 203 (1956)
E^{254}	1.5×10^5 y	A. Ghiorso *et al.*, unpublished results (1955)
Fm^{254}	200 d	G. R. Choppin *et al.*, Phys. Rev. **94**, 1080 (1954)
	220 ± 40 d	P.R. Fields *et al.*, Phys. Rev. **94**, 209, (1954)
	246 d	Jones *et al.*, Phys. Rev. 102, 203 (1956)
Fm^{255}	> 60 y	A. Ghiorso *et al.*, unpublished results (1955)
Fm^{256}	3 h	G.R. Choppin *et al.*, Phys. Rev. **98**, 1519 (1955)

y = years; d = days; h = hours.

Z^2/A is shown in figure 11.30. It is interesting to note that if the line is extrapolated to the region of instantaneous rate of spontaneous fission (i.e. half-life of the order of 10^{-20} seconds) the value obtained for Z^2/A is ~47 which corresponds nearly to the predicted $(Z^2/A)_{lim}$ of the Bohr-Wheeler theory.

From the regular spacing of the curves for the even-even isotopes of the heavy elements it is possible to estimate positions for the corresponding curves for higher even elements. It is apparent on the basis of this correlation that the longest lived even mass isotope of element 104 will have a half-life of about 1 second. In the region of element 108 the maximum half-life will be in the range of microseconds.

Another useful correlations of spontaneous-fission half-lives has been provided by STUDIER AND HUIZENGA[91] who revived the KRAMISH[92] correlation of the ratio of half-lives for spontaneous fission and alpha decay versus Z^2/A except that, instead of connecting consecutive alpha decay products, they were able to show a more consistent relationship by correlating nuclides differing by two Z units and six A units. The Studier-Huizenga systematics of spontaneous fission are shown in figure 11.31.

GHIORSO[90] pointed out that the measured spontaneous fission half-lives of Cf^{252}, Cf^{254}, Fm^{254} and Fm^{256} are substantially shorter than had been predicted by the systematics of the above mentioned types. GHIORSO interpreted this as additional evidence that a neutron subshell is closed at 152 neutrons and that the nuclear constitution for isotopes with more than 152 neutrons is somewhat different, leading to a much sharper drop in spontaneous fission half lives with increasing A. In this connection, it will be recalled that a discontinuity in alpha particle energies for the even-even isotopes of californium, einsteinium and fermium is observed indicating subshell closure at 152 neutrons. (See for example, figure 8.6 in Chapter 8).

If this 152 neutron effect is real the predictions of spontaneous-fission half lives for isotopes of elements 100 and above are markedly influenced. In figure 11.32 we show Ghiorso's modified plot of the spontaneous-fission systematics. The half-lives are plotted against neutron number. The vertical

---

[91] M. H. Studier and J. R. Huizenga, Phys. Rev. 96, 545 (1954)

[92] A. Kramish, Phys. Rev. 88, 1201,(1952)

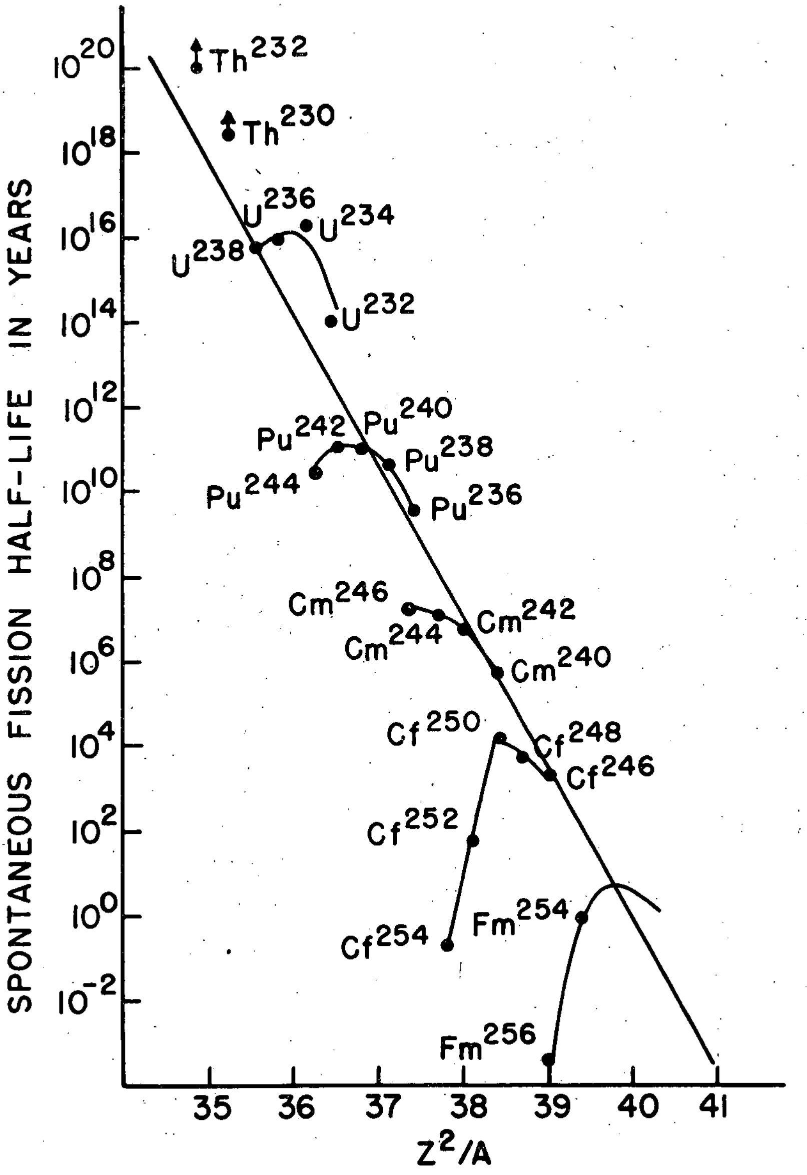

Fig. 11.30. Spontaneous fission half life of even-even nuclides versus Z^2/A.

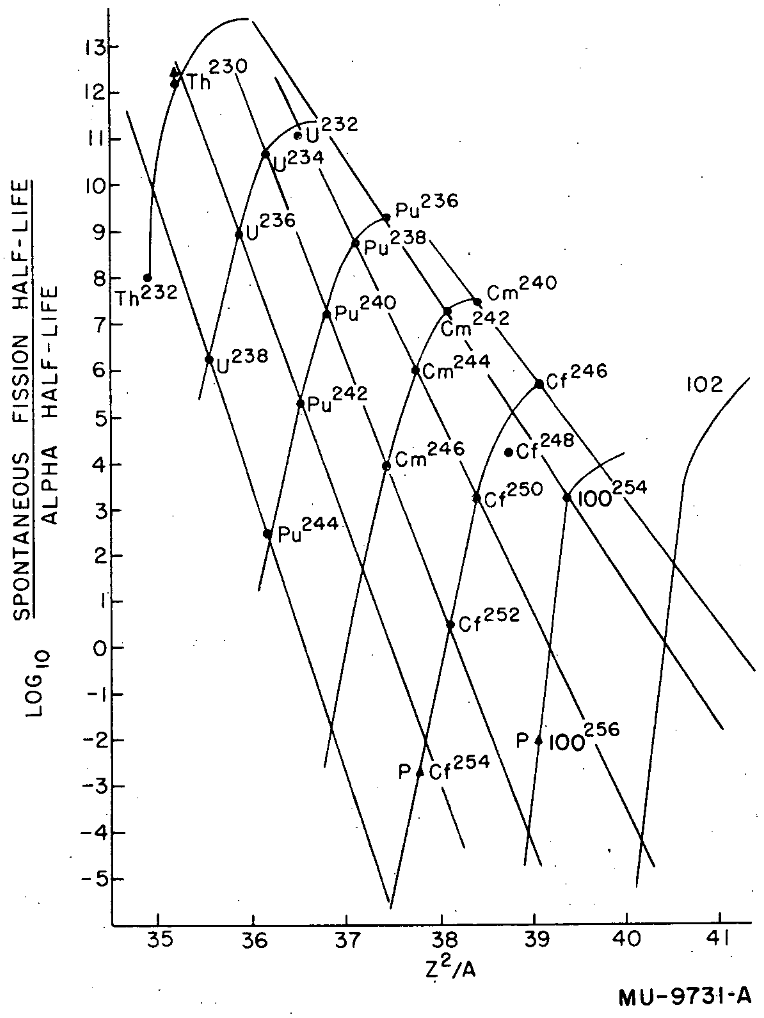

Fig. 11.31. The ratio of spontaneous fission half life and alpha half life versus Z^2/A. (Studier-Huizenga correlation).

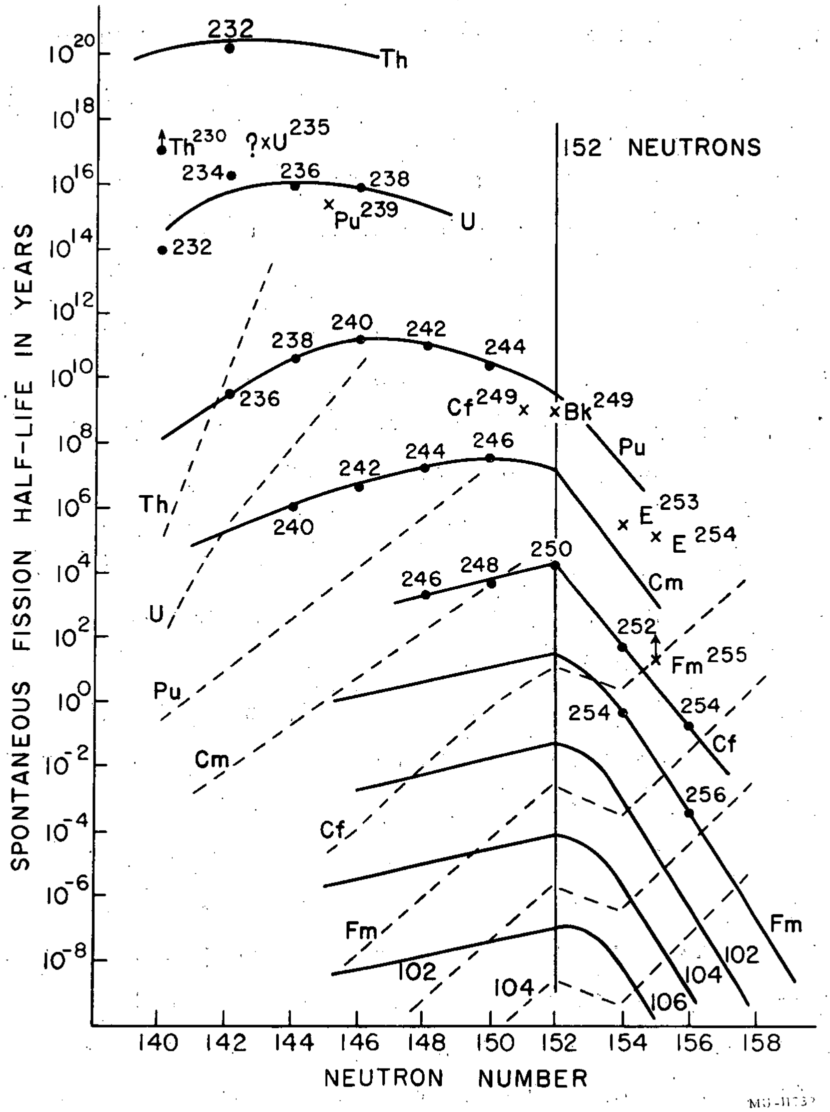

Fig. 11.32. Spontaneous fission half life versus neutron number. Dotted lines indicate the experimentally observed alpha half life variation except in the cases for elements 102 and 104 where the curves are estimates.

line shows the 152-neutron shell and the predicted lines for elements 100, 102, 104 and 106 show a strong prejudice for the hypothesized 152-neutron shell effect. This correlation is not completely established.

FOREMAN AND SEABORG[93] have replotted spontaneous fission half lives against mass number as shown in figure 11.33. This plot indicates that all even-even isotopes with neutron number equal to or greater than 152 lie on the same straight line so that the spontaneous fission half lives for these isotopes appears to depend only on the mass number. Some predictions of spontaneous fission half lives of unmeasured isotopes with atomic number 100 or greater are given in Table 11.8.

SWIATECKI[94] has made an important contribution to an understanding of the rate of spontaneous fission by pointing out the great sensitivity of the decay rate to the finer details of the ground state masses of nuclei. Swiatecki showed that any nucleus which had a special stability in the ground state as measured against some smooth reference is invariably associated with a longer lifetime than that given by a straight line Z^2/A relationship such as given in figure 11.30. Each millimass unit of extra ground state stability corresponds to about 10^5 times longer lifetime. Swiatecki corrected each experimental half life, t_{exp}, by adding a factor $k\delta M$ where k is an empirical factor and δM is the deviation of the ground state mass from the smooth reference mass surface given by GREEN[95]. Thus, in effect, Swiatecki has an explanation for the variation of the spontaneous fission half life with A for a given Z and for the dramatic effect which occurs at 152 neutrons. Figure 11.34 shows the remarkable smoothing of the data which occurs when this correction is applied.

The success of this correlation leads to the conclusion that the saddle-point energy surface is much smoother and freer of shell-effects than is the ground state surface. As the distance between the two surfaces decreases with increasing Z it might be expected that shell effects in the saddle-point surface might become important.

---

93. B. Foreman and G. T. Seaborg, J. Inorg. Nucl. Chem. 7, 305 (1958).
94. W. J. Swiatecki, Phys. Rev. 100, 937, (1955)
95. A. E. S. Green, Phys. Rev. 95, 1006 (1954)

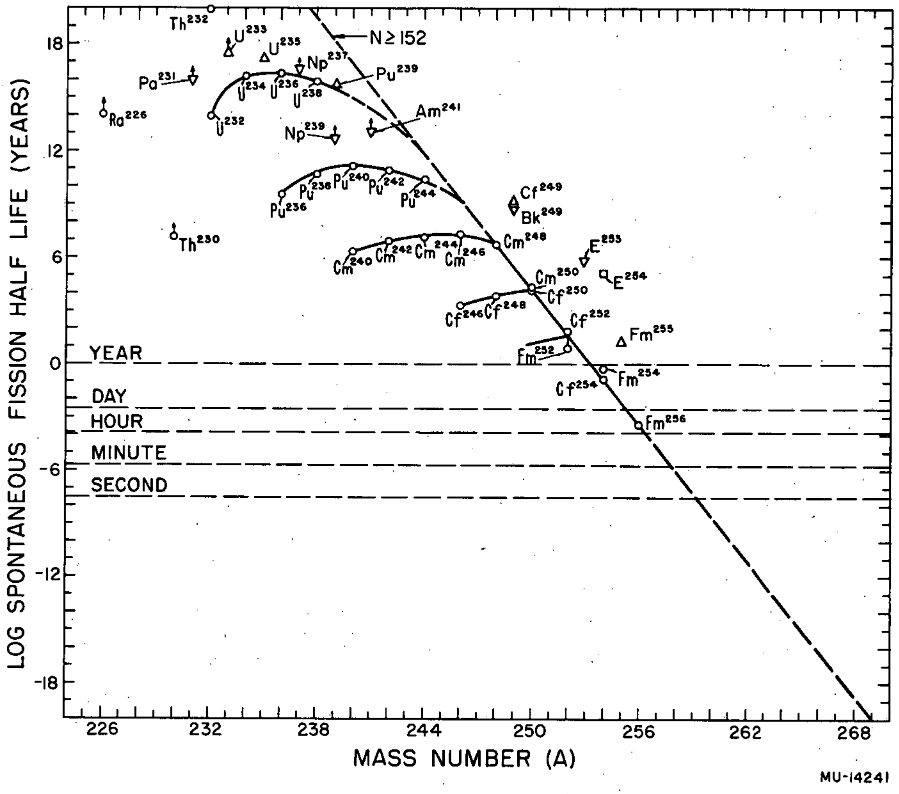

Fig. 11.33. Partial spontaneous fission half lives as a function of mass number o, even-even nuclide; △, even-odd nuclide; ▽, odd-even nuclide; ▢, odd-odd nuclide. From Foreman and Seaborg.93

Table 11.8 Some Prediction Half lives for Spontaneous Fission of Isotopes of Elements 100 through 104*

Nuclide	$T_{1/2}$ SF
Fm^{257}	1 min
Fm^{258}	30 sec
Mv^{252}	1 yr
Mv^{253}	2 yr
Mv^{254}	50 day
Mv^{255}	2 day
Mv^{257}	1 min
Mv^{258}	20 sec
102^{252}	10 day
102^{253}	20 day
102^{254}	50 day
102^{255}	2 day
102^{256}	5 hr
102^{257}	1 min
102^{258}	20 sec
103^{255}	2 day
103^{256}	5 hr
103^{257}	1 min
103^{258}	20 sec
103^{259}	2 sec
103^{260}	0.1 sec
104^{256}	5 hr
104^{257}	1 min
104^{258}	20 sec
104^{259}	2 sec
104^{260}	0.1 sec
104^{261}	5×10^{-3} sec

---

* As given by Foreman and Seaborg, J. Inorg. Nucl. Chem. 7, 305 (1958)

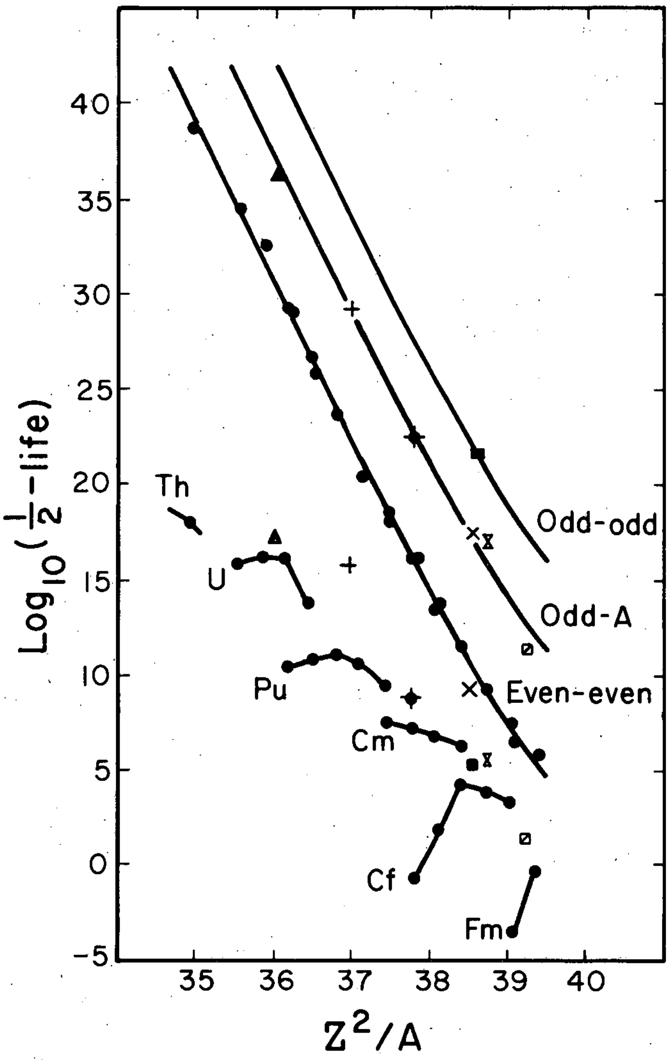

MU-19017

Fig. 11.34. Plot of spontaneous fission half-lives against Z^2/A. The observed lifetimes τ_{exp} occupy the bottom left-hand part of the figure; the "corrected" values $\tau_{exp} + k\delta M$ group themselves around the three curves. Experimental points for even-even nuclei are joined by straight lines. Odd-A nuclei are designated by special symbols which, reading from left to right along the odd-A curve, refer to U^{235}, Pu^{239}, Bk^{249}, Cf^{249}, E^{253} (einsteinium, Z = 99), and Fm^{255} (fermium, Z = 100). The odd-odd nucleus E^{254} is marked by a square. From Swiatecki, Phys. Rev. 100, 937 (1955).

J. O. NEWTON[96] and, later, WHEELER[97] have offered an attractive explanation for the reduced rates of spontaneous fission of odd-nucleon nuclides using the strong coupling approximation of the unified model of Bohr and Mottelson. This explanation follows from the quantization of the intrinsic angular momentum, $\Omega \hbar$, of the nucleonic system about the symmetry axis, and the fact that this intrinsic angular momentum for the state of lowest energy changes with increasing spheroidal deformation, δ, in the case of odd nuclei, whereas for even-even nuclei the nucleonic state $\Omega = 0$ lies lowest at all deformations. Thus in the case of even-even nuclei the top pair of protons or neutrons can readjust their orbits while conserving angular momentum as the energies associated with the orbital change with increasing deformation. In the case of odd nuclei a given nucleonic component of angular momentum Ω can only be maintained during the change of orbital position with increasing deformation by introducing nucleonic excitation energy into the system at the expense of kinetic energy in the fission mode. Wheeler makes a rough estimate of this excitation (which he terms specialization energy) using Nilsson's curves for the dependence of individual nucleon energy upon deformation. In this manner, Wheeler estimates sufficient additional activation energy for fission of odd nuclei to account on the average for the outstandingly slower spontaneous fission rates for odd nuclei.

Spontaneous fission half lives are competitive with alpha decay half lives for the higher mass, even-even isotopes of californium and fermium and presumably even more competitive for higher elements. Cf^{254} decays chiefly by spontaneous fission with a half life of 56 days; the alpha half life is estimated to be about 100 years. In Fm^{256} the observed mode of decay is spontaneous fission; the observed half life of 3.5 hours is much shorter than the predicted alpha half life of about 10 days.

The rapid shortening of spontaneous fission lifetimes makes it unlikely that elements beyond fermium can be made in measurable quantities by neutron irradiation techniques, at least not until much higher neutron fluxes are available. According to figure 2.5 in chapter 2, it is necessary to reach a mass number of 259 before a beta-emitting fermium isotope is reached. The estimated

---

96. J. O. Newton, Progr. Nuclear Physics, 4, 234-286 (1955)
97. J. A. Wheeler, "Nuclear Fission and Nuclear Stability", a contribution to Bohr 70th Anniversary Volume, Pergamon Press, London.

spontaneous fission rates of Fm^{258} and Fm^{260} are so large that most of the atoms of these isotopes will be destroyed by this process before they are converted to heavier isotopes by neutron capture. Hence very little buildup of element 101 and higher elements can be expected in heavy element samples irradiated in high flux reactors.

FIELDS et al.[98] and BENTLEY et al.[99] have discussed the possible usefulness of some of the short-lived, spontaneously-fissioning isotopes as sources of neutrons. Cf^{252} is attractive for this purpose because it can be made in appreciable yield by long time neutron irradiation of plutonium. (This isotope has a neutron emission rate of 3×10^{12} neutrons per second per gram.)

11.3.7 Probability of Photofission and of Fission Induced by Charged Particles. The discussion of photofission thresholds, fission excitation functions in photofission and in charged particle induced fission and in other characteristics of fission induced in these ways is reserved for Chapter 12.

---

[98] P. R. Fields, M. H. Studier, L. B. Magnusson and J. R. Huizenga, Nature, 174, 265 (1954)

[99] W. C. Bentley et al., paper P/809 "Proceedings of the Geneva Conference, Peaceful Uses of Atomic Energy," August 1955, United Nations.

11.4 DISTRIBUTION OF MASS IN FISSION

11.4.1 Introduction. The techniques of radiochemistry led to the discovery of nuclear fission and have contributed greatly to an elucidation of the main features of the fission reaction. One of the most characteristic features of fission is the asymmetric division of the fissioning nucleus and our most complete knowledge of the mass division has come from radiochemical research. HAHN and his co-workers working in Germany during World War II continued the initial studies of HAHN and STRASSMANN[100,101] on the fission product elements. At the same time radiochemists working in the United States and Canada were making an exhaustive study of these same products. The first goal of this work was to identify the atomic number, mass number, the half life, and the main features of the radioactive decay schemes of the individual fission products. A second goal was to measure quantitatively the yields of the individual fission product chains and, where possible, the independent yield of the individual fission product isotopes.

The first work on fission yield and the introduction of the concept of fission yield was due to FERMI[102] and his co-workers at Columbia.

The determination of the fission yield of a specific species consists of a number of steps.

(1) A measured amount of non-radioactive carrier material of a given fission product element is added to a solution of uranium in which a known number of fission events has occurred.

(2) If it is necessary, chemical treatment is given this solution to insure complete isotopic exchange of the stable and radioactive isotopes of the element. For most elements this consists merely of stirring the solution. For some elements the exchange is incomplete and experimental conditions have been investigate to determine the conditions under which isotopic exchange is complete. Iodine, for example, is a fission product element which does not show complete exchange with added iodine carrier unless a certain sequence of oxidation and reduction steps is carried through.

---

100. Hahn and Strassmann, Naturwissen. 27, 11 (1939).
101. Hahn and Strassmann, Naturwissen. 27, 529 (1939).
102. Anderson, Fermi, and Grosse, Phys. Rev. 59, 52 (1941).

(3) The solution is subjected to an analytical procedure to separate the element from the solution in a state of chemical and radiochemical purity.

(4) The fractional recovery of the inert carrier is determined by some quantitative analytical method. The chemical recovery of the tracer element is assumed equal to that for the inert carrier material.

(5) The radiations of the purified radioelements are measured to identify the isotopes and to determine the absolute amounts of each species. Corrections are made as required for back-scattering, absorption effects, branching decay etc. Correction is made for radioactive decay from the time of fission to the time of counting.

(6) From the counting data, the chemical yield data and the known number of fission events the fission yield is calculated. The fission yield is defined as the percentage of fissions leading to the formation of a measured product.

It is to be noted that the radiochemical results do not in general give the independent yield of the specific isotope measured. Usually the experimentally determined yield is the cumulative yield of the specific isotope including any precursers which have undergone decay to the specific isotope before the chemical isolation occurred.

The extensive American war-time studies by the workers in the Plutonium Project are recorded in Volume 9 of the Plutonium Project Record.[103] In this three-book set of research papers the chemical methods, decay scheme studies, counting techniques, and fission yields are summarized. The fission of U^{235}, U^{233}, Pu^{239}, and U^{238} are treated. Similar studies were reported by Grummitt and Wilkinson[104] from the Canadian project.

Since 1946 the war-time data have been substantially improved. With the great advances in radiation detection instruments and with more time for careful study it has been possible to establish more detailed decay schemes for the fission product nuclides. Chemical purification techniques and absolute counting also have greatly improved. Furthermore for certain elements the application of mass spectrographic techniques have made it possible to measure the yield of stable and long-lived isotopes with increased accuracy.

---

[103] Radiochemical Studies: The Fission Products, edited by C. D. Coryell and N. Sugarman, National Nuclear Energy Series, Division IV Plutonium Project Record, Volume 9, McGraw-Hill Book Company, New York, 1951.

[104] W. E. Grummitt and G. Wilkinson, Nature 161, 520 (1948).

11.4.2 Summary of Fission Yields in Slow Neutron Fission. Several critical summaries of fission yield studies have been prepared.[105-108] We reproduce here some tables and curves which summarize the data.

Table 11.9 is a summary of fission yields and fission chains for slow neutron fission of U^{235} as determined by radiometric and mass spectrometric methods. This table was compiled by Dr. Seymour Katcoff[107] and represents a comprehensive review of all data published by 1958. These same chains appear in the fission of other nuclei but with different yields than those given for U^{235}.

In the beginning, most data were accumulated by the radiochemical method but later the mass spectrometric method was used for most of the main products. Some of the mass-spectrometric measurements of the fission-produced isotopes of strontium, zirconium, molybdenum, cerium, barium, cesium, and neodymium were made on an absolute basis by the isotope dilution technique.[109] For ruthenium the number of atoms of 1 year Ru^{106} was determined by absolute beta counting since a suitable isotopic tracer was not available for isotopic dilution. The isotopic abundances of Ru^{101}, Ru^{102}, and Ru^{104} were determined relative to Ru^{106} by mass spectrometry. Relative isotopic abundances of fission

---

[105] J. O. Blomeke, Nuclear Properties of U^{235} Fission Products, Oak Ridge National Laboratory Report ORNL-1783, Nov. 1955; see also J. O. Blomeke and M. F. Todd, ORNL-2127, Aug. 1957.

[106] E. P. Steinberg and L. E. Glendenin, Survey of Radiochemical Studies of the Fission Process, Paper No. P/614, "Proceedings of the International Conference on the Peaceful Uses of Atomic Energy," Volume 7, United Nations, New York, 1956.

[107] S. Katcoff, Handbook of Nuclear Engineering, Addison-Wesley (1957); see also Nucleonics 4, 78 (1958).

[108] H. R. Fickel and R. H. Tomlinson, Can. J. Phys. 37, 916-936 (1959).

[109] Glendenin, Steinberg, Flynn, Hayden, and Inghram, unpublished work quoted by Glendenin and Steinberg in reference 106.

Table 11.9

Decay chains and yields from thermal-neutron fission of U^{235}.

Prepared by Dr. S. Katcoff from data available to 1958.

Underlined numbers give experimental fission yields. Last fission yield along any chain usually represents total chain yield. Lower values for yields of earlier chain members may be caused by (1) direct formation in fission of later chain members, (2) chain branching, (3) experimental uncertainty. Latter accounts for cases where early chain member has higher yield than later one. Where branching occurs, arrows are shown only for decay modes observed experimentally; fraction in each branch is given where known. Parentheses indicate nuclide probably occurs but has not been observed. References for fission yields are cited following chains.

References

1. C. D. Coryell, N. Sugarman, editors, "Radiochemical Studies: The Fission Products," National Nuclear Energy Series IV-9 (McGraw-Hill Book Co., New York, 1951)
2. J. M. Siegal, L. E. Glendenin, ref. 1, p. 549
3. E. P. Steinberg, Engelkemeir, ref. 1, p. 566
4. N. Sugarman, Phys. Rev. 89, 570 (1953)
5. J. G. Cuninghame, Phil. Mag. 44, 900 (1953)
6. L. E. Glendenin, ref. 1, p. 596
7. L. E. Glendenin, ref. 1, editors' note, p. 591
8. J. R. Arnold, N. Sugarman, J. Chem. Phys. 15, 703 (1947)
9. J. A. Petruska, H. G. Thode, R. H. Tomlinson, Can. J. Phys. 33, 696 (1955)
10. A. T. Blades, H. G. Thode, Z. Naturforschg. 10a, 838 (1955)
11. A. T. Blades, W. H. Fleming, H. G. Thode, Can. J. Chem. 34, 233 (1956)
12. J. E. Sattizahn, M. Kahn, J. D. Knight, Bull. Am. Phys. Soc., Ser. II, 2, 197 (1957)
13. L. E. Glendenin et al., quoted by E. Steinberg and L. E. Glendenin et al. in "Proceedings of the International Conference on the Peaceful Uses of Atomic Energy," Geneva, Vol. 7, p. 3 (United Nations, New York, 1956)

14. A. C. Wahl, private communication (October, 1956). Measured fractional cumulative yields of short-lived rare gases. These values were multiplied by the relevant total chain yields to obtain the respective rare gas fission yields.

15. A. F. Stehney, N. Sugarman, Phys. Rev. 89, 194 (1953)

16. G. W. Reed, A. Turkevich, Phys. Rev. 92, 1473 (1953)

17. A. P. Baerg, R. M. Bartholomew, Can. J. Chem. 35, 980 (1957)

18. G. W. Reed, Phys. Rev. 98, 1327 (1955)

19. W. E. Grummitt, G. M. Milton, J. Inorg. and Nucl. Chem. 5, 93 (1957)

20. E. J. Hoagland, S. Katcoff, ref. 1, p. 660

21. C. R. Dillard et al., ref. 1, p. 692

22. C. D. Coryell et al., Phys. Rev. 77, 755 (1950)

23. J. Terrell et al., Phys. Rev. 92, 1091 (1953)

24. D. Wiles, C. Coryell, Phys. Rev. 96, 696 (1954)

25. W. H. Hardwick, Phys. Rev. 92, 1072 (1953)

26. W. H Sullivan et al., ref. 1, p. 808

27. C. D. Coryell, J. W. Winchester, Progress Report, Laboratory for Nuclear Science, MIT (August 31, 1955)

28. D. W. Engelkemeir et al., ref. 1, p. 1372

29. J. A. Seiler, ref. 1, p. 860

30. A. Wahl, N. Bonner, Phys. Rev. 85, 570 (1952)

31. R. P. Metcalf, ref. 1, p. 905

32. E. P. Steinberg, ref 1, editors' note, p. 913

33. G. R. Leader, ref. 1, p. 919

34. J. A. Seiler, ref. 1, p. 910

35. C. W. Stanley, L. E. Glendenin, ref. 1, p. 947

36. G. R. Leader, W. H Sullivan, ref. 1, p. 934

37. A. C. Pappas, Technical Report No. 63, Lab. for Nuclear Science, Massachusetts Institute of Technology (Sept., 1953)

38. L. E. Glendenin, ref. 1, editors' note, p. 979

39. B. C. Purkayastha, G. R. Martin, Can. J. Chem. 34, 293 (1956)

40. A. C. Pappas, D. R. Wiles, J. Inorg. and Nucl. Chem. 2, 69 (1956)

41. R. M. Bartholomew et al., Can. J. Chem. 31, 120 (1953)

42. S. Katcoff, W. Rubinson, Phys. Rev. 91, 1458 (1953)

43. L. Yaffe et al., Can. J. Chem. 31, 48 (1953)

44. A. C. Wahl, Phys. Rev. 99, 730 (1955)

45. L. E. Glendenin, R. P. Metcalf, ref. 1, p. 992

46. S. Katcoff et al., ref 1, p. 1005

47. F. Brown, L. Yaffe, Can. J. Chem. 31, 242 (1953)

48. C. W. Stanley, S. Katcoff, J. Chem. Phys. 17, 653 (1949)

49. F. Brown, J. Inorg. and Nucl. Chem. 1, 248 (1955)

50. R. M. Bartholomew, A. P. Baerg, Can. J. Chem 34, 201 (1956)

51. Value 6.44 is average of 6.33 and 6.56 from refs. 9 and 13, respectively. It is assumed that these mass-spectrometric measurements on Ce^{140} are also accurate measure of Ba^{140} yield since independent yields of La^{140} and Ce^{140} are very small (ref. 19). Many fission yields have been determined relative to Ba^{140}; these are now normalized to yield of 6.44 for latter. Absolute radiochemical measurements of Ba^{140}, ref. 16 and 52, give 6.32.

52. L. Yaffe et al., Can. J. Chem. 32, 1017 (1954)

53. W. H. Burgus, N. E. Ballou, ref. 1, p. 1184

54. G. P. Ford, C. W. Stanley, AECD-3551 (1953)

55. S. Katcoff, B. Finkle, N. Sugarman, ref. 1, p. 1167

56. J. A. Marinsky, L. E. Glendinin, ref. 1, p. 1229 and p. 1254

57. H. G. Petrow, G. Rocco, Phys. Rev. 96, 1614 (1954)

58. L. Winsberg, ref. 1, p. 1284

59. L. Winsberg, ref. 1, p. 1302 and p. 1311
60. L. Winsberg, ref. 1, p. 1292
61. E. C. Freiling *et al.*, Phys. Rev. 96, 102 (1954)
62. Y. Y. Chu, UCRL-8926 (1959) unpublished.

72.

$$\begin{tikzcd} \begin{array}{c}\text{49-h Zn}^{72}\\ \underline{1.6 \times 10^{-5}}\end{array} \arrow[r] & \text{14.1-h Ga}^{72} \arrow[r] & \text{stable Ge}^{72} \end{tikzcd}$$

(1, 2)

73.

$$\begin{tikzcd} (\text{<2-m Zn}^{73}) \arrow[r] & \begin{array}{c}\text{5.0-h Ga}^{73}\\ \underline{1.1 \times 10^{-4}}\end{array} \arrow[r] & \text{stable Ge}^{73} \end{tikzcd}$$

(2)

77.

$$\begin{tikzcd} \text{54-s Ge}^{77m} \arrow[d, "0.22"] \arrow[dr, "0.78"] & & \\ \begin{array}{c}\text{12-h Ge}^{77}\\ \underline{0.0031}\end{array} \arrow[r] & \begin{array}{c}\text{38.7-h As}^{77}\\ \underline{0.0083}\end{array} \arrow[r] & \text{stable Se}^{77} \end{tikzcd}$$

(3, 4)

78.

$$\begin{tikzcd} \begin{array}{c}\text{86-m Ge}^{78}\\ \underline{0.019}\end{array} \arrow[r] & \begin{array}{c}\text{91-m As}^{78}\\ \underline{0.021}\end{array} \arrow[r] & \text{stable Se}^{78} \end{tikzcd}$$

(3, 4)

79.

$$\begin{tikzcd} & \text{3.89-m Se}^{79m} \arrow[d] & \\ \begin{array}{c}\text{9.0-m As}^{79}\\ \underline{0.056}\end{array} \arrow[ur] & \sim 6 \times 10^{4}\text{-y Se}^{79} \arrow[r] & \text{stable Br}^{79} \end{tikzcd}$$

(5)

81.

$$\begin{tikzcd} \begin{array}{c}\text{56.6-m Se}^{81m}\\ \underline{0.0084}\end{array} \arrow[d] & \text{stable Br}^{81} \\ \begin{array}{c}\text{17.6-m Se}^{81}\\ \underline{0.14}\end{array} \arrow[ur] & \end{tikzcd}$$

(6)

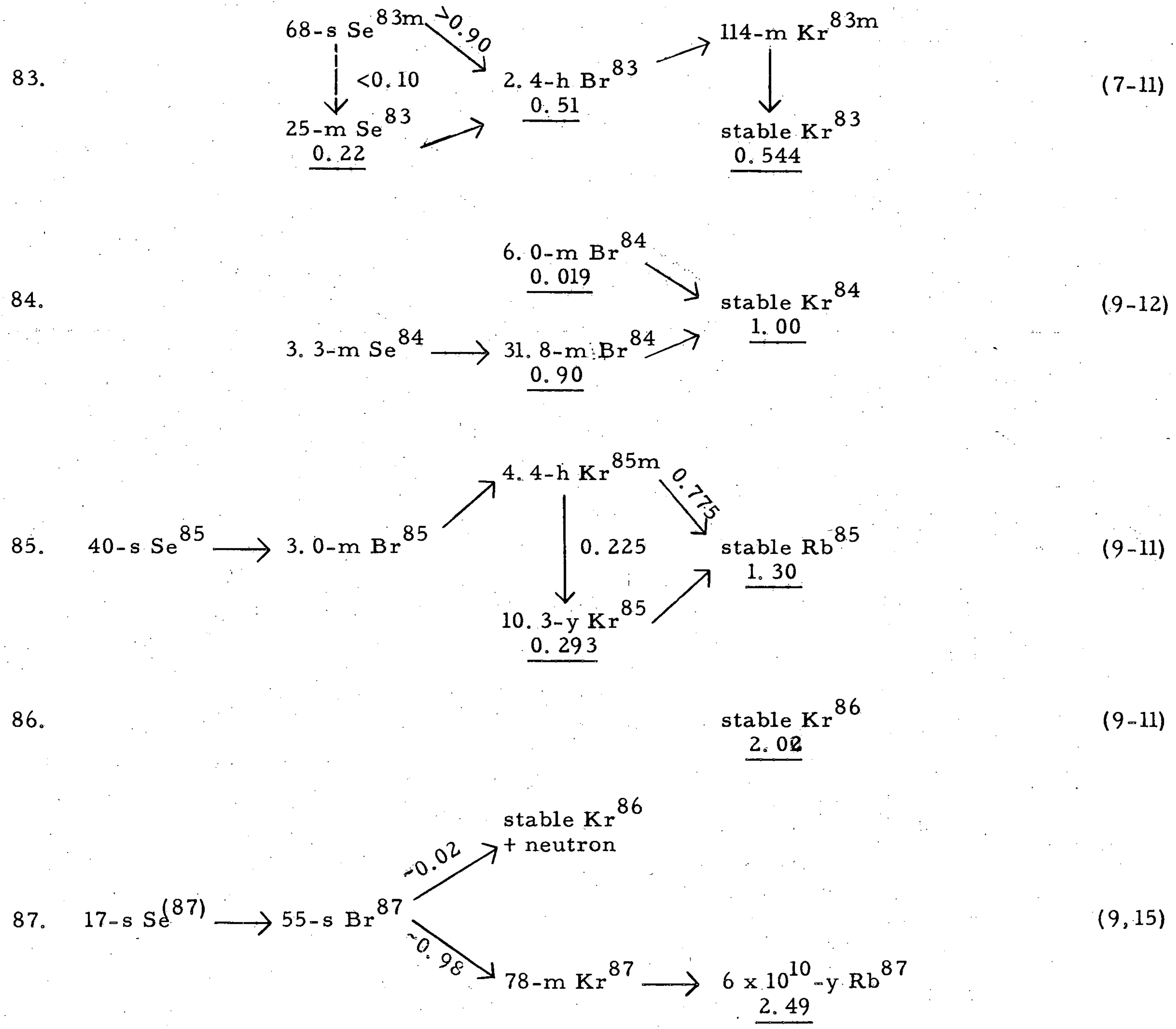
83.
68-s Se^{83m}
~0.90
<0.10
25-m Se^{83}
0.22
2.4-h Br^{83}
0.51
114-m Kr^{83m}
stable Kr^{83}
0.544
(7-11)
84.
6.0-m Br^{84}
0.019
3.3-m Se^{84}
31.8-m Br^{84}
0.90
stable Kr^{84}
1.00
(9-12)
85.
40-s Se^{85}
3.0-m Br^{85}
4.4-h Kr^{85m}
0.775
0.225
10.3-y Kr^{85}
0.293
stable Rb^{85}
1.30
(9-11)
86.
stable Kr^{86}
2.02
(9-11)
87.
17-s Se$^{(87)}$
55-s Br^{87}
~0.02
stable Kr^{86} + neutron
~0.98
78-m Kr^{87}
6 x 10^{10}-y Rb^{87}
2.49
(9,15)

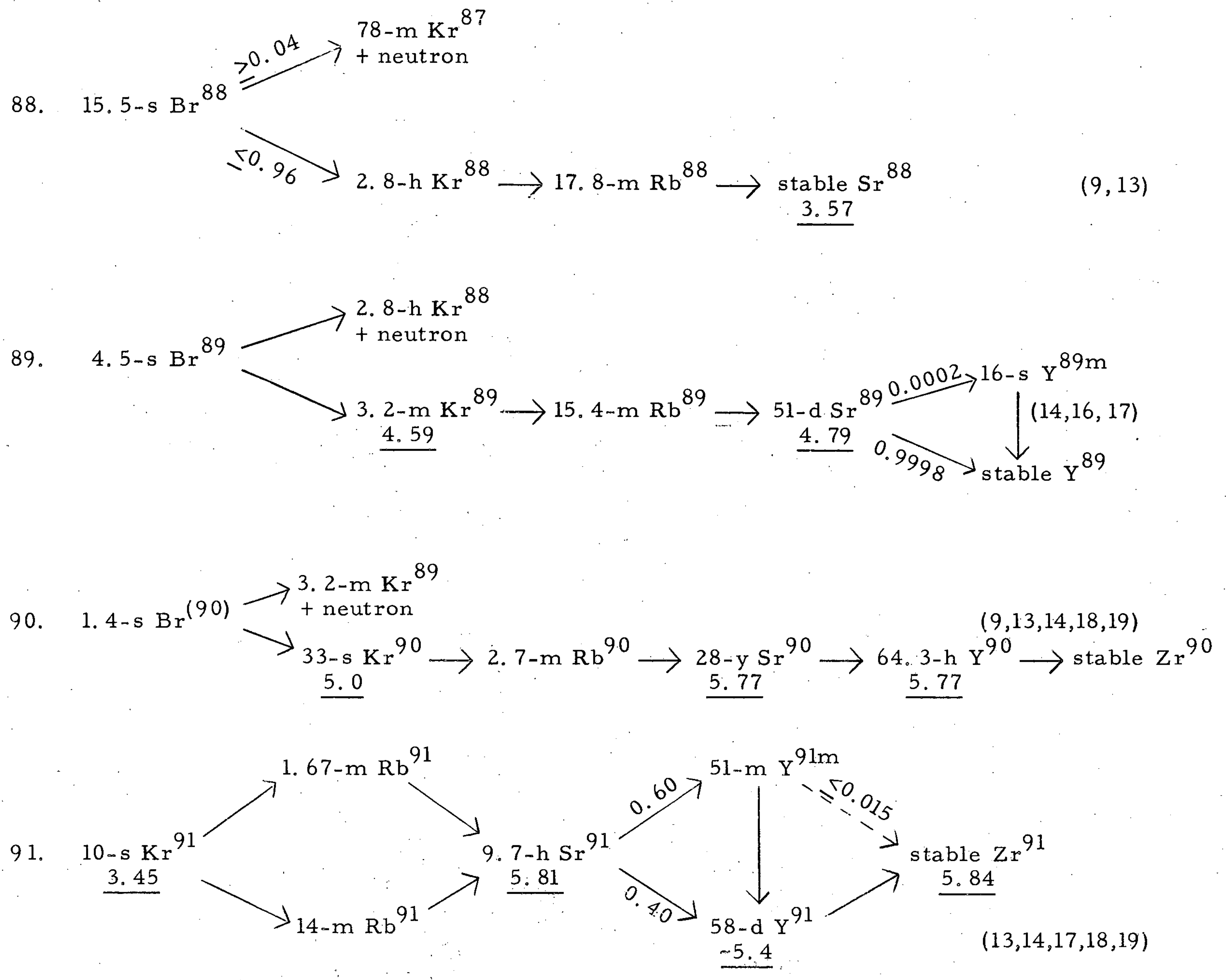
88.
15.5-s Br88
≥0.04
78-m Kr87 + neutron
≤0.96
2.8-h Kr88
17.8-m Rb88
stable Sr88
3.57
(9,13)
89.
4.5-s Br89
2.8-h Kr88 + neutron
3.2-m Kr89
4.59
15.4-m Rb89
51-d Sr89
4.79
0.0002
16-s Y89m
0.9998
stable Y89
(14,16,17)
90.
1.4-s Br(90)
3.2-m Kr89 + neutron
33-s Kr90
5.0
2.7-m Rb90
28-y Sr90
5.77
64.3-h Y90
5.77
stable Zr90
(9,13,14,18,19)
91.
10-s Kr91
3.45
1.67-m Rb91
14-m Rb91
9.7-h Sr91
5.81
0.60
51-m Y91m
0.40
58-d Y91
~5.4
≤0.015
stable Zr91
5.84
(13,14,17,18,19)

92.
$$\begin{tikzcd}\underset{\underline{1.87}}{\text{3.0-s Kr}^{92}} \arrow[r] & \text{80-s Rb}^{92} \arrow[r] & \underset{\underline{5.3}}{\text{2.7-h Sr}^{92}} \arrow[r] & \text{3.6-h Y}^{92} \arrow[r] & \underset{\underline{6.03}}{\text{stable Zr}^{92}} & (13,14,20)\end{tikzcd}$$

93.
$$\begin{tikzcd}
 & & & & & \text{\textasciitilde 6-y Nb}^{93m} \arrow[d] & \\
\text{2.0-s Kr}^{93} \arrow[r] & \text{(short Rb)} \arrow[r] & \text{7-m Sr}^{93} \arrow[r] & \text{10.5-h Y}^{93} \arrow[r] & \underset{\underline{6.45}}{1.1 \times 10^{6}\text{-y Zr}^{93}} \arrow[ur, "\sim 0.50"] \arrow[dr, "\sim 0.50"'] & & (13) \\
 & & & & & \text{stable Nb}^{93} &
\end{tikzcd}$$

94.
$$\begin{tikzcd}\text{1.4-s Kr}^{94} \arrow[r, dashed] & \text{(short Rb)} \arrow[r] & \text{\textasciitilde 2-m Sr}^{94} \arrow[r] & \underset{\underline{5.4}}{\text{16.5-m Y}^{94}} \arrow[r] & \underset{\underline{6.40}}{\text{stable Zr}^{94}} & (13,21)\end{tikzcd}$$

95.
$$\begin{tikzcd}
 & \text{90-h Nb}^{95m} \arrow[dd] & & \\
\underset{\underline{6.2}}{\text{65-d Zr}^{95}} \arrow[ur, "0.02"] \arrow[dr, "0.98"'] & & \underset{\underline{6.27}}{\text{stable Mo}^{95}} & (13,22) \\
 & \text{35-d Nb}^{95} \arrow[ur] & &
\end{tikzcd}$$

96.
$$\begin{tikzcd}\underset{\underline{6.33}}{\text{stable Zr}^{96}} & (13)\end{tikzcd}$$

97.
$$\begin{tikzcd}
 & \text{60-s Nb}^{97m} \arrow[dd] & & \\
\underset{\underline{5.9}}{\text{17.0-h Zr}^{97}} \arrow[ur] \arrow[dr, "\sim 0.02"'] & & \underset{\underline{6.09}}{\text{stable Mo}^{97}} & (13,16,22) \\
 & \text{73-m Nb}^{97} \arrow[ur] & &
\end{tikzcd}$$

98.
$$\begin{tikzcd}\underset{\underline{5.78}}{\text{stable Mo}^{98}} & (13)\end{tikzcd}$$

$$\begin{tikzcd}
 & & & & 6.0\text{-h Tc}^{99m} \arrow[dd] & & \\
99. & 30\text{-s Zr}^{99} \arrow[r] & 3\text{-m Nb}^{99} \arrow[r] & \begin{array}{c}66\text{-h Mo}^{99}\\ \underline{6.06}\end{array} \arrow[ur, "0.87"] \arrow[dr, "0.13"'] & & \text{stable Ru}^{99} & (16,23) \\
 & & & & 2.1 \times 10^{5}\text{-y Tc}^{99} \arrow[ur] & &
\end{tikzcd}$$

$$\begin{tikzcd}
100. & & & & & \begin{array}{c}\text{stable Mo}^{100}\\ \underline{6.30}\end{array} & (13)
\end{tikzcd}$$

$$\begin{tikzcd}
101. & & & \begin{array}{c}14.6\text{-m Mo}^{101}\\ \underline{\sim 5.6}\end{array} \arrow[r] & 14.3\text{-m Tc}^{101} \arrow[r] & \begin{array}{c}\text{stable Ru}^{101}\\ \underline{5.0}\end{array} & (13,24)
\end{tikzcd}$$

$$\begin{tikzcd}
 & & & & 4.1\text{-m Tc}^{102} \arrow[dr] & & \\
102. & & & \begin{array}{c}11.5\text{-m Mo}^{102}\\ \underline{\sim 4.3}\end{array} \arrow[ur] \arrow[dr] & & \begin{array}{c}\text{stable Ru}^{102}\\ \underline{4.1}\end{array} & (13,24) \\
 & & & & 5\text{-s Tc}^{102} \arrow[ur] & &
\end{tikzcd}$$

$$\begin{tikzcd}
 & & & & 57\text{-m Rh}^{103m} \arrow[dd] & \\
103. & & 1.2\text{-m Tc}^{103} \arrow[r] & \begin{array}{c}39.7\text{-d Ru}^{103}\\ \underline{3.0}\end{array} \arrow[ur] \arrow[dr, dashed, "<0.05"'] & & (25) \\
 & & & & \text{stable Rh}^{103} &
\end{tikzcd}$$

$$\begin{tikzcd}
104. & & (<2.5\text{-m Mo}^{104}) \arrow[r] & 18\text{-m Tc}^{104} \arrow[r] & \begin{array}{c}\text{stable Ru}^{104}\\ \underline{1.8}\end{array} & (13)
\end{tikzcd}$$

$$\begin{tikzcd}
 & & & & 38\text{-s Rh}^{105m} \arrow[d] & & \\
105. & (<2\text{-m Mo}^{105}) \arrow[r] & 10\text{-m Tc}^{105} \arrow[r] & \begin{array}{c}4.45\text{-h Ru}^{105}\\ \underline{0.9}\end{array} \arrow[ur] & 35.3\text{-h Rh}^{105} \arrow[r] & \text{stable Pd}^{105} & (24,26)
\end{tikzcd}$$

106. $\underset{\underline{0.38}}{1.01\text{-y Ru}^{106}} \rightarrow 30\text{-s Rh}^{106} \longrightarrow \text{stable Pd}^{106}$ (13,25)

107. $$\begin{tikzcd} & & 6\text{-s Rh}^{107m} \arrow[d] & & \\ (<1\text{-m Tc}^{107}) \arrow[r] & 4.8\text{-m Ru}^{107} \arrow[r] \arrow[ur] & \underset{\underline{0.19}}{22\text{-m Rh}^{107}} \arrow[r] & 7 \times 10^{6}\text{-y Pd}^{107} \arrow[r] & \text{stable Ag}^{107} \end{tikzcd}$$ (27)

108. $(<1\text{-m Tc}^{108}) \longrightarrow 4.4\text{-m Ru}^{108} \rightarrow 18\text{-s Rh}^{108} \longrightarrow \text{stable Pd}^{108}$

109. $$\begin{tikzcd} & 39.2\text{-s Ag}^{109m} \arrow[d] \\ \underset{\underline{0.030}}{13.4\text{-h Pd}^{109}} \arrow[ur] & \text{stable Ag}^{109} \end{tikzcd}$$ (28)

111. $$\begin{tikzcd} & 5.5\text{-h Pd}^{111m} \arrow[r] \arrow[dd, "0.75"] \arrow[ddr, dashed] & 74\text{-s Ag}^{111m} \arrow[ddr, dashed, "<0.01"] & \\ (\text{short Rh}^{111}) \arrow[ur, "\sim 0.01"] \arrow[dr, "\sim 0.99"'] & & & \\ & 23\text{-m Pd}^{111} \arrow[r] \arrow[uur] & \underset{\underline{0.019}}{7.6\text{-d Ag}^{111}} \arrow[r] & \text{stable Cd}^{111} \end{tikzcd}$$ (28)

112. $\underset{\underline{0.010}}{21.0\text{-h Pd}^{112}} \rightarrow 3.14\text{-h Ag}^{112} \rightarrow \text{stable Cd}^{112}$ (28,29)

113.

$$\begin{tikzcd}
 & 1.2\text{-m Ag}^{113m} \arrow[d] \arrow[dr] & \\
1.5\text{-m Pd}^{113} \arrow[ur] \arrow[dr] & & \text{stable Cd}^{113} \\
 & 5.3\text{-h Ag}^{113} \arrow[ur] &
\end{tikzcd}$$

114.

$$\begin{tikzcd}
2.4\text{-m Pd}^{114} \arrow[r] & 5\text{-s Ag}^{114} \arrow[r] & \text{stable Cd}^{114}
\end{tikzcd}$$

115.

$$\begin{tikzcd}
 & {\sim}20\text{-s Ag}^{115m} \arrow[ddr] & \begin{array}{c}43\text{-d Cd}^{115m}\\ \underline{0.0007}\end{array} \arrow[ddr] & 4.51\text{-h In}^{115m} \arrow[dd, "0.95"] \arrow[dr, "0.05"] & \\
45\text{-s Pd}^{115} \arrow[ur] \arrow[dr] & & & & \text{stable Sn}^{115} \\
 & \begin{array}{c}21\text{-m Ag}^{115}\\ \underline{0.0077}\end{array} \arrow[uur, "0.09"] \arrow[r, "0.91"'] & \begin{array}{c}53\text{-h Cd}^{115}\\ \underline{0.0097}\end{array} \arrow[uur] & 6\times10^{14}\text{-y In}^{115} \arrow[ur] &
\end{tikzcd} \tag{30}$$

116.

$$\begin{tikzcd}
2.5\text{-m Ag}^{116} \arrow[r] & \text{stable Cd}^{116}
\end{tikzcd}$$

117.

$$\begin{tikzcd}
 & \begin{array}{c}3.0\text{-h Cd}^{117m}\\ \underline{0.011}\end{array} \arrow[r, dashed, "<0.10"] \arrow[dd, ">0.60"] \arrow[ddr] & 2\text{-h In}^{117m} \arrow[r, "0.001"] \arrow[dd, "0.22"] \arrow[ddr, "0.78"] & 14\text{-d Sn}^{117m} \arrow[dd] \\
1.1\text{-m Ag}^{117} \arrow[ur] \arrow[dr] & & & \\
 & {\sim}50\text{-m Cd}^{117} \arrow[uur] & 70\text{-m In}^{117} \arrow[r] & \text{stable Sn}^{117}
\end{tikzcd} \tag{31}$$

119.

$$\begin{tikzcd}
\text{10-m Cd}^{119} \arrow[r] & \text{17.5-m In}^{119} \arrow[r] & \text{stable Sn}^{119}
\end{tikzcd}$$

121.

$$\begin{tikzcd}
\begin{array}{c}\text{27.5-h Sn}^{121}\\ \underline{0.015}\end{array} \arrow[r] & \text{stable Sb}^{121}
\end{tikzcd}$$

(32)

123.

$$\begin{tikzcd}
(\text{40-m Sn}^{123}) \arrow[dr] & \\
& \text{stable Sb}^{123} \\
\begin{array}{c}\text{136-d Sn}^{123}\\ \underline{0.0013}\end{array} \arrow[ur] &
\end{tikzcd}$$

(33)

125.

$$\begin{tikzcd}
(\text{9.5-m Sn}^{125}) \arrow[dr] & & \text{58-d Te}^{125m} \arrow[dd] \\
& \begin{array}{c}\text{2.0-y Sb}^{125}\\ \underline{0.021}\end{array} \arrow[ur, "0.25"] \arrow[dr, "0.75"'] & \\
\begin{array}{c}\text{9.6-d Sn}^{125}\\ \underline{0.013}\end{array} \arrow[ur] & & \text{stable Te}^{125}
\end{tikzcd}$$

(34-36)

126.

$$\begin{tikzcd}
\text{50-m Sn}^{126} \arrow[r] & \begin{array}{c}\text{9-h Sb}^{126}\\ \underline{0.05}\end{array} \arrow[r] & \text{stable Te}^{126}
\end{tikzcd}$$

127.

$$\begin{tikzcd}
& & \begin{array}{c}\text{105-d Te}^{127m}\\ \underline{0.035}\end{array} \arrow[dd, "0.98"] \arrow[dr, "0.02"] & \\
\text{1.9-h Sn}^{127} \arrow[r] & \begin{array}{c}\text{91-h Sb}^{127}\\ \underline{0.13}\end{array} \arrow[ur, "0.22"] \arrow[dr, "0.78"'] & & \text{stable I}^{127} \\
& & \text{9.3-h Te}^{127} \arrow[ur] &
\end{tikzcd}$$

(28, 37, 38)

128. $\substack{57\text{-m Sn}^{128}\\ \underline{0.37}} \longrightarrow 10.3\text{-m Sb}^{128} \longrightarrow \text{stable Te}^{128}$ (27)

129.

$$\begin{tikzcd}
 & \substack{37\text{-d Te}^{129m}\\ \underline{0.35}} \arrow[d] & & \\
4.6\text{-h Sb}^{129} \arrow[ur, "0.36"] \arrow[dr, "0.64"'] & & \substack{1.7\times10^{7}\text{-y I}^{129}\\ \underline{0.9}} \arrow[r] & \text{stable Xe}^{129} \\
 & 72\text{-m Te}^{129} \arrow[ur] & &
\end{tikzcd}$$

(37,39)

130. $\substack{2.6\text{-m Sn}^{130}\\ \underline{2.0}} \longrightarrow 10.0\text{-m Sb}^{130} \longrightarrow \text{stable Te}^{130}$ (40)

131.

$$\begin{tikzcd}
 & & \substack{30\text{-h Te}^{131m}\\ \underline{0.44}} \arrow[d, "0.20"] \arrow[dr, "0.80"] & & 12\text{-d Xe}^{131m} \arrow[dd, "(11,28,37,40,41,44)"] \\
3.4\text{-m Sn}^{131} \arrow[r] & \substack{23\text{-m Sb}^{131}\\ \underline{2.6}} \arrow[ur, "0.15"] \arrow[dr, "0.85"'] & & \substack{8.05\text{-d I}^{131}\\ \underline{\sim3.1}} \arrow[ur, "0.008"] \arrow[dr, "0.992"'] & \\
 & & 24\text{-m Te}^{131} \arrow[ur] & & \substack{\text{stable Xe}^{131}\\ \underline{2.93}}
\end{tikzcd}$$

132. $2.2\text{-m Sn}^{132} \longrightarrow 2.1\text{-m Sb}^{132} \longrightarrow \substack{77\text{-h Te}^{132}\\ \underline{\sim4.7}} \longrightarrow 2.30\text{-h I}^{132} \longrightarrow \substack{\text{stable Xe}^{132}\\ \underline{4.38}}$ (11,37,44)

133.

$$\begin{tikzcd}
 & \begin{array}{c}\text{63-m Te}^{133m}\\ \underline{4.9}\end{array} \arrow[dd] & & \text{2.3-d Xe}^{133m} \arrow[dd] & \\
\begin{array}{c}\text{4.1-m Sb}^{133}\\ \underline{4.0}\end{array} \arrow[ur, "0.72"] \arrow[dr, "0.28"'] & & \begin{array}{c}\text{20.8-h I}^{133}\\ \underline{\sim 6.9}\end{array} \arrow[ur, "0.024"] \arrow[dr, "0.976"'] & & \begin{array}{c}\text{stable Cs}^{133}\\ \underline{6.59}\end{array} \\
 & \text{2-m Te}^{133} \arrow[ur] & & \begin{array}{c}\text{5.27-d Xe}^{133}\\ \underline{6.62}\end{array} \arrow[ur] &
\end{tikzcd}$$

(9,37,43,44)

134.

$$\begin{tikzcd}
(\text{0.8-m Sb}^{134}) \arrow[r] & \begin{array}{c}\text{44-m Te}^{134}\\ \underline{6.9}\end{array} \arrow[r] & \begin{array}{c}\text{52.5-m I}^{134}\\ \underline{7.8}\end{array} \arrow[r] & \begin{array}{c}\text{stable Xe}^{134}\\ \underline{8.06}\end{array}
\end{tikzcd}$$

(11,37,43,44)

135.

$$\begin{tikzcd}
 & & \text{15.3-m Xe}^{135m} \arrow[dd] & & \\
(<\text{0.5-m Te}^{135}) \arrow[r] & \begin{array}{c}\text{6.7-h I}^{135}\\ \underline{6.1}\end{array} \arrow[ur, "0.30"] \arrow[dr, "0.70"'] & & \begin{array}{c}2.6\times10^{6}\text{-y Cs}^{135}\\ \underline{6.41}\end{array} \arrow[r] & \text{stable Ba}^{135} \\
 & & \begin{array}{c}\text{9.2-h Xe}^{135}\\ \underline{6.3}\end{array} \arrow[ur] & &
\end{tikzcd}$$

(9,37,42,45-47)

136.

$$\begin{tikzcd}
\begin{array}{c}\text{86-s I}^{136}\\ \underline{3.1}\end{array} \arrow[r] & \begin{array}{c}\text{stable Xe}^{136}\\ \underline{6.46}\end{array}
\end{tikzcd}$$

(11,48)

137.

$$\begin{tikzcd}
 & \begin{array}{l}\text{stable Xe}^{136}\\ \text{+ neutron}\end{array} & & \\
\text{24-s I}^{137} \arrow[ur] \arrow[dr] & & & \text{2.57-m Ba}^{137m} \arrow[dd] \\
 & \text{3.9-m Xe}^{137} \arrow[r] & \begin{array}{c}\text{29-y Cs}^{137}\\ \underline{6.15}\end{array} \arrow[ur, "0.92"] \arrow[dr, "0.08"'] & \\
 & & & \text{stable Ba}^{137}
\end{tikzcd}$$

(9,49)

138.
$$\begin{tikzcd} & \text{3.9-m Xe}^{137} \\ & + \text{ neutron} \\ \text{5.8-m I}^{138} \arrow[ur] \arrow[dr] \\ & \text{17-m Xe}^{138} \arrow[r] & \text{32.2-m Cs}^{138} \arrow[r] & \underset{\underline{5.74}}{\text{stable Ba}^{138}} \end{tikzcd}$$
(13,50)

139.
$$\text{2.7-s I}^{139} \longrightarrow \underset{\underline{5.5}}{\text{41-s Xe}^{139}} \longrightarrow \text{9.5-m Cs}^{139} \longrightarrow \underset{\underline{6.55}}{\text{84-m Ba}^{139}} \longrightarrow \text{stable La}^{139}$$
(14,16,17)

140.
$$\underset{\underline{3.8}}{\text{16-s Xe}^{140}} \longrightarrow \text{66-s Cs}^{140} \longrightarrow \underset{\substack{6.32\\(\underline{6.44})}}{\text{12.8-d Ba}^{140}} \longrightarrow \underset{\substack{6.32\\(\underline{6.44})}}{\text{40.2-h La}^{140}} \longrightarrow \underset{\underline{6.44}}{\text{stable Ce}^{140}}$$
(14,16,51,52,62)

141.
$$\underset{\underline{1.34}}{\text{1.7-s Xe}^{141}} \rightarrow \text{(short Cs)} \rightarrow \underset{\underline{6.3}}{\text{18-m Ba}^{141}} \rightarrow \underset{\underline{6.4}}{\text{3.7-h La}^{141}} \rightarrow \underset{\underline{\sim 6.0}}{\text{33-d Ce}^{141}} \rightarrow \text{stable Pr}^{141}$$
(14,17,53,54)

142.
$$\text{6-m Ba}^{142} \longrightarrow \text{75-m La}^{142} \longrightarrow \underset{\underline{5.95}}{\text{stable Ce}^{142}}$$
(9,13,62)

143.
$$\underset{\underline{0.051}}{\text{1-s Xe}^{143}} \rightarrow \text{(short Cs)} \rightarrow (\text{<0.5-m Ba}) \rightarrow \text{18-m La}^{143} \rightarrow \underset{\underline{5.7}}{\text{33-h Ce}^{143}} \rightarrow \text{13.7-d Pr}^{143} \rightarrow \underset{\underline{5.98}}{\text{stable Nd}^{143}}$$
(9,13,14,55,62)

144.
$$\underset{\underline{\sim 6.0}}{\text{285-d Ce}^{144}} \text{---} \text{17.4-m Pr}^{144} \longrightarrow \underset{\underline{5.67}}{5 \times 10^{15}\text{-y Nd}^{144}}$$
(9,13,62)

145.	$3.0\text{-m Ce}^{145} \rightarrow 5.95\text{-h Pr}^{145} \rightarrow \underset{\underline{3.95}}{\text{stable Nd}^{145}}$	(9,13,62)
146.	$13.9\text{-m Ce}^{146} \rightarrow 24.4\text{-m Pr}^{146} \rightarrow \underset{\underline{3.07}}{\text{stable Nd}^{146}}$	(9,13,62)
147.	$\underset{\underline{\sim 2.7}}{11.1\text{-d Nd}^{147}} \rightarrow 2.65\text{-y Pm}^{147} \rightarrow \underset{\underline{2.38}}{1.3 \times 10^{11}\text{-y Sm}^{147}}$	(9,56,62)
148.	$\underset{\underline{1.70}}{\text{stable Nd}^{148}}$	(9,13,62)
149.	$(2.0\text{-h Nd}^{149}) \rightarrow 54\text{-h Pm}^{149} \longrightarrow \underset{\underline{1.13}}{\text{stable Sm}^{149}}$	(9,56,62)
150.	$\underset{\underline{0.67}}{\text{stable Nd}^{150}}$	(9,13,62)
151.	$(13\text{-m Nd}^{151}) \rightarrow 27.5\text{-h Pm}^{151} \rightarrow \underset{\underline{0.45}}{80\text{-y Sm}^{151}} \longrightarrow \text{stable Eu}^{151}$	(9,62)
152.	$\underset{\underline{0.285}}{\text{stable Sm}^{152}}$	(9,62)
153.	$\underset{\underline{0.15}}{47\text{-h Sm}^{153}} \longrightarrow \text{stable Eu}^{153}$	(28,57,62)
154.	$\underset{\underline{0.077}}{\text{stable Sm}^{154}}$	(9,62)

155.	$\underset{\underline{0.033}}{\text{24-m Sm}^{155}} \longrightarrow \underset{\underline{\sim 0.03}}{\text{1.9-y Eu}^{155}} \longrightarrow \text{stable Gd}^{155}$	(58,59,62)
156.	$\underset{\underline{0.013}}{\sim\text{10-h Sm}^{156}} \longrightarrow \underset{\underline{0.014}}{\text{15.4-d Eu}^{156}} \longrightarrow \text{stable Gd}^{156}$	(28,57,59)
157.	$\underset{\underline{0.0078}}{\text{15.4- Eu}^{157}} \longrightarrow \text{stable Gd}^{157}$	(60)
158.	$\underset{\underline{0.002}}{\text{60-m Eu}^{158}} \longrightarrow \text{stable Gd}^{158}$	(60)
159.	$\underset{\underline{0.00107}}{\text{18.0-h Gd}^{159}} \longrightarrow \text{stable Tb}^{159}$	(57, 61)
161.	$(\text{3.6-m Gd}^{161}) \longrightarrow \underset{\underline{7.6 \times 10^{-5}}}{\text{6.9-d Tb}^{161}} \longrightarrow \text{stable Dy}^{161}$	(57, 61)

produced krypton, xenon, and cesium (references 110, 111 and 112) were normalized to the data of reference 109.

These mass abundances were converted to fission yields by imposing the criterion that the sum of all yields be 200 percent as expected theoretically for binary fission. Radiochemical data for mass numbers not determined mass spectrometrically were used as an aid in the summation. In general, the U^{235} fission yields of Table 11.9 which are based on radioactivity measurements are considered reliable to 10 to 20 percent although the uncertainty in a few cases may be only a few percent. The values based on mass spectrometry are believed to be somewhat more accurate and are considered reliable to about 5 percent. Values for total chain yields are plotted as a yield-mass curve in Fig. 11.35.

Fine structure is clearly indicated by the mass spectrometric data in the regions around mass 100 and mass 134. This effect is ascribed to the influence of closed neutron shells in fission and is discussed below in Section 11.4.3. Here we wish to describe only the broad features of the mass yield curves.

Detailed literature references to the yields of the products of the fission of Pu^{239} can be found in KATCOFF'S[107] 1958 review. Much of the earlier data has been superceded by later work. We quote here from a particularly comprehensive study of FICKEL and TOMLINSON[108] who used a mass spectrograph to measure relative yields of the isotopes of 6 elements in the light and 5 elements in the heavy group. In addition, they measured the absolute yield of one isotope of each element by the isotope dilution method. By combining these results they derived absolute yields for 36 mass chains. These results replace the earlier data of WILES, PETRUSKA and TOMLINSON[113] from the same laboratory. Table 11.10 is a summary table prepared by FICKEL and TOMLINSON.[108] It includes the results of FRITZE, McMULLEN and THODE[114] and of FLEMING and THODE[115]

---

110. H. G. Thode, Nucleonics (No. 3) 3, 14 (1948).
111. J. Koch, et al., Phys. Rev. 76, 279 (1949).
112. D. R. Wiles, et al., Can. J. Phys. 31, 419 (1953).
113. D. M. Wiles, J. A. Petruska and R. H. Tomlinson, Can. J. Chem. 34, 227 (1956).

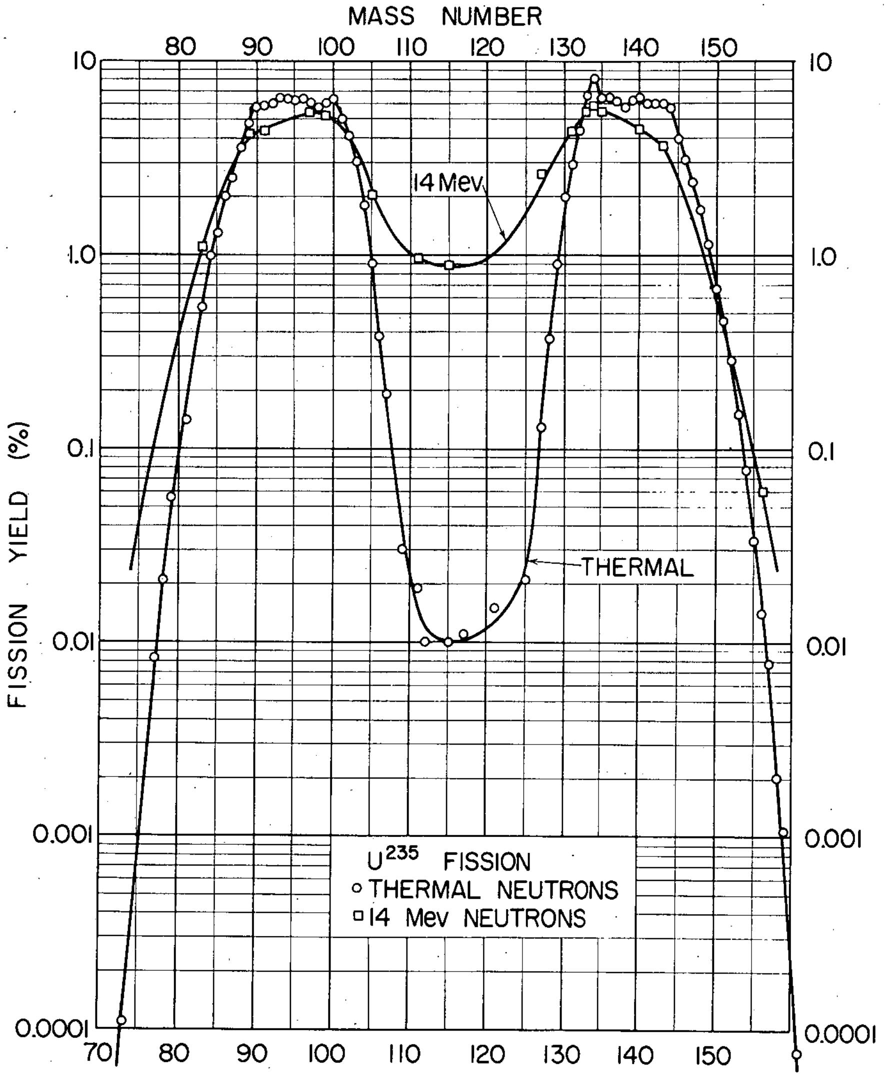

Fig. 11.35. Yield-mass curve for fission of U^{235} induced by slow neutrons. Curves plotted from "Best" values taken from literature by S. Katcoff.

Table 11.10

Cumulative Yields in the Slow Neutron Fission of Pu^{239}

Isotopic Mass	% yield	Isotopic Mass	% yield	Isotopic Mass	% yield
		Part 1. The Light Group			
72-82	0.59*	Zr^{94}	4.45	Ru^{106}	4.53
Kr^{83}	0.29	$\mathrm{Mo}^{95}(\mathrm{Zr}^{95})$	4.99	107	3.40*
Kr^{84}	0.47	Zr^{96}	5.13	108	2.44*
$\mathrm{Rb}^{85}(\mathrm{Kr}^{85})$	0.535	Mo^{97}	5.61	109	1.50**
Kr^{86}	0.75	Mo^{98}	5.84	110	0.76*
Rb^{87}	0.912	99	6.44*	111	0.27**
Sr^{88}	1.43	Mo^{100}	7.05	112	0.10*
Sr^{89}	1.71	Ru^{101}	5.86	113	0.080*
Sr^{90}	2.16	Ru^{102}	5.94	114	0.060*
Zr^{91}	2.60	Ru^{103}	5.63	115	0.041*
Zr^{92}	3.12	Ru^{104}	5.88	116-118	0.122*
Zr^{93}	3.94	105	5.50*	Total % yield	100.13
		Part 2. The Heavy Group			
Atomic No.	% yield	Atomic No.	% yield	Atomic No.	% yield
118-130	5.70*	140	5.58	150	1.02
131	3.77	141	5.23*	151	0.802
132	5.26	142	4.97	152	0.616
133	6.90	143	4.56	153	0.45*
134	7.46	144	3.84	154	0.293
135	7.25	145	3.12	155	0.17*
136	6.62	146	2.57	156	0.08*
137	6.48	147	1.99	159	0.02**
138	6.31	148	1.71	161	0.0041**
139	5.99*	149	1.30	166	7x10^{-5}**
				Total % yield	100

Table prepared by FICKEL and TOMLINSON.[108]

All values are based on mass spectrometric values except those marked.

* interpolated values

** radiochemical yields.

who determined absolute yields of the isotopes of krypton and xenon. A few yields for the very heavy rare earth products have been added to the table from the radiochemical results of BUNNEY and co-workers.[116] Figure 11.36 is plotted from the data of Table 11.10. A number of Russian workers have also contributed to the determination of Pu^{239} fission yields.[117-119]

Fission yield data for U^{233} are summarized in Table 11.11. In constructing this table we started with the 1955 summary of STEINBERG and GLENDENIN[106] and added to it data which have been published more recently. The Russian work[119] summarized in a 1958 Geneva Conference report gave two sets of data for U^{233}. We chose the set measured by the "integral" mass-spectrographic method. A fission yield curve for U^{233} is plotted in Fig. 11.37.

---

[114] K. Fritze, C. C. McMullen and H. G. Thode, Paper P/187, p. 436, Volume 15 Proceedings of the Second U.N. Conference on the Peaceful Uses of Atomic Energy, Geneva, 1958.

[115] W. H. Fleming and H. G. Thode, Can. J. Chem. 34, 193 (1956).

[116] R. Bunney, E. M. Scadden, J. O. Abriam and N. E. Ballou, Paper P/644, p. 444, Volume 15, Proceedings of the Second U N. Conference on the Peaceful Uses of Atomic Energy, Geneva, 1958.

[117] L. M. Krizhanskii and A. N. Murin, Soviet Journal of Atomic Energy (in English translation) 4, 95 (1958).

[118] L. M. Krizhanskii, Ya. Malyi, A. N. Murin and B. K. Preobrazhenskii, Soviet Journal of Atomic Energy 2, 334 (1957).

[119] M. P. Anikina et al., Paper P/2040, p. 446, Volume 15, Proceedings of the Second U.N. Conference on the Peaceful Uses of Atomic Energy, Geneva, 1958.

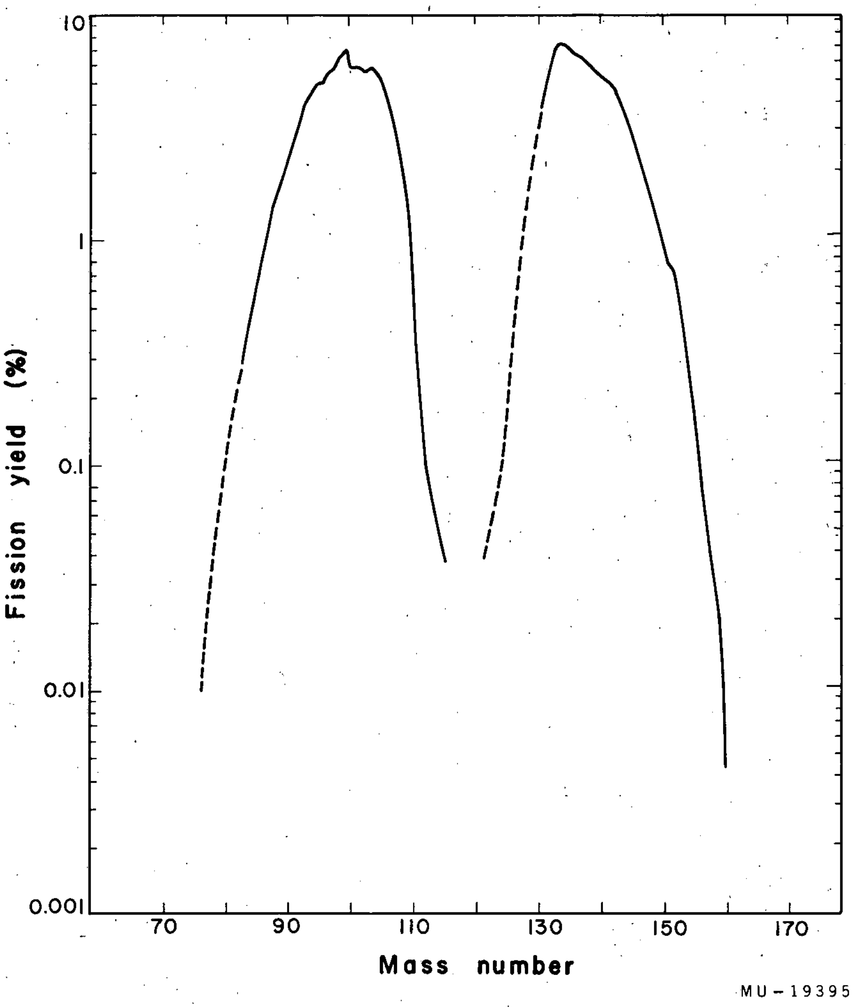

Fig. 11.36. The mass yield curve for the fission of Pu^{239} induced by slow neutrons. Curve plotted from table of Fickel and Tomlinson, reference 108.

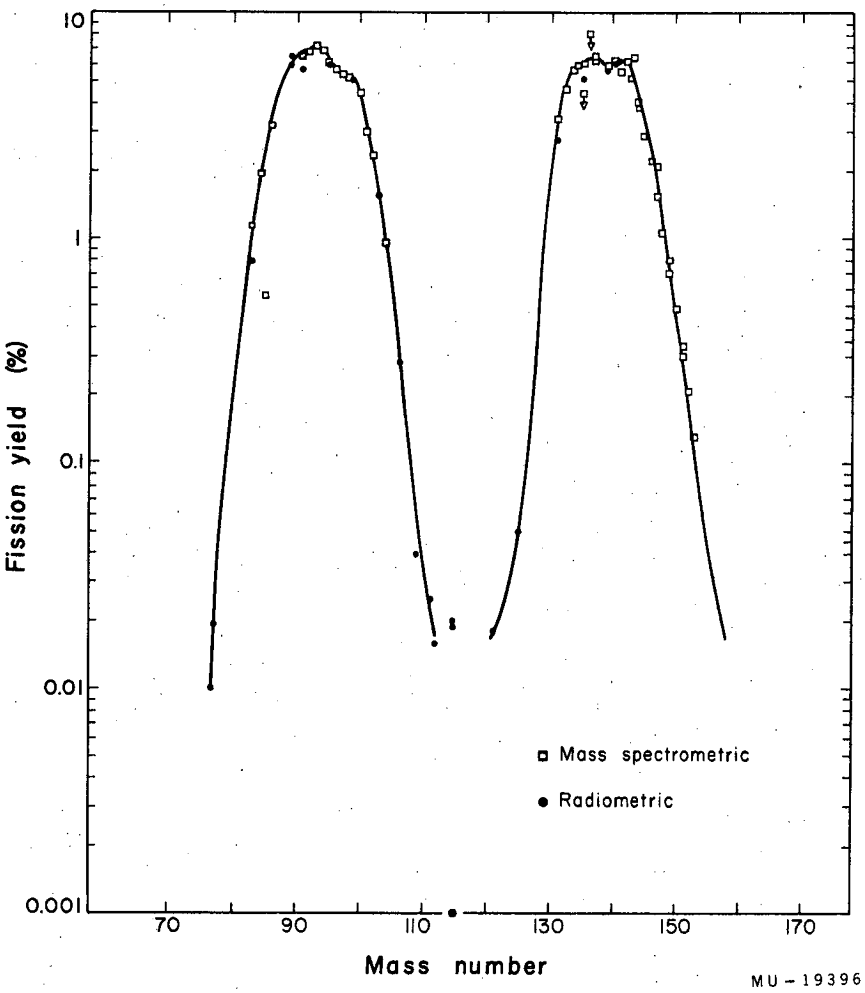

Fig. 11.37. Yield-mass curve for fission of U^{233} induced by slow neutrons.

Table 11.11

Cumulative Yields in the Slow Neutron Fission of U^{233}

Fission product	Mass number	U^{233}	
		Radiometric	Mass spectrometric
49.0-hr Zn	72		
5.0-hr Ga	73		
12-hr Ge	77	0.010(a)	
38-hr As	77	0.019(a)	
2.4-hr Br	83	0.79(a)	
Stable Kr	83		1.14(b)
Stable Kr	84		1.90(b)
10.27-yr Kr	85		0.56_2(b)
Stable Kr	86		3.1_8(b)
53-d Sr	89	6.5(a) 5.87(e)	
28-yr Sr	90		
9.7-yr Sr	91	5.61(e)	
61-d Y	91		
Stable Zr	91		6.5_3(c)
Stable Zr	92		6.7_0(c)
1.1×10^6-yr Zr	93		7.1_0(c)
Stable Zr	94		6.8_2(c)
63-d Zr	95	5.9(a)	
Stable Mo	95		6.1_0(c)
Stable Zr	96		5.6_0(c)
17.0-hr Zr	97		
Stable Mo	97		5.3_5(c)
Stable Mo	98		5.1_8(c)
67-hr Mo	99	5.1(a)	
Stable Mo	100		4.4_0(c)
Stable Ru	101		3.0_0(c)
Stable Ru	102		2.3_7(c)
39.8-d Ru	103	1.6(a)	

Table 11.11 (cont'd.)

		U^{233}	
Fission product	Mass number	Radiometric	Mass spectrometric
Stable Ru	104		0.96(c)
36.5-hr Rh	105		
1.0-yr Ru	106	0.28(a)	
13.6-hr Pd	109	0.040(a)	
7.6-d Ag	111	0.025(a)	
21-hr Pd	112	0.016(a)	
43-d Cd	115m	1×10^{-3}(a)	
53-hr Cd	115	0.19(a)	
Total Chain	115	0.020(a)	
27.5-hr Sn	121	0.018(a)	
9.4-d Sn	125	0.050(a)	
93-hr Sb	127		
8.1-d I	131	2.7(a)	
Stable Xe	131		3.4_0(b)
77.7-hr Te	132		
Stable Xe	132		4.6_4(b)
20.8-hr I	133		
Stable Cs	133		5.6_2(b) 5.6(f) (5.5)[g]
Stable Xe	134		5.9_5(b)
6.68-hr I	135	5.1(a)	
3.0×10^{6}-yr Cs	135		$>4.4_9$(b)
9.2-hr Xe	135		6.0(f)
86-sec I	136	1.7(d)	
Stable Xe	136		$<8.0_6$(b)
33-yr Cs	137		6.5_1(b) 6.16(g)
Stable La	139		5.91(g)
86-min Ba	139	5.59(e)	
12.8-d Ba	140	6.0(a)	
Stable Ce	140		6.16(g)
Stable Pr	141		5.57(g)

Table 11.11 (cont'd.)

Fission product	Mass number	U^{233}	
		Radiometric	Mass spectrometric
3.8-hr La	141	6.17(e)	
Stable Ce	142		6.06(g)
Stable Nd	143		5.19(g) 6.45(f)
282 d Ce	144		4.1(a)
Stable Nd	144		3.84(g)
Stable Nd	145		2.88(g)
Stable Nd	146		2.24(g)
2.6 yr Pm	147		1.53(g) 2.1(f)
Stable Nd	148		1.07(g)
Stable Sm	149		0.70(g) 0.8(f)
Stable Nd	150		0.49(g)
80 yr Sm	151		0.33(g) 0.3(f)
Stable Sm	152		0.21(g)
Stable Eu	153		0.13(g)
47 hr Sm	153	0.95(a)	0.95(a)

(a) Steinberg, E. P., Seiler, J. A., Goldstein, A., Dudley, A., Fission Yields in U^{233}, MDDC-1632 (1948); yields revised by Steinberg in 1954.

(b) Fleming, W., Tomlinson, R. H. and Thode, H. G., The Fission Yields of the Stable and Long-Lived Isotopes of Xenon, Cesium, and Krypton in Neutron Fission of U^{233}, Can. J. Phys. 32, 522 (1954); relative yield normalized to radiometric data of ref. (a).

(c) Steinberg, E. P., Glendenin, L. E., Inghram, M. G. and Hayden, R. J., Fine Structure in U^{233} Fission, Phys. Rev. 95, 867 (1954); relative yield normalized to radiometric data of ref. (a).

(d) Stanley, C. W. and Katcoff, S., The Properties of 86-second I^{136}, J. Chem. Phys. 17, 653 (1949).

(e) Bartholomew, R. M., Martin, J. S., Baerg, A. P., Can. J. Chem. 37, 660 (1959), accurate radiochemical measurements of yields relative to Ba^{140} were converted to absolute yield by setting Ba^{140} yield equal to 6.0.

(f) Bidinosti, D. R., Fickel, H. R. and Tomlinson, R. H., P/201, p. 459, Volume 15, Proceedings of the Second U. N. Conference on the Peaceful Uses of Atomic Energy, Geneva, 1958.

(g) Anikina, M. P., et al., Paper P/2040, Volume 15, Proceedings of the Second U.N. Conference on the Peaceful Uses of Atomic Energy, Geneva, 1958.

From an examination of the tables and curves showing the mass yield data for U^{235}, Pu^{239} and U^{233}, it is apparent at once that the heavy element nucleus does not split into two equal pieces. The two fragments have a mass ratio of 1.46 in the case of the most probable mass split in U^{235}. It is also clear at a glance that the fission process does not produce a unique pair of fragments. In any individual fission event it cannot be predicted which pair of products will be formed; nuclides ranging in mass from 72 to 161 and in atomic number from 30 to 65 have been identified among the fission products.

The preponderance of asymmetric fission compared to symmetrical fission is frequently expressed in terms of a peak-to-trough ratio defined as the ratio of the fission yields corresponding to the two maxima in the mass distribution and the fission yield at the minimum which occurs at the mass value corresponding to a symmetric split. The peak-to-trough ratio is greatest for spontaneous fission, next greatest for fission with neutrons of selected resonance energy, slightly lower for slow neutron fission and markedly lower for fission induced by high energy neutrons (Mev range). For fission with high energy neutrons (tens of Mev) and particularly for fission induced by charged particles symmetric fission becomes much more probable and in some cases becomes predominant. This is discussed fully in Chapter 12. The peak-to-trough ratio and certain other characteristics of the mass distributions for various fissile nuclides are tabulated in Table 11.12.

The sum of the values for the most probable mass numbers in the light and heavy peaks does not equal the mass of the initial heavy fissioning nucleus because of the neutrons emitted by the fragments. The difference of the two sums is the average number of neutrons, $\overline{\nu}$, emitted in fission. This quantity can be evaluated with much greater accuracy by direct measurement of the neutrons themselves as discussed in Section 11.7.

A principal effect of the increase in mass of the fissioning nucleus is to cause a shift in the light mass peak to higher values, the heavy mass peak remaining fixed. In some instances this rule has been taken as a guide in estimating the mass of the fissioning species in a complex reacting system. SWIATECKI[120] has shown from very general arguments based on the liquid drop model why this should be so. He has presented the correlation between asymmetry and the parameter Z^2/A given in Fig. 11.38, a correlation which should be useful for predictive purposes.

---

[120] W. J. Swiatecki, Phys. Rev. 100, 936 (1955).

Table 11.12

Comparison of Mass Distributions

Fissile nuclide	Type of fission	Most probable mass number Light group	Most probable mass number Heavy group	Mass width at half height	Ratio of most probable masses in heavy and light groups	Ratio of peak to trough yields
Th^{232}	Fast neutron (fission spectrum)	92	139	14	1.51	115
U^{233}	Slow neutron	94	138	14	1.47	~450
U^{235}	Slow neutron	95	139	15	1.46	650
U^{238}	Fast neutron (fission spectrum)	98	139	16	1.42	200
Pu^{239}	Slow neutron	99	138	16	1.40	150
Cm^{242}	Spont. fission	103	136	16	1.32	
Cf^{252}	Spont. fission	108	139	16	1.29	>600

This table may be compared with Table 11.21 which lists fragment energies and fragment mass ratios derived from fragment ionization and velocity measurements.

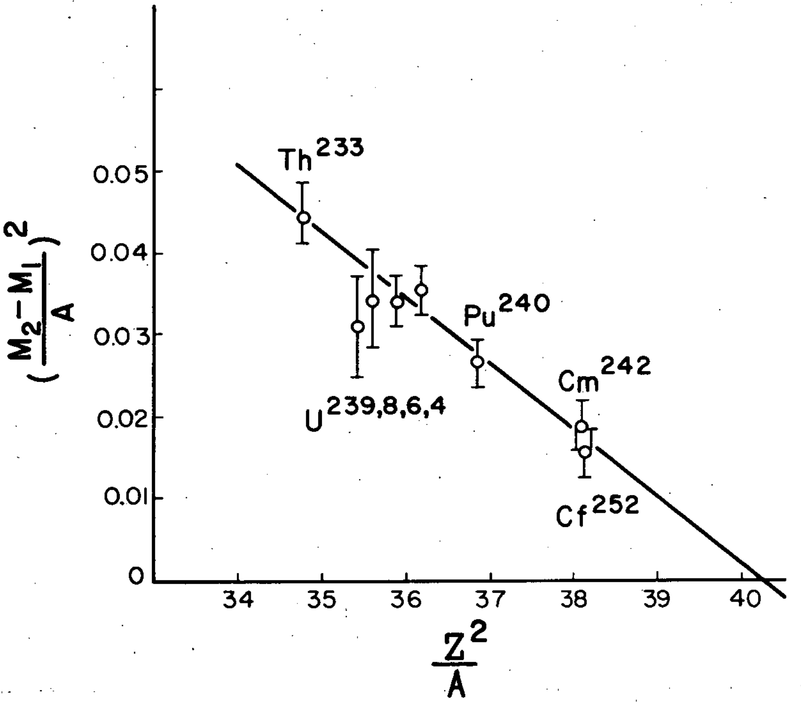

MU-19018

Fig. 11.38. The square of the relative degree of asymmetry, defined as M_2-M_1/A, as a function of Z^2/A. From SWIATECKI.[120]

11.4.3 Closed Shell Effects and Fine Structure in the Mass-Yield Curve. The early radiochemical investigations indicated that the mass-yield curves were rather smooth and there was no indication of fine structure "spikes" in the double humped distribution. Whenever a deviation from the smooth curve was found, further investigation usually revealed some error in the measurement. Some perturbations in the yield-mass curve are expected as a result of delayed neutron emission but such effects cannot be large because only 0.5 percent or less of the neutrons are delayed.

The first work which established the existence of large deviations from a smooth mass curve was the accurate mass spectrometric analysis measurements of THODE and co-workers[121-123] of the abundances of krypton and xenon isotopes produced in U^{235} fission. In particular, the yield of Xe^{134} was about 35 percent higher than had been expected. Radiometric determinations by STANLEY and KATCOFF[124] of the yield of I^{136} in the fission of U^{233}, U^{235}, and Pu^{239} also established a major departure from the smooth curve.

Since these isotopes lie close to the 82 neutron shell the explanation of the anomalous yields was sought in specific shell effects. Shell structure could influence fission yields by (1) specifying a preference in the fission act itself for fragments with a closed shell of neutrons or protons or (2) by causing additional boil-off of neutrons from fission fragments having one neutron in excess of a closed shell. GLENDENIN[125] proposed the second of these two alternatives to explain the anomalous yields in the 133 to 135 mass number region. This postulate of additional prompt neutron emission (beyond the usual number emitted from every fragment) would result in perturbations in fission yields near closed shells since the loss in yield from a given chain would not always be exactly compensated by a gain in yields from the chain one higher in mass number. Calculations based on this mechanism and utilizing the primary yields along fission chains as given by the charge distribution function (Fig. 11.46) indicated a fine structure pattern for the krypton and xenon isotopes and

---

121. H. G. Thode and R. L. Graham, Can. J. Research 25A, 1 (1947).
122. MacNamara, Collins and Thode, Phys. Rev. 78, 129 (1950).
123. R. K. Wanless and H. G. Thode, Can. J. Phys. 33, 541 (1955).
124. C. W. Stanley and S. Katcoff, J. Chem. Phys. 17, 653 (1949).
125. L. E. Glendenin, Phys. Rev. 75, 337 (1949).

an abnormally low yield for I^{136} in qualitative agreement with experimental observations.

PAPPAS[126] extended the GLENDENIN hypothesis by arguing from neutron binding energy systematics that prompt neutron emission should be extended to include the third, fifth and perhaps seventh neutron outside the closed shell. This post-fission, shell-influenced, neutron-boil-off effect runs into difficulty however in explaining other fission yield data. A requirement of the hypothesis is that any increase in yield of certain mass numbers over that expected from the "smooth curve" should be counterbalanced exactly by dips in the observed yields for higher-numbered mass chains. These dips have not been observed. WILES[127,128], for example, found a high yield for $Cs^{133,135,137}$ and for other products for which a low yield was expected on the basis of the GLENDENIN hypothesis.

WILES[127,128] suggested that the anomalous fine structure in fission must be caused, at least in substantial amount, by the favoring of fission fragments with 82 neutrons in the fission act itself. According to WILES' hypothesis nuclides with 82 neutrons such as Sb^{133}, Te^{134}, I^{135}, Xe^{136}, and Cs^{137} would be expected to have an increased independent yield due to selectivity in the primary fission act. Furthermore, due to the high binding energy of the last neutron the post-fission boil-off of neutrons would be low for such species. An important consequence of this hypothesis is that the high yield of these species must be reflected in the complementary fragments in the light mass region. Fission yield determinations in the mass region 99 to 101, the region complementary to Te^{134}, I^{135}, and Xe^{136}, should establish if such a selectivity is involved in the fission act. GLENDENIN, STEINBERG, INGHRAM, and HESS[129] looked for this reflection peak among the isotopes of molybdenum and zirconium and found abnormally high yields in the mass region 98 to 100.

---

[126] A. C. Pappas, Laboratory for Nuclear Science, M.I.T., Technical Report No. 63 (September 1953).

[127] D. R. Wiles, Thesis, McMaster University, Hamilton, Ontario, Canada (September 1950).

[128] Wiles, Smith, Horsley and Thode, Can. J. Phys. 31, 419 (1953).

[129] Glendenin, Steinberg, Inghram, and Hess, Phys. Rev. 84, 860 (1951).

Molybdenum-100 in particular was found to be high by over 40 percent. There is no reasonable basis for a preferential neutron boil-off effect for this mass region so it is quite likely that the high yields here are strictly a reflection of high yields for the 82-neutron nuclides in the heavy fragment.

Further evidence for a shell preference in the fission act comes from a study of the velocity distribution of fission fragments. LEACHMAN and SCHMITT[130] measured the velocity distribution of fragments slowed by passage through absorbers and detected fine structure in the velocity distribution of the fragments from U^{235}. No fine structure was observed for unslowed fragments.

A careful study of the yields of krypton isotopes has revealed abnormal yields in the region of the 50-neutron shell. This work, carried out by the mass spectrometer technique by WANLESS and THODE,[123] and by FLEMING, TOMLINSON and THODE,[131] showed fine structure effects in the neutron-induced fission of U^{235}, U^{238}, and U^{233}. Preference for a 50-proton configuration in the fission act has been proposed by WILES and CORYELL[132] on the basis of radiometric studies of 15 Mev deuteron induced fission of U^{235} and U^{238}. The influence of the 50 neutron or 50 proton shells is much harder to observe in yield studies than is the influence of the 82 neutron shell, because the nuclides which are affected all lie in a mass region where the normal chain yields are changing rapidly with mass.

The generally accepted conclusion is that the fine structure effects in the slow neutron fission of U^{235} are largely accounted for by shell-preference in the fission act, but that there is a definite contribution which is explained by the post fission boil-off hypothesis of GLENDENIN. PAPPAS[126] has given a detailed analysis of the operation of both effects in the case of slow neutron fission of U^{235}.

The fine structure effects have also been studied for the neutron-induced fission of U^{233}, U^{238}, and Pu^{239}, although not in as great detail.[133,134,135]

---

[130] R. B. Leachman and H. W. Schmitt, Phys. Rev. 96, 1366 (1954).

[131] Fleming, Tomlinson, and Thode, Can. J. Phys. 32, 522 (1954).

[132] D. R. Wiles and C. D. Coryell, Phys. Rev. 96, 696 (1954).

[133] See references to Tables 11.10 and 11.11, references 123 and 129.

[134] W. H. Fleming and H. G. Thode, Phys. Rev. 92, 378 (1953).

[135] D. M. Wiles, J. A. Petruska and R. H. Tomlinson, Can. J. Chem. 34, 227 (1956).

The PAPPAS[126] analysis should apply as well to these other nuclei; it does account qualitatively for many of the observed results but there are some unaccountable discrepancies between experiment and theory, particularly in the fission of U^{233}.

FLEMING, TOMLINSON and THODE[131] find a peak in the yields of the xenon isotopes from the fission of U^{238} with fast neutrons but the peak is lower than observed in the case of U^{235} fission, and lower than predicted by the PAPPAS[126] treatment. In the case of U^{233} fission, WANLESS and THODE[123] could find no evidence for a spike in the xenon yields. It is hard to understand this sudden disappearance of this fine structure in going from U^{235} to U^{233}. On the other hand, STEINBERG, GLENDENIN, INGHRAM, and HAYDEN[136] find clear evidence for a fine structure peak in the light fragment distribution for U^{233}. The maximum of the peak occurs at about mass 99 which is complementary to the heavy fission products containing 82 neutrons.

STEINBERG and GLENDENIN[137] measured the yields of fission products of the spontaneous fission of Cm^{242} and found pronounced fine structure around masses 105 and 134. The effect is attributed chiefly to 82-neutron preference in the fission act.

11.4.4 Distribution of Mass in Fission Induced by Neutron of Resonance Energy. Many of the characteristics of fission are probably strongly influenced by the specific fission channel or transition state through which fission occurs. The fission cross section as a function of neutron energy is known to have pronounced resonance structure in the electron-volt region (see Section 11.3.3). It is quite possible that different resonances may correspond to different transition states and that the mass-yield distributions resulting from different transition states may be markedly different. The mass yield distribution observed in thermal fission is probably some sort of average over two or more resonances. With these ideas in mind some investigations have been made of the shape of the mass-yield curve when fission is induced with neutrons of resonance energy.

---

[136] E. P. Steinberg, L. E. Glendenin, M. G. Inghram, and R. J. Hayden, Phys. Rev. 95, 867 (1954).

[137] E. P. Steinberg and L. E. Glendenin, Phys. Rev. 95, 431 (1954).

A detailed radiochemical study of resonance fission faces the severe difficulty that the available monoenergetic neutron sources are very weak. Nonetheless, some preliminary studies of this type have been made.

NASUHOGLU and co-workers[138] irradiated samples of U^{235} metal with neutrons of 1.1, 3.1 and 9.5 electron volts energy selected by a crystal spectrometer from the neutrons of the Argonne Research Reactor CP-5. The nuclides Sr^{89}, Ag^{111}, Cd^{115}, and Sb^{127} were isolated quantitatively with an accuracy of about 20 percent. The preliminary data indicated no detectable differences in the relative probabilities of asymmetric modes (represented by Sr^{89}) and near-symmetric modes (represented by Ag^{111}, Cd^{115} and Sb^{127}).

REIGIER, BURGUS and TROMP[139] performed a similar radiochemical experiment with U^{233} targets at the MTR reactor. The neutron resonance energies chosen by them were 1.8, 2.3, and 4.7 electron-volts. It was found that the ratio of asymmetric to symmetric fission is larger by about 20 percent at the 1.8 and 2.3 electron volt resonances than at thermal energies. At the 4.7 ev resonance, however, this ratio is the same as at thermal energies, to within experimental uncertainties.

The Los Alamos Radiochemistry group[140] did a somewhat similar study in which the relative yields of six selected fission products were measured for fission induced in a cadmium-wrapped U^{235} sample placed near the center of the Los Alamos Water Boiler reactor. The cadmium absorbed the neutrons of thermal energy and the observed fission products represented fission events induced by neutrons in the resonance energy region. No dramatic change was observed but there was a definite trend in the radiochemical yields indicating that the valley in the mass yield curve is deeper for fission induced by resonance neutrons than for fission induced by thermal neutrons.

The difficulty of obtaining a sufficient counting rate for a careful study of the mass-yield curve in resonance fission has prompted BOLLINGER and

---

138. Nasuhoglu, Raboy, Ringo, Glendenin and Steinberg, Phys. Rev. 108, 1522 (1957).

139. R. B. Regier, W. H. Burgus, and R. L. Tromp, Phys. Rev. Letters 2, 274 (1959). See also R. B. Regier, W. H. Burgus and B. H. Sorenson, Bull. Am. Phys. Soc. II 5, 33 (1960).

140. Phys. Rev. 107, 325 (1957).

his associates[141] at the Argonne National Laboratory to devise a clever method of obtaining a mass-yield curve by a physical method. In this method a thin sample of fissionable material is placed in a double ionization chamber and exposed to a beam of neutrons. The pulses produced by the two fission fragments in the double Frisch gridded ion chamber are amplified linearly to yield pulses proportional to the energy of the fragments. One of these pulses independently and also the sum of the two pulses is fed to an electronic circuit which converts the ratio of these two pulse heights to two pulses having a time difference proportional to the ratio of pulse heights. This time difference is recorded on a 1024 channel time analyzer. Because of conservation of momentum in the fission process the ratio of pulse heights is proportional to the mass of one of the fragments. The mass-yield curve obtained in this fashion from ionization chamber pulses is better than the mass-yield curve derived in the more conventional way from ionization chamber data as discussed in Sections 11.6.1 and 11.6.2. This difference can be attributed to the great spread in total fragment energy inherent in the fission process for a given mass split. ROELAND, THOMAS and BOLLINGER[141] applied this technique to the case of U^{235} and U^{233} fission in a filtered beam of neutrons with a high proportion of neutron energies near one of the prominent resonances. The upper part of Fig. 11.39 gives the measured mass distribution for thermal neutron fission of U^{235}. The peak-to-valley ratio is 400, a value that is almost as high as the value of 600 obtained radiochemically. The mass distribution was also measured in a filtered beam of neutrons containing chiefly neutrons centered at the prominent U^{235} resonance at 8.9 electron volts. The ratio of the yields in corresponding channels for the resonance neutrons compared to the thermal neutrons is plotted in the lower part of the figure. This ratio does not deviate markedly from unity but there does appear to be a slight increase in the center of the distributiom. If this effect is real it would indicate that U^{235} fission with 8.9 electron volt neutrons has a slightly lower peak to valley ratio than does thermal fission.

---

[141] L. W. Roeland, L. M. Bollinger and G. E. Thomas, Paper P/551, Volume 15, Proceedings of the Second U.N. Conference on the Peaceful Uses of Atomic Energy, Geneva, 1958.

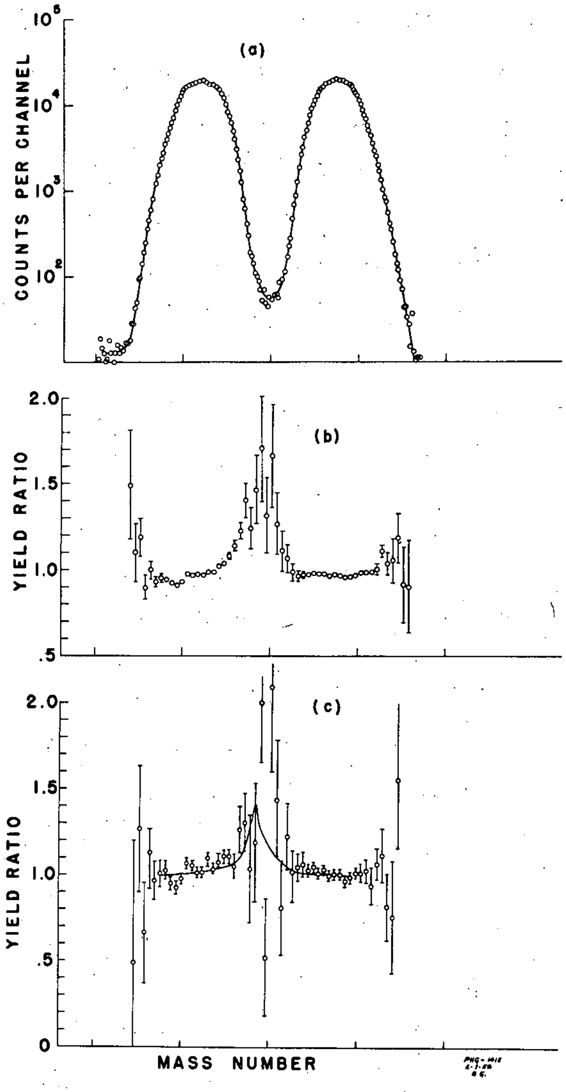

MU - 18902

Fig. 11.39. Mass distribution for U^{235} for thermal neutrons is given in (a) as determined by the special ion-chamber technique of Roeland, Bollinger, and Thomas. In part (b) the U^{235} is caused to fission with a filtered neutron beam in which 50 percent of the neutrons have the resonance energy 8.9 electron volts. What is plotted in (b) and (c) is the ratio of the yields in corresponding channels of the distribution for the resonance neutrons and for the thermal neutrons. (b) shows raw results (c) shows corrected results.

The Los Alamos radiochemistry group[142] overcame the neutron intensity problem by a novel experiment performed during field tests of nuclear explosive devices. In this experiment a fission explosion was used as a source of neutrons many orders of magnitude greater than are available on a resonable time-scale from the best laboratory neutron sources. The experimental arrangement is shown in Fig. 11.40(a). A rotating wheel with a U^{235} rim was located 100 feet from the explosion. Neutrons traveling with different velocities struck the U^{235} target at different points along the rim. The fluxes at the target were 10^{10} or more neutrons per cm^2 per ev with an energy spread at half width of the order of a few percent from energies below 10 ev to in excess of 100 ev. Radio-autographs of the target made it possible to identify many of the main resonances.

The rim was sectioned and radiochemical analysis was carried out for the specific products Mo^{99}, As^{77}, Ag^{111}, Cd^{115} and Ba^{140}. Molybdenum-99 yields were used as a measure of total fissions in each section of the U^{235} rim; several individual resonances were resolved below 60 ev as well as several packets of levels at higher levels. Comparison of the peak-to-valley yield ratios showed that there are no highly symmetric modes of fission (Ag^{111} or Cd^{115} yields $\geq$ 1 percent) in the energy interval 9 to 500 electron volts. Figure 11.40(b) shows the change in the Ag^{111}/Mo^{99} activity ratio as a function of neutron energy. Fluctuations of the order of 30 percent occur in this ratio.

It is clear that a series of experiments of this type would permit a very sensitive and fruitful analysis of many features of the fission of heavy nuclei with neutrons of resonance energy.

11.4.5 *Fission Product Yields in Spontaneous Fission*. It seems likely that spontaneous fission must involve a single fission channel. It might be expected that the mass distribution of the fission products, as well as other characteristics, of spontaneous fission would provide very exact information on the nature of fission in a single-channel process. However, the number of nuclei for which detailed studies of the characteristics of spontaneous fission can be made is limited by the strong dependence of the probability of spontaneous fission on atomic number and on nuclear type as discussed in Section 11.3.6.

---

[142] G. A. Cowan and A. Turkevich, Bull. Am. Phys. Soc. II, 4, 31 (1959) and private communication from G. A. Cowan. Detailed paper to be published. See also report of Plowshare Conference in Report UCRL-5679, May 15, 1959.

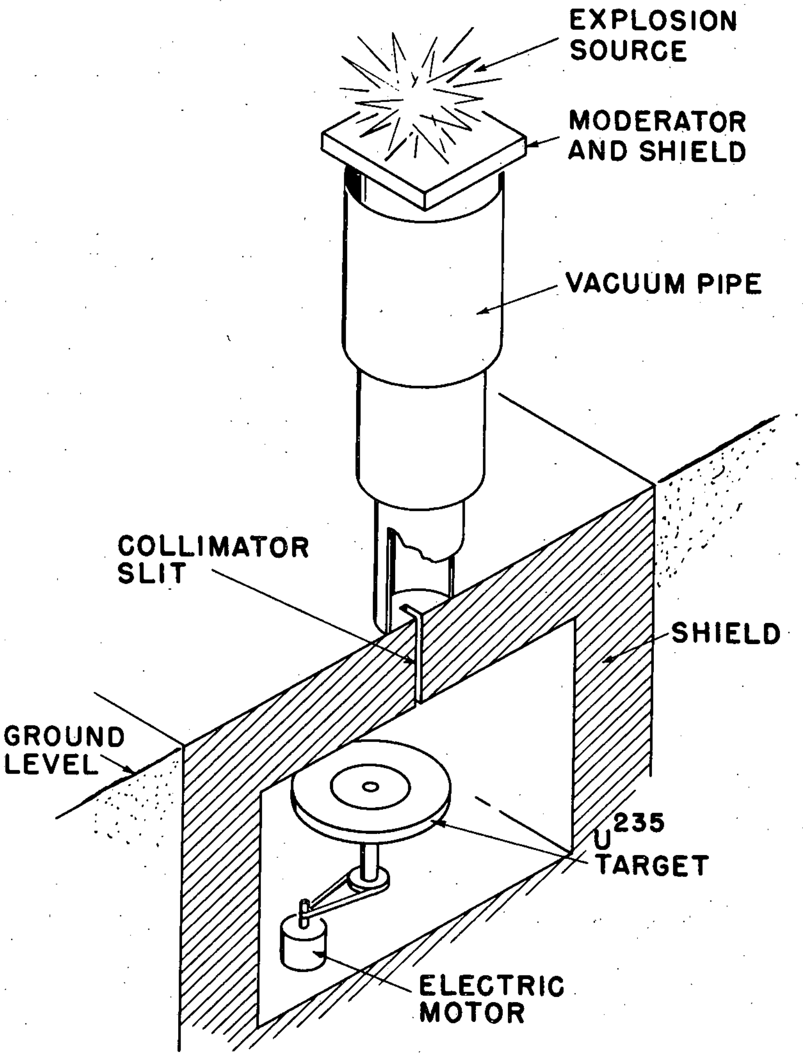
EXPLOSION SOURCE
MODERATOR AND SHIELD
VACUUM PIPE
COLLIMATOR SLIT
SHIELD
GROUND LEVEL
U^{235} TARGET
ELECTRIC MOTOR
MU-18872

Fig. 11.40(a). Sketch of Los Alamos "wheel" experiment for measurement of resonance fission characteristics. Figure supplied by G. A. Cowan.

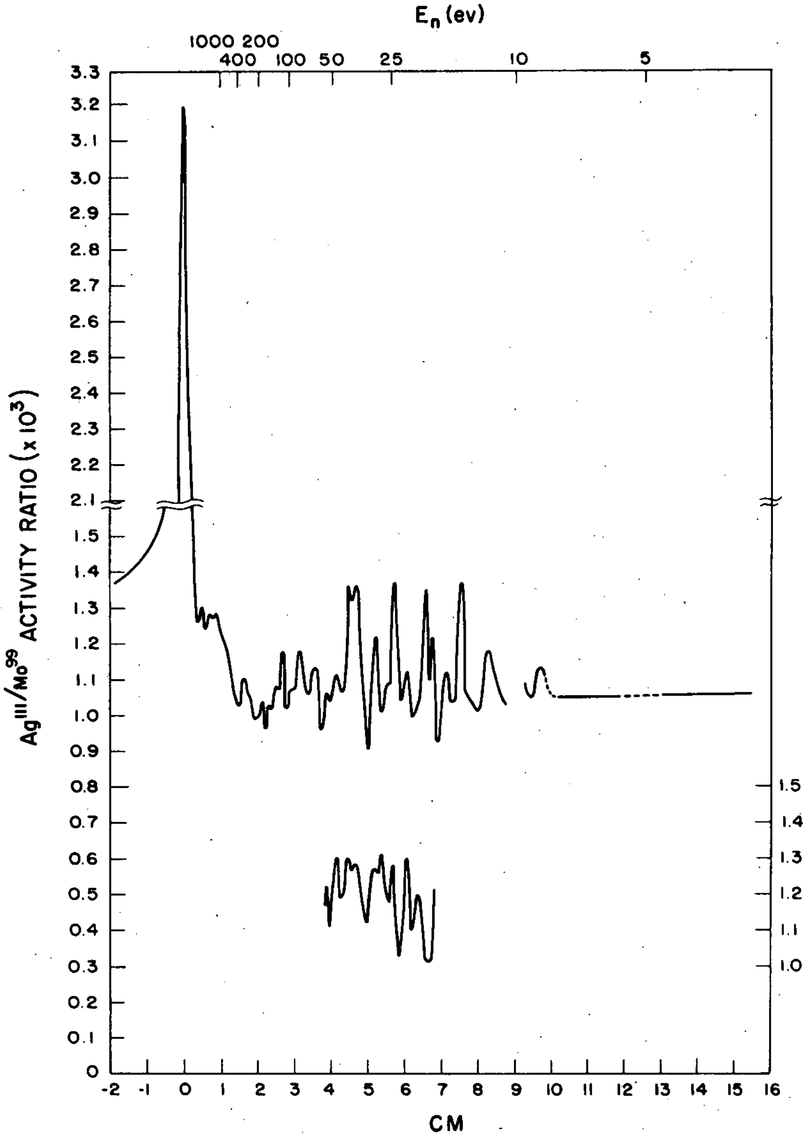

MU-18871

Fig. 11.40(b). Ratio of Ag^{111} to Mo^{99} in resonance fission of U^{235}. Figure supplied by G. A. Cowan.

The study of spontaneous fission of thorium or uranium is greatly hampered because of the measured half lives of greater than 10^{20} years and 1.3×10^{16} years, respectively, for these elements. See Table 11.7. Nonetheless, a few investigations have been carried out. The most successful have been the extraction from uranium and thorium minerals of the stable rare gas isotopes which have been accumulating in the minerals throughout geological time. For example, the spontaneous fission from one gram of uranium produces about 10^{-7} cc of Xe^{136} in 300 million years. In a 6% uranium mineral having this age the ratio of fission product Xe^{136} to normal Xe^{136} should be about 60. Thus in radioactive minerals the total amount of xenon and krypton as well as the isotopic distribution should be very different from that found in ordinary minerals. Modern techniques of mass spectrometry are so sensitive that the isotopic composition of gas volumes of this extremely small size can be determined accurately. In 1947, KHLOPIN, GERLING and BARONOVSKAYA[143] found that pitchblende contained more xenon than is usually found in minerals and that the quantity of xenon is in rough agreement with the assumption that the xenon was produced by spontaneous fission. In 1950 MACNAMARA and THODE[144] reported measurements on the isotopic abundances of xenon and krypton extracted from a sample of pitchblende with an age of about 1.4×10^{9} years. Five fission product isotopes of xenon (Xe^{129}, Xe^{131}, Xe^{132}, Xe^{134} and Xe^{136}) and three of kryton (Kr^{83}, Kr^{84}, Kr^{86}) were identified. It is interesting to note that Xe^{129} is an observed product of the spontaneous fission of U^{238} since it is not seen in the fission gases of the slow neutron fission of U^{235}. The reason for this is that its precursor I^{129} has a half life of 1.7×10^{7} years. WEATHERILL[145] measured the isotopes of xenon and krypton from samples of the uranium minerals, euxenite and pitchblende, and of the thorium mineral, monazite. FLEMING and THODE[146] measured the fission yields of these fission gases in six samples of pitchblende and one sample of uraninite. When all the results were compared it was clear that the

---

143. Khlopin, Gerling and Baronovskaya, Bull. Acad. Sci. USSR Classe Sci. Chim. 599 (1947); Chem. Abs. 42, 3664 (1948).

144. J. Macnamara and H. G. Thode, Phys. Rev. 80, 471 (1950).

145. G. W. Weatherill, Phys. Rev. 92, 907 (1953).

146. W. H. Fleming and H. G. Thode, Phys. Rev. 92, 378 (1953).

pattern of xenon isotopes varied to some extent from sample to sample. It became clear that one must be cautious about attributing all the observed xenon and krypton in a uranium mineral to the spontaneous fission of the U^{238}. Some fission of U^{235} with the neutrons of natural origin may contribute to the rare gas fraction. The extent to which neutron fission of U^{235} competes with natural fission of U^{238} depends on the concentration of uranium in the mineral, the age of the mineral and the nature of the impurities. The measurement of minute amounts of plutonium in uranium minerals[147] resulting from the capture of natural neutrons by U^{238} is a very direct indication of a measurable neutron concentration in uranium minerals. This is fully discussed in Section 3.6 of Chapter 3. The neutrons come chiefly from the spontaneous fission of U^{238} and from (α,n) reactions caused by the action of the alpha emitters from the uranium series on the light elements in the ore.

By an examination of the trends in the xenon isotope ratios in various uranium minerals it was possible for WEATHERILL[145] and for FLEMING and THODE[146] to state three important ways in which spontaneous fission yields differ from fission yields in neutron-induced fission.

1. The mass yield curve for spontaneous fission is much steeper indicating a more selective division of mass. The lighter isotopes of xenon are formed in much lower yield than they are in slow neutron induced fission.

2. The "fine structure" characteristics are different. In the case of U^{235} fission Xe^{133} and Xe^{134} have abnormally high yields, whereas in natural fission the yield of Xe^{132} is abnormally high and the yield of Xe^{134} is markedly down.

3. The yield of xenon relative to krypton is higher in spontaneous fission.

The measurement of the fission yields of other products by more standard radiochemical techniques has not proceeded far because of the extremely low counting rates of the fission elements which are to be found in uranium samples of manageable proportions. PARKER and KURODA[148] for example isolated molybdenum from 3420 grams of purified uranyl nitrate and found an equilibrium amount of 67 hour Mo^{99} equal to only 1 count per minute in their counter. They calculated an equilibrium activity of 1.26 x 10^{-14} curies of Mo^{99} per gram of U^{238} which corresponds to a spontaneous fission half life of 8.4 ± 0.8 x 10^{15} years for U^{238} assuming a Mo^{99} fission yield of 6.2 percent. ASHIZAWA and KURODA[149] measured the amounts of several iodine isotopes in 1.5 kilograms of highly purified uranium and found the following equilibrium amounts in units of 10^{-4} disintegrations per second per gram of U^{238}: I^{131}, 0.3 ± 0.1; I^{132}, 2.5 ± 0.3; I^{133}, 1.0 ± 0.2; I^{134}, 3.6 ± 0.4; I^{135}, 3.5 ± 0.4. KURODA and EDWARDS[150] measured Ba^{140} present in 4.5 kilograms of uranyl acetate and found 1.6 x 10^{-14} counts per minute per gram of U^{238}. Radiochemical studies of this type serve to verify that the natural fission rate of uranium measured by physical means is of the correct order of magnitude. The data are not extensive enough, and are not likely to become extensive enough, to permit a careful exploration of the structure of the spontaneous fission-yield curve in U^{238}. For example, a ton of U^{238} would be required to obtain a measurable activity of a fission product with a fission yield of 0.01 percent.

---

[147] C. A. Levine and G. T. Seaborg, J. Am. Chem. Soc. 73, 3278 (1951).

[148] P. L. Parker and P. K. Kuroda, J. Chem. Phys. 25, 1084 (1956).

RUSSELL and TURKEVICH[151] made the radiochemical determinations of spontaneous fission yields summarized in Table 11.13 using kilogram quantities of U^{238} as the fission source. Figure 11.41 combines these radiochemical results with the rare gas mass-spectrometric determinations of WETHERILL[145] into a mass-yield curve.

For a more complete radiochemical study of spontaneous fission products it is quite essential to study isotopes of heavier even-Z elements. Some of the more suitable candidates from the standpoint of their availability as well as their radiation characteristics are the ones listed in the table.

---

[149] F. T. Ashizawa and P. K. Kuroda, J. Inorg. Nucl. Chem. 5, 12 (1957); See also preliminary study by Kuroda, Edwards and Ashizawa, J. Chem. Phys. 25, 603 (1956).

[150] P. K. Kuroda and R. R. Edwards, J. Inorg. Nucl. Chem. 3, 345 (1957).

[151] I. J. Russell and A. Turkevich, unpublished results; I. J. Russell, Ph.D. Thesis, Department of Chemistry, University of Chicago, December, 1956.

Table 11.13

Fission yields in the spontaneous fission of U^{238} as reported by RUSSELL and TURKEVICH

Nuclide	Fission yield	Nuclide	Fission yield
Sr^{89}	2.9 ± 0.3	Y^{91}	6.9 ± 0.5
Mo^{99}	6.0 ± 0.5	Ag^{111}	0.05(upper limit)
Pd^{109}	0.02(upper limit)	Cd^{115}	0.02(upper limit)
Te^{132}	4.5 ± 0.5	Pr^{143}	7.5 ± 0.5
Ce^{144}	6.5 ± 0.5	Nd^{147}	4.2 ± 0.4

Specific fission rates of selected transuranium element nuclides

Isotope	Partial half life for spontaneous fission decay (years)	Spontaneous fissions per minute per milligram
Cm^{242}	7.2×10^{6}	4.66×10^{5}
Cf^{252}	66	4.5×10^{10}
Fm^{254}	0.60	5×10^{12}

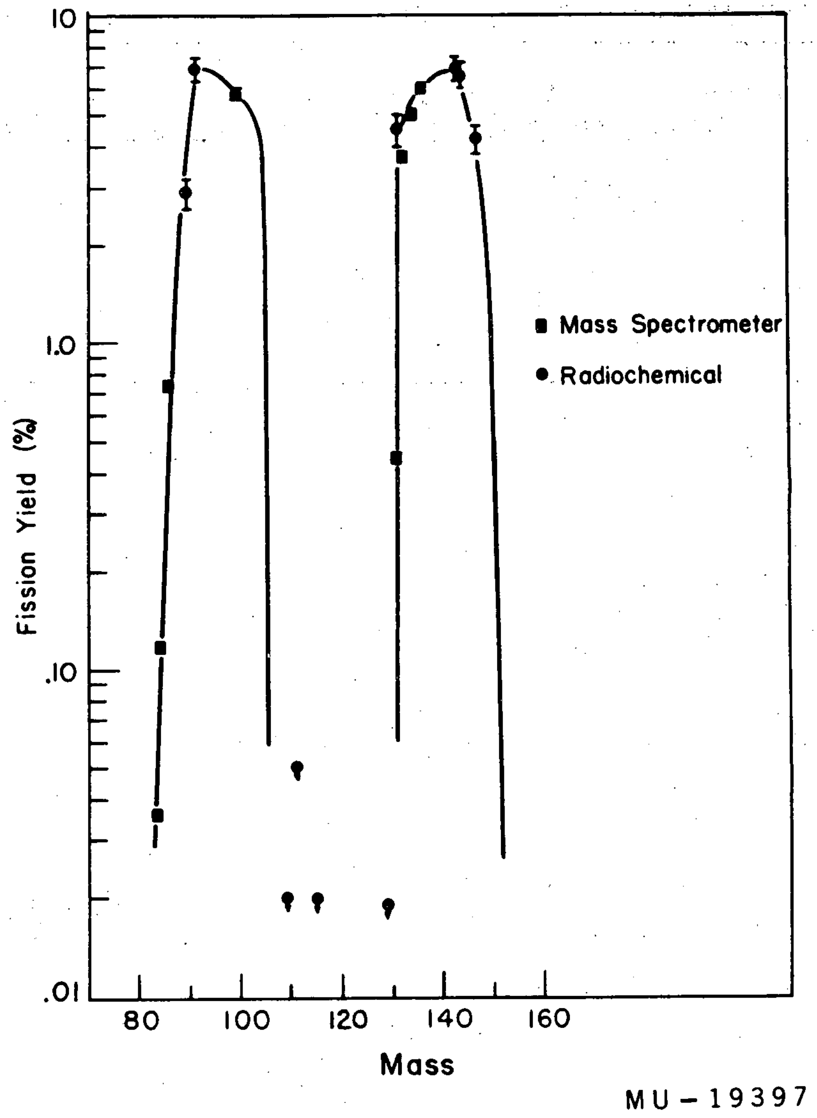

Fig. 11.41. U^{238} spontaneous fission yield distribution. The ordinate is the fission yield in percent. The abscissa is the mass of the fission product. Round points correspond to radiochemical determinations of Russell and Turkevich. Square points correspond to mass spectrometric determinations by G. W. Wetherill [Phys. Rev. 92, 907 (1952)]. Wetherill's data are normalized to 6.0% at Xe^{136}. Radiochemical data are based upon a spontaneous fission half life of 8.0×10^{15} years [E. Segre, Phys. Rev. 86, 21 (1952)].

STEINBERG and GLENDENIN[152] studied the fission products from a one milligram sample of Cm^{242}. Procedures were worked out for isolating several fission product elements from the 7 x 10^{12} alpha disintegrations per minute of Cm^{242}. The yields of 21 nuclides, enough to define the major features of the mass yield curve, were determined. Their procedure was to purify the parent sample of Cm^{242}, to let it stand for a certain period of time and then to isolate and measure specific fission products by quantitative radiochemical techniques. The results given in Table 11.14 and Fig. 11.42 show that spontaneous fission of Cm^{242} is more asymmetric than the thermal neutron fission of U^{235}, U^{233} or Pu^{239}. The peak-to-trough ratios are higher and the light and heavy peaks are higher and narrower. The light peak shifts toward heavier mass numbers. The fine structure effect in Cm^{242} due to preference for 82 neutrons in the fission act is very pronounced in both peaks. It was estimated that the excess yields due to this effect over the "smooth" curve was about 7 percent.

GLENDENIN and STEINBERG[153] also investigated radiochemically some products of spontaneous fission of Cf^{252} using a 10^{-10} gram source possessing a spontaneous fission rate of a few thousand per minute. CUNNINGHAME[154] also contributed to this investigation.

The most comprehensive radiochemical study was carried out by NERVIK and STEVENSON[155] with the assistance of several co-workers. One source of 1 x 10^{6} and another of 2 x 10^{7} fissions per minute were used to obtain the data. The results are presented in Table 11.15 and in Fig. 11.43. The fission yield curve has maxima of 6.2 percent at masses 107 and 141 with the width at 1/10 maximum of each peak being approximately 27 mass units. The peaks are much narrower than the comparable ones in the slow neutron fission of U^{235}. There is a very narrow "trough" with a minimum value of 1 x 10^{-2} percent at mass number 124. In addition, while the curve as a whole is symmetrical about mass 124, each peak is not symmetrical about its own maximum, being significantly

---

152. E. P. Steinberg and L. E. Glendenin, Phys. Rev. 95, 431 (1954).
153. L. E. Glendenin and E. P. Steinberg, J. Inorg. Nuclear Chem. 1, 45 (1955).
154. J. G. Cunninghame, J. Inorg. Nuclear Chem. 4, 1 (1957).
155. W. E. Nervik and P. C. Stevenson, unpublished results; abstract published in Bull. Amer. Phys. Soc. II, 4, 372 (1959), Nervik Stevenson, Hicks, Levy, Niday and Armstrong.

Table 11.14

Fission yields in spontaneous fission of Cm^{242}

Nuclide	Observed fission yield (%)	Calculated independent fission yield of daughter[c] (%)	Total fission yield of chain (%)
9.7-hr Sr^{91}	0.94 ± 0.3	0.01	0.95 ± 0.3
2.7-hr Sr^{92}	1.1 ± 0.3	0.1	1.2 ± 0.3
67-hr Mo^{90}	5.7 ± 0.7	0	5.7 ± 0.7
40-day Ru^{103}	7.2 ± 1.5	0	7.2 ± 1.5
4.5-hr Ru^{105}	9.5 ± 0.9	0.4	9.9 ± 1.0
1.0-yr Ru^{106}	7.4 ± 0.8	1.0	8.4 ± 1.0
13.1-hr Pd^{109}	2.9 ± 0.4	0	2.9 ± 0.4
21-hr Pd^{112}	0.95 ± 0.15	0.15	1.1 ± 0.2
53-hr Cd^{115}	0.033±0.01	0	
43-day Cd^{115m}	(0.003)[a]	0	0.036±0.01
3.0-hr Cd^{117m}	<0.01	0	<0.01
93-hr Sb^{127}	0.35 ± 0.1	0.02	0.37 ± 0.1
4.2-hr Sb^{129}	1.3 ± 0.3	0.4	1.7 ± 0.4
30-hr Te^{131m}	2.3 ± 0.5	---	
8.0-day I^{131}	2.0 ± 0.4[b]	0	4.3 ± 0.7
77-hr Te^{132}	5.8 ± 0.9	1.6	7.4 ± 1.3
21-hr I^{133}	5.7 ± 0.8	0.3	6.0 ± 0.9
52.5-min I^{134}	6.9 ± 1.0	1.1	8.0 ± 1.3
6.7-hr I^{135}	3.9 ± 0.6	3.4	7.3 ± 1.4
13.7-day Cs^{136}	0.80 ± 0.12	---	
85-min Ba^{139}	6.6 ± 0.7	0	6.6 ± 0.7
12.8-day Ba^{140}	5.9 ± 0.8	0	5.9 ± 0.8

a. Assumed yield from known branching ratio in induced fission.

b. Yield independent of 30-hr Te^{131m}.

c. Calculated independent yields assume validity of equal charge displacement hypothesis and a $\bar{\nu}$ value of 3.

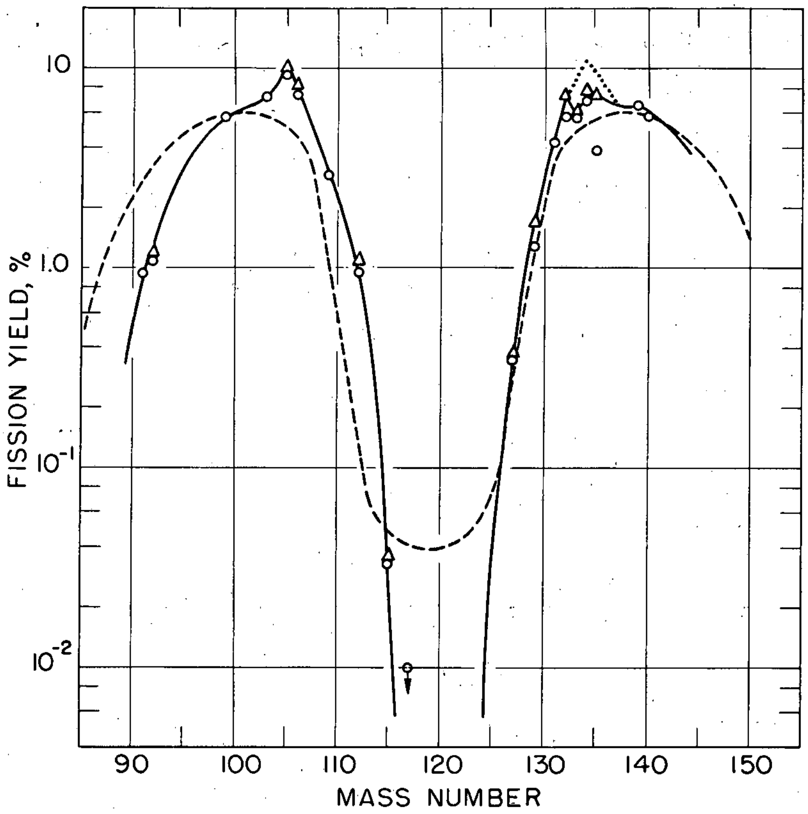

MU-18710

Fig. 11.42. Yield mass curves for spontaneous fission of Cm^{242} (solid line) and pile neutron fission of Pu^{239} (dashed line). Circles represent observed yields and triangles estimated total chain yields. Steinberg and Glendenin.[152]

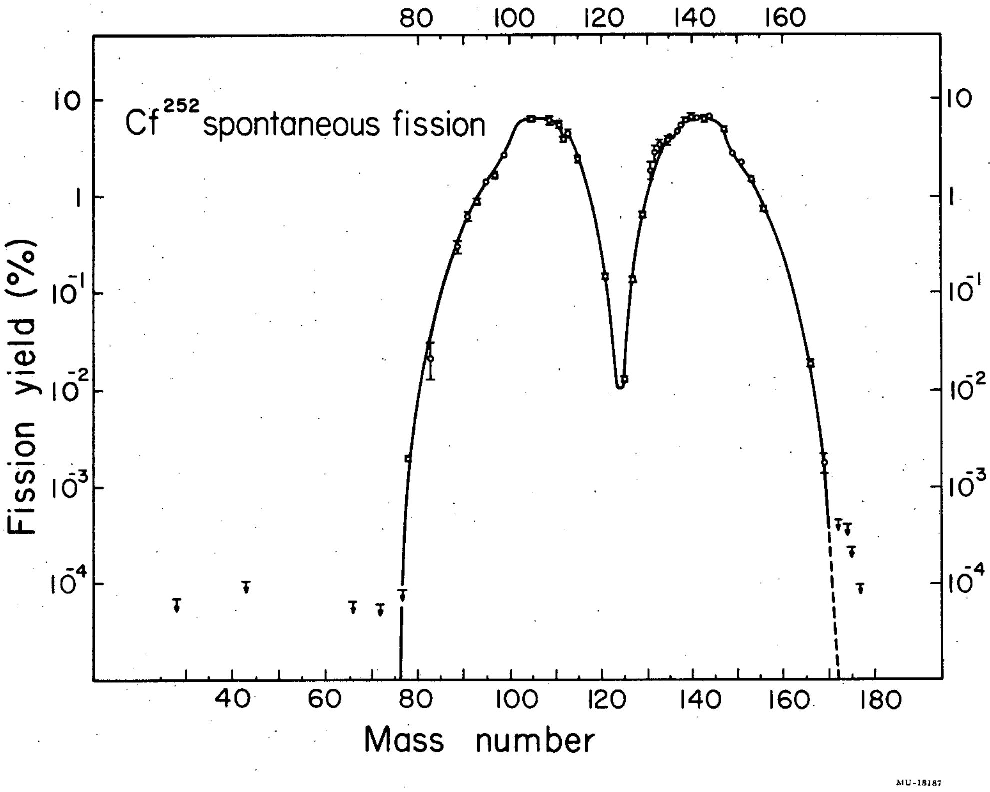

Fig. 11.43. Mass-yield curve for Cf^{252} spontaneous fission. Figure prepared by W. Nervik.

Table 11.15

Spontaneous fission yields of Cf^{252}

Nuclide	Number of determinations	Fission yield %		
		Nervik et al.[155]	Glendenin and Steinberg[153]	Cunninghame[154]
Mg^{28}	1	$\leq 7.1\times10^{-5}$		
K^{43}	2	$\leq 1.1\times10^{-4}$		
Ni^{66}	2	$\leq 6.8\times10^{-5}$		
Zn^{72}	2	$\leq 6.2\times10^{-5}$		
As^{77}	2	$\leq 8.8\times10^{-5}$		
As^{78}	3	$1.97\times10^{-3}\pm0.18$*		
Br^{83}	3	$2.14\times10^{-2}\pm0.93$		
Sr^{89}	2	0.32±0.01		
Y^{91}	2	0.61±0.06		
Y^{93}	3	0.87±0.03		
Zr^{95}	1	1.42		
Zr^{97}	3	1.60±0.16		2.1±0.3
Mo^{99}	3	2.60±0.08	2.2±0.5	3.0±0.45
Mo^{101}				4.1±0.8
Rh^{105}	4	6.22±0.22		
Ru^{105}			9.2±1.4	
Pd^{109}	5	5.91±0.61	6.8±1.3	
Ag^{111}	4	5.39±0.30	4.5±0.9	
Pd^{112}	5	3.79±0.18	4.5±0.9	
Ag^{113}	4	4.39±0.39	4.2±0.8	
Cd^{115}	4	2.37±0.13	2.8±0.5	
In^{117}			<1.0	
Sn^{121}	3	0.148±0.009		
Sn^{125}	3	$1.25\times10^{-2}\pm0.005$		
Sb^{127}	3	0.135±0.009		
Sb^{129}	3	0.639±0.017		
I^{131}	3	1.84±0.38		
Te^{132}	3	2.79±0.44	2.8±0.4	
I^{133}	3	3.37±0.42	4.8±0.7	
I^{134}	3	[illegible]	4.2±0.6	

Table 11.15 (cont'd.)

Nuclide	Number of determinations	Fission yield % Nervik et al.[155]	 Glendenin and Steinberg[153]	 Cunninghame[154]
I^{135}	3	3.61±0.30	4.0±0.6	
Cs^{136}	1	$3.7\text{x}10^{-2}$ (independent yield)		
Cs^{137}	1	4.57		
Cs^{138}	1	5.13	6.3±0.9	
Ba^{139}	2	5.96±0.17	6.2±0.9	
Ba^{140}	7	6.56±0.57		
Ce^{141}	1	6.39		
Ce^{143}	3	6.17±0.36	7.8±1.5	
Pr^{143}				7.4±1.5
Ce^{144}	1	6.69		
Nd^{147}	6	4.83±0.09		4.0±0.8
Pm^{149}	1	2.75		
Pm^{151}	1	2.26		
Sm^{153}	6	1.47±0.035		1.3±0.3
Eu^{156}	3	0.73±0.009		
Dy^{166}	3	$1.80\text{x}10^{-2}$±0.16		
Er^{169}	3	$1.72\text{x}10^{-3}$±0.41		
Tm^{172}	3	$\leq 0.44\text{x}10^{-4}$		
Tm^{174}	3	$\leq 4.0\text{x}10^{-4}$		
Yb^{175}	2	$\leq 2.3\text{x}10^{-4}$		
Lu^{177}	1	$\leq 9.6\text{x}10^{-5}$		

---

*Average deviation of multiple determinations.

spread toward the most asymmetric fission modes. No evidence was seen of fine structure in either peak; nor was there evidence of activities which could be ascribed to ternary fission events, upper limits of 10^{-4}% fission yield being set for individual nuclides between mass numbers 28 and 72.

11.4.6 *Ternary Fission*. All studies of low-energy fission indicate that the process results predominantly in the division of the fissioning nucleus into two fragments plus two or three neutrons. PRESENT[156] showed that the liquid drop model of fission does not rule out the possibility of ternary fission into three fragments of roughly equal masses. Evidence for tripartite fission has been sought by a variety of methods, chiefly by the examination of fission tracks in nuclear emulsions impregnated with fissile material and by studies using multiple ionization chambers.[‡] The findings of these studies can be grouped in three categories for the case of U^{235} caused to fission with slow neutrons.

(1) The most prominent and best-established type of ternary fission is the emission of high speed alpha particles in coincidence with two heavy fragments of the conventional type. The abundance of this type of fission is roughly one in 400 of normal binary fission events. The alpha particles have a distribution in energy up to 29 Mev but the distribution shows a definite broad peak at 15 Mev. The angular distribution of the alpha particles shows a strong peaking at an angle a few degrees less than 90° with respect to the direction of the lighter of the two heavy fragments.

(2) The second type of ternary fission is the splitting of the nucleus into three fragments of roughly equal mass. A conservative upper limit to this process for low-energy fission is one such event in 100,000 normal binary events. The low incidence of this process puts severe conditions on its study. In nuclear emulsion studies, aside from the necessity to investigate hundreds of thousands of events, there is the difficulty of positively distinguishing between a triple track due to a triple fission event and a triple track due to

---

156. R. D. Present, Phys. Rev. 59, 466 (1941).

[‡] An excellent and detailed discussion of ternary fission is given by Demers in his book "Ionographe; les Emulsions Nucleaires", Montreal University Press, Ottawa (1958).

a binary fission event plus a heavy recoil originating in the emulsion at approximately the point of fission. On the other hand when tripartite fission is investigated by observing the three fragments in a multiple ionization counter coincidence experiment it is necessary to eliminate accidental coincidences produced by two binary fissions occurring within the resolving time of the coincidence equipment. ROSEN and HUDSON[157] made a particularly careful study by the coincidence method and in the case of U^{235} they arrived at a frequency of ternary fission of 6.7 ± 3.0 in 10^6 binary fissions. PERFILOV[158] points out that this measurement does not apply to the possibility of an asymmetric division which led to a kinetic energy < 40 Mev for one fragment.

In the wartime radiochemical research on the fission products[159] a determined search was made for possible products of ternary fission in which one fragment might have a mass in the range of 35-60 units. Nuclides of sulfur, chlorine, calcium, scandium and iron were investigated and upper limits of 10^{-4} percent or less were set on the total number of fissions resulting in the production of such nuclides.

MUGA and THOMPSON[160] have looked at fission tracks of Cf^{252} in nuclear emulsions impregnated with this spontaneously-fissioning nuclide. They found several definite events in which true triple fission of type 2 had occurred and set a conservative lower limit of one triple fission to 20,000 binary fission cases. The true rate may be several-fold greater. Hence triple fission of this type is considerably more frequent in the spontaneous fission of Cf^{252} than it is in the slow neutron fission of U^{235}.

(3) A third type of triple fission consists of the emission of light particles of low Z (variously reported as 1, 2 or, in some cases, higher than 2) and of low energy (of the order of 1 Mev). These particles are distinguished by their

---

157. L. Rosen and A. M. Hudson, Phys. Rev. 78, 533 (1950).

158. N. A. Perfilov in Physics of Fission, English Translation of a Conference of this title published as Supplement 1 to the Soviet Journal of Atomic Energy, 1957,

159. See papers by Metcalf, Seiler, Steinberg, and Winsberg in Book 1, of "Radiochemical Studies: The Fission Products", National Nuclear Energy Series, edited by C. D. Coryell and N. Sugarman, McGraw-Hill Book Co., New York, 1951.

160. L. Muga and S. G. Thompson, results to be submitted for publication in the Phys. Rev. (1960).

frequency and their energy from the energetic α-particles comprising type (1)

Several studies[161-164] dealing with these light fragments of low-energy assign rather high probability to their occurrence (about one percent). It is difficult to distinguish such particles from protons and other nuclear recoils produced by fission fragments in their passage through nuclear emulsion or counter gas and the interpretation of these data is open to some question.[165] It has been suggested also that some of these light fragments might have nuclear charges greater than 2. The emission of light fragments with the nuclear charge of beryllium seems to be ruled out conclusively by radiochemical experiments. COOK[166] set an upper limit of 10^{-5} percent to the formation of Be^7 in uranium fission. FLYNN, GLENDENIN and STEINBERG[167] set an upper limit of 4×10^{-4} percent to the formation of 2.5 million year Be^{10}.

We shall not consider further triple fission of type 3.

We turn now to a fuller account of triple fission of the first type. ALVAREZ[168] in 1943 was the first to observe triple fission into two heavy particles and one light particle, but this discovery was not reported until after the war. The first published literature was that by SAN-TSIANG ZAH-WEI, CHASTEL and VIGNERON.[169] The literature on the subject up to 1950 is well reviewed by

---

161. Tsien, Ho, Chastel and Vigneron, J. Phys. radium 8, 165, 200 (1947).
162. K. W. Allen and J. T. Dewan, Phys. Rev. 82, 527 (1951).
163. L. L. Green and D. L. Livesey, Trans. Royal Soc. (London) A241, 323 (1948).
164. E. W. Titterton, Nature 168, 590 (1951).
165. See for example the discussion by Demers p357 IONOGRAPHE; Les Emulsions Nucleaires, Montreal University Press, Ottawa (1958).
166. G. B. Cook, Nature 169, 622 (1952).
167. K. F. Flynn, L. Glendenin and E. P. Steinberg, Phys. Rev. 101, 1492 (1956).
168. L. W. Alvarez as reported by Farwell, Segre and Wiegand, Phys. Rev. 71, 327(1947).
169. San-Tsiang Zah-Wei, Chastel and Vigneron, Compt. Rendus 223, 986 (1946); 224, 272 (1947); and Phys. Rev. 71, 382 (1947).
170. L. Rosen and A. M. Hudson, Phys. Rev. 78, 533 (1950).

ROSEN and HUDSON[170] and by ALLEN and DEWAN.[162] An excellent later review is that of DEMERS.[171] The ionization and range characteristics of the light particles leave no doubt that they are helium ions. Experiments dealing with the frequency of this type of triple fission are summarized in Table 11.16. It is not clear why there is such a spread in the reported results. It has been suggested that the variation might be attributed to differences in the energy of the neutrons causing fission but the preliminary results of AUCLAIR[172] argue against this interpretation.

The energy distribution of the long-range alpha particles has been studied by measurement of ranges in nuclear emulsions,[164] by ionization chamber measurements[173] and by magnetic analysis.[174] The results, which agree rather well, are summarized in Fig. 11.44. MUGA and THOMPSON[160] investigated the energy distribution of the long-range alpha particles in the spontaneous fission of Cf^{252}. Their results, summarized in Fig. 11.45 show a peaking at a somewhat higher energy than in the U^{235} case.

The angular distribution follows that to be expected of an alpha particle formed at the instant of fission and traveling away from the origin in the Coulombic field of the heavy fragments. TITTERTON[164] investigated a huge number of events by the emulsion technique and found a strong peaking of the angular distribution at 82° with respect to the lighter of the fission fragments. MUGA and THOMPSON[160] studied Cf^{252} and reported a strong peaking at 85° with respect to the lighter of the fragments.

The observation of these alpha particles with the reported energy and angular distribution can be explained from a simple qualitative picture based on the liquid drop model of nuclear division. This explanation has been well stated by HILL and WHEELER[175] whom we quote here.

---

171. P. Demers, Ionographie, Les Emulsions Nucleaires, Montreal University Press, Ottawa (1958), pp. 353-355.

172. J. M. Auclair, Proceedings of the International Conference on the Neutron Interactions with the Nucleus, held at Columbia University, Sept. 9-13, 1957, Report TID-7547, p. 139.

173. K. W. Allen and J. T. Dewan, Phys. Rev. 80, 181 (1950).

174. C. B. Fulmer and B. L. Cohen, Phys. Rev. 108, 370 (1957).

175. D. L. Hill and J. A. Wheeler, Phys. Rev. 89, 1102 (1953).

Table 11.16

Probability of Emission of Long-Range Alpha Particles in Low-Energy Fission

Investigators	Target nucleus	Neutron source	Frequency compared to total fission events
Fulmer and Cohen	U^{235}	pile neutron	1 to 310
Allen and Dewan	U^{233}	thermal neutrons	1 to 405 ± 30
Allen and Dewan	U^{235}	thermal neutrons	1 to 505 ± 50
Allen and Dewan	Pu^{239}	thermal neutrons	1 to 445 ± 35
Titterton	U^{235}	thermal neutrons	1 to 422 ± 50
Farwell, Segre and Wiegand	U^{235}	cyclotron slow neutrons	1 to 250
Farwell, Segre and Wiegand	Pu^{239}	cyclotron slow neutrons	1 to 500
Green and Livesey	U^{235}	cyclotron slow neutrons	1 to 300
Demers	U^{235}	Ra-Be source	1 to 250
Marshall	U^{235}	thermal	1 to 230
Muga and Thompson	Cf^{252}	spontaneous fission	1 to 415

C. B. Fulmer and B. C. Cohen, Phys. Rev. 108, 370 (1957).

K. W. Allen and J. T. Dewan, Phys. Rev. 80, 181 (1950).

K. T. Titterton and F. K. Goward, Phys. Rev. 76, 142 (1949).

K. T. Titterton, Nature 168, 590 (1951).

G. Farwell, E. Segre and C. Wiegand, Phys. Rev. 71, 327 (1947).

L. L. Green and D. L. Livesey, Nature 159, 332 (1947).

P. Demers, Phys. Rev. 70, 974 (1946).

L. Marshall, Phys. Rev. 75, 1339 (1949).

L. Muga and S. G. Thompson, unpublished results, 1959.

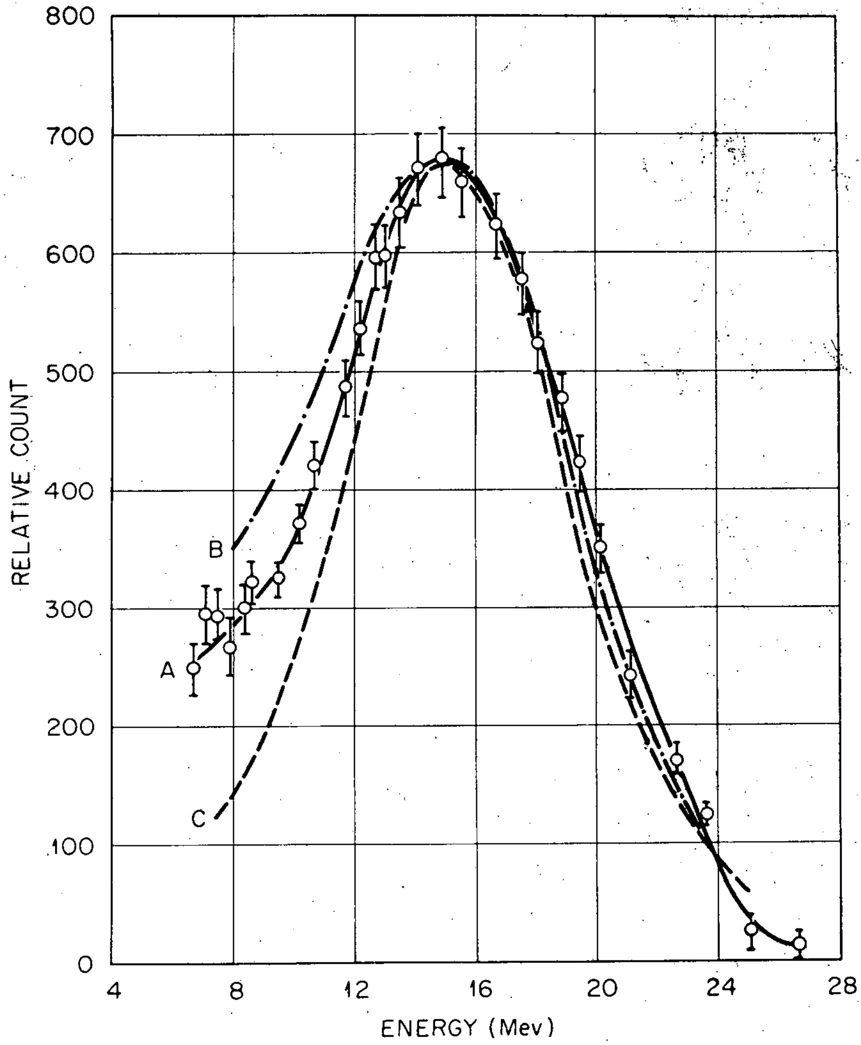

MU-19358

Fig. 11.44. Energy distribution of long-range alpha particles from the pile neutron fission of U^{235}. Curve A is the distribution determined by FULMER and COHEN[174] by magnetic analysis. Curve B is the work of ALLEN and DEWAN.[173] Curve C is the distribution determined by TITTERTON[164] using an emulsion technique. Figure reproduced from FULMER and COHEN.[174]

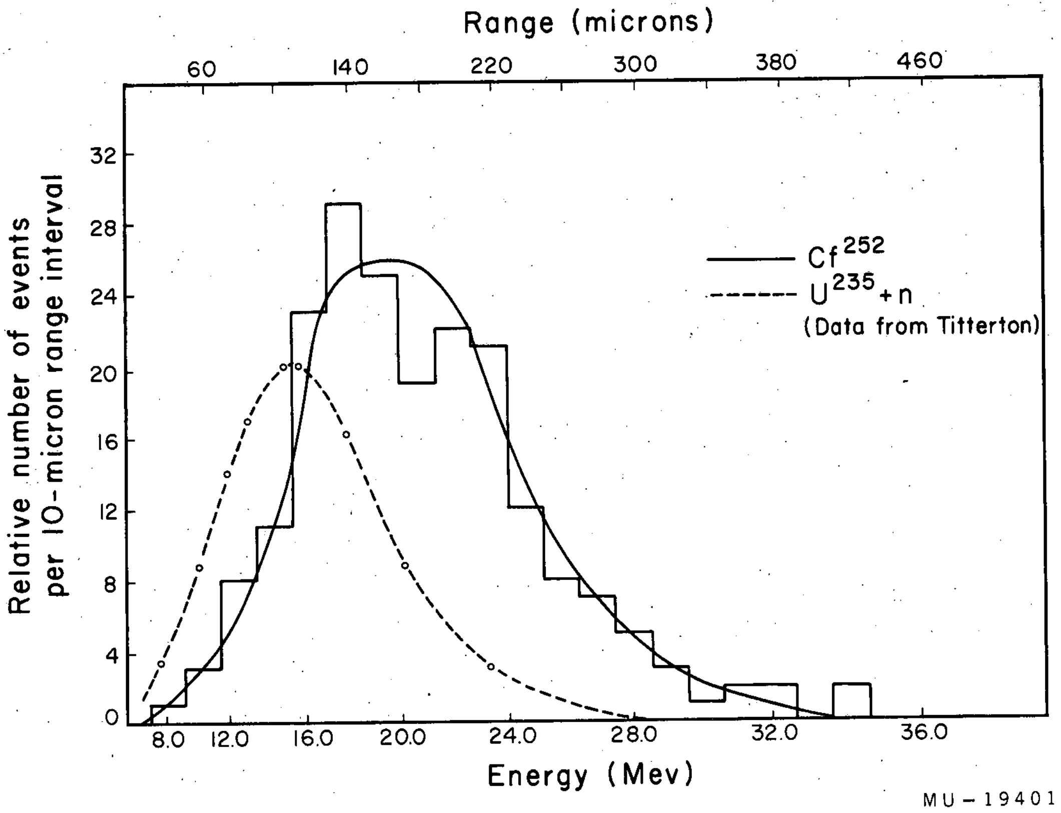

Fig. 11.45. Comparison of the energy distribution of long-range alpha particles from the spontaneous fission of Cf^{252} (MUGA and THOMPSON[160]) and from the slow neutron fission of U^{235} (TITTERTON[164]). Figure prepared by L. Muga.

"From classical hydrodynamics it is well known that the disintegration of a liquid jet into drops leads to the formation between these fragments of tiny droplets. Likewise in the case of nuclear fission it is not surprising to find some portion of the nuclear substance set free between the fission fragments in the act of scission. It is necessary to distinguish between alpha-particles, protons and neutrons. Of these only the alpha-particles represent nearly saturated nuclear matter, and only they are energetically capable of emerging from the original nucleus already in its unexcited state. But an alpha-particle at the surface of the original nucleus is far below the level of the Coulomb potential, on account of the coupling to its surroundings. In contrast, an alpha-particle in the region of scission lies at the point of maximum Coulomb potential, and yet has less than the normal amount of nuclear matter immediately around it with which to form bonds. This particular alpha-particle has in effect been raised to a point but little lower than the top of the barrier, by means of the changes of nuclear form which took place up to the moment of scission. An alpha-particle in such a position will have a significant probability to pass through the barrier. Thus it is reasonable to connect up the energy of the observed alpha-particles with the value of the electrostatic potential in the small interval between the newly formed fission fragments. On this view the alpha-particle will be expelled in a direction roughly perpendicular to the line of separation with an energy of about 20 Mev. The unequal repulsion by the lighter and heavier fission fragments will be responsible for some deviation from perpendicular emission, as observed.

Similar effects will be expected for other light nuclear fragments, except that here the relevant potential barriers will be higher, and emission probabilities lower.

Emission of protons will be practically forbidden in comparison with alpha-particle emission, because the binding of the particle to nuclear matter--even near the scission neck--places its energy far below the top of the Coulomb barrier. Those protons which are observed have rather to be interpreted as due to processes of impact between fission fragments and the stopping material through which they pass. Their energy distribution is consistent with this view, and quite contrary to what would be expected if they came directly from either the dividing system or the fission fragments."

11.5 DISTRIBUTION OF NUCLEAR CHARGE IN FISSION

In the discussion of this section we shall use the term primary fission product to refer to the nuclear species formed after emission of the prompt neutrons but before any beta decay has occurred. The general term fission product will refer to the primary fission products plus any nuclear species produced by the beta decay of the primary products.

An important part of the information that one would like to have about the fission process is the division of nuclear charge between the primary fission fragments. Unfortunately, to determine this is a difficult experimental problem and the available data are limited. The reason for the difficulty is that the primary fragments are so far from beta stability that most of the radioactive decay half-lives are very short. Hence by the time the necessary chemical separations have been carried out the primary fragments have been completely converted into another element. This is not true in the case of shielded nuclides and their fission yields are of necessity independent rather than cumulative chain yields. A shielded nuclide is one which cannot be formed by beta decay because the isobaric nuclide of the next lower atomic number is stable. There is another group of nuclides whose independent yields may be measured; namely, those nuclides which can be chemically isolated in a time shorter than the half life of their beta-decaying precursors. For example, La^{140} is formed in fission chiefly from the decay of its parent, 12.8 day Ba^{140}, but if La^{140} is isolated within a few minutes of the completion of a short irradiation of uranium with neutrons, the activity isolated will be chiefly attributable to the La^{140} formed as a primary fission product.

Before the matter of charge division was subjected to much study, various conjectures were put forth as to what might be expected. One might have expected the neutron to proton ratio of the light and heavy fragments to be identical with that of the fissioning nucleus. This postulate of unchanged charge distribution would lead one to expect much longer beta-emitter chains in the light fragments, which is not in accord with the facts. One might also have postulated, as did WAY and WIGNER[176] in an early unpublished report that the most probable charge distribution would correspond, to that division giving rise to the maximum kinetic energy of the fragments and the minimum potential energy in the form of radioactivity decay energy. This postulate predicts a longer average chain length for the heavy fragments which also is not in accord with the facts.

---

[176] See K. Way and E. P. Wigner, Phys. Rev. 73, 1318 (1948).

The problem of nuclear charge distribution may be considered to have two aspects: (1) the determination of the most probable mode of charge division for a given mass split, and (2) the distribution function for primary formation (independent yield) about the most probable nuclear charge among fission products of the same mass number.

The empirical facts regarding the division of charge in slow-neutron induced fission are satisfactorily summarized by the hypothesis of equal charge displacement put forth by GLENDENIN, CORYELL and EDWARDS.[177-178] According to this hypothesis the most probable charges for one fission fragment and for its complementary fragment lie an equal number of units away from beta stability. It was further postulated, to cover point (2) above, that the distribution about the most probable charge is a symmetrical function with the same form for all mass splits and all fissile nuclides. The empirical charge distribution curve is shown here in Fig. 11.46.

From the equal charge displacement hypothesis

$$Z_A - Z_p = Z_A^* - Z_p^* \qquad (11.44)$$

where Z_A and Z_A^* are the most stable charges of the complementary fission product chains and Z_p and Z_p^* are the most probable charges for the primary fission products of mass numbers A and A^*. Z_A and Z_p (and Z_A^* and Z_p^*) are not restricted to integral values and in nearly all cases are non-integral. The sum of the primary charges Z_p and Z_p^* must equal the charge of the fissioning nucleus Z_f. The complementary fission product masses A and A^* are related by

$$A + A^* = A_f - \overline{\nu} \qquad (11.45)$$

---

177. Glendenin, Coryell, and Edwards, Distribution of Nuclear Charge in Fission, Paper 52 in "Radiochemical Studies: The Fission Products" C. D. Coryell and N. Sugarman, editors, National Nuclear Energy Series, Plutonium Project Record, McGraw-Hill Book Co., Inc., New York, (1951).

178. L. E. Glendenin, Laboratory for Nuclear Science, Massachusetts Institute of Technology, Technical Report No. 35, December, 1949.

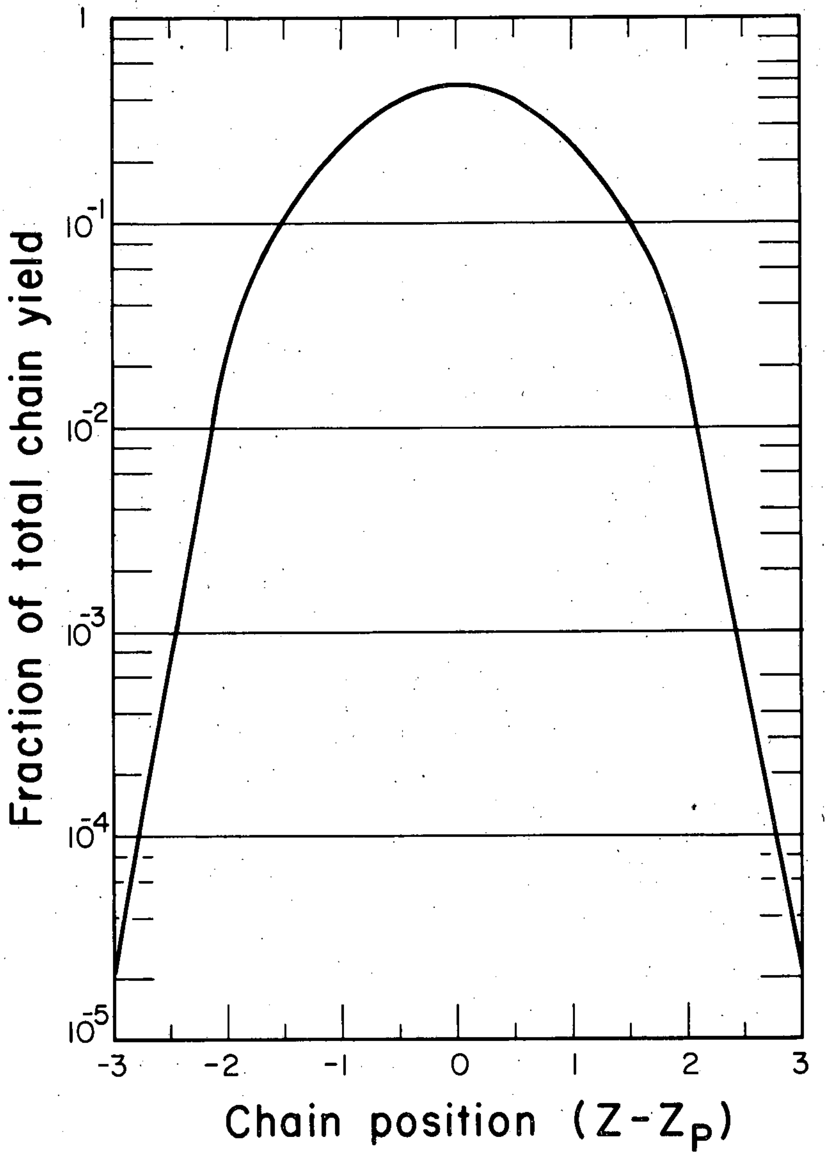

MU-19011

Fig. 11.46. The empirical charge distribution curve as based on the original suggestion of GLENDENIN, CORYELL and EDWARDS. The curve is a probability curve with the Gaussian approximation

$$P(Z) = \frac{1}{\sqrt{c\pi}} e^{-\frac{(Z-Z_p)^2}{c}}$$

where c is an empirical constant ~1.5.

where A_f is the mass number of the fissioning nucleus and $\bar{\nu}$ is the average number of neutrons emitted per fission. The equation for the most probable charge of a fission product of mass A is then

$$Z_p = Z_A - 1/2\ (Z_A + Z_A^* - Z_f) \qquad (11.46)$$

In the original treatment of GLENDENIN, CORYELL and EDWARDS,[177] the values of Z_A were evaluated from the BOHR-WHEELER[179] mass equation. This continuous Z_A function smooths over the mass discontinuities involved in crossing shell edges; hence appreciable error in estimating Z_A and Z_p is likely to result for those fission products having proton numbers close to the 50 proton shell or a neutron number close to the 50 or 82 neutron shell. To eliminate this difficulty PAPPAS[180] modified the method of estimating Z_A and based his calculations of Z_A on the treatment of beta stability of CORYELL, BRIGHTSEN and PAPPAS.[181] In this treatment empirical Z curves are used which are essentially straight lines for nuclides whose nucleon numbers lie within a given shell but separate Z_A lines are used in different shell regions and discontinuities appear at the shell edges. Hence the calculated Z_p curves show discontinuities at the shell edges and at points complementary to the shell edges. In PAPPAS treatment attention is focused on the fragments at the time of scission before prompt neutrons have been emitted; in this respect his approach also differs from that of GLENDENIN, CORYELL and EDWARDS.

Table 11.17 shows the values of Z_A in the mass ranges of interest in fission and gives values of $\frac{\partial Z_A}{\partial A}$ for convenience in interpolation. For mass numbers in the vicinity of shell closures there is an uncertainty in the Z_A value to be used in Eq. (11.46). This is indicated in column 2 of Table 11.17 by the occurrence of mass numbers 87-90, 116-120, 137-140 and 155-158 in two

---

[179] N. Bohr and J. A. Wheeler, Phys. Rev. 56, 426 (1939).

[180] A. C. Pappas, "A Radiochemical study of fission yields in the region of shell perturbations and the effect of closed shells in fission" Laboratory for Nuclear Science, Massachusetts Institute of Technology, Tech. report No. 63, September, 1953; see also A. C. Pappas, Paper P/881, Volume 7, Proceedings of the U.N. Conference on the Peaceful Uses of Atomic Energy, United Nations, Geneva, 1955.

[181] Coryell, Brightsen, and Pappas, Phys. Rev. 85, 732 (1952); see also C. D. Coryell, Beta Decay Energetics, Ann. Rev. Nucl. Sci. 2, 305 (1953).

Table 11.17

Values of Z_A

Shell group	A	Z_A	$\delta Z_A/\delta A$
$Z < 50$, $N < 50$	70 90	31.2 38.9	0.38_4
$Z < 50$, $N > 50$	87 120	38.6 51.7	0.39_7
$Z > 50$, $N < 82$	116 140	49.0 57.4	0.35_0
$Z < 64$, $N > 82$	137 158	57.8 65.3	0.35_7
$Z > 64$, $N > 82$	155 165	63.6 67.3	0.37_0

A. C. Pappas, as quoted in reference 182.

shell groups. In these mass regions STEINBERG and GLENDENIN[182] suggest the use of the average of the Z_A values from the two groups.

A summary of the experimental data on independent fractional chain fission yield is given in Table 11.18. In the previous discussion of "fine structure" in the mass-yield curve it was suggested that certain nuclides may be preferentially formed in fission giving rise to regions of fine structure in the mass yield curve. For the purposes of an analysis of charge distribution the "excess" yields of such nuclides are considered anomalous, and a "normal" chain yield is used to calculate the fraction of chain yield represented by the observed independent fission yield. These "normal" chain yields represent the yields which would have occurred without the extra contribution of a specific preferred member of the chain. In their 1955 Geneva Conference report STEINBERG and GLENDENIN[182] compared the charge distribution curve shown here as Fig. 11.46 with the data available at that time from several fissile nuclides and found reasonably good agreement with the equal charge displacement hypothesis.

In 1956 KENNETT and THODE[183] reported some new results which were not in good agreement with the curve shown in Fig. 11.46 and indicated a need for a revision in the theory. These authors used ultrasensitive mass-spectrometer techniques to measure the yields of Xe^{128} and Xe^{130} relative to the heavier isotopes Xe^{131} whose fission yield was accurately known. The amount of Xe^{128} and Xe^{130} so found could be taken as the measure of the primary yields of I^{128} and I^{130} which had decayed into the stable xenon daughters before analysis. KENNETT and THODE obtained yields which were too high by a factor of more than 100 to fit Fig. 11.46.

They reasoned that while PAPPAS[180] was correct in allowing for shell effects in the evaluation of Z_A it was necessary to go further and made a correction for shell effects in Z_p. KENNETT and THODE[183] postulated a charge division such that the greatest energy release occurs in the fission act. To make

---

[182] E. P. Steinberg and L. E. Glendenin, Paper P/614 in Volume 7, Proceedings of the International Conference on the Peaceful Uses of Atomic Energy, August 1955, United Nations, Geneva (1956).

[183] T. J. Kennett and N. G. Thode, Phys. Rev. 103, 323 (1956).

Table 11.18

Independent Fractional Chain Yields: Fission of U^{235} with Thermal Neutrons

Fission product	Independent fractional chain yield[a]	Reference
91 min As^{78}	0.09	b
*36 hour Br^{82}	$\simeq 6 \times 10^{-4}$	c
	1.4×10^{-4}	d
	1.6×10^{-4}	e
*19 day Rb^{86}	1.2×10^{-5}	e
	1.5×10^{-6}	f
64 hour Y^{90}	$<3 \times 10^{-4}$	h
	$<8 \times 10^{-5}$	w
	$<5 \times 10^{-4}$	e
14 min Rb^{91}	0.35 ± 0.05	v
9.7 hour Sr^{91}	0.06 ± 0.04	v
58 day Y^{91}	$<9 \times 10^{-3}$	h
	~0.01	w
*23 hour Nb^{96}	9×10^{-5}	e
	1.4×10^{-4}	i
	$(1.0 + 0.2) \times 10^{-4}$	y
72 min Nb^{97}	$(1.7 \pm 1.3) \times 10^{-3}$	y
*10^6 year Tc^{98}	0.011 ± 0.004	y
*210 day Rh^{102}	$<2 \times 10^{-7}$	k
*25 min I^{128}	1.0×10^{-4}	c
*12.6 hour I^{130}	2.8×10^{-4}	c
24 min Te^{131}	0.14	l
	0.15 ± 0.07	m
	0.04 - 0.12	n
8.05 day I^{131}	<0.01	n
77 hour Te^{132}	0.36 ± 0.17	o
2.3 hour I^{132}	<0.01	n
20.8 hour I^{133}	<0.05	n
5.3 day Xe^{133}	<0.001	p
52.5 min I^{134}	0.12	f,n
9.2 hour Xe^{135}	0.035	p
	0.049	q
	0.027	r

Table 11.18 (cont'd.)

Fission product	Independent fractional chain yield[a]	Reference
*13 day Cs^{136}	1.0×10^{-3}	f
	9×10^{-3}	e
27 yr Cs^{137}	~0.025	z
32 min Cs^{138}	0.045 ± 0.005	z
9.5 min Cs^{139}	0.17 ± 0.03	v
84 min Ba^{139}	0.011 ± 0.005	v
66 sec Cs^{140}	0.34 ± 0.05	v
12.8 day Ba^{140}	0.07 ± 0.03	v
40.2 hour La^{140}	7.0×10^{-4}	w
26 sec Cs^{141}	0.52 ± 0.08	x
18 min Ba^{141}	0.27 ± 0.06	x
3.7 hour La^{141}	$(4 \pm 2) \times 10^{-3}$	x
77 min La^{142}	0.018 ± 0.006	x
1.0 sec Xe^{143}	8.5×10^{-3}	g
*5.3 day Pm^{148}	$<10^{-4}$	e

*Indicates shielded isotopes.

a. based on measured total chain yield.

b. N. Sugarman, Phys. Rev. 89, 570 (1953).

c. T. J. Kennett and H. G. Thode, Phys. Rev. 103, 323 (1956).

d. M. H. Feldman, L. E. Glendenin, and R. R. Edwards, p. 598 in ref. u.

e. G. B. Cook, results cited in m.

f. L. E. Glendenin, Technical report No. 35, Laboratory for Nuclear Science, M.I.T. (1949).

g. A. C. Wahl, J. Inorg. and Nuclear Chem. 6, 263 (1958).

h. G. W. Reed, Phys. Rev. 98, 1327 (1955).

i. J. S. Gilmore, unpublished results cited in g.

j. G. D. O'Kelley and Q. V. Larson, unpublished results cited in g.

k. J. A. Swartout and W. H Sullivan, p. 856 in u.

l. L. E. Glendenin, unpublished results cited in g.

m. A. C. Pappas, Proceedings of the International Conference on the Peaceful Uses of Atomic Energy, Geneva, 1955, Vol. 7, pp. 3-14, United Nations (1956).

Table 11.18 (cont'd.)

n. A. C. Wahl, Phys. Rev. 99, 730 (1955). Data for Te^{131} corrected for the 5% Sb^{131} decaying to Te^{131}.

o. A. C. Pappas, Technical Report No. 63, Laboratory for Nuclear Science, M.I.T., September, 1953.

p. S. Katcoff and W. Rubinson, Phys. Rev. 91, 1458 (1953).

q. E. J. Hoagland and N. Sugarman, p. 1030 of u.

r. F. Brown and L. Yaffe, Can. J. Chem. 31, 242 (1953).

s. N. Sugarman, p. 1139 of u.

t. G. P. Ford and C. W. Stanley, Atomic Energy Commission Document, AECD-3551 (1953).

u. "Radiochemical Studies: The Fission Products", edited by C. D. Coryell and N. Sugarman, NNES, Plutonium Project Record, Div. IV, Vol. 9, McGraw-Hill Book Co., Inc., New York (1951).

v. R. L. Ferguson, Thesis, Department of Chemistry, Washington University, January, 1959.

w. W. E. Grummitt and G. M. Milton, J. Inorg. Nuclear Chem. 5, 93 (1957).

x. D. R. Nethaway, Ph.D. Thesis, Washington University, September, 1959.

y. D. E. Troutner, Ph.D. Thesis, Washington University (1959).

z. K. Wolfsberg, Ph.D. Thesis, Washington University (1959).

quantitative predictions it was necessary to have some means for estimating masses of nuclides far removed from stability. They used the mass formula of KUMAR and PRESTON[184] which includes shell effects and spin terms. The calculations of KENNETT and THODE[183] based on this mass equation resulted in a Z_p curve which remained near 50 for fission masses from A = 128 to A = 132, which is quite different from the behavior of Z_p determined from the treatments of GLENDENIN, CORYELL and EDWARDS[178] or of PAPPAS.[180] The primary yields for I^{128} were accounted for much more satisfactorily. GRUMMITT and MILTON[185] also discussed the maximum energy release hypothesis.

ALEXANDER and CORYELL[186] asserted that the general application of the method of KENNETT and THODE[183] to all mass regions is open to serious question. This method of calculating Z_p predicts longer chain lengths in the heavy fragments than in the light. They attempted to correlate measured fractional chain yields in low energy fission, with Z_p calculated according to the postulate of maximum energy release and concluded that the scatter of the data was worse than for the original postulate of equal charge displacement.

Subsequent to these reports WAHL[187] made a substantial new contribution to the problem of charge distribution in fission. First of all he materially increased the data by using an ingenious method to measure the primary and cumulative yields of nine short-lived isotopes of krypton and xenon. In his experimental method the fission products recoiling from a thin sample of U^{235} were caught in a layer of barium stearate powder, a material which has a negligible tendency to retain occluded gases (a characteristic referred to as high emanating power). The rare-gas fission products then immediately escaped into a large evacuated space. There the inert gases decayed depositing their longer-lived descendents on a filter-paper liner. Comparison of the descendent activities found on the liner and in the barium stearate powder gave the fractional cumulative yields of the inert gases.

---

184. K. Kumar and M. A. Preston, Can. J. Phys. 33, 298 (1955).

185. W. E. Grummitt and G. M. Milton, Chalk River Laboratory Report CRC-694, AECL-453 (1957).

186. J. M. Alexander, and C. D. Coryell, Phys. Rev. 108, 1274 (1957).

187. A. C. Wahl, J. Inorg. Nuclear Chem. 6, 263 (1958).

WAHL[187] combined his new data with all the previous data on independent yields. Because of the uncertainties which we have just recounted about the proper method of calculating the Z_p function, WAHL reasoned that it might be a good idea to determine it empirically. He assumed that the charge distribution curve of Fig. 11.46 was correct. Then when each independent fractional chain yield (plus a few cumulative yields) was placed precisely on the assumed charge distribution curve, the corresponding value of Z_p was automatically fixed. The results are plotted in Fig. 11.47 in which the light and heavy regions are folded so that the total $Z = 92$ and the total $A = 233.5$ ($\nu = 2.5$). A smooth continuous curve passes through all the points except those for mass numbers 96 and 98 in which case reasonable explanations could be given for the small discrepancy. Some general features of the empirical Z_p curve are the following:

(1) In the regions where the Z_A functions are not influenced by shell edges, the Z_p curve is approximately equi-distant (for complementary mass numbers) from the two Z_A lines as proposed in the postulate of equal charge displacement. The Z_A lines shown are those proposed by CORYELL.[181]

(2) In the regions where the Z_A functions are discontinuous due to crossing of the 50 and 82 neutron shell edges the Z_p curve makes a smooth continuous transition. There are no large discontinuities in the Z_p function of the type observed in the PAPPAS treatment.[180]

(3) The Z_p line tends to approach and remain close to the 50-proton shell edge as proposed by KENNETT and THODE.[183] However, there is no pronounced tendency for it to remain close to the 82 (or 50) neutron shell as they proposed.

Several of WAHL's students[188] have contributed newer data on independent and cumulative yields which are significant for an analysis of the equal charge displacement hypothesis in its various formulations. Much of this data is listed in Table 11.18. NETHAWAY[188] developed the charge distribution curve shown in Fig. 11.48 which is very similar to GLENDENIN'S curve (Fig. 11.46) but gives somewhat better agreement with the data available in 1959. Experimental data are shown in the figure to indicate the extent of the agreement or

---

[188] See 1959 thesis studies, Department of Chemistry, Washington University, by Ferguson, Nethaway, Troutner and Wolfsberg.

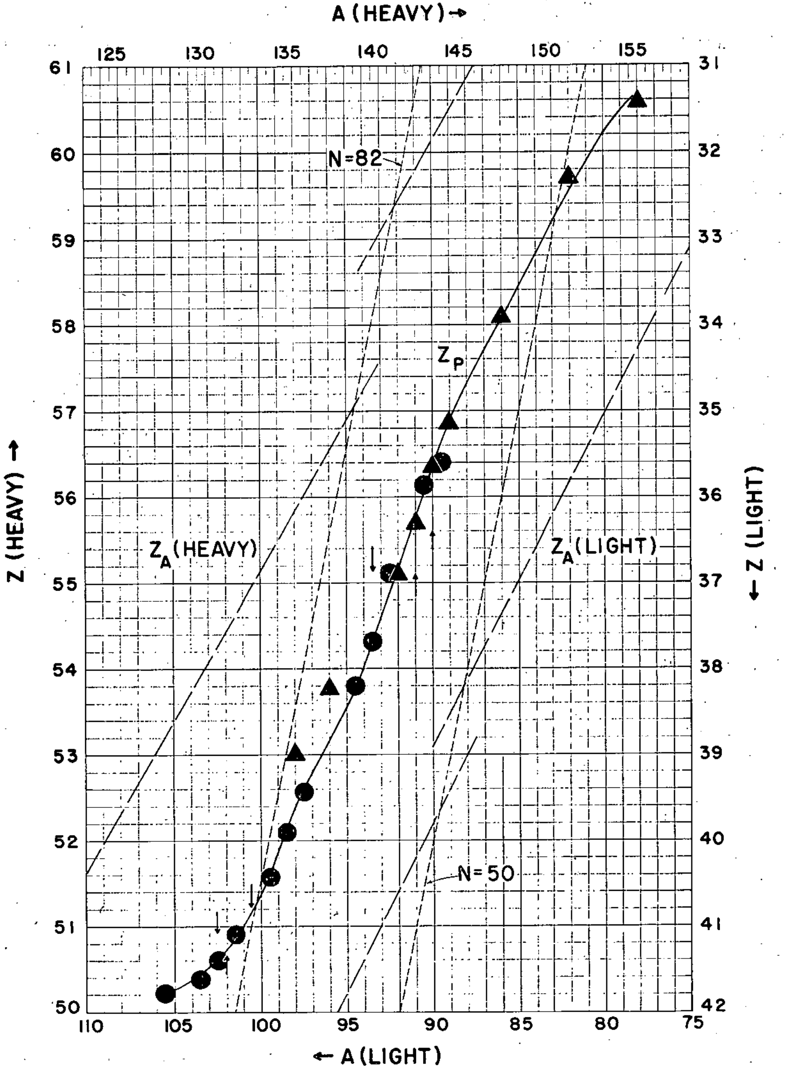

Fig. 11.47. Wahl's empirical Z_p function. ● heavy fission products; ▲ light fission products; upper limits indicated by tips of arrows. The Z_A lines are those proposed by CORYELL. From A. C. Wahl, reference 187.

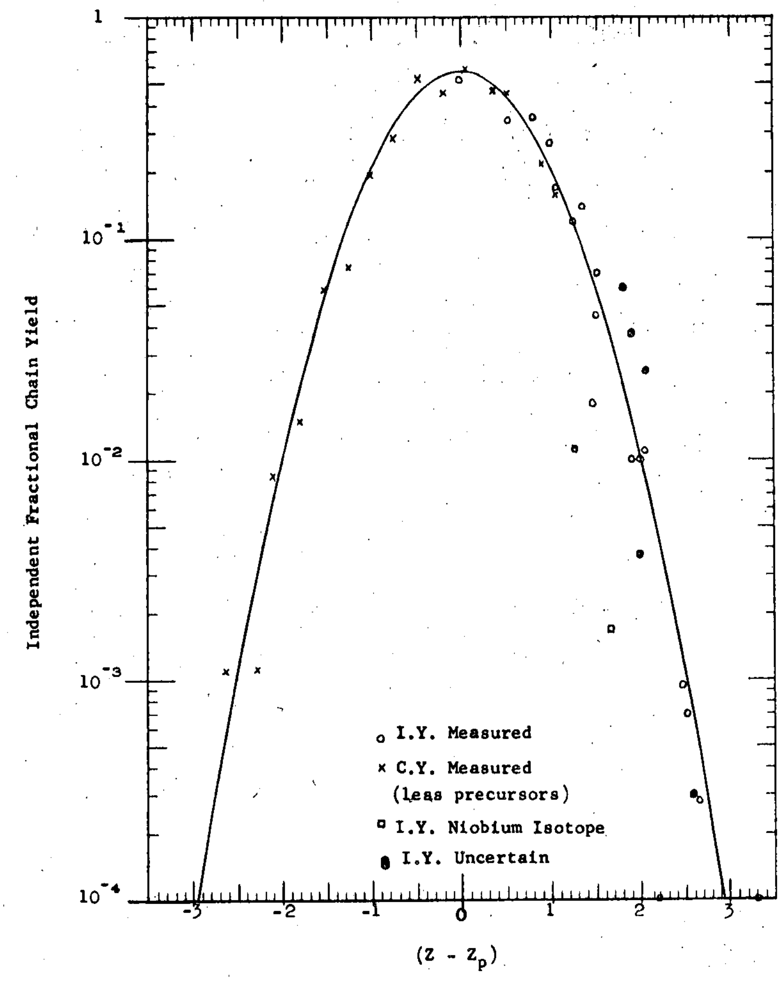

MU-19257

Fig. 11.48. Charge distribution curve as given by NETHAWAY and WAHL.

$$P(Z) = \frac{1e}{\sqrt{c\pi}} - \frac{(Z-Z_p)^2}{c} \quad , \; c = 1.00.$$

I.Y. and C.Y. indicates independent yield and cumulative yield respectively.

disagreement. NETHAWAY evaluated the Z_p's from Eq. (11.46) using Z_A values as given by GRUMMITT and MILTON[189]. A similar fit is obtained if WAHL'S[187] empirical method of determining the Z_p function is used.

Since so much depends on the validity of this charge distribution curve it is important to check its correctness by determining the independent yields of several members of the same fission product chain. FERGUSON[190] collected data on three members each of the chains of mass 91, 139 and 140 and found that the data for all three chains was consistent with the standard curve.

It would appear that a combination of WAHL'S[187] empirical Z_p curve and the empirical curves of either Fig. 11.46 or 11.47 provides a satisfactory basis for correlating the data on low energy fission and for predicting the independent yield of products which cannot be directly determined. It must be emphasized that the correlation is strictly an empirical one. The fundamental factors governing the division of charge have not been explained by any comprehensive theory of fission.

The correlations of nuclear charge distribution which we have just reviewed seems to fit well nearly all the available data for slow neutron fission of U^{233}, U^{235} and Pu^{239} and for the spontaneous fission of several heavy element nuclei. The question arises whether these same correlations hold in the case of nuclei caused to fission with high energy neutrons or high energy charged particles. WAHL[189a] measured fission yields for U^{235} induced to fission with 14 Mev neutrons and discussed nuclear charge distribution. He showed that the $Z - Z_p$ correlation could be taken to be the same as that for low-energy fission by assuming $\bar{\nu}$ of about 5 but he considered that there was insufficient evidence that the nuclear-charge distribution pattern remains the same. FORD[190a] presents the case for close similarity in the distribution patterns, using data for Br^{82}, I^{132}, I^{134}, and Cs^{136} from U^{235} irradiated with 14 Mev neutrons. ALEXANDER and CORYELL[186] considered the cases of U^{238} and

---

189. W. E. Grummitt and G. M. Milton, J. Inorg. Nucl. Chem. 5, 93 (1957).

189a. A. C. Wahl, Phys. Rev. 99, 730 (1955).

190. R. L. Ferguson, Thesis, Washington University, January, 1959. Some of Ferguson's data is given in Table 11.18.

190a. G. P. Ford, U.S. Atomic Energy Commission Report AECD-3597, unpublished.

Th^{232} caused to fission by capture of 13.6 Mev deuterons and by capture of fast neutrons (produced in a beryllium target at a cyclotron and containing a spread of energies up to 19 Mev). Using independent fission yields on 5 products in each case they found reasonable agreement with the equal charge displacement postulate in every instance and poor agreement with the hypothesis that the neutron-to-proton ratio of the fission products was the same as that of the fissioning nucleus.

On the other hand, a thesis study by GIBSON[191] of fission induced in the following cases--(Pu^{239} + 20 Mev deuterons), (Np^{237} + 31 Mev deuterons), (Np^{237} + 46 Mev helium ions), and (U^{233} + 23 Mev deuterons) indicated better agreement with the postulate that the most probable primary fission products have the same neutron to proton ratio. There was very poor agreement with the equal charge displacement hypothesis. However, certain features of the independent yield distributions which GIBSON got when he plotted his data according to the constant-charge-to-mass-ratio hypotehsis led him to the conclusion that the actual charge distribution may be intermediate to the two cases.

CHU and MICHEL[192] studied independent fission yields of several isotopes in the fission of U^{235} and U^{238} targets bombarded with 45.7 and 24 Mev helium ions. They agree with GIBSON[91] that the true charge distribution must fall between the two postulates but that the equal-charge-displacement hypothesis in its typical form gives the poorer fit. CHU and MICHEL[192] tried various prescriptions for computing the Z_p and Z_A parameters. One interesting fact they noted was that if one abandons the Z_A functions[181,189] which trace out all the shell influenced discontinuities in the ground state masses of stable nuclei and uses instead a smooth Z_A function which ignores pronounced shell effects then one can use the equal-charge-displacement treatment and obtain an excellent fit of the experimental fractional chain yield data to a smooth curve. This may mean that fission at this level of excitation is not greatly affected by the shell properties of the fragments, whereas in low energy fission it clearly is.

---

191. W. M. Gibson, Thesis, University of California, November, 1956; also published as University of California Radiation Laboratory Report UCRL-3493; see also B. M. Foreman, Jr., W. M. Gibson, R. A. Glass, and G. T. Seaborg, Phys. Rev.

192. Y. Y. Chu and M. C. Michel, unpublished results (1959); see thesis study by Y. Y. Chu, issued as University of California Radiation Laboratory Report UCRL-8926, Nov. 1959.

In the case of fission induced by charged particles of large energy (> 50 Mev say) it becomes more difficult to interpret data on independent yields in terms of the correlations we are discussing in this chapter. One of the chief reasons for this is that the identity and excitation energy of the fissioning nucleus is not unique. Instead the fission products come from a variety of fissioning nuclei excited to a variety of energies. This is fully discussed in the next chapter. PATE, FOSTER, and YAFFE[193] give a typical discussion of this problem in a study of nuclear charge distribution in the fission of thorium with protons at nine proton energies between 8 and 87 Mev.

It is known definitely from the work of PERLMAN and GOECKERMANN[194] on the fission of bismuth with 190 Mev deuterons that in this case at least the equal charge displacement hypothesis appears to be inapplicable. For this system the fission product yields show a definite preference for those nuclides, with the same neutron to proton ratio as the fissioning nucleus.

A method of investigating the nuclear charges of the primary fragments which is fundamentally different from any discussed so far, in this section is the one tried by CARTER, WAGNER, and WYMAN.[195] These experimentalists observed the energy spectrum of x-rays in coincidence with fission fragments by using a thin NaI crystal for K x-rays and a proportional counter for L x-rays. The resolution of this method is only fair but with improved technique this approach may give a good picture of the entire distribution in nuclear charges. The observed x-ray spectra are influenced by several effects which need further examination and which may severely limit the applicability of this method. These include (1) internal conversion of prompt gamma rays, (2) fluorescent yield corrections and (3) the number of K and L vacancies produced by the formation of the fragments.

Further comments on charge distribution in high energy fission are deferred until the next chapter.

---

[193] B. D. Pate, J. S. Foster, and L. Yaffe, Can. J. Chem. 36, 1691 (1958); B. D. Pate, Can. J. Chem. 36, 1707 (1958).

[194] R. H. Goeckermann and I. Perlman, Phys. Rev. 76, 628 (1949); see section

[195] Carter, Wagner and Wyman as reported by Leachman in Paper P/665, Proceedings of the Second International Conference on the Peaceful Uses of Atomic Energy, United Nations, 1958.

11.6 KINETIC ENERGY OF THE FISSION FRAGMENTS

Shortly after nuclear fission was discovered by the radiochemical work of HAHN and STRASSMANN,[196] the large energy release in fission was measured experimentally by FRITSCH.[197] He measured ionization pulses produced in an ionization chamber containing a uranium sample irradiated with neutrons. A short time later JENTSCHKE and PRANKL[198] resolved the ionization pulses into two groups which corresponded to fragment energies of about 60 and about 100 kev. JOLIOT[199] demonstrated the large kinetic energy of the fission fragments by radiochemical measurements of the penetration of the fission fragments through thin foils. Since this early work, a great body of information on the kinetic energy of the fission fragments has been collected by refined experimental techniques. We discuss four types of experiments in the following pages: (1) ionization chamber measurements of kinetic energy release, (2) time-of-flight measurement of fragment velocity, (3) ranges of the fragments in gases and foils, and (4) calorimetric measurement of total energy release.

11.6.1 Ion-Chamber Measurement of Fragment Energy Distribution in Slow Neutron Fission of U^{235}, U^{233} and Pu^{239}. The energy of fission fragments can be obtained from the measurement of the total ionization produced in the gas of a suitable ionization chamber. Fission fragments are heavily ionizing particles with a maximum range in air at NTP of about 2.5 centimeters; hence, a shallow ionization chamber is sufficient to stop the fragments completely. The ionization charge collected is very closely proportional to the fragment kinetic energy. The method involves (1) an ionization chamber into which a sample of fissionable material can be inserted and at the same time be exposed to a flux of neutrons; for the study of spontaneous fission a neutron source is not required. (2) An electrode system in which the rapidly collected charge generates across the chamber capacity a voltage pulse of many millivolts, the magnitude of which is proportional to the fragment energy, (3) a linear pulse amplifier which amplifies this pulse up to a voltage suitable for detection and (4) an oscilloscope, a pulse height analyzer, or other device for determining the relative number of pulses of various sizes. If the pulse height to energy relationship is correctly calibrated, a plot of the number of recorded events versus pulse height gives the distribution of fragment energies. The reader is referred elsewhere[200-206] for a detailed discussion of the ionization process and of the design of ionization chambers.

---

[196] O. Hahn and F. Strassmann, Naturwiss. 27, 11, 89 (1939).

[197] O. R. Frisch, Nature 143, 276 (1939).

[198] W. Jentschke and F. Prankl, Naturwiss. 27, 134 (1939).

[199] F. Joliot, Compt. rend. 208, 341, 647 (1939).

If fission fragment energies are studied in a simple ionization chamber, only one fragment from each fission event is observed, since the other is stopped in the foil upon which the fissionable material is deposited or in the wall of the chamber. Since it is completely random whether the light or the heavy fragment in any one case is slowed down in the ionization chamber gas, a study of the pulses from a large number of fissioning atoms will show a double humped distribution corresponding to the light and heavy fragments.

More information is obtained if both fragments are studied simultaneously in a twin-back-to-back ionization chamber in which the fissionable material is mounted on a thin film, which serves as a common cathode.[207-209] This method was highly developed by BRUNTON and HANNA[210] and BRUNTON and THOMPSON.[211]

---

[200] Ghiorso, Jaffey, Robinson, and Weissbourd, Paper No. 16.8, "The Transuranium Elements", National Nuclear Energy Series, Div. IV, Vol. 14B, McGraw-Hill Book Co., Inc., New York, 1949.

[201] Bunneman, Cranshaw, and Harvey, Can. J. Research 27A, 191 (1949).

[202] D. H. Wilkinson, "Ionization Chambers and Counters", Cambridge University Press, Cambridge (1950).

[203] Herwig, Miller and Utterback, Rev. Sci. Inst. 26, 929 (1955).

[204] B. Rossi and H. H. Staub, "Ionization Chambers and Counters", McGraw-Hill Book Co., Inc., New York, 1949.

[205] H. H. Staub, "Detection Methods", Vol. I, "Experimental Nuclear Physics", edited by E. Segre, John Wiley and Sons, New York, 1953.

[206] H. A. Bethe and J. Ashkin, "Passage of Radiations through Matter", Vol. I "Experimental Nuclear Physics", edited by E. Segre, John Wiley and Sons, New York, 1953.

[207] W. Jentschke, Z. Phys. 120, 165 (1942).

[208] Flammerfeld, Jensen and Gentner, Z. Phys. 120, 450 (1942).

[209] M. Deutsch and M. Ramsey, Report MDDC-945 (1945).

[210] D. C. Brunton and G. C. Hanna, Can. J. Res. 28A, 190 (1950).

[211] D. C. Brunton and W. B. Thompson, Can. J. Res. 28A, 498 (1950).

These experimenters constructed a double ionization chamber of the type shown in Fig. 11.49. A thin sample of uranium or plutonium mounted on a thin backing was placed in the center of the chamber on the common cathode. When the chamber was placed in a flux of slow neutrons to induce fission, the two fragments travelled in opposite directions into the two chambers. The electrons formed by ionization in the argon-carbon dioxide gas mixture were collected on the two collecting anodes. Frisch grids were used to shield the collecting electrodes from charges induced by the slowly-moving positive ions. The fissioning sample was mounted on one side of a collimator consisting of a plate with closely spaced holes. The purpose of this was to reject all fragments coming off at a low angle from the source. These would have excessive ionization losses owing to oblique passage through the source, and to loss of electrons to the chamber walls caused by fringing field effects. Only coincident pulses were accepted for measurement. In addition, pulse-height analyzers were used to determine the size of the coincident pulses. On the gate side the analyzer consisted usually of a single-channel analyzer with a window width of 5 Mev, although operation with a wide open gate was also possible. The coincident pulses from the second chamber were passed into a 30-channel analyzer.

To convert the observed pulse heights to energy it was necessary to determine the amount of energy required to produce an ion pair in the chamber gas. In practice this was done by measuring pulses due to the alpha particles of known energy from U^{233}, U^{235} and Pu^{239} and assuming that the number of electron volts per ion pair in argon is the same for fission fragments as for alpha particles. Appreciable error is involved in this assumption, as is discussed a few pages later.

When the gate discriminator was adjusted to pass fission pulses of all energies, the energy spread of the pulses from the second chamber appeared as shown in Fig. 11.50. The double-humped curve is reminiscent of the radiochemical mass yield distribution. Certain properties of these three curves are given in Table 11.19.

The results obtained by BRUNTON and HANNA[210] for U^{235} are shown in Fig. 11.51. In this series of experiments the gate was systematically moved from the low-energy side of the low-energy peak to the trough region and across the high-energy peak. Similar curves (not reproduced here) were taken

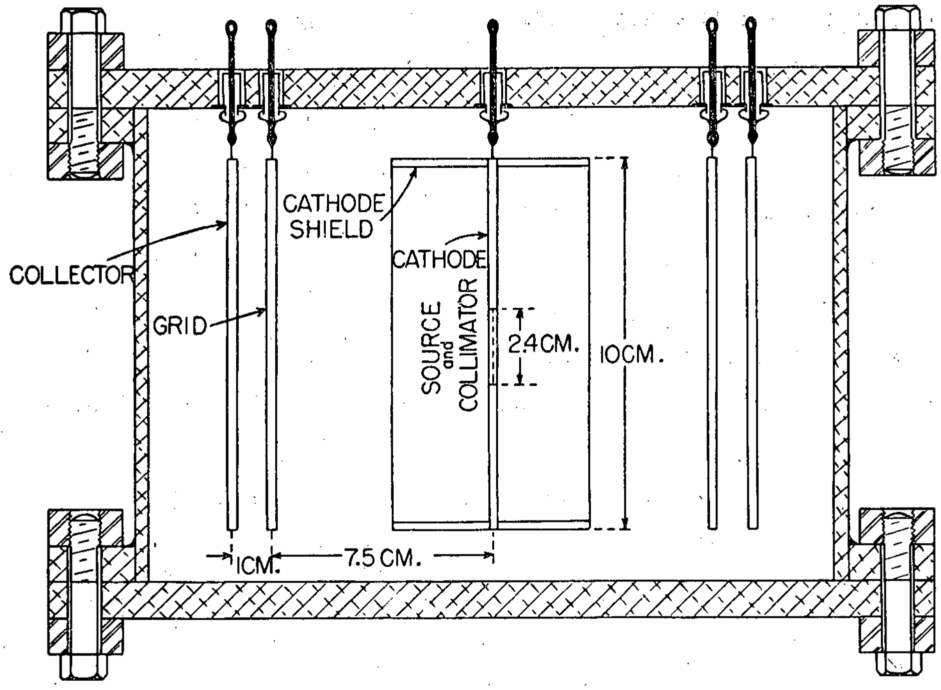
CATHODE SHIELD
COLLECTOR
CATHODE
GRID
SOURCE and COLLIMATOR
2.4CM.
10CM.
1CM.
7.5 CM.

MU-19019

Fig. 11.49. Double ionization chamber of BRUNTON and HANNA (1950). The chambers employ electron collection to secure fast rising pulses. Frisch grids are used to shield the collecting electrodes from charges induced by the slowly-moving positive ions. From Can. J. Research, reference 210.

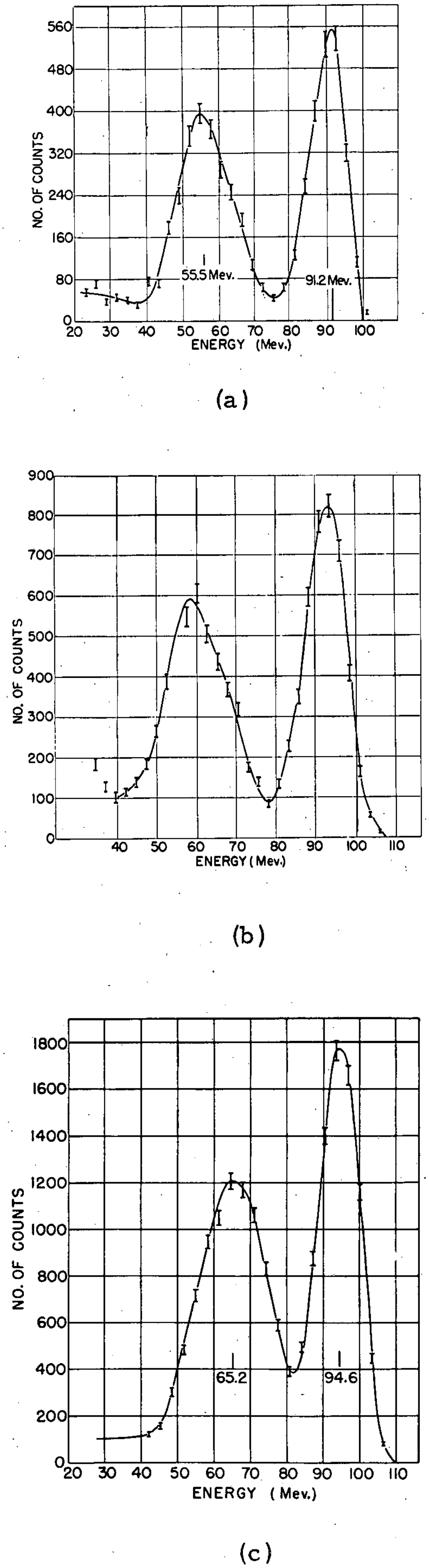

Fig. 11.50. Energy spectrum of fission fragments. 1950 data of BRUNTON, HANNA and THOMPSON. Data not corrected for an ionization loss of about 7 Mev in each fragment. From Can. J. Research, reference 211.

(a) U^{233} (b) U^{235} (c) Pu^{239}

MUB-364

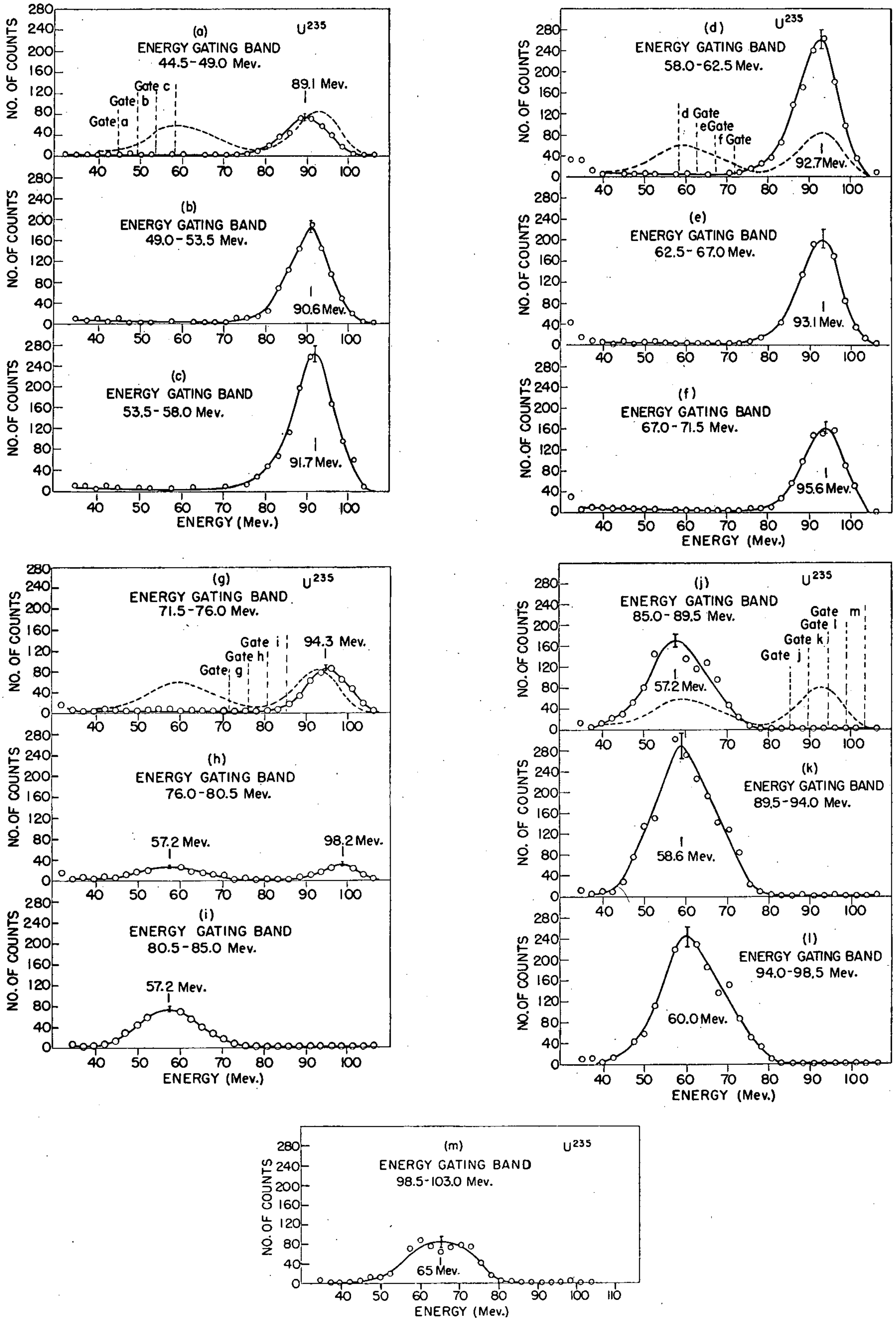
(a) U^{235}
ENERGY GATING BAND
44.5-49.0 Mev.
Gate a
Gate b
Gate c
89.1 Mev.
(b)
ENERGY GATING BAND
49.0-53.5 Mev.
90.6 Mev.
(c)
ENERGY GATING BAND
53.5-58.0 Mev.
91.7 Mev.
(d) U^{235}
ENERGY GATING BAND
58.0-62.5 Mev.
d Gate
e Gate
f Gate
92.7 Mev.
(e)
ENERGY GATING BAND
62.5-67.0 Mev.
93.1 Mev.
(f)
ENERGY GATING BAND
67.0-71.5 Mev.
95.6 Mev.
(g) U^{235}
ENERGY GATING BAND
71.5-76.0 Mev.
Gate g
Gate h
Gate i
94.3 Mev.
(h)
ENERGY GATING BAND
76.0-80.5 Mev.
57.2 Mev.
98.2 Mev.
(i)
ENERGY GATING BAND
80.5-85.0 Mev.
57.2 Mev.
(j) U^{235}
ENERGY GATING BAND
85.0-89.5 Mev.
Gate j
Gate k
Gate l
Gate m
57.2 Mev.
(k)
ENERGY GATING BAND
89.5-94.0 Mev.
58.6 Mev.
(l)
ENERGY GATING BAND
94.0-98.5 Mev.
60.0 Mev.
(m) U^{235}
ENERGY GATING BAND
98.5-103.0 Mev.
65 Mev.
NO. OF COUNTS
0 40 80 120 160 200 240 280
ENERGY (Mev.)
40 50 60 70 80 90 100 110

MUB-356

Fig. 11.51. Spectra of fission fragments of U^{235} in coincidence with companion fragments of the energy specified (BRUNTON and HANNA)[210] Gate width was 5 Mev. From Can. J. Research.

Table 11.19

Comparison of fragment energy distribution in slow-neutron fission of U^{235}, U^{233} and Pu^{239} (Refs. 210,211)

	U^{233}	U^{235}	Pu^{239}
Most probable energy of light fragment (Mev)	93.0	94.5	94.6
Most probable energy of heavy fragment (Mev)	56.6	60.2	65.2
Ratio of most probable energies	1.64	1.57	1.45
Width at half maximum of high-energy peak (Mev)	14	12	14
Width at half maximum of low-energy peak (Mev)	22	20	24
Width at half maximum of total energy curve (Mev)	22	25	27
Mass ratio for most probable total energy	1.26	1.23	1.20
Total energy for most probable fission mode* (Mev)	149.6	154.7	159.8

---

*Note: These values are not corrected for an ionization defect; see Table 11.20.

in the case of U^{233} and Pu^{239}. The results of these runs are interesting and somewhat different than might have been expected.

1. When the energy gate is set on the heavy fragment group the energy distribution of the corresponding light group is almost independent of the position of the gate, and, conversely, when the gate is set on the light fragment group the energy distribution of the coincident heavy group is almost independent of the position of the gate.
2. The partial distribution covers nearly the whole range of the complete spectrum of one group. The distributions are not identical however, and the shift that does occur is such that as the gate energy is increased, the corresponding distribution maximum also increases.
3. Item (2) may be restated in this way: a heavy fragment of lower than average energy for the heavy group will be paired on the average with a light fragment of lower than average energy. The corresponding situation with the mass distribution curve is quite different. Since the sum of the masses is constant, a heavy fragment of higher than average mass for the heavy group must be paired with a light fragment of lower than average mass. Thus the double-humped energy distribution curve is not even approximately a simple inversion of the double-peaked mass distribution curve, as was first pointed out by JENTSCHKE and PRANKL[211a] and re-emphasized by BRUNTON and HANNA.
4. A particularly interesting curve is Fig. 11.51 (h) which shows that if the gate pulse is chosen to correspond to the central energy minimum the coincident pulse distribution instead of being a single peak also centered at the central energy minimum (as one might have expected) is a double-humped curve with maxima close to the energy peaks of the total distribution. If the energy curves were an inverse picture of the mass curves, this experiment would have resulted in a single maximum at the same energy as the gate or perhaps two small maxima very close to this energy.

[211a] W. Jentschke and F. Prankl, Z. Physik 119, 696 (1942).

5. Making use of the fact that the energy ratio is the inverse of the mass ratio ($E_L M_L = E_H M_H$ where M and E refer to mass and energy, and L and H to light and heavy fragments, respectively) it is possible to calculate the most probable mass ratios.
6. Wide ranges in the release of kinetic energy are observed. The maximum variation associated with a fixed mass ratio is about 50 Mev which is close to the maximum variation for the total distribution. The spread at half the maximum probability is 20 Mev. A corollary of this is that a coincidence measurement of the energy or velocity of the fragment pairs is needed to obtain the total energy or mass distribution in any fission event. Observations of energy or velocity of only a single fragment, even if carried out with great accuracy, are insufficient to give this information.
7. The variation in the most probable total kinetic energy with mass ratio is shown in Fig. 11.52. The interesting fact is that total kinetic energy does not show a linear variation with fragment mass ratio. The maximum kinetic energy release occurs for a mass ratio of 1.2 to 1.3 instead of for 1.0. This hump in the kinetic energy curve was also noticed by KATCOFF, MISKEL and STANLEY[212] in an analysis of fission fragment ranges. See Fig. 11.70.

The results of all measurements by the back-to-back ionization chamber coincidence method can be summarized compactly in a contour diagram of the type shown in Fig. 11.53. The masses M_L and M_H, the velocities V_L and V_H and the total kinetic energy, E_k, are determined at any point on this diagram through conservation of momentum except for uncertainties resulting from variations in neutron emission and by ionization dispersion. Several types of probability distributions may be read from this contour diagram.

The values for kinetic energy given in these reports of BRUNTON and HANNA[210] and BRUNTON and THOMPSON[211] do not check within experimental error with the values obtained by calorimetric measurements or by velocity measurements on the fragments discussed later. This discrepancy has prompted a reconsideration of the assumptions of the calibration method. The basic assumption has been that fission fragments and alpha particles expend the same

---

[212] S. Katcoff, J. A. Miskel, and C. W. Stanley, Phys. Rev. 74, 631 (1948).

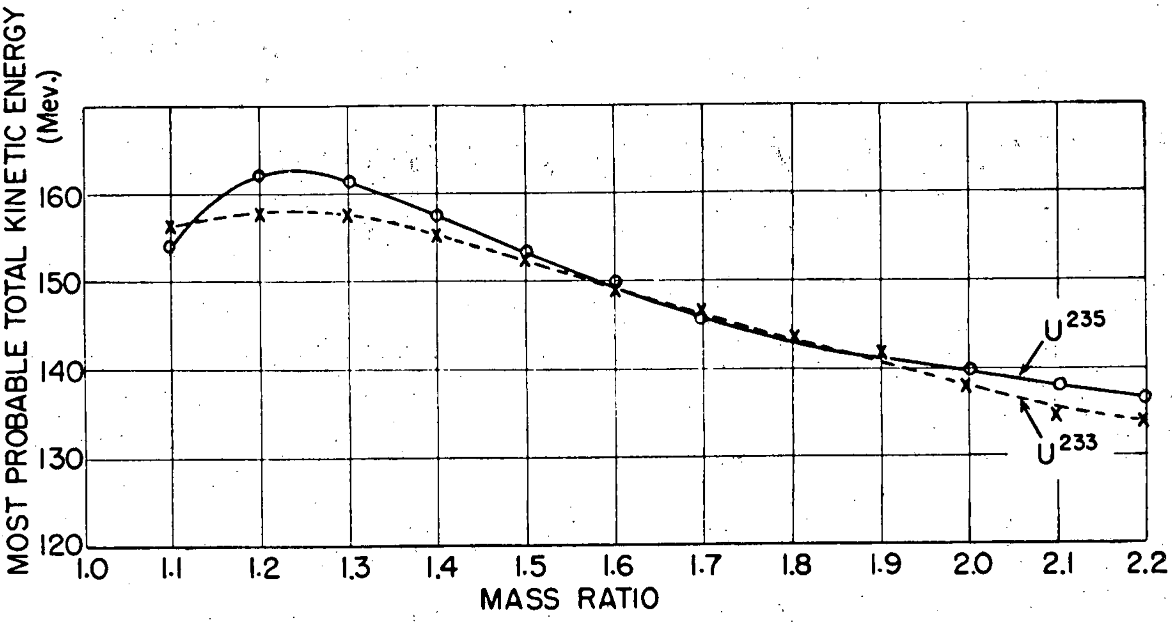

MU-19021

Fig. 11.52. Variation of the most probable kinetic energy with mass ratio. Data not corrected for ionization defect. From Can. J. Research, reference 210.

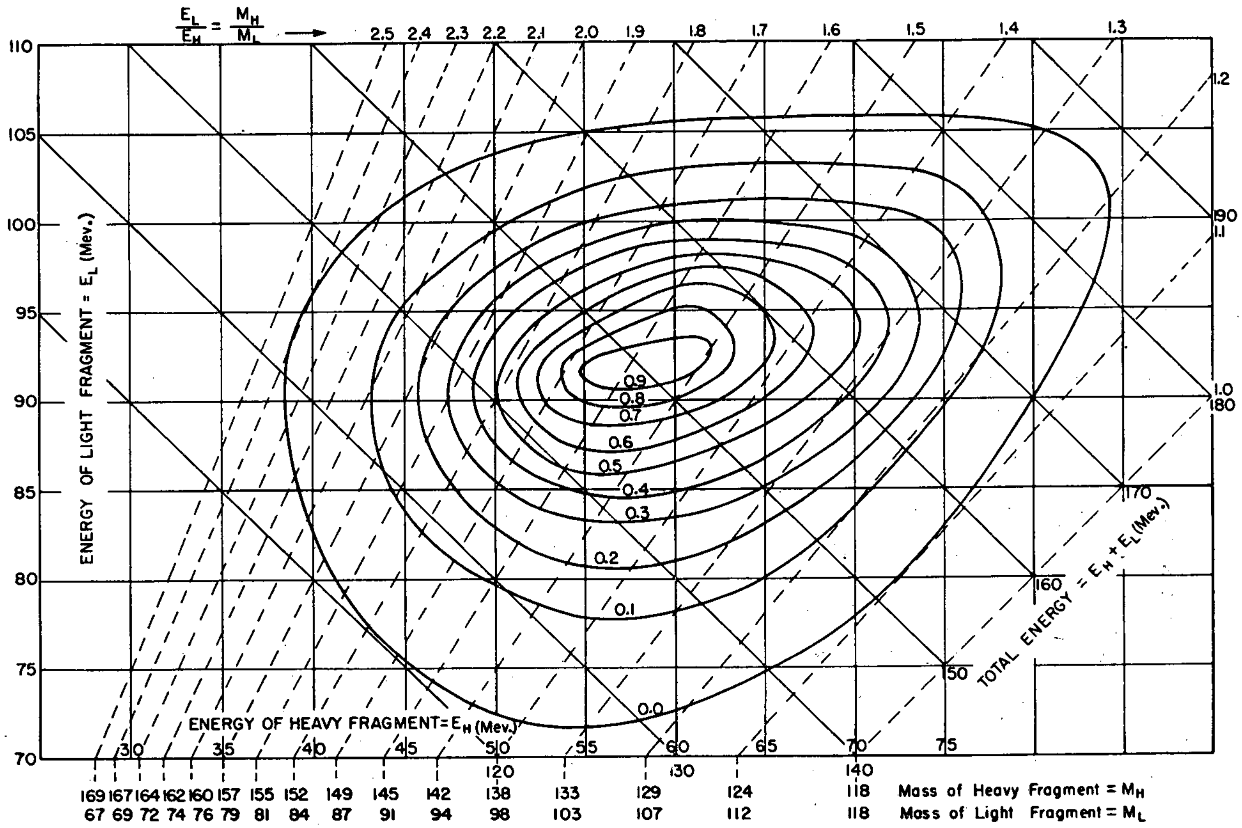

MU-19020

Fig. 11.53. Contour diagram of fission modes of U^{235}. BRUNTON and HANNA, Can. J. Research 28A, 190 (1950). The energy of the light and heavy fission fragments is given by the rectangular coordinates. Total kinetic energy and mass ratio are given by the oblique coordinates. The contours represent the relative frequency of occurrence of the fission modes. Energies in this figure are not corrected for ionization loss. The chamber gas was argon plus 1.5% CO_2. About 20,000 events were recorded.

average energy per ion pair formed so that alpha particles of known energy can be used to calibrate the chamber. KNIPP and LING[213] pointed out that the energy loss of a slow heavy particle is due predominantly to recoiling atoms so that ionization by secondary heavy particles contributes a large fraction of the total ionization resulting from a slow heavy primary particle stopped in a gas. If the secondary heavy particle ionization efficiency is low, as it is in argon, the overall efficiency for the production of ion pairs is greatly reduced for low energies of the primary particle. The decrease in ionization over that expected from the energy-ionization ratio, ω_α, derived from data on alpha particles is referred to as the ionization defect. Because of this ionization defect fission fragments expend larger averages of energy per ion-pair in the counter gas. Furthermore the energy-ionization ratio of the heavy and light fragments, ω_H and ω_L respectively, are slightly different.

LEACHMAN[214-216] has analyzed ionization chamber data to deduce the factors leading to these discrepancies. He found that to make the mass-yield curve derived from ionization chamber data agree with the radiochemical results he needed an ionization dispersion of 8 Mev per fragment (full-width at half-maximum) in the resolution of fission fragment energies. In addition, Leachman had to assume an ionization defect of 6 to 7 Mev in the ionization energies at the most probable mode. The existence of the defect was confirmed by transforming the ionization energy contours of BRUNTON and HANNA[211] to a velocity distribution and comparing the position of these distributions with the directly observed single fragment velocity distributions. The shift in energy from BRUNTON and HANNA'S value is then computed from the equation:

$$\frac{\Delta E_i}{E_i} = \frac{\Delta m_i}{m_i} + \frac{2\Delta V_i}{V_i}$$

where i stands for light or heavy fragment and E, m, and V are energy, mass, and velocity respectively. The result of this calculation is that an ionization defect of 5.7 Mev and 6.5 Mev were found for the light and heavy fragments, respectively, of U^{235} when the chamber gas was argon plus a few percent of CO_2. If ω_α is the energy/ionization ratio for alpha particles these figures correspond to fragment energy/ionization ratios, $\omega_L = 1.06\ \omega_\alpha$, and $\omega_H = 1.11\ \omega_\alpha$. When this total energy differential of $\langle \Delta E_L \rangle_{AV} + \langle \Delta E_H \rangle_{AV} = 5.7 + 6.5$ Mev = 12.2 Mev is added to the 154.7 Mev reported for the average total kinetic of the fragments from U^{235}, a corrected value of 166.9 Mev is obtained in excellent agreement with the calorimetric value of 167.1 ± 1.6 Mev and the fragment velocity value of 167.1 Mev.

---

[213] J. K. Knipp and R. C. Ling, Phys. Rev. 82, 30 (1951).

[214] R. B. Leachman, "Ionization Yields of Fission Fragments", Phys. Rev. 83, 17 (1951).

[215] R. B. Leachman, Phys. Rev. 87, 444 (1952).

[216] H W. Smitt and R. B. Leachman, Phys. Rev. 102, 183 (1956).

STEIN[217] performed a similar series of velocity measurements and confirmed fully LEACHMAN'S analysis. Figure 11.54 shows the energy distributions of single fragments computed from STEIN'S velocity distributions and compared with BRUNTON and HANNA'S[210] and BRUNTON and THOMPSON'S[211] ionization data. The shift of the two sets of data with respect to each other clearly reveals the ionization defect. The two sets of data are compared again in Table 11.20 where the ionization defect values are given in numerical form.

SCHMITT and LEACHMAN[216] studied the ionization-versus-energy relationship for fission fragments of U^{235} in several gases. The values of ionization defect which they obtained for these gases are given in Table 11.21. HERWIG and MILLER[218] have measured relative ionization yields for fission fragments in various gases.

11.6.2. Ion-Chamber Measurements of Fragment Energy Distribution in Spontaneous Fission. The distribution in the kinetic energy of fragments from the spontaneous fission of natural uranium and of Pu^{240} has been determined in a preliminary way by the ionization chamber method.[219,220] Such experiments are difficult because of the low specific activity toward spontaneous fission. Plutonium-240 has a spontaneous fission rate of only 1.6×10^6 per gram per hour and the corresponding figure for U^{238} has the much smaller value of 25.

---

[217] W. E. Stein, Phys. Rev. 108, 94 (1957).

[218] L. O. Herwig and G. H. Miller, Phys. Rev. 95, 413 (1954).

[219] W. J. Whitehouse and Galbraith, Phil. Mag. 41, 429 (1950).

[220] E. Segre and C. Wiegand, "Energy Spectrum of Spontaneous Fission Fragments", Phys. Rev. 94, 157 (1954).

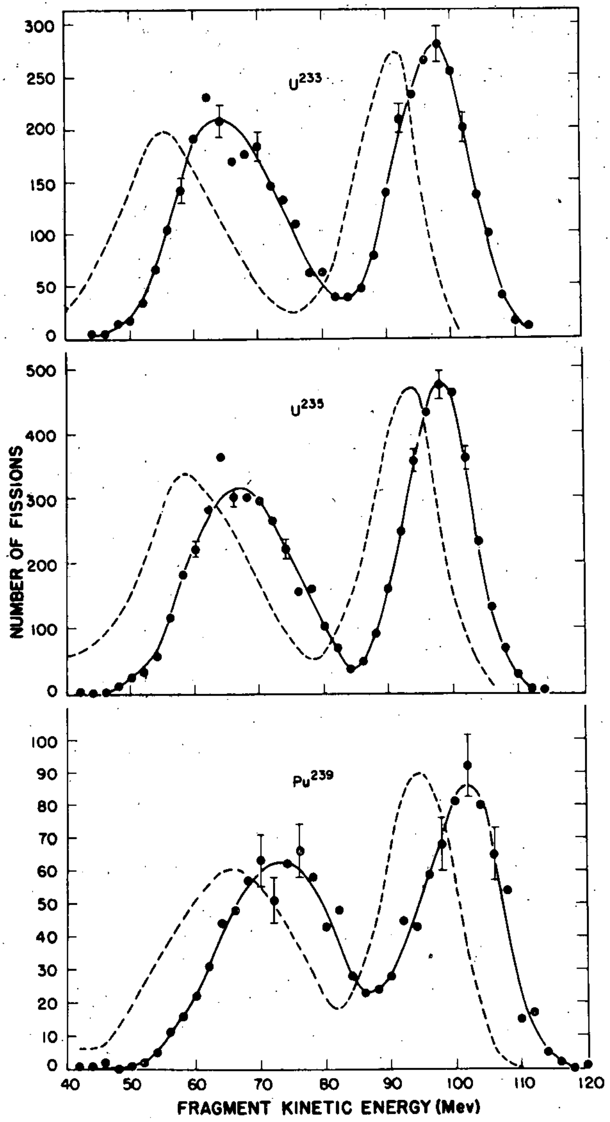

MU — 18709

Fig. 11.54. Energy distributions of single fragments from U^{233}, U^{235} and Pu^{239}. The solid curves represent conversion of STEIN'S[217] velocity data into an energy distribution. The dashed curves are renormalized data from double-ionization-chamber measurements of BRUNTON and HANNA,[210] and BRUNTON and THOMPSON.[211] Figure from Stein, reference 217.

Table 11.20

Comparison of ionization data and velocity data on the fission fragments of U^{233}, U^{235} and Pu^{239} — ionization defect values

	Ionization data				Velocity data			
	U^{233}	U^{235}	Pu^{239}	Ref.	U^{233}	U^{235}	Pu^{239}	Ref.
Light fragment energy	93.0	94.5	94.6	210, 211	97	98	100	217
Heavy fragment energy	56.6	60.2	65.2	210, 211	66	67	72	217
Light fragment ionization defect	6.1	5.7	5.2	215				
Heavy fragment ionization defect	7.3	6.5	6.4	215				
Total energy	163.0	166.9	171.4		163±2	165±2	172±2	

Note: The ionization data refer to most probable values whereas the time-of-flight data refer to average values.

Table 11.21

Ionization defect and energy/ionization ratio of U^{235} fission fragments in various gases
[Schmitt and Leachman, Phys. Rev. 102, 183 (1956)]

Gas	Fragment group	Ionization defect	$\overline{\omega}$ fragment/w_α
Argon + 3% CO_2	Heavy	6.3 ± 0.5	1.10 ± 0.02
	Light	6.5 ± 0.8	1.07 ± 0.02
Argon	Heavy	5.5 ± 0.5	1.09 ± 0.02
	Light	5.1 ± 0.8	1.05 ± 0.02
Nitrogen	Heavy	5.3 ± 0.5	1.09 ± 0.02
	Light	6.3 ± 0.8	1.07 ± 0.02
Neon	Heavy	4.8 ± 0.7	1.08 ± 0.02
	Light	4.3 ± 1.0	1.05 ± 0.02

MOSTOVAYA has nonetheless measured the fragment energy distribution in the case of Pu^{240} using the double ionization-chamber techniques.[220a]

In the case of even-even isotopes of higher Z elements the spontaneous fission half lives are much shorter, as is apparent at a glance in Fig. 11.30 of Section 11.3.6. This opens up the possibility of a detailed study of fission fragment energy distributions. HANNA and co-workers[221] reported some preliminary measurements on Cm^{242} using a single ionization chamber. SHUEY[222] has studied Cm^{242} using a double ionization chamber similar in general design to that of BRUNTON and HANNA.[210] Instead of electronic pulse height analysis SHUEY used photographic measurement of pulse height as registered on an oscilloscope to determine ionization caused by individual pulses. One scope was provided for each chamber and suitable circuitry was provided to make it possible to identify pulses which occurred simultaneously. SHUEY[222] collected data on a few thousand events and plotted a contour diagram similar to Fig. 11.53. The principal characteristics of the energy distribution in the spontaneous fission of Cm^{242} are given in Table 11.22; the numbers quoted there have been corrected for ionization defect.

SMITH, FIELDS, and FRIEDMAN[223-226] have used the double chamber technique to collect fission fragment data for the spontaneous fission of Cm^{244}, Pu^{240}, Pu^{242}, Cf^{252} and Fm^{254}. These authors have also studied fragment energy distributions for neutrons induced fission in Th^{229} and Pu^{241}.

The isotope of most general interest has turned out to be Cf^{252} as it is almost ideal for studies of this type. This nuclide has a half life of only

---

[220a] T. A. Mostovaya, Paper P/2031, Volume 15, Proceedings of the Second United Nations International Conference on the Peaceful Uses of Atomic Energy, Geneva, 1958.

[221] Hanna, Harvey, Moss, and Tunnicliffe, "Spontaneous Fission in Cm^{242}", Phys. Rev. 81, 466 (1951) (Letter).

[222] R. L. Shuey, "Fragment Energy Distribution in the Spontaneous Fission of Cm^{242}", University of California Radiation Laboratory Report, UCRL-959 (1950).

[223] A. Smith, P. Fields, and A. Friedman, Phys. Rev. 106, 779 (1957).

[224] A. Smith, A. Friedman, and P. Fields, Phys. Rev. 102, 813 (1956).

[225] A. Smith, P. Fields, A. Friedman, and R. Sjoblom, Phys. Rev. 111, 1633 (1958).

[226] Smith, Fields, Friedman, Cox, and Sjoblom, Paper P/690 in the Proceedings of the Second United Nations International Conference on the Peaceful Uses of Atomic Energy, Geneva, 1958, United Nations Publication, 1959.

Table 11.22

Summary of fission fragment properties (numbers refer to "most probable" values)

	Z^2/A	Energy[†] of light fragment in Mev	Energy[†] of heavy fragment in Mev	Total fragment energy[†] in Mev	M_H/M_L ion-chamber measurements[††]	M_H/M_L radiochemical measurements	Primary heavy fragment mass	Primary light fragment mass	Ref.[*]	Ref.[**]
Th^{229}+n	35.22	100	60	160±3	1.57	---	---	---	a	-
U^{233}+n	36.17	97[†††]	66[†††]	163±2	1.47±0.02	1.46	139	95	b	g
U^{235}+n	35.86	98[†††]	67[†††]	165±2	1.46±0.02	1.45	140	96	b	g
Pu^{239}+n	36.82	100[†††]	72[†††]	172±2	1.39±0.02	1.39	140	100	b	g
Pu^{241}+n	36.51	101	73	174±3	1.38±0.02	---	140	102	d	-
Pu^{242} sp.fiss.	36.51	101	73	174±3	1.38±0.02	---	140	102	d	-
Cm^{242}	38.08	110.8	85.9	196.7	1.29	1.32	138	104	e	f
Cm^{244}	37.77	105.5	80	185.5±5	1.32±0.05	---	139	105	c	-
Cf^{252}	38.11	105.0	80	185±4	1.33±0.04	1.33	144	108	i,j	h
Fm^{254}	39.37	101.5	74.5	176±6	1.36±0.05	---	146	108	c	-

[*] Ref. to ion chamber data.

[**] Ref. to radiochem. data.

[†] All ionization chamber measurements corrected for an ionization defect of about 7 Mev per fragment.

[††] M_H/M_L from ion-chamber measurements refers to primary fragments.

[†††] These values are taken from the time-of-flight measurements of STEIN;[217] they are average values rather than most probable values.

References to Table 11.22

a. See reference 225.

b. See reference 217.

c. See reference 226.

d. See reference 223.

e. Shuey, reference 222.

f. E. P. Steinberg and L. E. Glendenin, Phys. Rev. 95, 431 (1954).

g. Refer to Section 11.4.2.

h. L. Glendenin and E. Steinberg, J. Inorg. and Nuclear Chem. 1, 45 (1955).

i. See reference 224.

j. See reference 227.

82 years for spontaneous fission and an alpha-decay-to-spontaneous-fission-decay ratio of only 30. One microgram of Cf^{252} gives rise to 4×10^7 spontaneous fission events per minute; hence a very thin source provides a very convenient number of fission events for rapid collection of data and there is only a modest background of alpha particle radiation, from which the fission fragments can be discriminated easily. In addition to the work of SMITH, FIELDS, and FRIEDMAN[224] the double ionization chamber technique has been applied to Cf^{252} by BOWMAN and THOMPSON[227], and by HICKS and co-workers.[228] This nuclide has also been carefully studied by the time-of-flight techniques as is discussed below.

Figure 11.55 gives a contour plot of the results taken from an analysis of 5000 spontaneous fission events. Fragment mass distribution, energy distribution and asymmetry can be obtained directly from this diagram. It is perhaps easier to visualize the kinetic energy distribution by the plot shown in Fig. 11.56. The gross probability distribution for the fission fragment energies are shown and in addition, the distribution in the energy of one fragment when the energy of the second is selected. This figure is similar in all respects to Fig. 11.51 which shows the analogous energy distributions in the fission of U^{235} induced by slow neutrons. All the comments made previously about Fig. 11.51 apply to Fig. 11.56 as well. Again it can be noted that if the gate energy is selected at the minimum between the two peaks the energy distribution in coincidence does not peak at the same energy but is a two-humped distribution very similar to the total distribution. Curves of this type can be obtained directly from the contour diagram of Fig. 11.55.

The fragment energy distributions can be converted into mass-ratio distributions using the approximate* equality

---

227. H. Bowman and S. G. Thompson, University of California Radiation Laboratory Report, UCRL-5038, March, 1958; see also Paper P/652 in Proceedings of the Second United Nations Conference on the Peaceful Uses of Atomic Energy, Geneva, 1958.

228. Hicks, Ise, Pyle, Choppin, and Harvey, Phys. Rev. 105, 1507 (1957).

229. W. E. Nervik and co-workers, unpublished data, 1958.

*These two ratios are not precisely the same but for the present purpose they can be considered identical. A good discussion of the relation of these two ratios is given in an appendix of a paper by Terrell, Phys. Rev. 113, 527 (1959); see also Brunton and Hanna.[210]

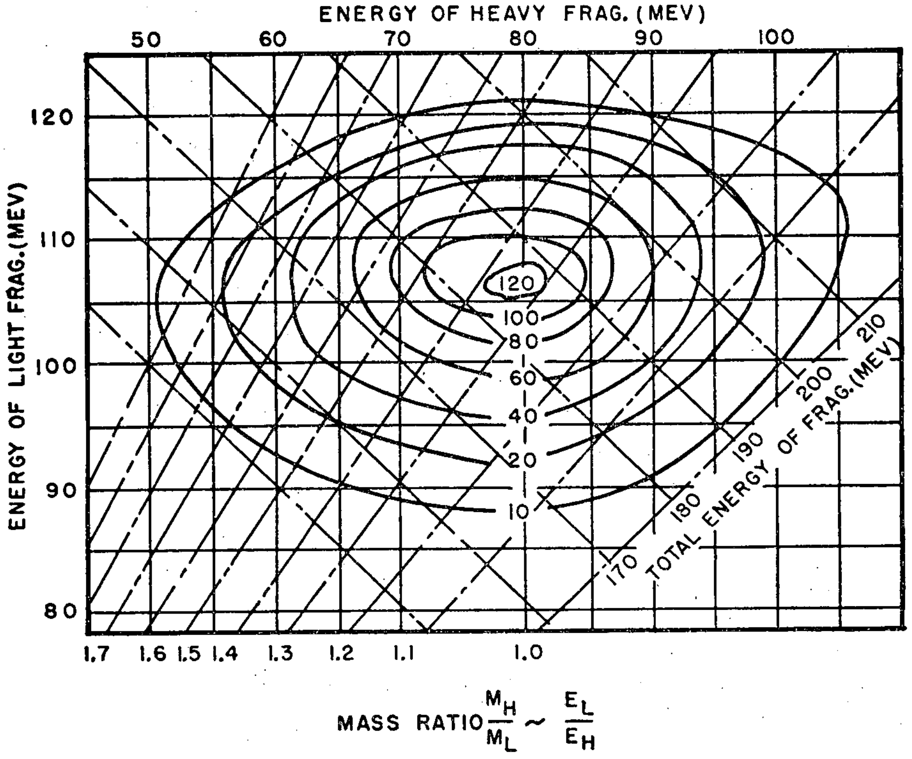

MU-18903

Fig. 11.55. Relative probabilities of Cf^{252} spontaneous fission modes. All energies have been corrected for an ionization defect amounting to 7 percent per fragment. SMITH, FRIEDMAN and FIELDS.[224]

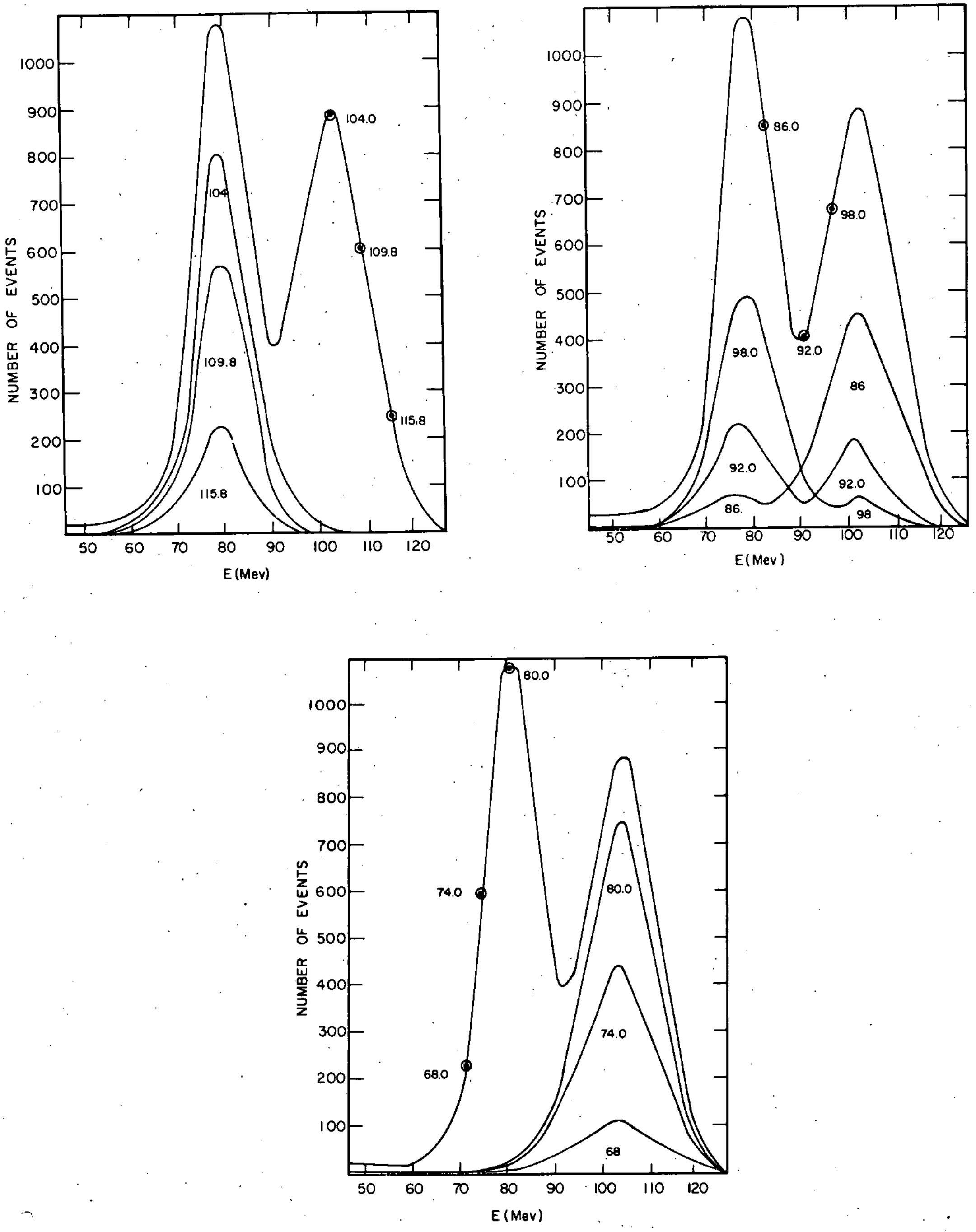

MUB-381

Fig. 11.56. The fission fragment kinetic energy distribution for Cf^{252}. The top curve in each case is the total distribution. The circled points indicate energy intervals selected by 3 Mev window on gate pulses from one-half of a double ionization chamber. The correspondingly labelled distributions are the coincident energies measured in the other chamber. BOWMAN and THOMPSON.[227] An ionization defect correction of 6.1 Mev has been added to all experimental data.

$$\frac{M_L}{M_H} = \frac{E_H}{E_L} .$$

This conversion has been made in Fig. 11.57 where the resulting mass-ratio distribution is compared with the radiochemical yield data of NERVIK.[229] The ionization data give a most probable mass ratio of 1.33 compared to the value of 1.34 obtained from the chemical analysis. These data are in excellent agreement with the time-of-flight measurements reported in Section 11.6.3.

It is interesting to make an overall comparison of fragment energy data for many fissioning nuclides obtained by the double ionization chamber technique. This is done in Table 11.22. We note that the properties of fission are very much the same in general features for all the fissioning nuclei listed. The total fragment energy is a slowly increasing function of the fission parameter Z^2/A up through Cm^{242}. At Cf^{252} the trend is reversed with decreasing total energy for higher values of Z^2/A. The mass of the most probable heavy fragment stays constant at about 140 except for the heaviest nuclei, Cf^{252} and Fm^{254}. To compensate for this the mass of the most probable light fragment must shift steadily upward with the mass of the fissioning nucleus, except for Cf^{252} and Fm^{254}. These trends are summarized in Fig. 11.58.

The double ionization chamber technique of establishing fission modes can be used in coincidence with other detectors to measure other properties of fission. Such applications are discussed in later sections of this chapter. We wish also to call attention again to the neat use of the double ionization chamber technique by BOLLINGER to deduce the mass-yield curve. This application is discussed in Section 11.4.4 and a sample curve is shown in Fig. 11.39.

11.6.3 Time-of-Flight Measurements of Fission Fragment Velocity.

LEACHMAN[230] introduced the time-of-flight method for determining the velocities (and hence indirectly the energies) of the fission fragments. As is shown schematically in Fig. 11.59, velocities were measured by the time-of-flight of the fission fragments through an evacuated drift tube. The time origin of each measurement is provided by the pulse P_o from the fission fragment traveling the

---

[230] R. B. Leachman, "Velocity of Fragments from Fission of U^{233}, U^{235}, and Pu^{239}", Phys. Rev. 87, 444 (1952).

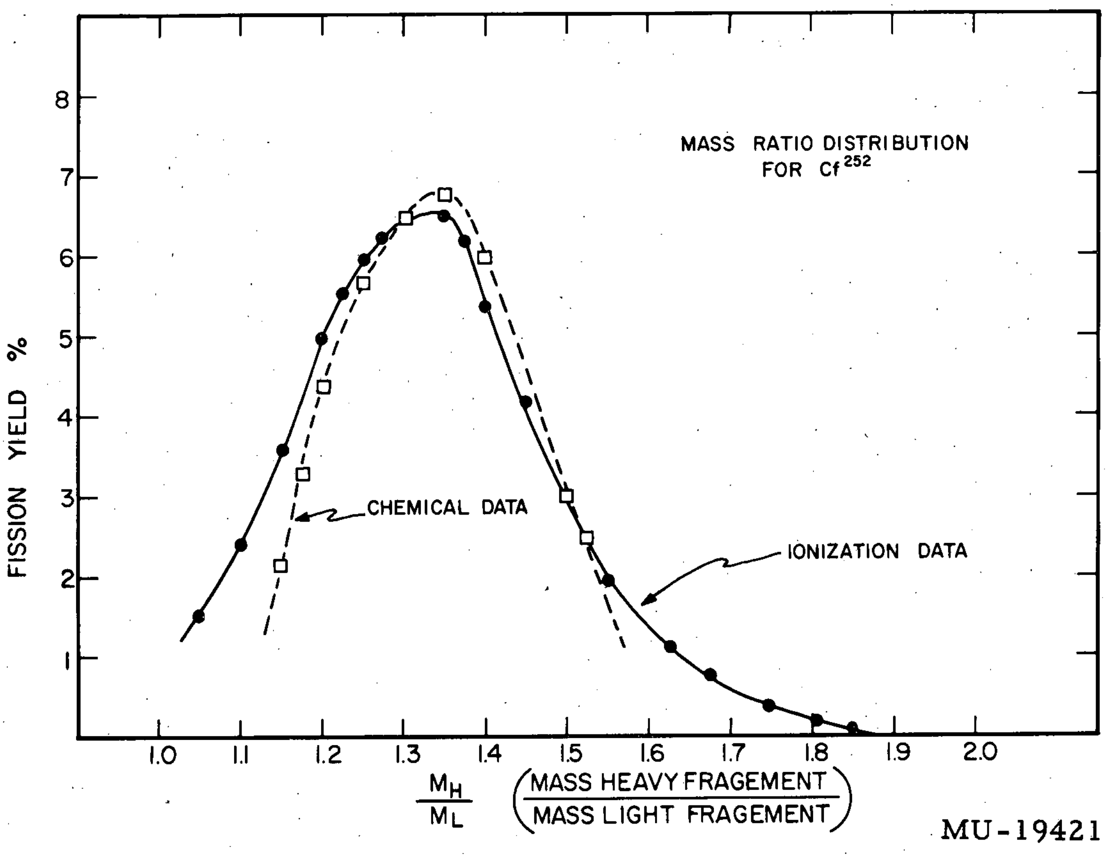

Fig. 11.57. The mass ratio distributions for Cf^{252} from ionization measurements and radiochemical yield data. BOWMAN and THOMPSON.[227]

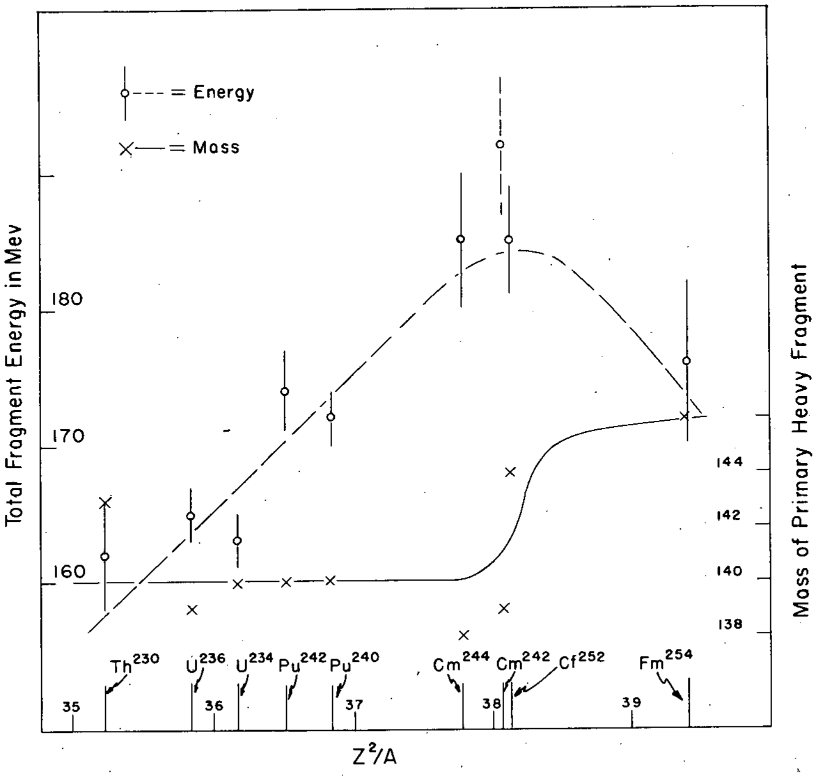

MU-18905

Fig. 11.58. Shifts in total fragment energy and the mass of the most probable heavy fragment with Z^2/A. Figure from Geneva paper by Smith, Fields, Friedman, Cox and Sjoblom[226].

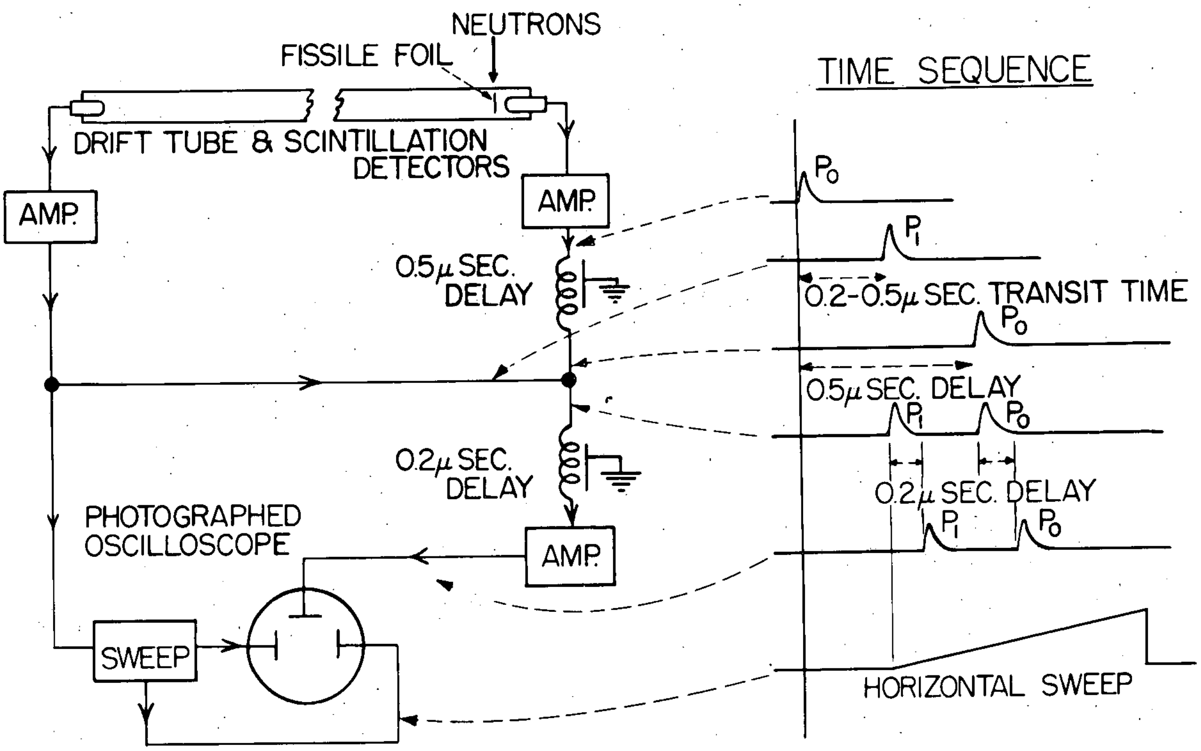
NEUTRONS
FISSILE FOIL
DRIFT TUBE & SCINTILLATION DETECTORS
AMP.
AMP.
0.5μ SEC. DELAY
0.2μ SEC. DELAY
AMP.
PHOTOGRAPHED OSCILLOSCOPE
SWEEP
TIME SEQUENCE
P0
P1
0.2-0.5μ SEC. TRANSIT TIME
P0
0.5μ SEC. DELAY
P1
P0
0.2μ SEC. DELAY
P1
P0
HORIZONTAL SWEEP

MU-18851

Fig. 11.59. Schematic diagram of LEACHMAN's[230] time-of-flight equipment. The time sequence illustrates that the less frequent pulses P_1 from the fragments which travel the length of the drift tube initiate the oscilloscope display, the pulses P_0 from the complementary fragments are delayed by the maximum transit time, and the mixture of P_1 and P_0 are in addition, delayed for proper oscilloscope presentation.

1 cm distance from the fission source to the nearest anthracene scintillation detector. The time-of-flight of the complementary fragment through the 343-cm drift distance determines the time of occurrence of P_1, the pulse from the remote detector. Fission was induced by a beam of thermal neutrons from a reactor. In order to decrease the number of the recorded data the less frequent pulses P_1 from the remote detector were used to initiate the oscilloscope displays of the pulses. Photographs of these sweeps were analyzed for the distribution in time-of-flight. The detectors and circuits used in the experiment gave pulses with rise times of $\sim 10^{-8}$ seconds, short compared to the 0.2 to 0.5 microsecond flight time of fragments through the 343-cm drift distance.

LEACHMAN[230] measured the velocity distribution of fragments from the fission of U^{233}, U^{235}, and Pu^{239} and compared his results with velocity distributions derived from the earlier ionization measurements[210,211] of fragment energy distributions. The time-of-flight data were more satisfactory because of the lower dispersion introduced by this method of measurement and because of the ionization defect inherent in the ion-chamber technique. The time-of-flight technique can achieve, with reasonable fragment flight distances, energy dispersions perhaps half the size of those estimated to be inherent in the ionization-chamber method. Furthermore, since the time-of-flight measurements permit the mass ratio of the fragments to be determined from a velocity ratio, rather than from an energy ratio, the dispersion in the measurement of a mass ratio by time-of-flight is slightly less than half the corresponding dispersion obtained by the ion chamber method. The limitation in the time-of-flight precision in principle lies in the effects of the fragment recoil from neutron emission.

LEACHMAN and SCHMITT[331] measured the velocity distribution of fission fragments slowed by passage through aluminum or nickel absorbers and detected fine structure in the velocity distribution of the fragments from U^{235}. No fine structure was observed for unslowed fragments. Comparison of this velocity fine structure with the fine structure in the fission mass yield confirms the influence of the 82-neutron shell in the fission act as distinguished from its

---

331. R. B. Leachman and H. W. Schmitt, "Fine Structure in the Velocity Distributions of Slowed Fission Fragments", Phys. Rev. 96, 1366 (1954).

influence in post-fission boil-off. No velocity fine structure was observed by this method in the fragments from U^{233} and Pu^{239}.

The usefulness of the time-of-flight technique was greatly increased by providing for the measurement of the velocity of both fragments in a double drift tube apparatus[332-334] analogous in conception to the double ionization chamber apparatus we have discussed previously. A schematic diagram of the apparatus is shown in Fig. 11.60. A thin sample of fissionable material mounted on a thin foil is placed in the center of the double drift tube. The velocities of the two fragments from a single fission event are measured by their time-of-flight through flight paths of 269 centimeters. The flight time for the light fragment is about 180 millimicroseconds; the time resolution is about 5 millimicroseconds corresponding to a mass resolution of two to three mass units. Fission was induced in the fissile material by a beam of thermal neutrons. The apparatus may also be used for a spontaneously-fissioning sample. One difficulty in this type of experiment is setting the initial time of fission since neither fragment is available to trigger the recording sequence. This problem is solved by utilization of the large number of electrons (about 50 to 100) ripped out of the thin backing foil when one of the fragments passes through it on its way down the drift tube. These electrons are accelerated to a high potential and electrostatically focused on a plastic phosphor mounted on a photomultiplier tube. This δ-ray electron detection system[335] produces a pulse P_0 which signals the beginning of the fission event with a time resolution of 5×10^{-9} seconds. The fission fragments are detected in scintillation crystals of 2-inch diameter and 8-inch diameter, respectively, mounted on photomultiplier tubes at the opposite ends of the drift tubes. The larger diameter detector corrects for non-collinearity introduced by neutron emission and by fragment scattering in the source. The time sequence of detector pulses is displayed in the schematic diagram.

---

332. W. E. Stein, Phys. Rev. 108, 94 (1957).

333. W. E. Stein and S. L. Whetstone, Jr., Phys. Rev. 110, 476 (1958).

334. J. C. D. Milton and J. S. Fraser, Phys. Rev. 111, 877 (1958); also published as Paper P/199, Proceedings of the Second United Nations Conference on the Peaceful Uses of Atomic Energy, Geneva, 1958.

335. W. E. Stein and R. B. Leachman, Rev. Sci. Instr. 27, 1049 (1956).

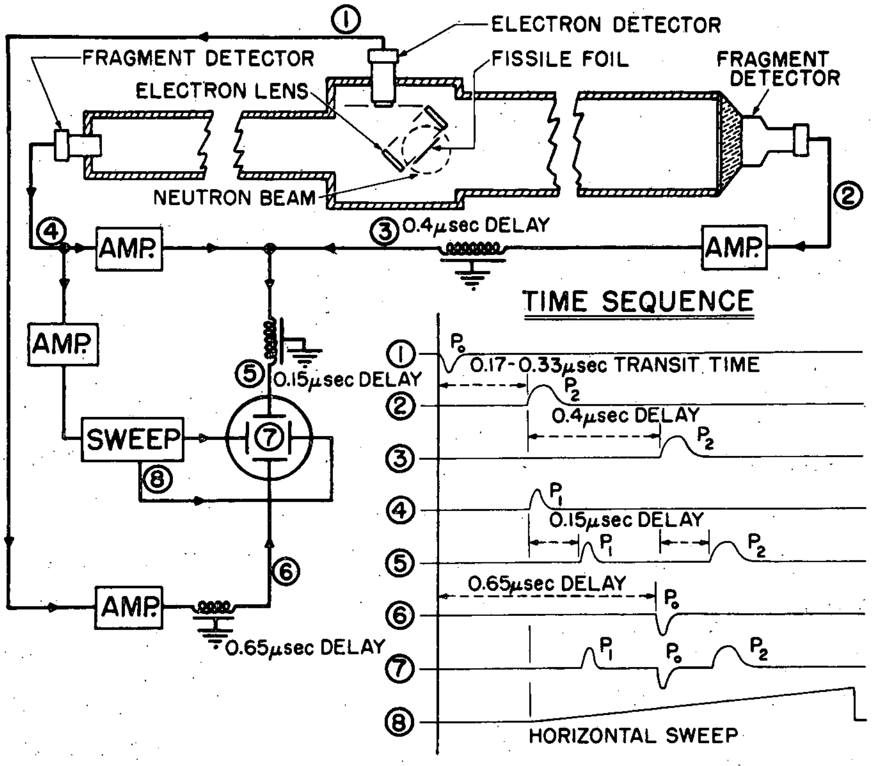
①
ELECTRON DETECTOR
FRAGMENT DETECTOR
FISSILE FOIL
FRAGMENT DETECTOR
ELECTRON LENS
NEUTRON BEAM
②
④
AMP.
③ 0.4μsec DELAY
AMP.
TIME SEQUENCE
AMP.
⑤ 0.15μsec DELAY
SWEEP
⑦
⑧
⑥
AMP.
0.65μsec DELAY
① P₀ 0.17-0.33μsec TRANSIT TIME
② P₂
0.4μsec DELAY
③ P₂
④ P₁
0.15μsec DELAY
⑤ P₁ P₂
0.65μsec DELAY
⑥ P₀
⑦ P₁ P₀ P₂
⑧ HORIZONTAL SWEEP

MU-18867

Fig. 11.60. Schematic diagram of STEIN'S[332] time-of-flight apparatus. Pulses were amplified by Hewlett-Packard 460A and 460B amplifiers and delayed by appropriate lengths of RG7/U cable. The fragment time-of-flight is the time between the occurence of P_0 and P_1 and that of the complementary fragment is the time between the occurrence of P_0 and P_2. The P_1 pulses were used to initiate the oscilloscope displays of the pulses. Photographs of these sweeps were analyzed for the times between pulses. The time scale was provided at frequent intervals by photographs of a 50-Mc/sec signal from a crystal-controlled oscillator.

STEIN'S[332] data on the slow neutron fission of U^{233}, U^{235} and Pu^{239} are shown in Fig. 11.54 and Table 11.20 which appear in Section 11.6.1. In his paper STEIN presents contour plots of his data, from which more detailed examination of fission properties can be made. One interesting correlation is shown in Fig. 11.61 which displays the average total kinetic energy as a function of mass ratio. There is a dip in this curve for mass ratios close to 1. This same dip is seen in the ion-chamber measurements (compare Fig. 11.52) and in radiochemical range measurements (compare Fig. 11.70).

Velocity measurements have also been made[333,334] on the fragments from the spontaneous fission source, Cf^{252}. Kinetic energy distributions and primary mass-yield distributions determined by STEIN and WHETSTONE[333] are shown in Figs. 11.62 and 11.63. The time-of-flight technique has been employed in coincidence with neutron[333] and gamma ray detectors[334] to measure neutron multiplicity and gamma ray spectra coincident with specific modes of fission as characterized by total kinetic energy and mass ratio of the fragments. These studies are summarized later in this chapter.

11.6.4 Measurement of Fission Fragment Ranges.[‡] The calculation of the interaction of fission fragments with matter is a difficult undertaking as can be seen by considering the process in only moderate detail. At the time of scission the fragments are accelerated to quite high velocities. These fragments are highly charged due to serious disruption of the uranium electron cloud during the fission process. As early as 1940 PERFILOV[336] measured the deflection of fission fragments expelled from thin layers of U_3O_8 and reported a net charge of about 20. The later measurements of COHEN and co-workers[337] show that the most probable electronic charge of a Zr^{97} fragment is 21 units. Due to this charge the fragments ionize and excite atoms which are at some distance from the fragment path and thereby lose energy. Some of these elctrons are captured by the fragment and the net charge of the fragment is gradually reduced. Occasionally there are direct collisions with atoms resulting in a complicated rearrangement of the electronic system of the fragment and the

---

336. N. A. Perfilov, Compt. rend. Acad. Sci. USSR 28, 5 (1940).

337. B. L. Cohen, A. F. Cohen and C. D. Coley, Phys. Rev. 104, 1046 (1956).

[‡] The subject matter of this section was reviewed by G. N. Walton, "Fission Recoil and Its Effects", Prog. Nuclear Phys. 6, 193-232 (1957).

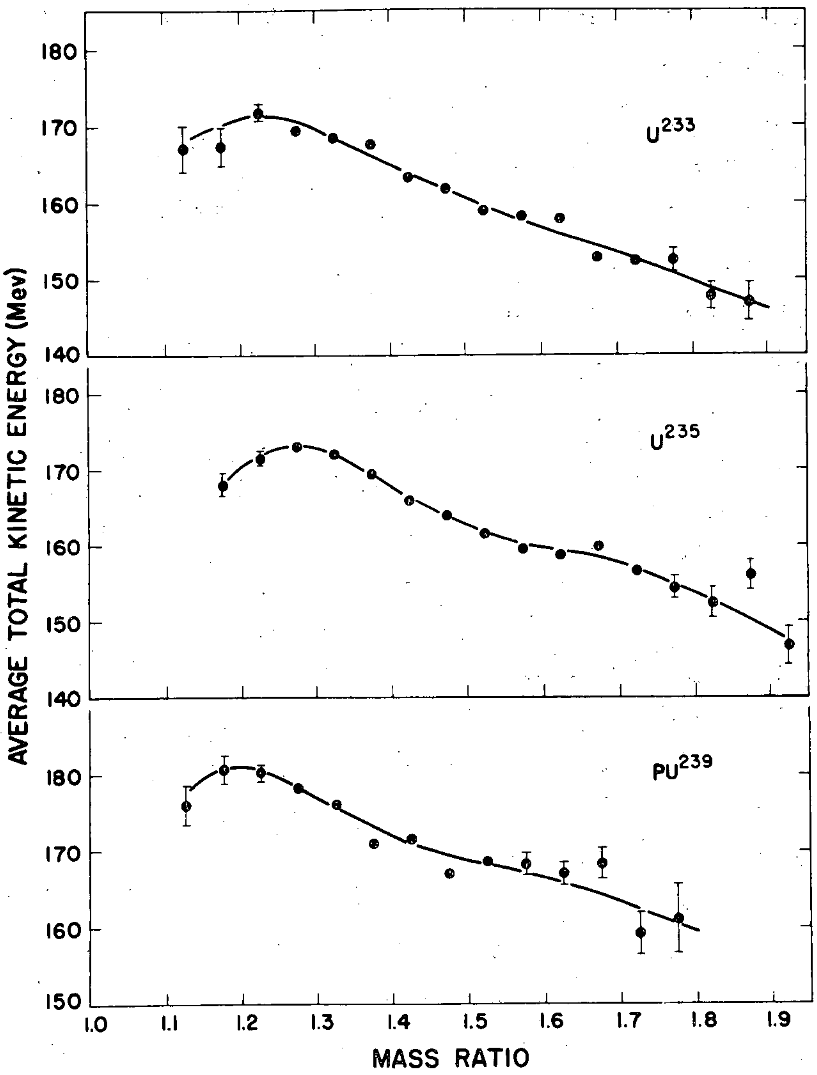

MU-18866

Fig. 11.61. Variation of the average total kinetic energy with mass ratio. Kinetic energy computed from STEIN'S velocity data. Figure from reference 332.

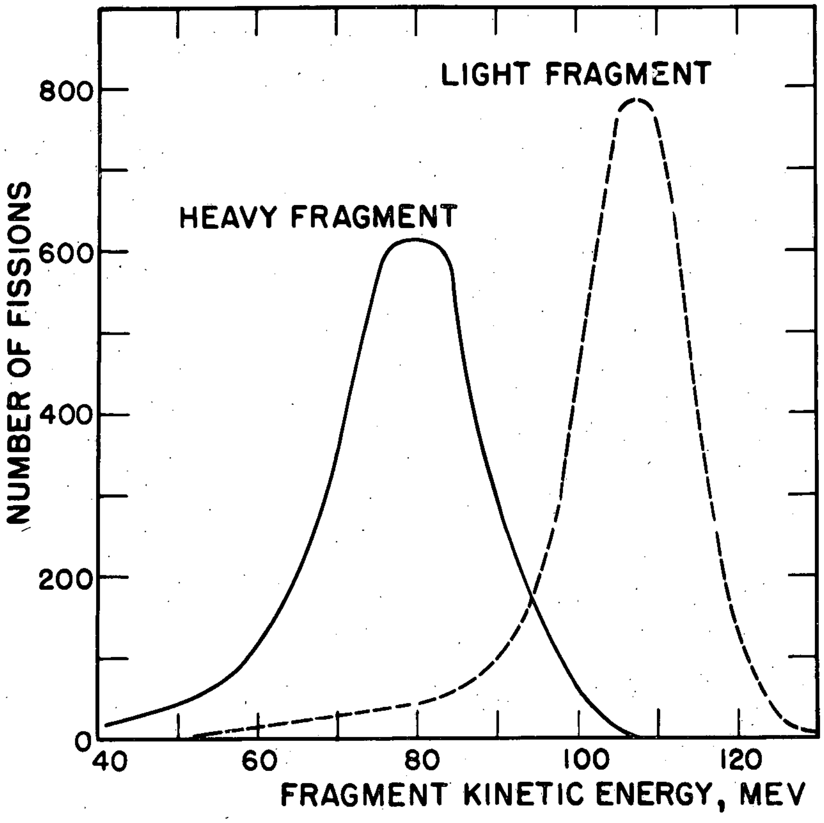

MU-18865

Fig. 11.62. Kinetic energy distributions of fission fragments of Cf^{252}. From STEIN and WHETSTONE.[333]

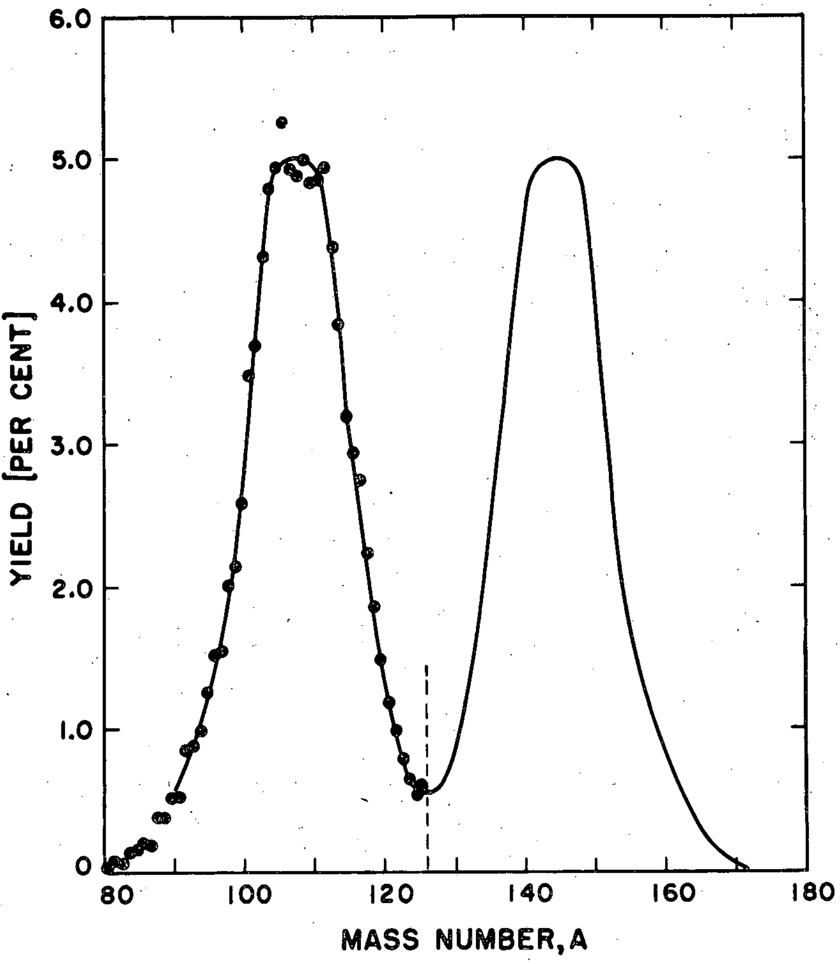

MU-18864

Fig. 11.63. The primary mass-yield distribution of the fragments of Cf^{252}. The measured distributions are necessarily symmetric about the mass number A = 126. From STEIN AND WHETSTONE.[333]

struck atom. These nuclear encounters in which kinetic energy is imparted to the stopping atom as a whole play an important part at the end of the range. As the fragment slows down at the end of the range its average net charge will tend to decrease and eventually reach zero, when only close collisions will be of any importance in reducing the fragment energy to the thermal equilibrium value.

This slowing down process would be very difficult to calculate for a single fragment species with a well defined initial energy and charge. This calculation is all the more difficult for the fission fragments which consist of a wide variety of products. Even when a single species is considered there is an appreciable dispersion in energy and net charge. COHEN, COHEN, and COLEY[337] used magnetic analysis to study the charge and energy distribution of Zr^{97} fragments ejected from a thin film of uranium and found a width of 11.4 percent for the energy distribution corrected for broadening due to prompt neutron emission. STEIN[332] found the somewhat lower value of 8.1 percent from an analysis of the velocity distribution of fragments of mass 97. From COHEN'S[337] work the most probable charge for Zr^{97} fragments was 21 but large percentages of charge-states 20, 22 and others were present.

There are important qualitative differences between the energy loss of fission fragments and alpha particles along their range. Due to the slower velocities and continual decrease in net charge of fission fragments the ionization sharply decreases along the range in contrast to the case of alpha particles or protons which exhibit an increasing ionization with decreasing velocity. At the very end of the range of fission fragments the energy loss due to nuclear collision increases. In alpha tracks observed in cloud chambers nuclear branching due to nuclear collisions is rare, occurring only once in several thousand tracks. Nuclear scattering is prominent in fission fragment tracks and sometimes occurs repeatedly in a single track.

Theoretical treatments of the energy loss of fission fragments have been made[338-341] by several authors with reasonably good success as far as the

---

338. N. Bohr, Phys. Rev. 58, 654 (1940); 59, 270 (1941); Kgl. Danske. Videnskab. Selskab, Mat.-Fys.Medd. 18, 8 (1948).

339. W. E. Lamb, Jr., Phys. Rev. 58, 696 (1940).

340. J. Knipp and E. Teller, Phys. Rev. 59, 659 (1941); see also Brunings, Knipp and Teller, Phys. Rev. 60, 657 (1941).

341. See general review of Bethe and Ashkin in Vol. 1 of "Experimental Nuclear Physics", edited by E. Segre, John Wiley and Sons, Inc., New York, 1953.

general features go. It is beyond the scope of our review to discuss these theories and we limit ourselves to a few comments about the results due to BOHR.[338]

According to BOHR'S development the total energy loss per centimeter is expressed as:

$$\frac{1}{N}\frac{dE}{dx} = \frac{4\pi e^4}{mv^2}\left(Z_1^{eff}\right)^2 Z_2 \log \frac{1.123\, mv^3}{\omega e^2\, Z_1^{eff}} + \frac{4\pi e^4}{M_2 v^2} Z_1^2\, Z_2^2 \log \frac{M_1 M_2}{M_1 + M_2}\, \frac{v^2\, a_{12}^{scr}}{Z_1 Z_2\, e^2} \,. \qquad (11.47)$$

The terms in this expression have these meanings:

N is number of atoms of the stopping medium per cubic centimeter.

M_1 and M_2 are the masses of the fragment and of the absorber.

Z_1 and Z_2 are the charges of the fragment and of the absorber.

e is the electronic charge and m is the electronic mass

v is the fragment velocity

Z_1^{eff} is the effective charge of the fragment; at the beginning of the range this quantity is about 20.

a_{12}^{scr} is an impact parameter which tells at what distance the energy loss in nuclear collisions is effectively zero owing to the screening of the charges of the nuclei by atomic electrons.

$\omega = I/\hbar$ is an average oscillation frequency of the electrons in the atom.

The first term expresses the energy loss attributable to electronic excitation of the absorber atoms while the second describes the transfer of energy by nuclear collisions. At the beginning of the range, where Z_1^{eff} is about 20, the electronic term is dominant but toward the end of the range, when Z_1^{eff} drops toward 2, the fractional contribution of the nuclear term rises rapidly and becomes more important. When protons or alpha particles are stopped in matter the nuclear scattering never becomes important because of the low value of Z_1. The greater importance of nuclear scattering in the total range of heavy fragments has the important consequence that the range will show an appreciable straggling. The dissipation of an appreciable fraction of the total kinetic energy by nuclear scattering also accounts for the ionization defect which is discussed in Section 11.6.1. In stopping gases such as argon, commonly used in ionization chambers, several Mev of kinetic energy may be lost in the motion of recoiling atoms which do not lose electrons but remain neutral.

A critical step in the application of the Bohr relation is the evaluation of Z_1^{eff}. As the fragment passes through matter it continuously gains and loses electrons and it is very difficult to calculate the equilibrium charge at every value of the kinetic energy. BOHR assumed as a first approximation that the fragment loses all of its electrons whose orbital velocity is smaller than the velocity of the fragment itself. This assumption has been commonly used in evaluating this and related equations. More recently FULMER and COHEN[342] have measured the equilibrium charges of fission fragments of a variety of fragment masses and velocities by magnetic analysis of fission fragments slowed by gases at various pressures. Their results indicate that BOHR'S assumption is only a rough approximation. An earlier study by LASSEN[343-344] also gathered data on the variation of equilibrium charge with gas pressure.

We turn now to a discussion of experimental data on the stopping of fission fragments. In the first years after the discovery of fission, a number of authors[345] studied the mean ranges of the two main groups of fission products. Ranges were measured in air, in various gases, in plastic films, aluminum and various other materials. These studies indicated a maximum range of about 2.0 cm air equivalent for the heavy group and 2.5 cm for the light group.

From studies carried out by the cloud chamber technique, BØGGILD and co-workers[346,347] determined the mean ranges of the fragments in the gases listed in Table 11.23.

LASSEN[348] studied the ionization produced in an ionization chamber by fission fragments after passage through various amounts of the chamber gas and thus obtained a differential ionization curve along the range. Measurements

---

[342] C. B. Fulmer and B. L. Cohen, Phys. Rev. 109, 94 (1958).

[343] N. O. Lassen, Phys. Rev. 69, 137 (1946).

[344] N. O. Lassen, Kgl. Danske. Videnskab. Selskab. Mat-fys. Medd. 26, No. 12 (1951); see also Vol. 30, No. 8 (1955).

[345] See for example the references and discussion given in Ref. 353 below and the review article of L. A. Turner, Rev. Modern Phys. 12, 23 (1940).

[346] Bøggild, Arroe, and Sigurgeirsson, Phys. Rev. 71, 281 (1947).

[347] Bøggild, Minnhagen and Nielsen, Phys. Rev. 76, 988 (1949).

[348] N. O. Lassen, Dan. Matt. Fys. Medd. 25, No. 11 (1949).

Table 11.23

Mean Range of Fission Fragments of U^{235}

	Air (mm)	Hydrogen (mm)	Helium (mm)	Argon (mm)	Xenon (mm)
Light fragment	25.4	17.7	23	19.4	18
Heavy fragment	19.5	21.1	28	23.9	23
(Total range)	44.9	38.8	51	43.3	41

Values for air taken from Bøggild, Minnhagen and Nielsen, Phys. Rev. 76, 988 (1949).

Other values taken from Bøggild, Arrøe, and Sigurgeirsson, Phys. Rev. 71, 281 (1947).

were made in argon, xenon, hydrogen, deuterium and helium. Such measurements show clearly the predicted rapid drop in specific ionization during the first part of the range where electronic interactions are dominant. By combining his results with experimental range values of others and by use of that part of BOHR'S stopping formula which should describe the nuclear collision part of the energy loss expression, LASSEN constructed curves such as that shown in Fig. 11.64 showing energy loss along the entire range. The ionization defect effect was not found until later and a proper correction of the data would change LASSEN'S curves somewhat as FULMER[349] has pointed out.

FULMER[349] measured the energy of fission fragments after passage through various thicknesses of absorbers. The energy measurement was made with a CsI scintillation detector whose pulse height-versus-energy curve was well calibrated by reference to the data of LEACHMAN and SCHMITT.[350] These latter authors used the very accurate time-of-flight technique (Section 11.6.3) to measure the velocity distributions of fission fragments of U^{235}, U^{233} and Pu^{239} which had passed through a thin metallic absorber. Three absorber thicknesses of aluminum, two of nickel, one of gold and one of platinum were used. FULMER[349] separated fission fragments of U^{235} into light and heavy groups by means of a magnetic fission-fragments spectrometer placed close to a research reactor. These selected fragments were reduced in energy by passage through gaseous or metallic stopping materials and then allowed to impinge on a CsI scintillation crystal. The data are summarized in Figs. 11.65 and 11.66. These figures show the energy of median-mass light and heavy fragments as a function of the thickness of absorbers through which they have passed the intercepts of these curves on the zero energy axis are based on the radiochemical range measurements of SUZOR[352] and of KATCOFF, MISKEL and STANLEY[353] cited below.

In a related series of measurements FULMER and COHEN[342] used their high resolution magnetic spectrometer to measure the equilibrium charges of U^{235} fission fragments as a function of velocity after passage through an absorber gas. The results are summarized in Figs. 11.67 and 11.68.

---

[349] C. B. Fulmer, Phys. Rev. 108, 1113 (1957).

[350] R. B. Leachman and H. W. Schmitt, Phys. Rev. 96, 1366 (1954).

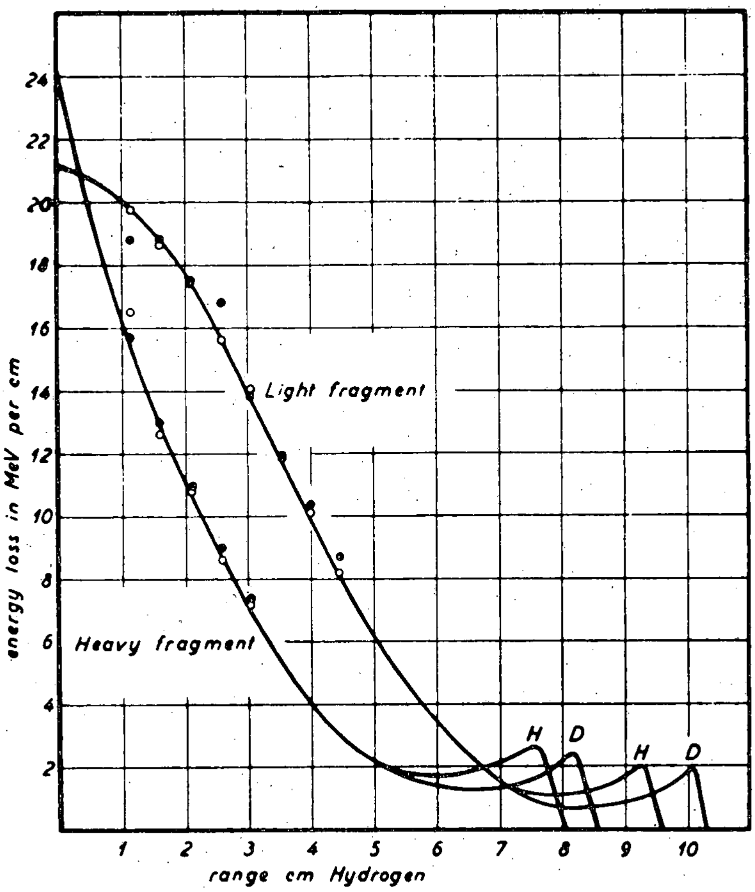

MU-18826

Fig. 11.64. Energy loss curve for fission fragments stopping in hydrogen and deuterium. Curves were constructed by LASSEN[348] from his experimental measurements and the N. BOHR energy loss formula.[338] The open circles are the experimental values found in H_2 (after normalization) and the full circles are the corresponding values in D_2. Data uncorrected for ionization defect; see reference 349.

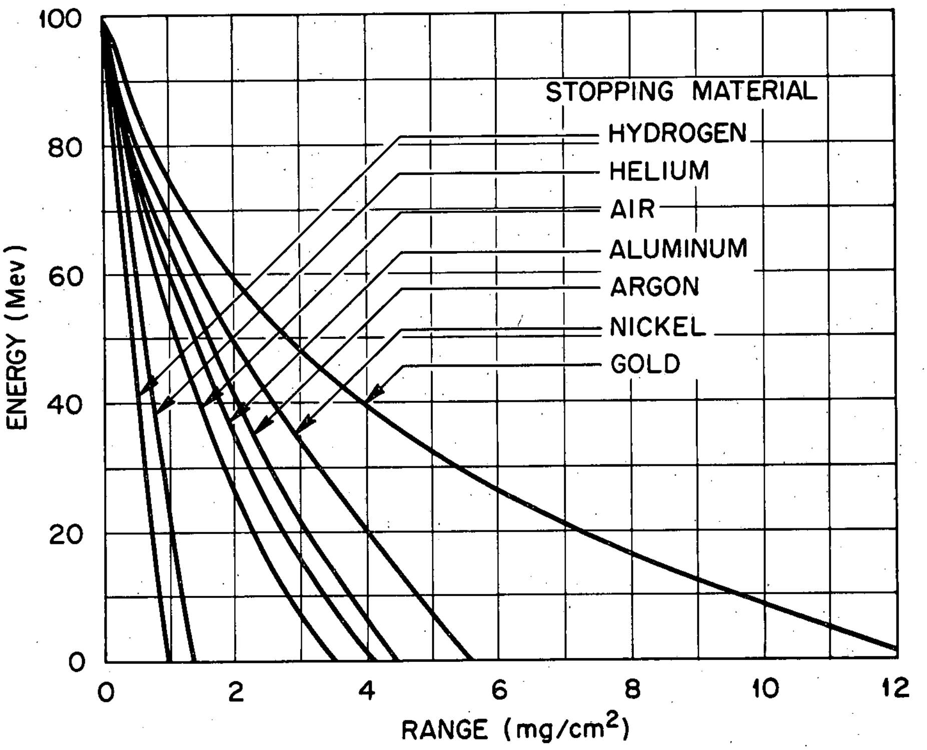

MU-18840

Fig. 11.65. FULMER'S[349] curves showing energy of median-mass light fission fragments of U^{235} (magnetically selected) as a function of range in various materials. The residual energy after traversing the absorber was measured by a CsI (Tl) scintillator.

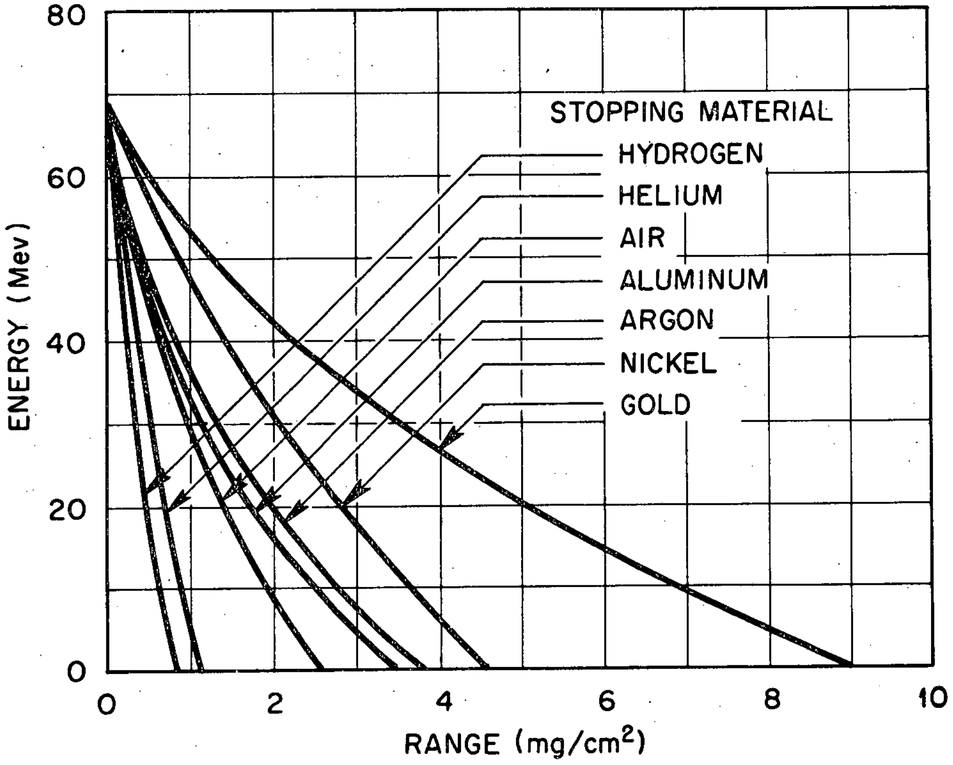

MU-18843

349

Fig. 11.66. FULMER'S curves showing energy of median-mass heavy fission fragments of U^{235} (magnetically selected) as a function of range in various materials.

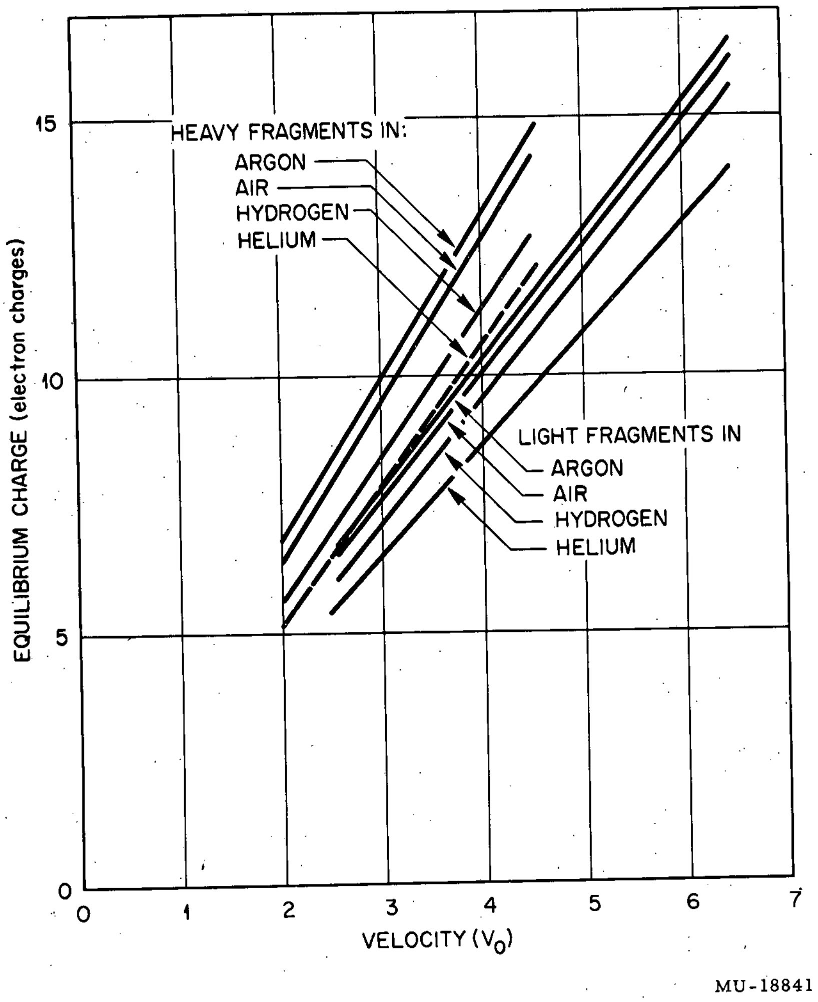

Fig. 11.67. Equilibrium charges of median-mass light and heavy fission fragments as functions of velocity in various gases as measured by FULMER and COHEN.[342]

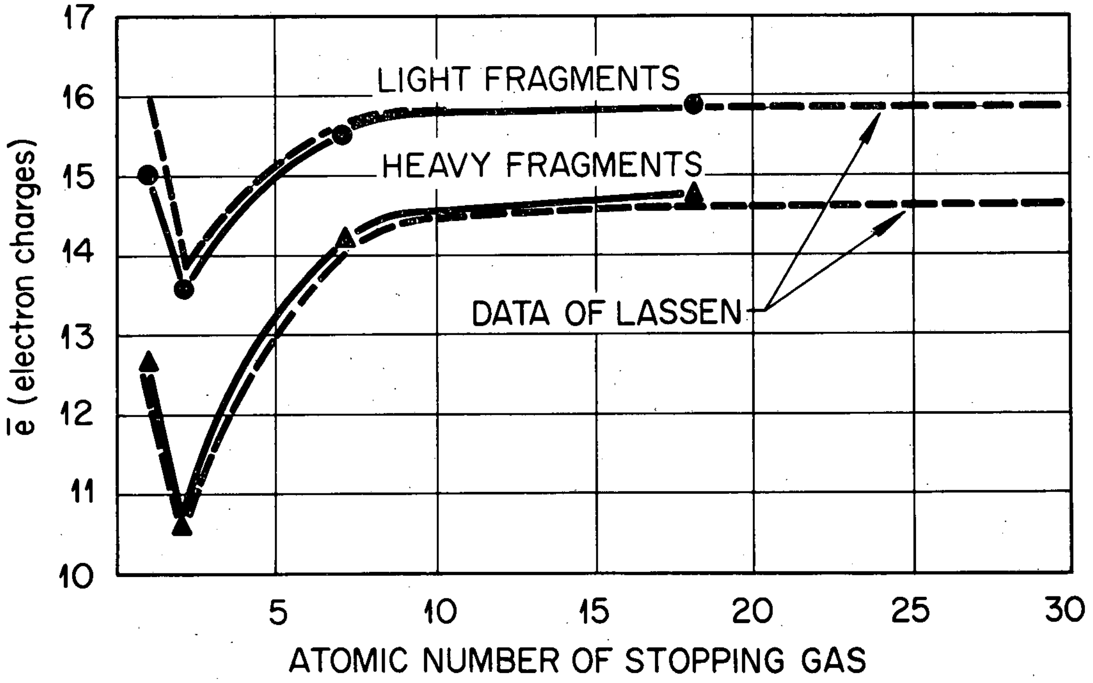

MU-18842

Fig. 11.68. Equilibrium charges of unslowed fission fragments as functions of atomic number of stopping gas. Solid lines are data of FULMER and COHEN[342]; broken lines are data of LASSEN.[348] Figure by FULMER AND COHEN [342].

Radiochemical studies of the range of specific fission fragments have been carried out. In one type of experiment the fragments are allowed to penetrate a stack of thin foils which are dissolved separately and analyzed radiochemically for specific fission products. FINKLE, HOAGLAND, KATCOFF, and SUGARMAN[351] studied the ranges in aluminum of light fission products from the slow-neutron induced fission of U^{235}. SUZOR[352] studied the ranges of Te^{132}, Mo^{99}, and Zr^{97} from U^{235} fission in several foil materials. He studied the effect of slow neutrons and fast neutrons. Some of his results for aluminum are given in Table 11.24. SUZOR made a very careful determination of the shape of the range curve and gave a good description of the factors influencing range straggling. He also studied the stopping power of several materials relative to aluminum. ALEXANDER and GALLAGHER[354] measured several ranges in aluminum and compared them with the results of previous studies. When plotted on one curve the data shown in Table 11.24 form a smooth curve provided the numbers of FINKLE, HOAGLAND, KATCOFF and SUGARMAN[351] are multiplied by the factor 1.084.

A more detailed radiochemical study of fission fragment ranges was made by KATCOFF, MISKEL, and STANLEY[353] who studied the ranges of twenty individual nuclides with mass numbers between 83 and 157 formed in the slow neutron fission of Pu^{239}. Collimated fission fragments passing through air at 120 or 140 mm pressure were deposited after being stopped by the air on a series of 14 extremely thin Zapon lacquer films. These foils were analyzed radiochemically for individual fission products. The corrected activities were plotted against distance traversed yielding differential range curves whose widths at half maximum were 11.7 ± 1.3 percent. (See Fig. 11.69). This range straggling can be attributed to a distribution in the initial energy of the fragments, to an experimental dispersion caused by the analytical method, and to true range straggling attributable mainly to the nuclear collision part of the stopping

---

351. B. Finkle, E. J. Hoagland, S. Katcoff, and N. Sugarman, Papers 45 and 46, "Ranges of Fission-Recoil Fragments of Known Mass Numbers" in "Radiochemical Studies — The Fission Products", Div. IV, Vol. 9, McGraw-Hill Book Co., Inc., New York, 1951.

352. F. Suzor, Ann. de Phys. 4, 269 (1949).

354. J. Alexander and M. F. Gallagher, University of California Lawrence Radiation Laboratory Report, UCRL-8978, December, 1959, unpublished.

353. S. Katcoff, J. A. Miskel and C. W. Stanley, Phys. Rev. 74, 631 (1948).

Table 11.24

Ranges of Specific Fission Products in Aluminum. U^{235}+slow neutrons.

Fission product	Extrapolated range (mg/cm^2)	Uranium target	Author
Zr^{97}	4.20	U on Ni backing	Suzor[352]
	4.27	U on Cu backing	
Te^{132}	3.62	U on Ni backing	
	3.55	U on Cu backing	
Mo^{99}	4.27	U on Cu backing	
Sr^{89}	4.12	U on Al backing	Alexander and Gallagher[352a]
Sr^{91}	4.02		
Ag^{111}	3.51		
Cd^{115}	3.33		
I^{131}	3.37		
Ba^{140}	2.98		
Sr^{89}	3.74	U on Pt backing	Finkle et al.[351]
Zr^{95}	3.64		
Ru^{103}	3.57		
Te^{129}	3.34		
I^{131}	3.16		
Ba^{140}	2.75		
Ce^{141}	2.69		
Ce^{144}	2.54		

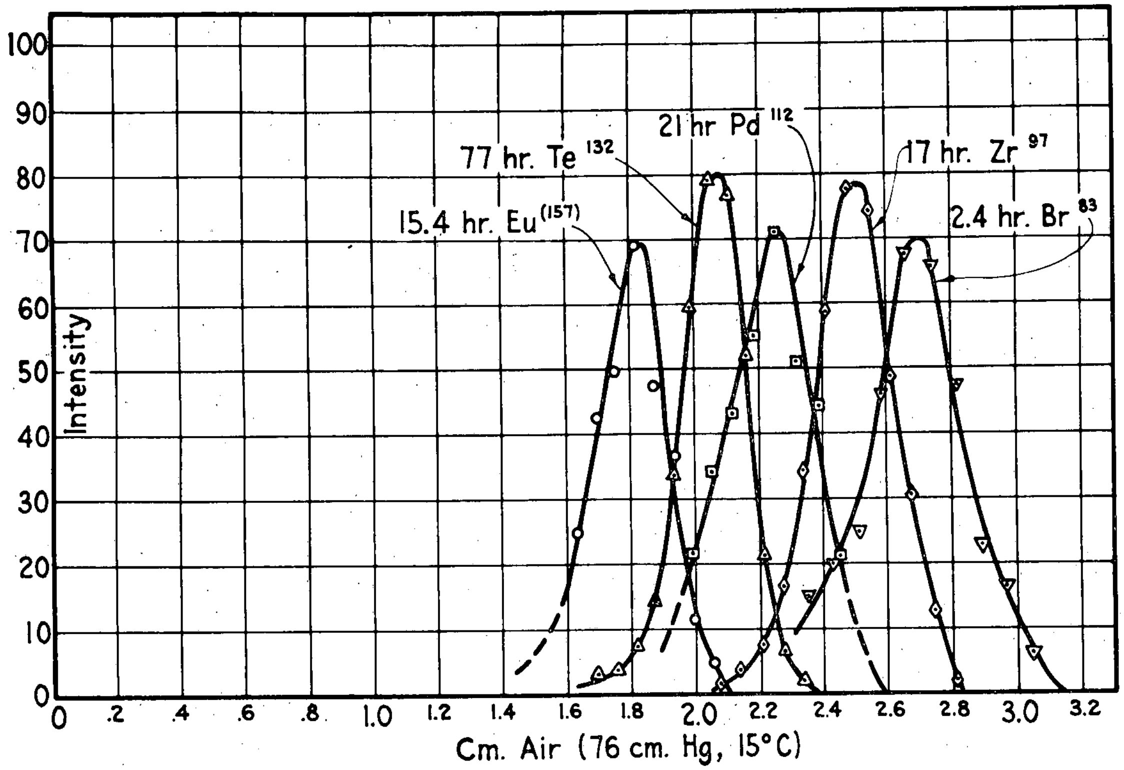

MU-18844

Fig. 11.69. Differential range curves for typical fission products as determined by KATCOFF, MISKEL and STANLEY.[353] The ordinate for each curve is entirely arbitrary.

process. The major part of the observed straggling is caused by the first of these factors.

The activities found beyond each distance were plotted against distance yielding integral range curves from which mean and extrapolated ranges could be derived. These ranges are tabulated in Table 11.25 and presented graphically in Fig. 11.70. The most striking feature of this figure is the dip in the center which suggests that the division of the nucleus into two equal fragments minimizes the kinetic energy release. Similar dips are seen in the ionization chamber measurements of kinetic energy and time-of-flight measurement of the velocities of the fragments as can be seen in Figs. 11.52 and 11.61, respectively; however, the mass resolution of these other methods is much poorer so that the dip and the interpretation are less definite.[†]

NIDAY[355] has remeasured ranges of about 20 selected fission products of U^{235} by an integral range technique. A foil[‡] of U^{235} was irradiated with slow neutrons and those fission products which escape from the uranium were caught in an aluminum catcher foil. The thickness of both the uranium and the aluminum foil was greater than the range of the fragments so that only those fragments formed in a thin layer of the target foil escaped into the catcher. Quantitative radiochemical analyses were made of specific fragments in both foils. From the relative amounts of specific fragments in both foils, and from the thickness of the uranium foil it was possible to compute the range of the product in uranium metal. NIDAY'S results are given in Table 11.26 and Fig. 11.71. The shape of the curve is very similar to that of Fig. 11.70. One interesting result, for which the explanation is not clear, is the low values of the ranges for Cs^{136} and Rb^{86}, both of which are "shielded" nuclides. Their ranges fall about 10 percent below the curve.

---

355. J. Niday, University of California Radiation Laboratory, Livermore, Report UCRL-5816 (1960) unpublished.

[†] SWIATECKI has made the interesting suggestion that the central dip in Fig. 11.70 may be caused by a strong preference for symmetric mass division in those fission events which are accompanied by the emission of an energetic alpha particle. W. J. Swiatecki, private communication.

[‡] Foils of normal uranium and of uranium enriched in U^{235} were used.

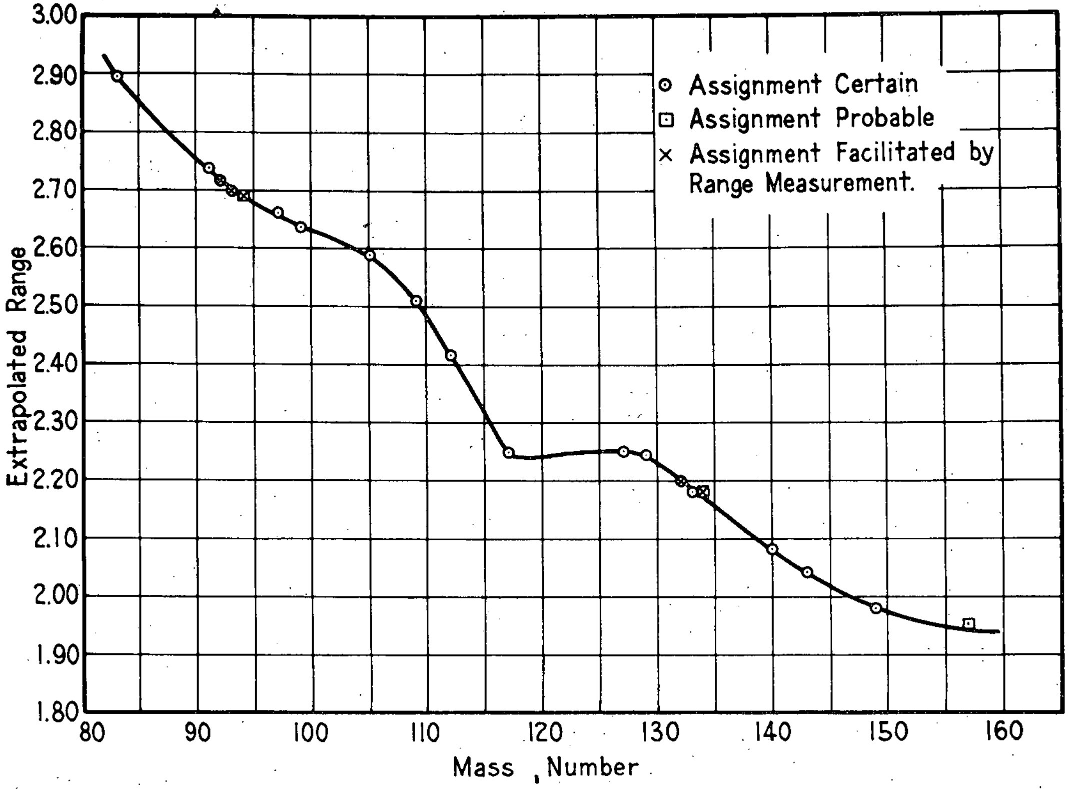

MU-18845

Fig. 11.70. Extrapolated range (76 cm pressure, 15°C) of plutonium fission fragments in air as a function of mass. Figure from KATCOFF, MISKEL, and STANLEY.[353]

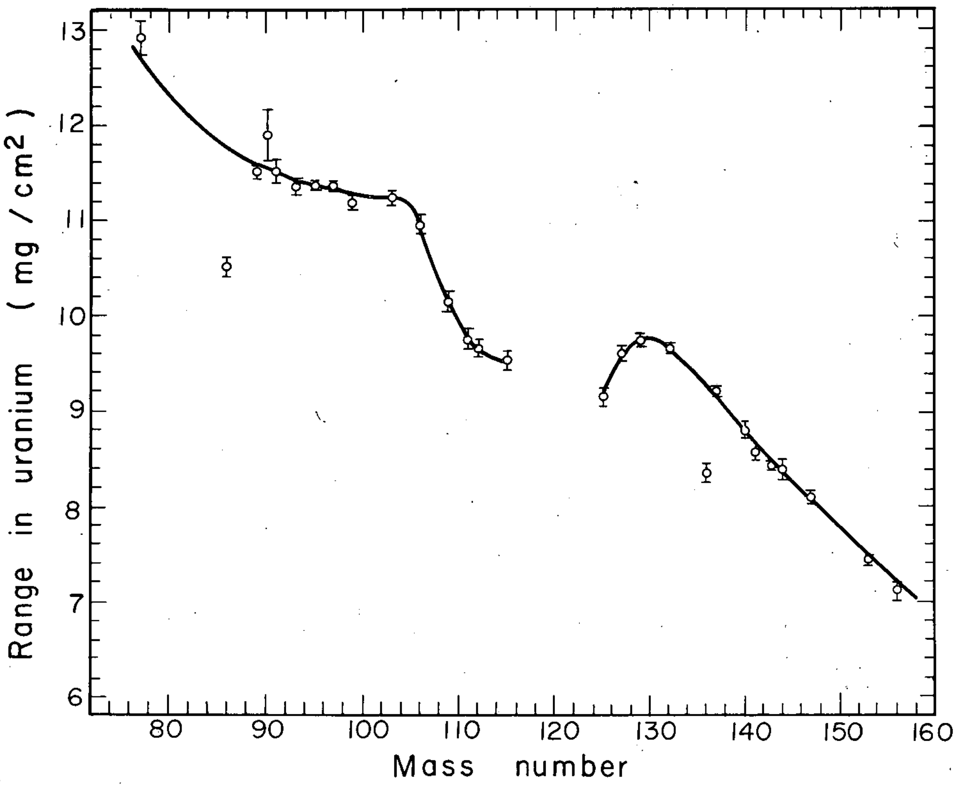

MU-19398

Fig. 11.71. Integral ranges of fission products of U^{235} measured in uranium metal. J. NIDAY 355.

Table 11.25

Extrapolated and mean ranges of plutonium fission fragments in normal air, and the straggling as indicated by the widths at half-height of the differential range curves. KATCOFF, MISKEL and STANLEY[353]

Mass number	Isotope	Normalized extrapolated range (cm)	Normalized mean range (cm)	Average width at half-maximum (percent)
83	2.4-hr. Br	2.895	2.63	13.4 ± 1.5
91	9.7-hr. Sr	2.738	2.55	11.4 ± 0.7
92	3.5-hr. Y	2.717	2.55	10.5 ± (0.6)
93	10-hr. Y	2.697	2.53	10.1 ± 0.7
(94)	20-min. Y	2.687	2.52	10.5 ± 0.7
97	17-hr Zr	2.661	2.50	10.7 ± 1.1
99	67-hr. Mo	2.635	2.48	10.8 ± 0.5
105	36.5-hr. Rh	2.587	2.42	11.4 ± 0.6
109	13.4-hr. Pd	2.508	2.36	10.7 ± 0.9
112	21-hr. Pd	2.416	2.24	13.4 ± (0.2)
117	1.95-hr. In	2.246	2.08	10.1 ± 1.7
127	93-hr. Sb	2.248	2.09	11.9 ± (1.3)
129	4.2-hr. Sb	2.243	2.09	12.5 ± 0.5
132	77-hr. Te	2.198	2.05	11.5 ± 0.6
133	60-min. Te	2.180	2.04	11.8 ± 0.8
(134)	43-min. Te	2.180	2.04	11.4 ± 1.3
140	12.8-day Ba	2.080	1.92	12.6 ± 1.3
143	33-hr. Ce	2.040	1.89	11.8 ± 0.6
149	47-hr. 61	1.977	1.82	13.1 ± 1.2
(157)	15.4-hr. Eu	1.949	1.79	15.1 ± 1.3

Table 11.26

Integral ranges of fission products of U^{235} measured in uranium metal
J. Niday, unpublished results

Element	Mass number	Number of determinations	Range mg/cm^2	Standard deviation σ
As	77	1	12.9	0.2
Rb	86	1	10.5	0.1
Sr	89	6	11.55	0.05
Sr	90	1	11.9	0.3
Sr, Y	91	3	11.54	0.07
Y	93	1	11.35	0.08
Zr	95	2	11.36	0.04
Zr	97	2	11.36	0.03
Mo	99	7	11.17	0.06
Ru	103	2	11.23	0.08
Ru	106	2	10.94	0.10
Pd	109	2	10.14	0.1
Ag	111	2	9.74	0.1
Pd	112	2	9.61	0.05
Cd	115	3	9.52	0.09
Sn	125	3	9.14	0.09
Sb, Te	127	3	9.58	0.06
Te	129m	2	9.75	0.03
Te	132	3	9.63	0.03
Cs	136	2	8.36	0.06
Cs	137	2	9.18	0.06
Ba	140	4	8.74	0.05
Ce	141	3	8.55	0.06
Ce	143	4	8.42	0.04
Ce	144	2	8.37	0.11
Nd	147	1	8.07	0.05
Sm	153	1	7.43	0.07
Eu	156	1	7.1	0.1

ALEXANDER and GALLAGHER[354] carried through a series of experiments in which the penetration of selected fission products through a stack of thin collector foils of aluminum and gold was measured radiochemically. The data were used to derive average ranges and relative rates of energy loss in the two materials. In addition, by combining these radiochemical data with the velocity data of LEACHMAN and SCHMITT[356] on fission fragments which had penetrated various thicknesses of absorber ALEXANDER and GALLAGHER[354] were able to construct curves showing range-versus-velocity and range-versus-energy for fission fragments of median-light mass and median-heavy mass. This is an important paper for those who use range measurements on fission fragments or other heavy energetic charged ions as a way to determine the energy of such ions. The curves derived by these authors are appreciably different from those of FULMER[349] given in Figs. 11.65 and 11.66

11.6.5 Calorimetric Measurement of the Energy Released in Fission. In 1940 HENDERSON[360] made a calorimetric measurement of the energy released in a 13 gram sample of metallic natural uranium when the sample was irradiated with moderated neutrons from a beryllium target bombarded with protons. He obtained a value of 177 Mev ± 1 percent per fissioning nucleus.

In 1955 LEACHMAN and SCHAFER[361] were able to repeat the measurement under considerably more favorable conditions and obtained a value of 167.1 ± 1.6 Mev. LEACHMAN and SCHAFER[361] used a differential type calorimeter employing a null indicator for heat measurement. To determine both the heat produced by the fissions and the number of fissions producing the heat a combination of a calorimeter and a fission pulse counter was used. The number of thermal neutrons passing through the sample was determined by small U^{235} monitor foils placed in front of and in back of the calorimeter. The amount of heat released in a 220 mg sample of U^{235} (93 percent isotopic purity) was determined by the amount of electrical energy required to heat the sample to the same temperature. The uncorrected result indicated 170.1 Mev ± 1.0 Mev per fission. The possible effects of beta-particles, gamma-rays and neutrons in producing heat had to be considered. It was calculated that energy supplied to the calorimeter by gamma-rays and neutrons was negligibly small. For the beta rays a correction of 3.0 ± 1 Mev was estimated. The final result was 167.1 ± 1.6 Mev. It is gratifying that this agrees so well with the value of 167.1 ± 2 Mev determined by LEACHMAN[362] by velocity measurements of fragment velocities. It is significantly larger than the value of 154.7 originally reported by BRUNTON and HANNA[363] from ionization chamber measurements and confirms the necessity for applying a correction for ionization defect as described in Section 11.6.1.

---

[356] R. B. Leachman and H. W. Schmitt, Phys. Rev. 96, 1366 (1954).

[360] M. C. Henderson, Phys. Rev. 58, 774 (1940).

[361] R. B. Leachman and W. D. Schafer, Can. J. Phys. 33, 357 (1955).

GUNN, HICKS, LEVY and STEVENSON[364] redetermined the average total kinetic energy of the fragments by a very similar calorimetric measurement and obtained a value of 166 ± 2 Mev in excellent agreement with LEACHMAN and SCHAFER.[361]

STEVENSON, HICKS, ARMSTRONG and GUNN[365] repeated this measurement on the heat released in the fission of U^{235} and U^{238} by 14 Mev neutrons. The average total fragment kinetic energies were found to be 174 ± 4 and 175 ± 2 Mev, respectively.

---

[362] R. B. Leachman, Phys. Rev. 87, 444 (1952).

[363] D. C. Brunton and G. C. Hanna, Can. J. Research A28, 190 (1950); see Section 11.6.1.

[364] S. R. Gunn, H. G. Hicks, H. B. Levy and P. C. Stevenson, Phys. Rev. 107, 1642 (1957).

[365] P. C. Stevenson, H. G. Hicks, J. C. Armstrong, Jr., and S. R. Gunn, University of California Lawrence Radiation Laboratory Report UCRL-5455, March, 1959; see also Phys. Rev. 116, Dec. 1959.

11.7 PROMPT NEUTRONS EMITTED IN FISSION

11.7.1 The average number of neutrons emitted in fission. The average number of neutrons released in nuclear fission is of the utmost practical importance in the application of the nuclear chain reaction in nuclear reactors or explosions. The measurement of $\bar{\nu}$, the average number of neutrons emitted per fission event, of α, the ratio of the cross sections for radioactive capture and fission, and of η, the average number of neutrons emitted per neutron captured*, has been carried out in many laboratories in many countries for the important isotopes U^{233}, U^{235} and Pu^{239}. Many of these determinations were discussed in the papers presented at the 1955 and 1958 Geneva Conferences on the Peaceful Uses of Atomic Energy. The cross sections group at the Brookhaven National Laboratory compiled and evaluated all data published up to May 1958 and arrived at the "world consistent set" of values reproduced in Table 11.27.

The variation in $\bar{\nu}$ as a function of the energy of the neutrons causing fission is shown in figure 11.72 plotted from the data listed in Table 11.28. The figure and the table are taken from a paper by LEACHMAN[366]. Table 11.29 also taken from LEACHMAN'S[366] paper lists data on $\bar{\nu}$ for a few other nuclei.

Values of $\bar{\nu}$ do not change greatly with the energy of the neutrons over the range of neutron energies encountered in most nuclear reactors. However, the quantity α undergoes strong fluctuations in the range of neutron energies where resonance absorption gives considerable structure to the cross section curve. See Section 11.3.3. Therefore the value of η must also go through strong fluctuations with neutron energy. This variation in η, the number of neutrons emitted per neutron absorbed, is an important quantity in reactor design; for example in calculating the temperature coefficient of reactivity. Hence considerable experimental work has gone into a study of this variation by direct counting of the fission neutrons ejected from a sample irradiated with a monochromatic beam of neutrons. A discussion of such data is given by HARVEY AND SANDERS.[368]

All neutrons, except for the small percentage of delayed neutrons, discussed later, are emitted within a very brief period of time after the moment

---

* These quantities are related by the expression $\eta = \frac{\bar{\nu}}{1+\alpha}$

366. R.B. Leachman, Paper P/2467, Proceedings of the Second United Nations Conference on the Peaceful Uses of Atomic Energy, Geneva, 1958.
367. R.B. Leachman, Phys. Rev. 101, 1005 (1956)
368. J.A. Harvey and J.E. Sanders, Chapt. 1, Progress in Nuclear Energy, Ser. 1, Vol. 1. Physics and Mathematics, McGraw-Hill Book Co., New York, 1956.

Table 11.27 Values of $\bar{\nu}$, α, and η for fission induced by neutrons of 0.0253 electron volts energy (2200 meters/sec)*,**

Target nucleus	$\bar{\nu}$	$1 + \alpha$	η
U^{233}	2.51 ± 0.03	1.102 ± 0.005	2.28 ± 0.02
U^{235}	2.47 ± 0.03	1.19 ± 0.001	2.07 ± 0.02
Pu^{239}	2.90 ± 0.04	1.38 ± 0.02	2.10 ± 0.02

* "World Consistent Set", as given by D. J. Hughes and R. B. Schwartz, "Neutron Cross Sections", Report BNL-325, Second Edition, July, 1958, for sale by Superintendent of Documents, U. S. Government Printing Office Washington, D. C.

** Other determinations and discussions of these quantities are given in: "Proceedings of the International Conference on the Peaceful Uses of Atomic Energy", Volume 4, United Nations, New York, 1956.

$\bar{\nu}$ = average number of neutrons emitted per fission event.

η = average number of neutrons emitted per neutron captured.

α = ratio of radiative capture to fission.

$1 + \alpha$ = ratio of absorption cross section to fission cross section.

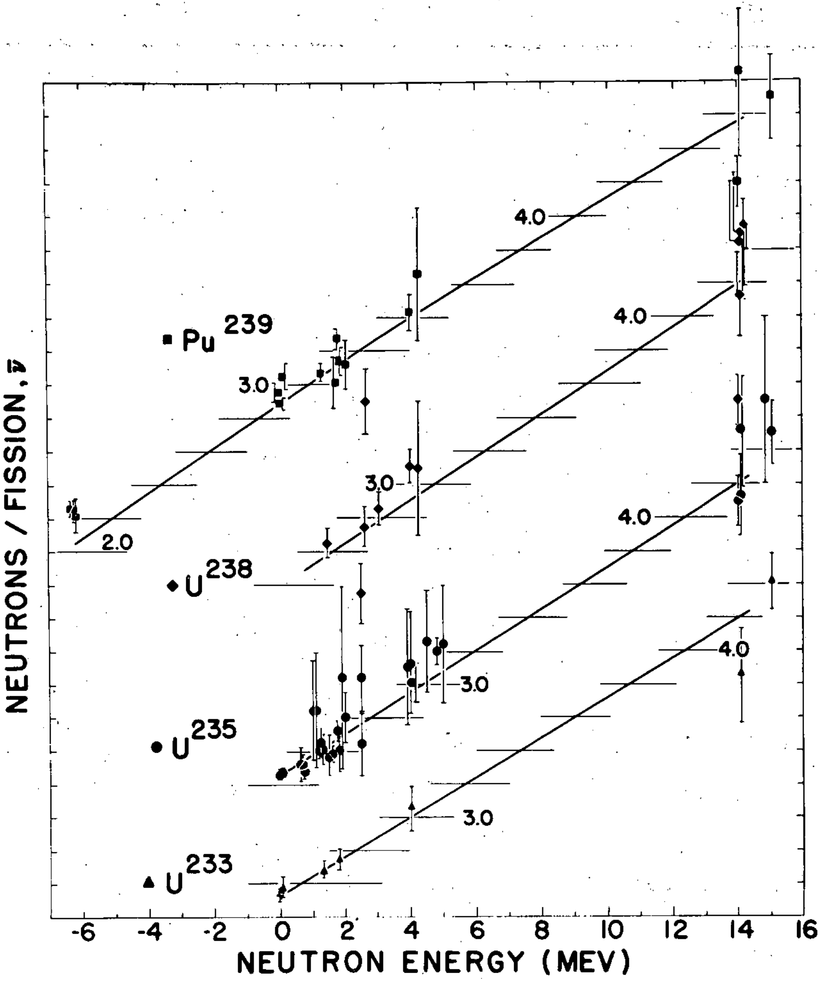

MU-18847

Fig. 11.72. Dependence of $\overline{\nu}$ on the energy of the neutrons inducing fission. The data and references are given in Table 11.28. The lines show the dependence of $\overline{\nu}$ on E_n given by the theoretical considerations of LEACHMAN[367] normalized to the thermal neutron experimental values. Figure from a paper by LEACHMAN.[366]

Table 11.28 The Average Number of $\overline{\nu}$ of Fission Neutrons* as a Function of the Neutron Energy E_n. Table prepared by R. B. Leachman

E_n (Mev)	U^{233}+n	U^{235}+n	U^{238}+n	Pu^{239}+n
0		2.47 ± .05(x)**		
	2.54 ± .04(a)‡	2.46 ± .03(a)‡		2.88 ± .04(a)‡
	2.55 ± .05(b)‡‡			2.95 ± .06(b)‡‡
-6.3				2.26 ± .05(b)‡
				2.26 ± .05(c)‡
				2.22 ± .11(d)‡
0.08	2.58 ± .06(c)	2.47 ± .03(c)		3.05 ± .08(c)
0.7		2.52 ± .10(d)		
		2.52 ± .06(f)		
0.74‡‡		2.48 ± .05(g)		
1.0		2.84 ± .30(h)		
		2.84 ± .35(f)		
1.2		2.60 ± .05(i)		
1.25		2.65 ± .09(c)		
1.3‡‡	2.69 ± .05(j)	2.61 ± .09(g)		3.08 ± .05(j)
1.5		2.57 ± .12(j)	2.65 ± .09(c)	
1.6‡‡		2.58 ± .05(g)		
1.8‡‡	2.75 ± .06(l)	2.72 ± .06(l)		3.28 ± .06(l)
				2.15 ± .08(m)
		2.60 ± .13(n)		3.01 ± .15(n)
1.9		3.04 ± .55(h)		
2.0		2.80 ± .15(o)		
2.1				3.12 ± .15(o)
2.5		2.64 ± .19(p)	2.35 ± .18(p)	
2.5‡‡		3.04 ± .20(f)		
2.6‡‡			3.5 ± .2(q)	
			2.75 ± .12(j)	
3.1			2.86 ± .10(i)	
4.0		3.11 ± .35(h)		
		3.13 ± .31(n)		

Table 11.28 (cont'd.)

E_n (Mev)	U^{233}+n	U^{235}+n	U^{238}+n	Pu^{239}+n
	3.06 ± .12(r)	3.01 ± .12(r)	3.11 ± .10(r)	3.43 ± .11(r)
4.25			3.10 ± .40(n)	3.66 ± .40(n)
4.5		3.26 ± .31(n)		
4.8		3.20 ± .08(b)		
5.0		3.24 ± .35(h)		
14.0		4.1 ± .15(s)	3.5 ± .15(s)	4.2 ± .15(s)
14.1	3.86 ± .28(p)	4.52 ± .32(p)	4.13 ± .25(p)	4.85 ± .50(p)
		4.13 ± .24(t)	4.50 ± .32(t)	
			4.45 ± .35(u)	
14.22			4.55 ± .15(v)	
14.8		4.7 ± .5(w)		
15.0	4.42 ± .17(r)	4.51 ± .19(r)		4.71 ± .20(r)

---

* References given in parentheses. Uncertainties include that of the standard value.

** Not plotted in Fig. 11.72. This value was used as a standard to convert data reported as a ratio with thermal-neutron induced fission of U^{235}.

† Calculations normalized to these values.

†† These values were used as a standard to convert data reported as a ratio with thermal-neutron induced fission of U^{233} or Pu^{239}.

‡ Spontaneous Pu^{240} fission.

‡‡ Effective energy of a neutron energy spectrum.

---

a. Hughes, D. J. and Harvey, J.A., "Neutron Cross Sections", Brookhaven National Laboratory Report BNL-325, Superintendent of Documents, Washington, D.C., (1955).

b. Colvin, D. W. and Sowerby, M. G., "Precision Measurements of $\overline{\nu}$ by the Boron Pile", P/52, Proceedings Second Geneva Conference.

c. Diven, B. C., Martin, H. C., Taschek, R. F., and Terrell, J. Date given by Terrell, J, "Distributions of Fission Neutron Numbers", Physical Review, 108, 783-9 (1957).

d. Kalashnikova, V. I., Krasnushkin, A. V., Levedov, V. I., Pevzner, M. I., and Zakharova, V. P., "Dependence of the Number of Neutrons Emitted in the Fission of Heavy Nuclei on the Excitation Energy of the Fissionable Nucleus", Conference of the Academy of Sciences of the USSR on the Peaceful Uses of Atomic Energy, 156-70 (1955).

e. Terrell, J., and Leland, W. T., (see Reference c).

f. Usachev, L. N. and Trubitsyn, V. P., "Neutrons Emitted by the Fission of U^{235} and its Dependence on the Energy of the Neutron Producing Fission, OTCHET FIGUIAE (1955). (see Bondarenko, I. I., P/2187, proceedings Second Geneva Conference.)

g. Hanna, R. C., Atomic Energy Research Establishment, Harwell, unpublished report, (1956).

h. Fowler, J. L., Oak Ridge National Laboratory unpublished report, (1956).

i. Kuzminov, B. D., Kutsaeva, L. S., and Bondarenko, I. I., "Prompt Neutron Numbers for the Fast Neutron Fission of U^{235}, U^{238}, Th^{232}, and Np^{237}, Atomnaya Energiya, 4:187-8, (1958).

j. Hansen, G. E., Los Alamos unpublished report (1958). (See Leachman, R. B., P/665, proceedings Second Geneva Conference).

k. Blair, J. M., Los Alamos unpublished report, (1945).

l. Kalashnikova, V. I., Lebedov, V. I., and Spivak, P.E., "Relative Measurements of the Mean Number of Neutrons Emitted in Fission of U^{233}, U^{235}, and Pu^{239} by Thermal Neutrons and by Neutrons Characteristic of a Fission Spectrum", Atomnaya Energiya, 2:18-21 (1957).

m. Auclair, J. M., Landon, H. H., and Jacob, M., "Measurement of the Dependence of $\bar{\nu}$ on Neutron Energy," Physica, 22:1187-8 (1956).

n. Bethe, H. A., Beyster, J. R., and Carter, R. E., Los Alamos unpublished report, (1955).

o. Anreev, V. N., "Effective Number of Neutrons Produced by the Fission of U^{235} and Pu^{239} with Energies 30, 140, 220 and 900 kev" OTCHET FIGUIAE, (1957). (see Bondarenko, I. I., et al., P/2187, proceedings Second Geneva Conference.)

p. Johnstone, I., Atomic Energy Research Establishment, Harwell, unpublished report (1956).

q. Nargundkar, V. R., Prabhu, R. B., Ramanna, R., Umakantha, N., and Khopkar, P. K., "Number of Neutrons Emitted per Fission from the Fast Fission of U^{238}", P/1632, proceedings Sec ond Geneva Conference.

r. Smirenkin, G. M., Bondarenko, I. I., Kutsaeva, L. S., Mischenko, Kh.D., Prokhorova, L. I., and Shemetenko, B. P., "Mean Prompt Neutron Numbers in the Fission of U^{233}, U^{235}, and Pu^{239} by 4- and 15-Mev Neutrons," Atomnaya Energiya, 4:188-90 (1958).

s. Graves, E. R., Los Alamos unpublished report (1954).

t. Flerov, N. N. and Taltszin, V. M., "Measurement of ν and η for Fission of U^{235} and U^{238} by 14.1-Mev Neutrons," Atomnaya Energiya (in press).

u. Flerov, N. N. and Tamanov, E. A., "Measurement of ν for Fission of U^{238} by 14.1 Mev Neutrons", Atomnaya Energiya (in press).

Table 11.28 references (cont'd.)

v. Gaudin, M. and Leroy, J. L., "Measurements of Fission Cross-Sections and of Neutron Production Rates", P/1186 (b), proceedings Second Geneva Conference.

w. Protopopov, A. N. and Blinov, M. V., "Determination of Mean Neutron Numbers Emitted from the 14.8-Mev Neutron Fission of U^{235}", Atomnaya Energiya, 4:374-6, (1958).

x. Harvey, J. A., and Sanders, J. E., "Summary of Data on the Cross Sections and Neutron Yields of U^{233}, U^{235}, and Pu^{239}", Progress in Nuclear Energy, Series I, 1:1-54 (1956).

Table 11.29 Variation of the Average Neutron Number* $\bar{\nu}$ from Fission Induced by Neutrons with Energy E_n for Nuclides not Shown in Fig. 11.72

E_n(Mev)	Th^{232}+n	Np^{237}+n	Pu^{240}+n	Pu^{241}+n
0				3.03±.06(d)
-6.1				2.18±.09(e)
1.4†		2.81±.09(b)		
1.47†			3.26±.21(b)	
1.67†		2.90±.04(b)	3.37±.10(b)	
2.5		2.72±.15(a)		
3.5	2.35±.07(a)			
14.2	4.64±.20(c)			

* References given in parentheses. Uncertainties include that of the standard value.

** Spontaneous Pu^{242} fission.

† Average energy of neutron spectrum. Unlike Table 11.28, the spectra are not combined with $\sigma_f(E)_n$.

---

a. Kuzminov, B. D., Kutsaeva, L.S., and Bondarenko, I. I., "Prompt Neutron Numbers for the Fast Neutron Fission of U^{235}, U^{238}, Th^{232}, and Np^{237}," Atomnaya Energiya, 4:187-8, (1958).

b. Hansen, G. E., Los Alamos unpublished report (1958). (See Leachman, R. B., P/665, proceedings Second Geneva Conference.)

c. Gaudin, M. and Leroy, J. L., "Measurements of Fission Cross-Sections and of Neutron Production Rates", P/1186(B), proceedings Second Geneva Conference.

d. Average of USSR, U.K., and U.S.A. values given by Egelstaff, P. A., Morton, K. W., and Sanders, J. E., unpublished Atomic Energy Research Establishment report (1955).

e. Hicks, D. A., Ise, J., Jr., Pyle, R. V., "Probabilities of Prompt Neutron Emission from Spontaneous Fission", Phys. Rev., 101, 1016-20 (1956).

of scission, the moment of separation of the fragments. FRASER[369] set a limit for the time of emission of prompt neutrons of less than 4×10^{-14} seconds.

The value of $\bar{\nu}$ for nuclides decaying by spontaneous fission is given in Table 11.30. The most accurate values reported in this table were measured by counting neutrons absorbed in large tanks of cadmium-loaded liquid scintillator solution. The efficiency of this detector (~80 percent) is much superior to that of other detection methods. Because of the importance of this neutron-counting technique for the determination, not only of $\bar{\nu}$, but of the probability distribution P (ν) for the emission of 0,1,2 ,.. neutrons we shall give a few details of the method in the next section.

An interesting correlation of $\bar{\nu}$ with mass number of the spontaneously fissioning nucleus is revealed by figure 11.73. The significance of this trend is not obvious since there is no apparent correlation with the total energy available or with Z^2/A.

11.7.2 Measurements of P(ν). REINES AND CO-WORKERS[370] developed the use of large scintillator tanks as neutron detectors in connection with the Los Alamos Neutrino experiment. Several groups have applied these neutron detectors as counters for the neutrons emitted in fission. The dimensions of the tank are not critical so long as a large volume is enclosed. A typical tank consists of a right cylinder 3 feet long and 3 feet in diameter made of steel. The inside surfaces are coated with a highly reflective and protective coating such as tygon plastic paint. The scintillator solution consists of toluene in which are dissolved several organic compounds including cadmium propionate. Fast neutrons entering the tank are slowed by collisions with hydrogen atoms. After thermalization the neutrons are captured by cadmium which has a huge thermal neutron capture cross section. The mean capture time is roughly 10 microseconds. The gamma rays released in the (n,γ) reaction excite fluorescent radiation in the liquid scintillator which is reflected from the walls and partially gathered up by the numerous large, photomultpilier tubes facing into the solution from the periphery of the tank. The efficiency for detection depends on several factors but is usually 70-85 percent. Each cap-

---

[369] J. S. Fraser, Phys. Rev. 88, 536 (1952)

[370] Reines, Cowan, Harrison and Carter, "Detection of Neutrons with a Large Liquid Scintillation Counter," Rev. Sci. Instr. 25, 1061 (1954)

Table 11.30

Average Number of Neutrons ($\bar{\nu}$) Released in Spontaneous Fission

Isotope	$\bar{\nu}$	Neutron Detector	Standard	Ref.
U^{238}	2.4±0.2	BF_3 proportional counter	Standard Ra-Be source	1
		Subcritical pile experiment		2
Th^{232}	2.6±0.10	BF_3 proportional counter	$U^{238}(\bar{\nu} = 2.4)$	2
Pu^{236}	1.89±0.20	LiI(Eu)	Ra-Be n-source	3
	2.30±0.19	Large scintillaotr tank	$Pu^{240}(\bar{\nu} = 2.257)$	4
Pu^{238}	2.04±0.10	LiI(Eu)	Standard Ra-Be source	3
	2.33±0.08	Large scintillator tank	$Pu^{240}(\bar{\nu} = 2.257)$	4
Pu^{240}	2.09±0.11	LiI(Eu)	Standard Ra-Be source	3
	2.257±0.046	Large scintillator tank	$U^{235}+n(\bar{\nu} = 2.46)$	5
Pu^{242}	2.32±0.16	LiI(Eu)	Standard Ra-Be source	3
	2.18±0.09	Large scintillator tank	$Pu^{240}(\bar{\nu} = 2.257)$	4
Cm^{242}	3.0 ± 0.3			6
	2.33±0.11	LiI(Eu)	Standard Ra-Be source	3
	2.65±0.09	Large scintillator tank	$Pu^{240}(\bar{\nu} = 2.257)$	4
Cm^{244}	2.61±0.13	LiI(Eu)	Standard Ra-Be source	3
	2.84±0.09	Large scintillator tank	$Pu^{240}(\bar{\nu} = 2.257)$	4
	2.810±0.059	Large scintillator tank	$U^{235}+n(\bar{\nu} = 2.46)$	5
	2.60±0.11	Manganous sulfate solution	Standard Po-Be source	9
Bk^{249}	3.72±0.16	Large scintillator tank	$Pu^{240}(\bar{\nu} = 2.257)$	11
Cf^{246}	2.92±0.19	Large scintillator tank	$Pu^{240}(\bar{\nu} = 2.257)$	11
Cf^{252}	3.52±0.16	LiI(Eu)	Standard Ra-Be source	3
	3.53±0.15	Manganous sulfate solution	Cm^{244}	
			Ra-Be source	7
	3.82±0.12	Large scintillator tank	$Pu^{240}(\bar{\nu} = 2.257)$	4
	3.869±0.078	Large scintillator tank	$U^{235}+n(\bar{\nu} = 2.46)$	5
	3.8 ± 0.16	Large scintillator tank	Ra-Be source	10
Cf^{254}	3.90±0.14	Large scintillator tank	$Pu^{240}(\bar{\nu} = 2.257)$	11
Fm^{254}	4.05±0.19	Large scintillator tank	$Cf^{252}(\bar{\nu} = 3.82)$	8

Table 11.30 (References)

1. D. J. Littler, Proc. Phys. Soc. (London) A64, 638 (1951); A65, 203 (1952).
2. Barclay, Galbraith and Whitehouse, Proc. Phys. Soc. (London) A65, 73 (1952).
3. W. W. T. Crane, G. H. Higgins and H. R. Bowman, Phys. Rev. 101, 1804 (1956); There is a systematic difference of 7 percent between the $\bar{\nu}$ values from this report and those from reference 4; this is caused by a difference in standardization of neutron counting efficiency.
4. D. A. Hicks, J. Ise, Jr., and R. V. Pyle, Phys. Rev. 101, 1016 (1956).
5. B. C. Diven, H. C. Martin, R. F. Taschek, and J. Terrell, Phys. Rev. 101, 1012 (1956).
6. F. R. Barclay and W. J. Whitehouse, Proc. Phys. Soc. (London) A66, 447 (1953).
7. W. W. T. Crane, G. H. Higgins, and S. G. Thompson, Phys. Rev. 97, 242 (1955); erratum Phys. Rev. 97, 1727 (1955).
8. Choppin, Harvey, Hicks, Ise, and Pyle, Phys. Rev. 102, 766 (1956).
9. G. H. Higgins, W. W. T. Crane, and S. Gunn, Phys. Rev. 99, 183 (1955).
10. H. R. Bowman and S. G. Thompson, University of California Radiation Laboratory Report UCRL-5038, March 1958; also published as Paper P/652. Proceedings of the Second Geneva Conference on the Peaceful Uses of Atomic Energy, Geneva, 1958.
11. R. V. Pyle, "The Multiplicities of Neutrons from Spontaneous Fission", Unpublished results.

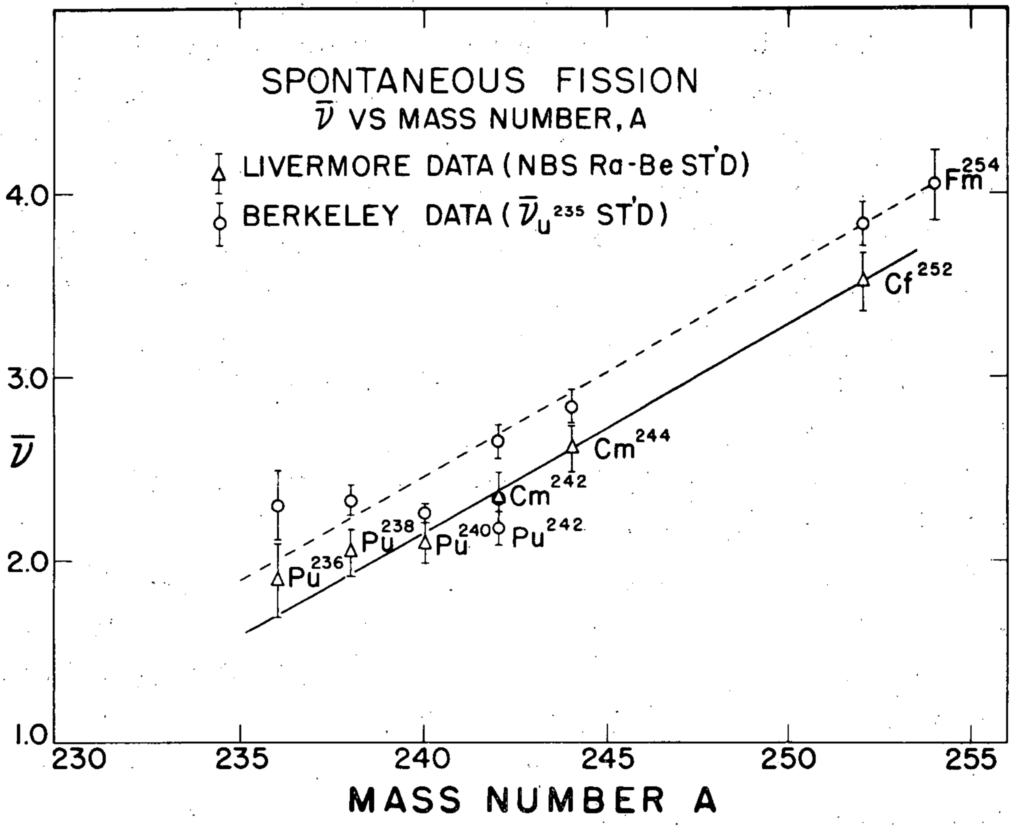

MU-19279

Fig. 11.73. Average number of neutrons $\overline{\nu}$ as a function of mass number in spontaneous fission.

tured neutron gives rise to a pulse in the photomultiplier circuits. Since the capture times are not identical, the neutron indicator pulses from a single fission event are separated in time.

The large tank is provided with a well along the axis of the cylinder or a passage going clear through, into which an ionization chamber containing a spontaneously fissionable sample can be placed. A typical circuit arrangement is shown in figure 11.74. The sequence of events in the experiment is the following:

The fragments from a spontaneous fission event give rise to a pulse in the ionization chamber which serves to trigger the sweep of the oscilloscope. This fission event is accompanied by prompt gamma rays and neutrons. The neutrons transmit practically all of their energy to recoil protons in a time much shorter than a microsecond. These recoil protons and any of the absorbed prompt gamma rays from the fission appear as one prompt pulse from the phototubes looking into the scintillator tank. The thermalized neutrons then are captured exponentially in time by the cadmium-113 (σ = 27,000 barns) or the hydrogen (σ = 0.33 barns) in the solution. The Cd^{113} radiative capture immediately releases a gamma ray cascade with a total energy of 9.2 Mev some fraction of which is converted to scintillation photons in the tank and gives a pulse in the phototube circuits indicating a neutron capture. A photograph of the oscilloscope screen gives a permanent record of the type shown in figure 11.75.

From such experiments accurate values are obtained not only for $\bar{\nu}$ the average number of neutrons but also for P(ν) the probability of emitting ν neutrons per spontaneous fission. The $\bar{\nu}$ measurements reported by several groups using this technique for spontaneous fission are recorded above in Table 11.30. Values P(ν) are summarized in Tables 11.31, 11.32 and 11.33.

DIVEN, MARTIN, TASCHEK AND TERRELL[371] were able to use this technique for the measurement of neutron multiplicities in the neutron induced fission of U^{233}, U^{235} and Pu^{239} by using the apparatus diagrammed in figure 11.76. It was possible to use thermalized neutrons from a Pu-Be source or 80 kev neutrons from the T (p,n) He^3 reaction to initiate fission. Values of $\bar{\nu}$ are

---

[371] Diven, Martin, Taschek and Terrell, "Multiplicities of Fission Neutrons," Phys. Rev. 101, 1012 (1956).

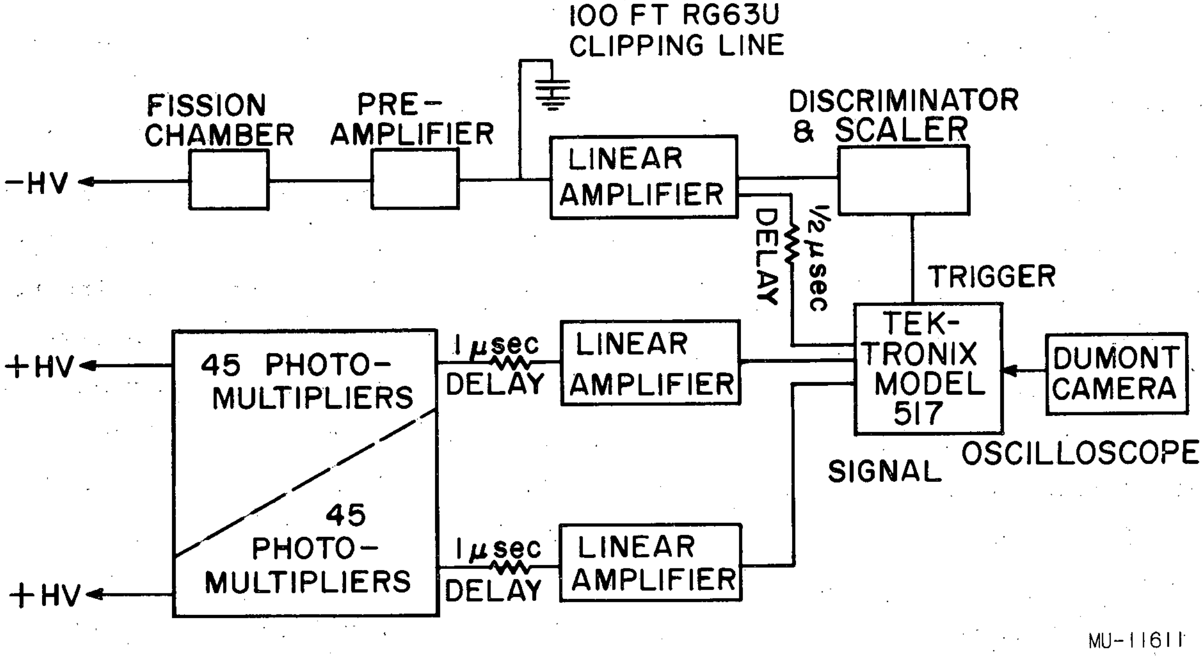
100 FT RG63U
CLIPPING LINE
FISSION CHAMBER
PRE-AMPLIFIER
LINEAR AMPLIFIER
DISCRIMINATOR & SCALER
−HV
½ μsec DELAY
TRIGGER
+HV
45 PHOTO-MULTIPLIERS
1 μsec DELAY
LINEAR AMPLIFIER
TEK-TRONIX MODEL 517
OSCILLOSCOPE
DUMONT CAMERA
SIGNAL
45 PHOTO-MULTIPLIERS
+HV
1 μsec DELAY
LINEAR AMPLIFIER
MU-11611

Fig. 11.74. Typical circuit arrangement for measuring the number of neutrons emitted in individual spontaneous fission events. See HICKS, ISE, and PYLE, Phys. Rev. 101, 1016 (1956).

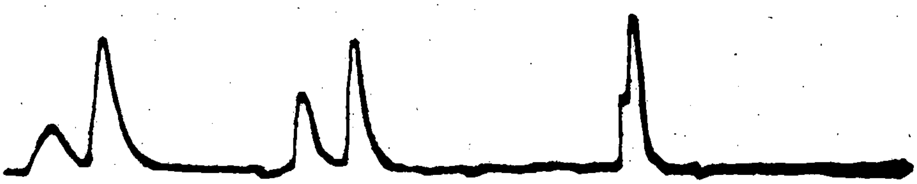

MU-10453

Fig. 11.75. Oscilloscope trace of pulses showing neutron pulses from a single fission event. Sweep triggered by fission chamber pulse. Pulse produced by prompt gamma rays and recoil protons in the scintillator tank is delayed 1 microsecond and appears as the first peak on the left-hand side. This pulse is followed in this case by four neutron-capture pulses. From HICKS, ISE AND PYLE, Phys. Rev. 101, 1016 (1956).

Table 11.31* Probabilities of emitting ν neutrons per spontaneous fission, $P(\nu)$, and the average number of neutrons per spontaneous fission, $\bar{\nu}$, based on $\bar{\nu}$ = 2.257 ± 0.046 for Pu^{240}

P_ν	Pu^{236}	Pu^{238}	Pu^{240}	Pu^{242}	Cm^{242}	Cm^{244}	Cf^{252}
P_0	0.062 ±0.035	0.044 ±0.009	0.041 ±0.009	0.063 ±0.013	0.011 ±0.005	0.001 ±0.004	0.001 ±0.001
P_1	0.156 ±0.090	0.175 ±0.026	0.219 ±0.021	0.192 ±0.034	0.126 ±0.018	0.099 ±0.017	0.021 ±0.007
P_2	0.38 ±0.13	0.384 ±0.026	0.351 ±0.021	0.351 ±0.041	0.323 ±0.018	0.281 ±0.022	0.111 ±0.019
P_3	0.28 ±0.12	0.237 ±0.027	0.241 ±0.020	0.324 ±0.047	0.347 ±0.020	0.365 ±0.018	0.271 ±0.019
P_4	0.096 ±0.086	0.124 ±0.021	0.127 ±0.018	0.033 ±0.026	0.139 ±0.013	0.198 ±0.220	0.326 ±0.018
P_5	0.033 ±0.036	0.036 ±0.009	0.020 ±0.006	0.036 ±0.013	0.050 ±0.009	0.049 ±0.009	0.178 ±0.016
P_6			0.001 ±0.002		0.004 ±0.002	0.007 ±0.002	0.077 ±0.013
P_7					0.001 ±0.001		0.013 ±0.004
P_8							0.003 ±0.001
$\bar{\nu}$	2.30 ±0.19	2.33 ±0.08	2.257 ±0.046	2.18 ±0.09	2.65 ±0.09	2.84 ±0.09	3.82 ±0.12

---

* D. A. Hicks, J. Ise, Jr., and R. V. Pyle, Phys. Rev. 101, 1016 (1956).

Table 11.32[*] Measurement of ν and the probability, of $P(\nu)$, of emitting ν neutrons in spontaneous fission

Nuclide	Cm^{244}	Cf^{252**}	Pu^{240}
Fissions analyzed	3301	4545	8355
$\bar{\nu}$	2.810±0.059	3.869±0.078	2.257±0.045
$(\nu)^2_{av}$	9.20±0.34	16.59±0.62	6.37±0.21
$(\nu)^2_{av} - \bar{\nu})/\bar{\nu}^2$	0.810±0.008	0.850±0.006	0.807±0.008
P_0	0.009±0.005	0.005±0.002	0.049±0.006
P_1	0.109±0.016	0.004±0.009	0.214±0.012
P_2	0.292±0.023	0.138±0.019	0.321±0.014
P_3	0.315±0.027	0.223±0.032	0.282±0.017
P_4	0.224±0.027	0.356±0.035	0.112±0.013
P_5	0.030±0.017	0.175±0.034	0.021±0.008
P_6	0.021±0.010	0.071±0.028	0.001±0.003
P_7	0.000±0.003	0.022±0.017	0.000±0.002
P_8	0.000±0.000	0.006±0.007	0.000±0.000

---

[*] Diven, Martin, Taschek and Terrell, Phys. Rev. 101, 1012 (1956)

[**] Similar data for Cf^{252} taken by STEIN AND WHETSTONE, Phys. Rev. 110, 476 (1958)

$\bar{\nu}$ and $\langle \nu^2 \rangle_{av}$ are the average and the average square of the number of neutrons per fission; P_0, P_1, P_2 .... are the respective probabilities of emission of 0, 1, 2 .... neutrons per fission. The quantity $[(\nu^2)_{av} - \bar{\nu}\,]/\bar{\nu}^2$ is a measure of the relative width of the neutron multiplicity distribution. It would be equal to 1.0 for a Poisson distribution.

Table 11.33* Probability of emission, $P(\nu)$ of ν neutrons in the spontaneous fission of Pu^{240} determined by large scintillator tank technique.

Number of events recorded = 4197 fissions	
P_0	0.062 ± 0.006
P_1	0.198 ± 0.017
P_2	0.374 ± 0.022
P_3	0.228 ± 0.024
P_4	0.114 ± 0.022
P_5	0.027 ± 0.013
P_6	0.000 ± 0.005

$\overline{\nu} = 2.20 \pm 0.03$

(value used to calibrate neutron detection efficiency)

* J. E. Hammel and J. F. Kephart, Phys. Rev. 100, 190 (1955)

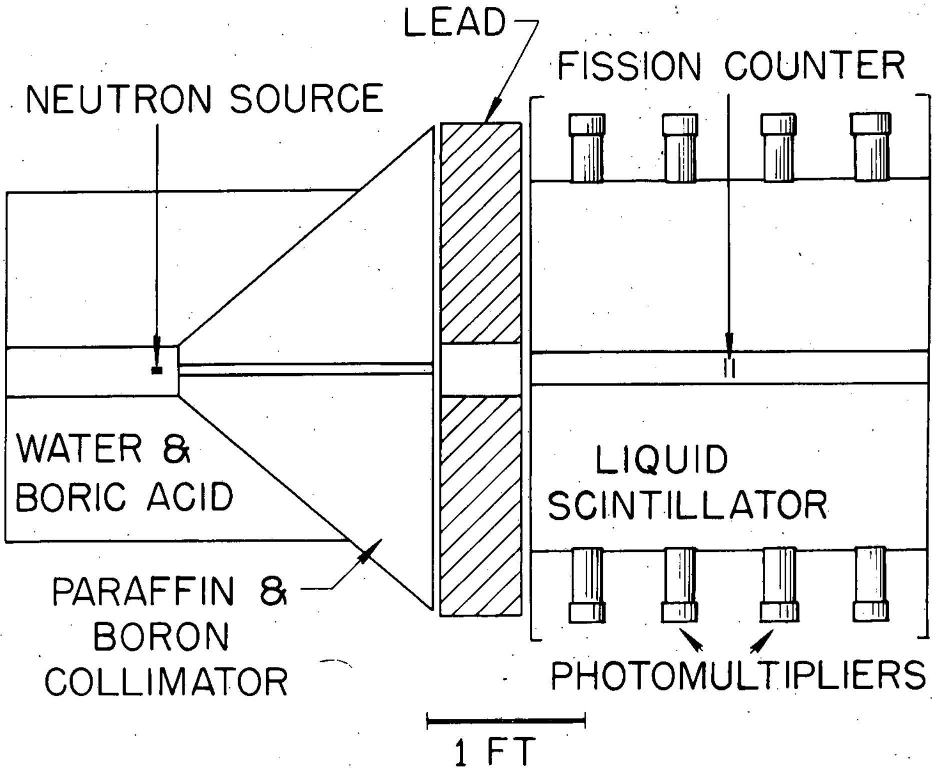
LEAD
FISSION COUNTER
NEUTRON SOURCE
WATER &
BORIC ACID
LIQUID
SCINTILLATOR
PARAFFIN &
BORON
COLLIMATOR
PHOTOMULTIPLIERS
1 FT

MU-18853

Fig. 11.76. Schematic diagram of experimental equipment used to measure neutron multiplicities for samples which underwent the fission reaction in a collimated beam of 80 kev neutrons from the T(p,n)He3 reaction. The shielding serves to eliminate spurious counts in large liquid scintillator. From DIVEN et al. Phys. Rev. 101, 1012 (1956).

given in Table 11.28. Values of P(ν) are given in Table 11.34.

In section 11.7.5 the experimental data on neutron multiplicity are correlated with simple models of the evaporation of neutrons from excited fission fragments.

11.7.3 Measurements of P(ν) as a function of fission mode. It is possible to carry this experimental technique a step further to get even more detailed information on individual fission events. HICKS AND COWORKERS[372] and BOWMAN AND THOMPSON[373] have combined the back-to-back double ionization chamber method for the simultaneous measurement of fragment energies (discussed in Sections 11.6.1 and 11.6.2) with the large scintillator tank in order to measure neutron multiplicities as a function of the specific mode of fission. A schematic drawing of BOWMAN AND THOMPSON'S[373] apparatus is given in figure 11.77. The shallow back-to-back ionization chambers are placed in the center of a cylindrical passageway installed along the axis of the tank. When a spontaneous fission event occurs the sequence of events is the following: first the ionization pulses developed by both fragments are applied to the vertical and horizontal deflection plates corresponding to the first oscilloscope electron beam. This produces a spot on the scope screen whose location gives the sizes of the two pulses and hence, the kinetic energy of both fragments. Simultaneously, the pulse from fragment one is used to initiate the sweep circuit for the second electron gun in the oscilloscope. The pulse developed in the scintillator tank-photomultiplier system is applied to the vertical deflection plate (after a built-in delay of one microsecond) producing a peak in the trace of the second electron beam. The neutrons emitted in fission are quickly moderated and then captured after delays of many microseconds. Each neutron at the time it is captured produces a pulse in the tank-photomultiplier system which is displayed as a peak on the scope screen. A camera photographs the screen during all this time and records simultaneously the spot specifying the fragment energies and the trace indicating the number of neutrons captured. The film is then advanced to be ready to photograph the next spontaneous fission event separately. With this technique, BOWMAN AND THOMPSON[373] recorded data on 20,000 spontaneous fission events in Cf^{252}. These data were recorded on IBM

---

[372] Hicks, Ise, Pyle, Choppin, and Harvey, "Correlations Between the Neutron Multiplicities and Spontaneous Fission Modes of Californium-252", Phys. Rev. 105, 1507 (1957)

[373] H.R. Bowman and S. G. Thompson, Univ. of Calif. Radiation Laboratory Report, UCRL-5038, March 1958; also published as paper P/652 in the Proceedings of the 2nd Geneva Conference on the Peaceful Uses of Atomic Energy, Geneva, 1958.

Table 11.34 Probability of emission $P(\nu)$ of ν neutrons in the fission of U^{233}, U^{235} and Pu^{239} induced by 80-kev neutrons

	Neutron-induced fission[a]		
Nuclide	U^{233}	U^{235}	Pu^{239}
Fissions analyzed	1632	10715	1376
$\bar{\nu}$	2.585±0.062	2.47^{b}±0.03	3.048±0.079
$(\nu)^2_{av}$	7.84±0.34	7.32±0.15	10.62±0.53
$[(\nu)^2_{av} - \nu] / \bar{\nu}^2$	0.786±0.013	0.795±0.007	0.815±0.017
P_0	0.010±0.008	0.027±0.004	-0.01±0.01
P_1	0.151±0.024	0.158±0.010	0.11±0.03
P_2	0.326±0.037	0.339±0.014	0.13±0.06
P_3	0.301±0.044	0.305±0.015	0.56±0.08
P_4	0.176±0.041	0.133±0.013	0.11±0.08
P_5	0.042±0.028	0.038±0.009	0.06±0.09
P_6	-0.010±0.017	-0.001±0.003	0.05±0.08
P_7	0.006±0.009	0.001±0.002	0.00±0.06
P_8	-0.002±0.002	0.000±0.000	-0.01±0.03

a. Results given are for 80-kev neutrons.

b. Normalizing value.

* DIVEN, MARTIN, TASCHEK AND TERRELL, Phys. Rev. 101, 1012 (1956).

See bottom of Table 11.32 for meaning of terms.

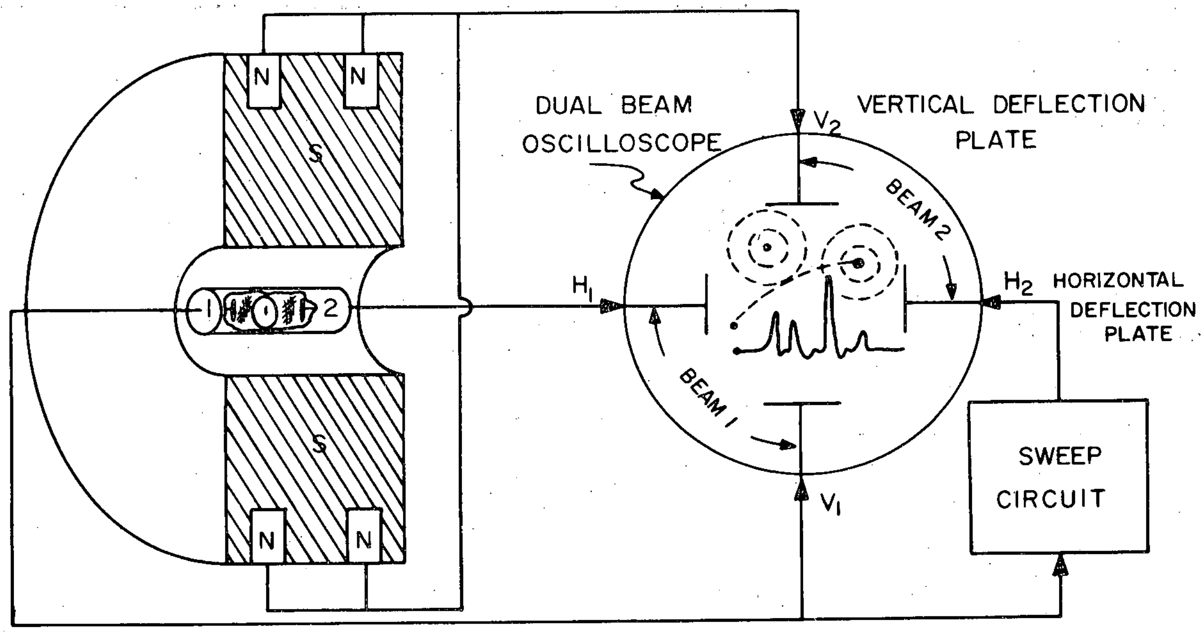
N
N
S
1
2
S
N
N
DUAL BEAM OSCILLOSCOPE
V2
VERTICAL DEFLECTION PLATE
BEAM 2
H1
H2
HORIZONTAL DEFLECTION PLATE
BEAM 1
V1
SWEEP CIRCUIT

AVERAGE NUMBER OF NEUTRONS AND FISSION FRAGMENT KINETIC ENERGIES

MU-19422

Fig. 11.77. Schematic diagram of H. BOWMAN and S. G. THOMPSON'S[373] apparatus for measuring neutron multiplicity and kinetic energies of both fragments simultaneously in spontaneous fission. S denotes large volume of cadmium-loaded scintillator. N denotes phototubes. The oscilloscope used in this experiment had two electron beams.

cards which make it easier to examine neutron multiplicity as a function of many variables. Such correlations can provide many crucial tests of fission theories. As examples of the many possible correlations BOWMAN AND THOMPSON show the variation of $\overline{\nu}$ with change in the fragment mass ratio and with change in the total kinetic energy of the fragments.

Rather than discuss these data we wish to turn to a description of a similar experiment done by a technique with inherently higher resolution. STEIN AND WHETSTONE[374] combined the high resolution provided by the fragment time-of-flight method of determining the fission mode and the high-detection efficiency of the large cadmium-loaded liquid scintillator as a neutron counter. With this combination of apparatus they determined how the total number of prompt neutrons emitted in the spontaneous fission of Cf^{252} is affected by the division of mass between the fragments and by the amount of energy going into kinetic energy of the fragments.

A schematic diagram of the apparatus and of the electronic recording system is shown in figure 11.78. Data were collected on 15,333 events and processed on an IBM-704 data processing machine. We show two correlations of the data in figures 11.79 and 11.80, In the first of these we see that there is a correlation between $\overline{\nu}$ and the total fragment kinetic energy E_k particularly in the interval of E_k containing the majority of the events. The observed correlation is what one would expect qualitatively if there is a given average amount of available energy to be shared between the kinetic and excitation energies of the fragments. In figure 11.80 it is readily apparent that $\overline{\nu}$ varies with the mass ratio R_A but the variation is complex and not easily explained. In the range of mass ratio covering the great majority of fission events the variation is approximately linear. STEIN AND WHETSTONE[374] also show the variation of $\overline{\nu}$ with E_k for data separated into intervals of R_A and similarly the variation of $\overline{\nu}$ with R_A for data separated into intervals of E_k. The authors subjected the data covering the majority of fission events to a detailed analysis to correct for the resolution effects in their experimental technique and derived the "true" dependence of $\overline{\nu}$ on R_A and E_k listed in Table 11.35. The quantity $\partial \overline{\nu}(E_k,R_A)/\partial E_k = -0.143$ neutrons fission^{-1} Mev^{-1} is in reasonably good agree-

---

[374] W. E. Stein and S. L. Whetstone, Jr., Phys. Rev. 110, 476 (1958)

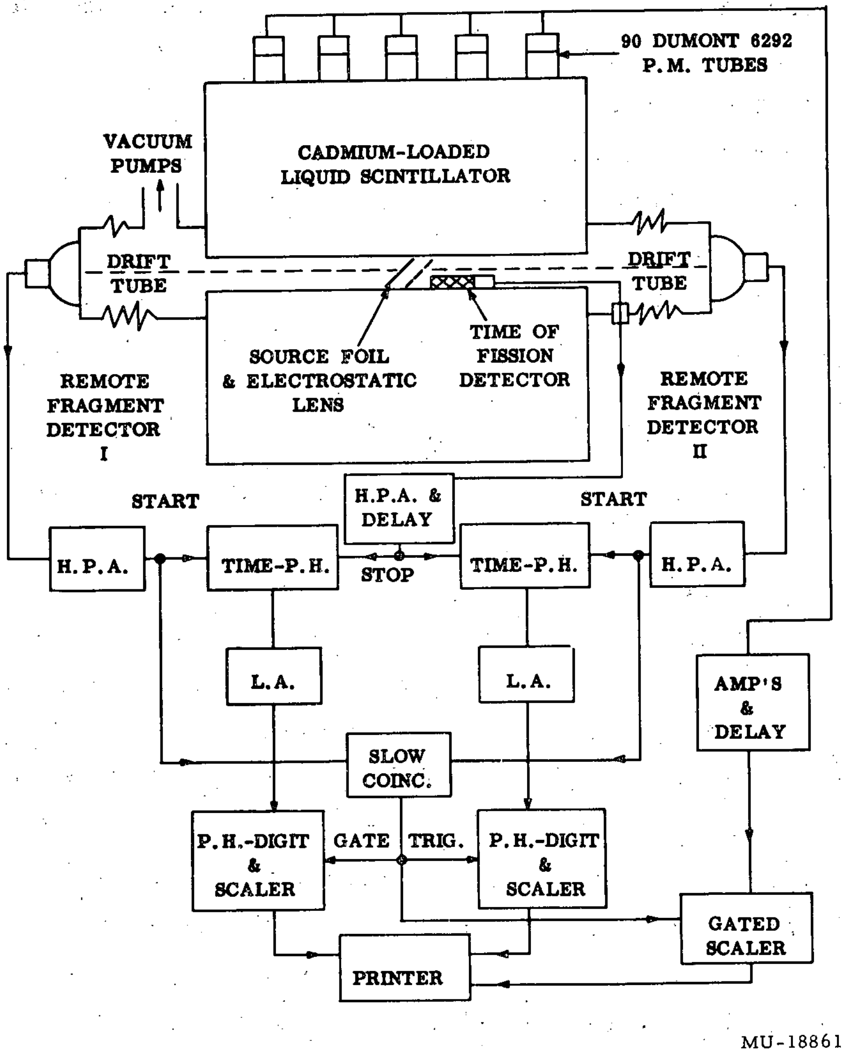
90 DUMONT 6292 P.M. TUBES
CADMIUM-LOADED LIQUID SCINTILLATOR
VACUUM PUMPS
DRIFT TUBE
DRIFT TUBE
SOURCE FOIL & ELECTROSTATIC LENS
TIME OF FISSION DETECTOR
REMOTE FRAGMENT DETECTOR I
REMOTE FRAGMENT DETECTOR II
START
START
H.P.A. & DELAY
H.P.A.
TIME-P.H.
STOP
TIME-P.H.
H.P.A.
L.A.
L.A.
AMP'S & DELAY
SLOW COINC.
P.H.-DIGIT & SCALER
GATE
TRIG.
P.H.-DIGIT & SCALER
GATED SCALER
PRINTER
MU-18861

Fig. 11.78. Schematic diagram of the STEIN and WHETSTONE[374] equipment for determining the correlation between neutron emission and the Cf^{252} fission mode. Drift lengths were each 152 cm. The scintillator tank was approximately 75 cm in diameter and height with a 6.8 cm transverse hole in which the time-of-flight drift tube was placed. Pulses from the bank of 90 photomultiplier tubes fed through Hewlett-Packard distributed amplifiers (HPA) time-to-pulse-height converters (Time-P.H.), conventional linear amplifiers (AMP'S and L.A.) to pulse-height-to-digital converters (P.H.-Digit). The time of fission detector was a thin plastic scintillator which collected the electrons ripped out of the backing foil supporting the Cf^{252} source as one of the fragments passed through this backing foil.

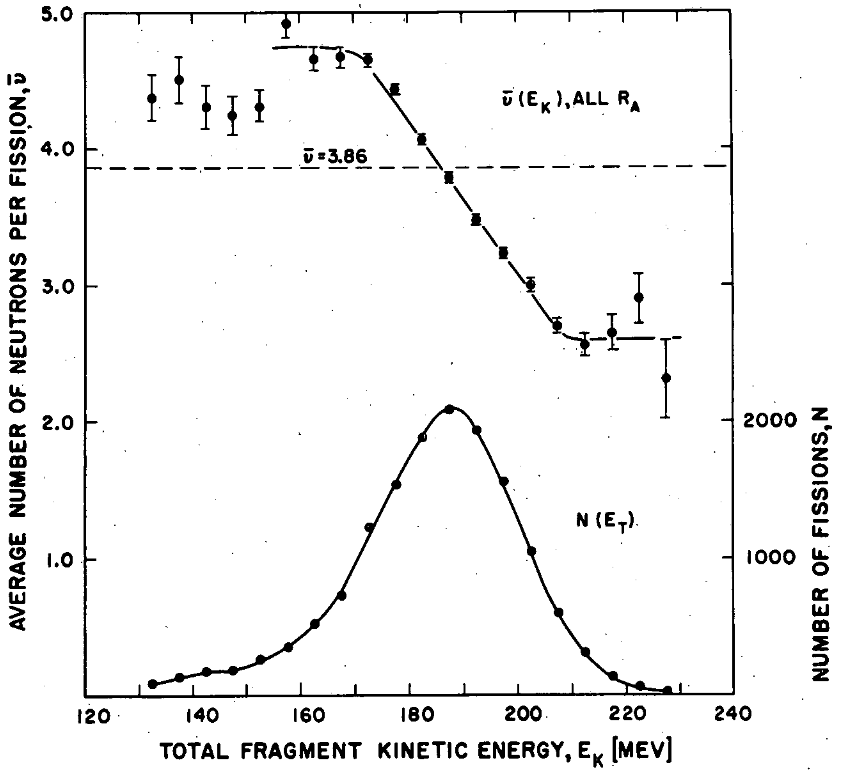

MU-18860

Fig. 11.79. The average number of neutrons per fission and the number distribution of Cf^{252} spontaneous fission events as functions of the total kinetic energy of the fragments with no discrimination on the mass ratio of the fragments. Uncertainties shown are relative standard errors. Data are corrected for the 78 percent efficiency of the neutron detector. STEIN and WHETSTONE.[374]

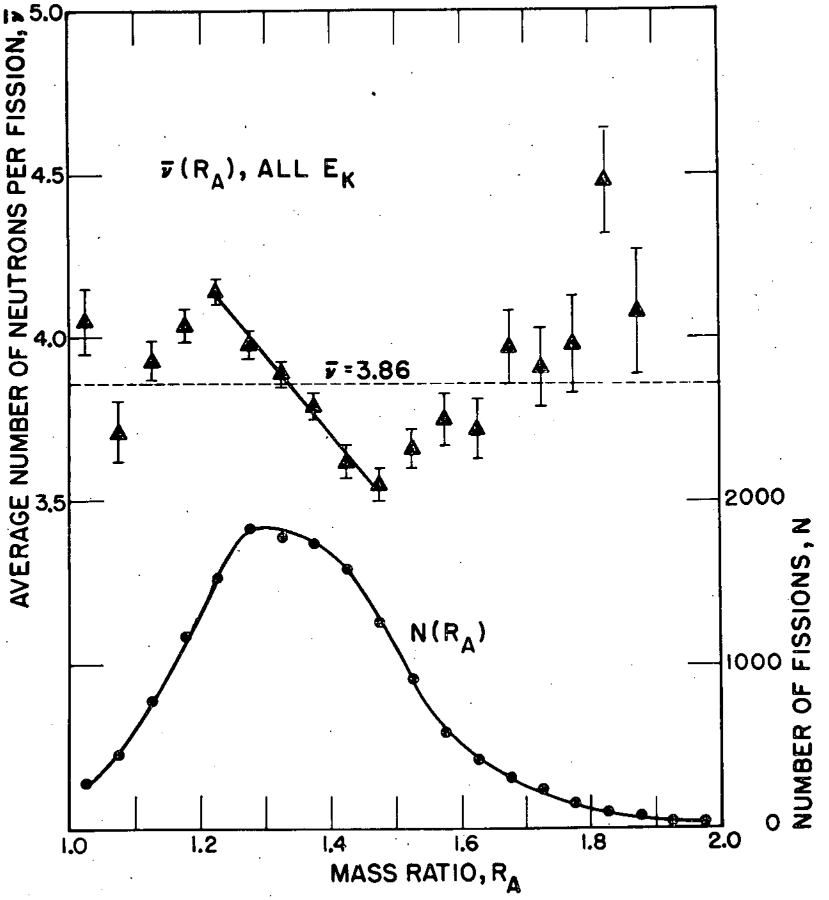

MU-18839

Fig. 11.80. The average number of neutrons per spontaneous fission of Cf^{252} and the number distribution of fission events as functions of the mass ratio of the fragments with no discrimination on the total kinetic energy of the fragments. STEIN and WHETSTONE.[374]

Table 11.35 Variation of $\bar{\nu}$ with mass ratio and fragment kinetic energy in the spontaneous fission of Cf^{252} according to STEIN AND WHETSTONE[374].

Slope	Observed value	Corrected value
$\partial\bar{\nu}(E_k, R_A)/\partial E_k$	-0.070 ± 0.004^a	-0.143 ± 0.020^a
$\partial\bar{\nu}(E_k, R_A)/\partial R_A$	-3.8 ± 0.8^b	-6.3 ± 1.1^b
$[\partial\bar{\nu}(E_k)/\partial E_k]_{\text{all } R_A}$	-0.056 ± 0.003^a	-0.079 ± 0.008^a
$[\partial\bar{\nu}(R_A)/\partial R_A]_{\text{all } E_k}$	-2.5 ± 0.5^b	-2.8 ± 0.6^b

a. In units of (neutrons/fission)/Mev.

b. In units of (neutrons/fission)/unit mass ratio.

ment with calculations based on a theory of LEACHMAN AND KAZEK[375] discussed in Section 11.7.5 below. The results imply a nuclear "temperature" of ≤ 1 Mev and a 7.0 Mev decrease in the average excitation energy for the emission of each neutron.

FRASER AND MILTON[376] have also studied the variation in prompt neutron emission probability as a function of fission mode for thermal neutron induced fission of U^{233}. This study, carried out earlier than the studies just described, makes use of a different type of neutron detector. The apparatus is shown schematically in Fig. 11.81. The kinetic energies of both fragments were measured in a double gridded ionization chamber. The U^{233} source was deposited on the common cathode and covered with a collimator. The pulse heights of the pulses from the two ionization chambers were recorded only when coincident with prompt fast neutrons detected in either one of two neutron counters placed on opposite sides of the fission chamber. These neutron detectors consisted of ionization chambers two inches in diameter filled to a high pressure of methane. The angle subtended by these counters at the fission source is small but the strong angular correlation of the direction of motion of the prompt neutrons with the direction of motion of the emitting fragment overcomes this disadvantage somewhat. Nevertheless, the neutron detection efficiency is much less than for large scintillator tank detectors and in most respects the characteristics of prompt neutron emission could not be studied as completely as in the methods just described. On the other hand, the method of FRASER AND MILTON[376] has the distinct advantage that it identifies the fragment from which each recorded neutron originates. This also is a consequence of the strong peaking (in the lab system) of the neutrons in the direction of the fragments.

One of the interesting conclusions which FRASER AND MILTON came to after an analysis of 20,000 events measured in their experimental apparatus is that neutrons are emitted preferentially by the heaviest light fragments and by the heaviest heavy fragments.

WHETSTONE[377] later restudied the variation in prompt neutron emission

---

375. R. B. Leachman and C. S Kazek, Jr., Phys. Rev. 105, 1511 (1957)

376. J.S. Fraser and J.C.D. Milton, "Distribution of Prompt-Neutron Emission Probability for the Fission Fragments of U^{233}," Phys. Rev. 93, 818 (1954)

377. S. L. Whetstone, Jr., Phys. Rev. 114, 581 (1959)

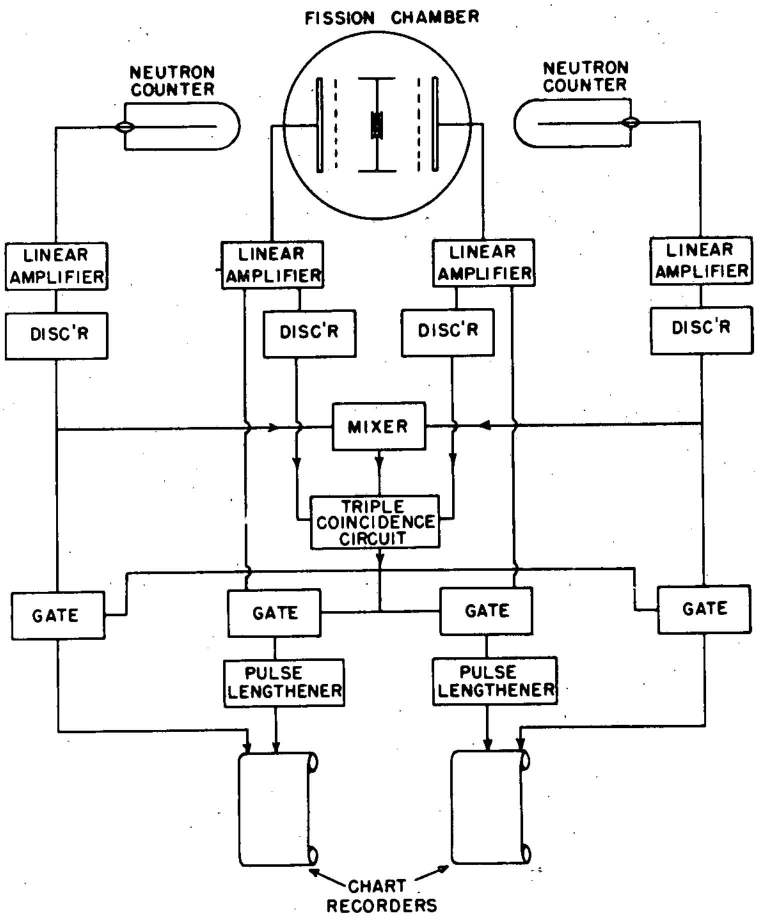
FISSION CHAMBER
NEUTRON COUNTER
NEUTRON COUNTER
LINEAR AMPLIFIER
LINEAR AMPLIFIER
LINEAR AMPLIFIER
LINEAR AMPLIFIER
DISC'R
DISC'R
DISC'R
DISC'R
MIXER
TRIPLE COINCIDENCE CIRCUIT
GATE
GATE
GATE
GATE
PULSE LENGTHENER
PULSE LENGTHENER
CHART RECORDERS

MU-18838

Fig. 11.81. Schematic diagram of FRASER and MILTON'S[376] apparatus for measurement of prompt-neutrons in coincidence with fragment pairs whose energies are measured in a double back-to-back gridded ion chamber. The neutron detectors are ionization chambers filled with high pressure methane.

Events are recorded only when triple coincidences are registered between a pair of fragments and one or the other of the neutron detectors. The record of each event consists of pen deflections proportional to the ionization energies of the two fragments and a side pen deflection specifying the neutron-emitting fragment.

probability as a function of the mass number of the fragment from which the neutrons are emitted. His experimental technique was superior in some respects to that of FRASER AND MILTON[376] and some striking results were obtained.

The experimental apparatus was similar to that used by STEIN AND WHETSTONE[374] and illustrated in Fig. 11.78. The chief difference was that the Cf^{252} spontaneous fission source was located at the end of the large cadmium-loaded liquid scintillator rather than in the center. Because of the strong forward peaking of neutron emission in the direction of travel of the fragments (assuming isotropic neutron emission in the frame of the moving fragment) the neutrons detected in the scintillator tank can be attributed almost entirely to one of the fragments. From the simultaneous measurement of the velocity of both fragments the approximate mass number of each fragment could be obtained.

The chief result of the experiment is given in Fig. 11.82 which shows the average number of neutrons as a function of mass number. There is a striking discontinuity of one whole unit at the mass number corresponding to symmetric fission. The average number of neutrons emitted from all the light fragments compared to the average number emitted from all the heavy fragments turns out to be 1.02 ± 0.02.

If this neutron emission discrepancy is real, it is very difficult to reconcile with the passage of the dividing nucleus over a symmetric saddle point[378] since in the picture of a symmetric saddle point shape leading to two fragments of almost equal mass one would expect to get two fragments with almost equal shapes and internal excitation. WHETSTONE[377] speculated on a possible explanation of the effect based on the idea that the saddle point shape is actually asymmetric. He takes this idea from the writings of VLADIMIRSKII[378] who showed by some qualitative calculations that within the framework of the unified model of the nucleus one might explain a marked softening of the distorted nucleus toward asymmetric shapes in terms of a favoring of nucleonic states of high Ω quantum number. If one assumes that this is true and that asymmetric shapes are favored at the state of critical deformation, then one can devise a simple model of the fission process which will reproduce qualitatively both the observed mass distribution and the strange dependence of $\overline{\nu}$ on mass number.

---

[378] V. V. Vladimirskii, Soviet Physics 5, 673 (1957).

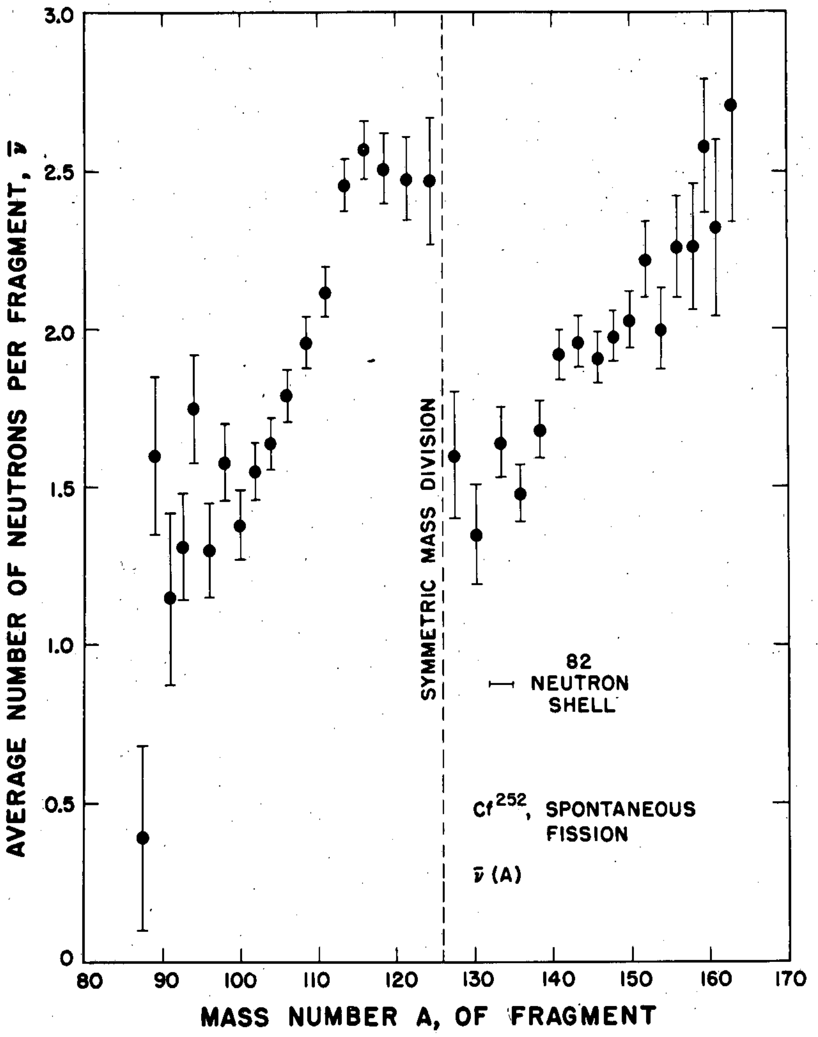

MU-18863

Fig. 11.82. The average number of neutrons per fragment as a function of the fragment mass number. WHETSTEONE.377 Isotropic emission of the neutrons in the fragment frames has been assumed and the curve has been normalized to give $\bar{\nu}$ = 3.86 averaged over all fission modes.

Quoting WHETSTONE[377], "One can easily imagine that just before the fissioning nucleus breaks in two, there exists a fairly long neck connecting two relatively large volumes, and that usually, if not always, these volumes are of unequal size (see figure 11.83). The nucleus will be expected to break with greatest probability somewhere near the middle of the neck, which will favor the asymmetric mass divisions observed and which will partition the deformation energy of the neck fairly equally between the two fragments. Since the two ends of the nucleus would be expected to have fairly small internal excitation energies before the split, the excitation energies of the fragments after the split, and therefore the number of neutrons emitted from each fragment, should be on the average, equal for the most probable mass division. The shape and volume of the neck can now be tailored to imply a point-of-splitting probability, such as is drawn schematically in figure 11.83 which will reproduce the observed fragment mass distribution. It is obvious that symmetric mass division will correspond to the relatively very rare splitting close to the large end of the nucleus, and it is seen that this kind of a split gives almost all of the large amount of deformation energy to the light fragment. Splittings very far from mass symmetry correspond to breaking points close to the small end, with the deformation energy of the neck given to the heavy fragment. Thus the observed $\overline{\nu}(A)$ dependence is obtained." This hypothetical picture of the fission process is discussed also by HALPERN[379].

---

[379] I. Halpern in "Nuclear Fission", a review prepared for Annual Reviews of Nuclear Science, 9, 245 (1959).

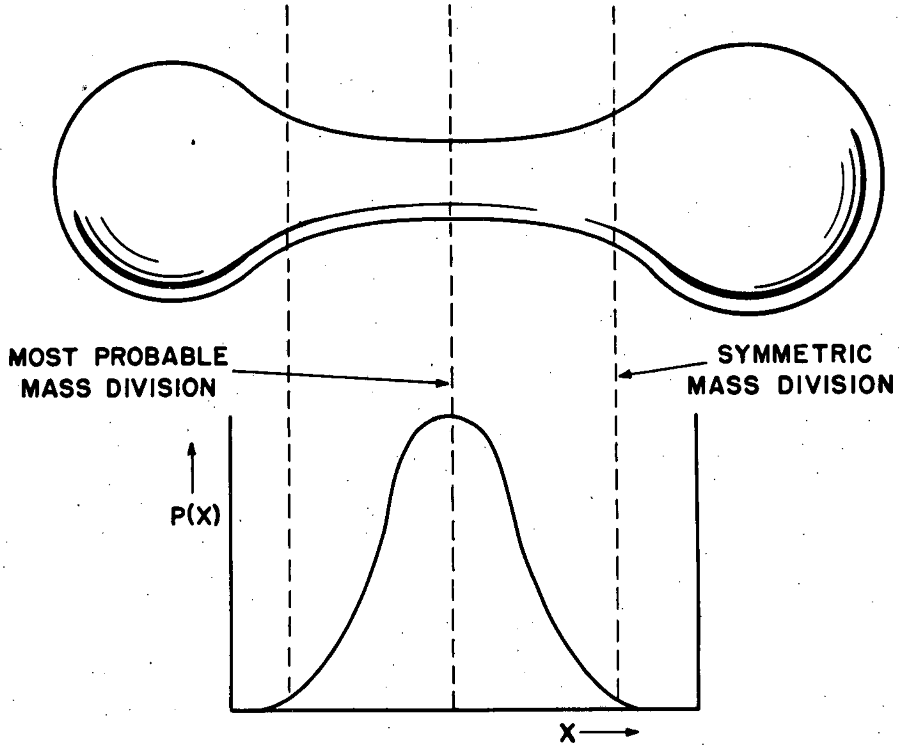

MU-18862

Fig. 11.83. A picture of a fissioning nucleus shortly before it breaks in two. The two lobes are unequal in size. The mass ratio is determined by the point along the neck at which division occurs. The P(x) curve is a probability curve for the points of division adjusted to give an overall distribution of fragment mass ratios in agreement with the observed distribution. According to this picture a division of the nuclear mass into two equal parts will produce a nearly spherical heavy fragment and a markedly distorted (hence excited) light fragment. From WHETSTONE.[377]

11.7.4 **The Energy Spectrum and Angular Distribution of the Prompt Neutrons from Fission.** The distribution in energy of the neutrons emitted in the fission of U^{235}, U^{233} and Pu^{239} has been studied by two fundamentally different methods.[380-387] In the first, the energy of the neutrons is obtained from the ranges of knock-on protons in photographic emulsions, cloud chambers, ionization chambers, proportional counters, etc. In the second, the velocity of the neutrons is measured by time-of-flight techniques. A combination of the two methods is often used to cover the whole range of neutron energies.

A compilation of three sets of data taken at the Los Alamos Scientific Laboratory is presented in Fig. 11.84. These data are compared with a semi-

---

380. N. Nereson, "Fission Neutron Spectrum of U^{235}", Phys. Rev. 85, 600 (1952); "Fission Neutron Spectrum of Pu^{239}", Phys. Rev. 88, 823-4 (1952).

381. Bonner, Ferrell and Rinehart, "A Study of the Spectrum of the Neutrons of Low Energy from the Fission of U^{235}", Phys. Rev. 87, 1032 (1952). These authors cite many earlier references.

382. D. L. Hill, "The Neutron Energy Spectrum from U^{235} Thermal Fission," Phys Rev., 87, 1034 (1952).

383. B. E. Watt, "Energy Spectrum of Neutrons from Thermal Fission of U^{235}," Phys. Rev. 87, 1037 (1952)

384. Unpublished data of Barton, Cranberg and Nereson, and of Frye and Rosen, quoted by R. B. Leachman in Paper P/592, Vol. 2, "Proceedings of the International Conference on the Peaceful Uses of Atomic Energy", United Nations, New York (1956).

385. L. Cranberg, G. Frye, N. Nereson and L. Rosen, "Fission Neutron Spectrum of U^{235}", Phys. Rev. 103, 662 (1956).

386. K. N. Mukhin, L. M. Barkov and Gerasimova; see B.G. Erozolimsky, Neutron Fission, Supplement No. 1 to Atomnaya Energiya 74-98 (1957).

387. D. B. Nicodemus and H.H. Staub, Phys. Rev. 89, 1288 (1953)

388. L. Cranberg, "Proceedings of the International Conference on the Peaceful Uses of Atomic Energy," Geneva 1955 (United Nations, New York, 1956), Vol. 2, Paper P/577.

389. K. M. Henry and M. P. Haydon, Oak Ridge National Laboratory Report, ORNL-2081, 1956, unpublished.

390. A. B. Smith, P. R. Fields, R. K. Sjoblom, and J. H. Roberts, Phys. Rev. 114, 1351 (1959).

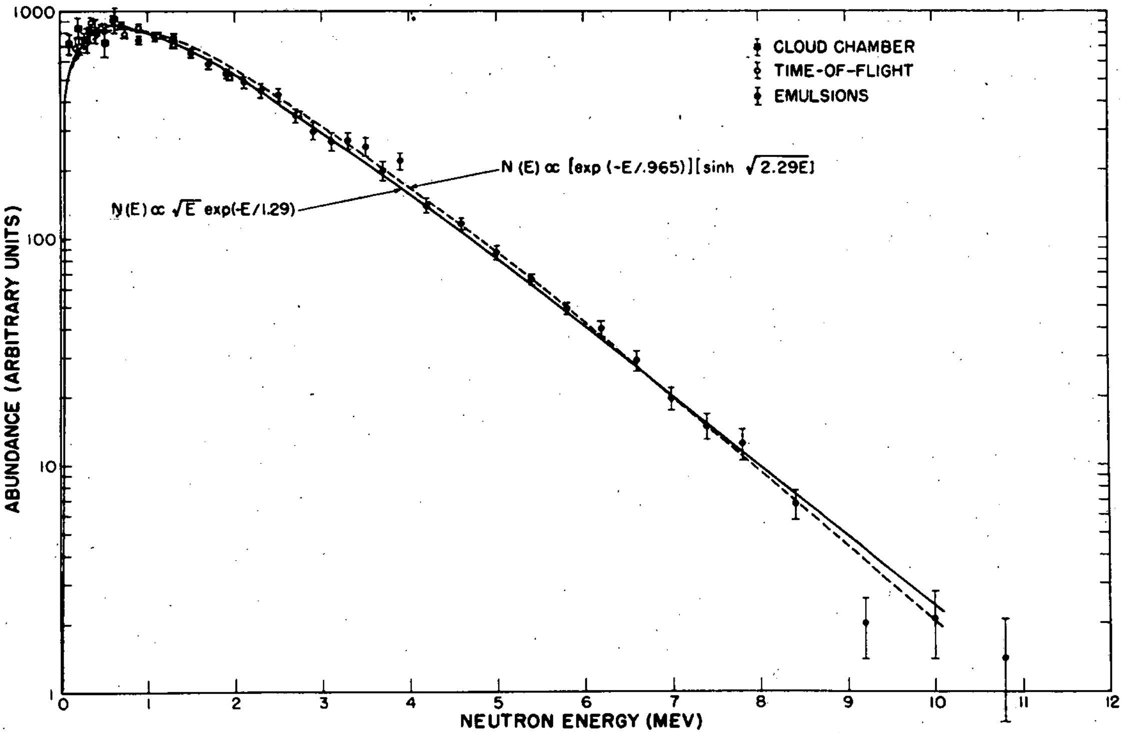

MU-18981

Fig. 11.84. Comparison of semi-empirical expressions of the energy spectrum of fission neutrons with experimental measurements at Los Alamos on neutrons from thermal fission of U^{235}. Figure from reference 384.

empirical expression published by WATT[383] for the U^{235} neutron spectrum.

$$N(E) \propto \left[\exp \frac{-E}{0.965}\right] \left[\sinh \sqrt{2.29\, E}\right] \qquad (11.48)$$

(N(E) is the probability of emission of a fission neutron with energy E. This expression is derived from simple considerations of neutron emission mechanisms and transformation of velocity frames. The constants in the equation are derived from nuclear "temperatures" and fragment energy choices adjusted to fit the experimental data. A further simplification of this semi-empirical expression reported by LEACHMAN[384] results in the form

$$N(E) \propto \sqrt{E}\ \exp\left[\frac{-E}{1.29}\right] \qquad (11.49)$$

which is shown in the figure similarly to provide a satisfactory fit to the experimental data. This expression assumes a Maxwellian distribution for the neutron spectrum but it is based on no simple theoretical derivation. The constant 1.29 is defined as the nuclear "temperatures". This temperature is not the nuclear temperature as defined by WEISSKOPF for the statistical model of the nucleus. This fit with such a simple expression containing only the coefficient in the exponent as a parameter is regarded as fortuitous in view of the dependence of the neutron spectrum on many variables such as fragment excitation, neutron binding energy, angular dependence of neutron emission, etc.

The neutron spectra of the fission neutrons from U^{235}, U^{233} and Pu^{239} caused to fission with slow neutrons are very similar[380, 383, 385, 386]. TERRELL[391] has analyzed all three spectra using the LEACHMAN expression given above and gets a good fit to the experimental spectra by setting the nuclear temperature constant equal to 1.290 Mev, 1.307 Mev and 1.333 Mev, respectively. See Fig. 11.85

The fission neutron spectrum of the spontaneously-fissioning Cf^{252} has also been measured.[392-394] We show the results of SMITH, FIELDS AND ROBERTS[394]

---

[391] J. Terrell, "The Fission Neutron Spectrum and Nuclear Temperature," Phys. Rev. 113, 527, 1959.

[392] E. Hjalmar, H. Slatis and S.G. Thompson, "Photographic Emulsion Measurements of the Energy Distribution of Neutrons from Spontaneous Fission of Cf^{252}", Phys. Rev. 100, 1542 (1955).

[393] H. R. Bowman and S. G. Thompson, "The Prompt Radiations in the Spontaneous Fission of Cf^{252}" University of Calif. Rad. Lab. Report, UCRL-5038, March 1958; also published as Paper P/652, Proceedings of the 2nd International Conference on the Peaceful Uses of Atomic Energy, Geneva, 1958.

[394] A. B. Smith, P.R. Fields, and J.H. Roberts, "Spontaneous Fission Neutron Spectrum of Cf^{252}", Phys. Rev. 108, 411, (1957).

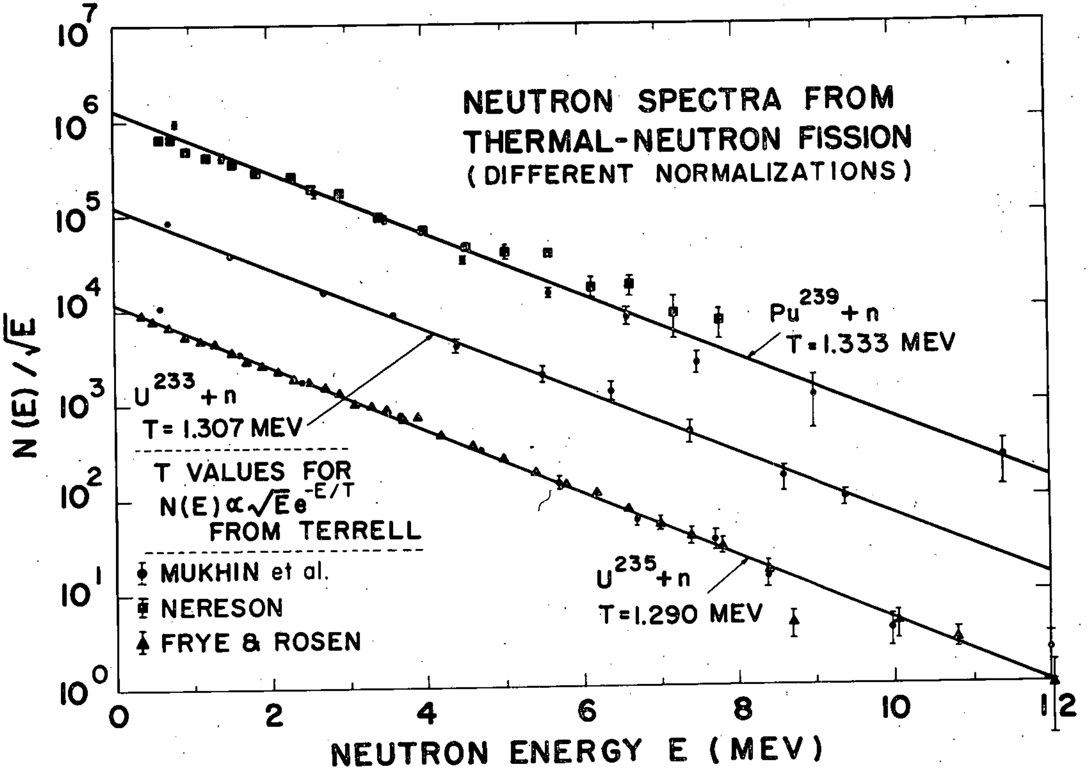

MU-18846

Fig. 11.85. Experimental data on fission neutron energy compared to the expression

$$N(E) \propto \sqrt{E} \quad \exp\left(\frac{-E}{T}\right).$$

This comparison made by TERRELL[389] as quoted by LEACHMAN.[384]

in figure 11.86. The spectrum is very similar to that of the neutron-induced fission of U^{235} except that it is shifted slightly to higher energies. The solid line follows the Watt formula (equation 11.48) evaluated as follows:

$$N(E) \propto \exp(-0.88E) \sinh \sqrt{2.0E} \qquad (11.50)$$

TERRELL[391] was able to get a good fit also with a Maxwellian distribution of the type given by equation 11.49.

It is apparent that all measured fission neutron spectra are fitted rather well by the WATT formula and perhaps slightly better by an equation based on a simple Maxwellian distribution (equation 11.49). The neutron intensity varies as $E^{1/2}$ at low energies and exponentially at high energies.

Many attempts have been made to derive neutron spectra using WEISSKOPF's[395] concepts of the statistical model of the nucleus since it has seemed that excited fission fragments should be quite appropriate systems for the application of the model. In its most approximate form this model leads to a simple evaporation spectrum of the form

$$E \exp\left(\frac{-E}{T}\right)$$

which gives a poor fit to the experimental data if the nuclear temperature T is single-valued throughout the neutron evaporation process. A great improvement can be made by consideration of the fact that the second and subsequent neutrons will be emitted from a less-excited nucleus for which a lower nuclear temperature would be appropriate. Several authors[391,396-8] have shown that even a simple combination of two evaporation components with different values of T can produce good agreement with the neutron spectra in the laboratory system. TERRELL[391] has carried out a more sophisticated analysis in which the wide distribution in initial fragment excitation energies is converted into a distribution of nuclear temperatures appropriate for the evaporation of $\bar{\nu}$ neutrons. In the U^{235} case he carried through a sample calculation by weighting together 14 evaporation spectra using a separate fragment velocity for the light and heavy fragments and seven different nuclear temperatures weighted according to his derived temperature distribution. This calculation yields a laboratory neutron spectrum in excellent agreement with experiment but not significantly better

---

395. V. F. Weisskopf, Phys. Rev. 52, 295 (1937); J. M. Blatt and V. F. Weisskopf, Theoretical Nuclear Physics, John Wiley and Sons, Inc., N.Y., 1952, pp.365-374.

396. J.S. Fraser, Phys. Rev. 88, 536 (1952)

397. J.C.D. Milton, unpublished data

398. Smith, Fields and Roberts, Phys. Rev. 108, 411 (1957).

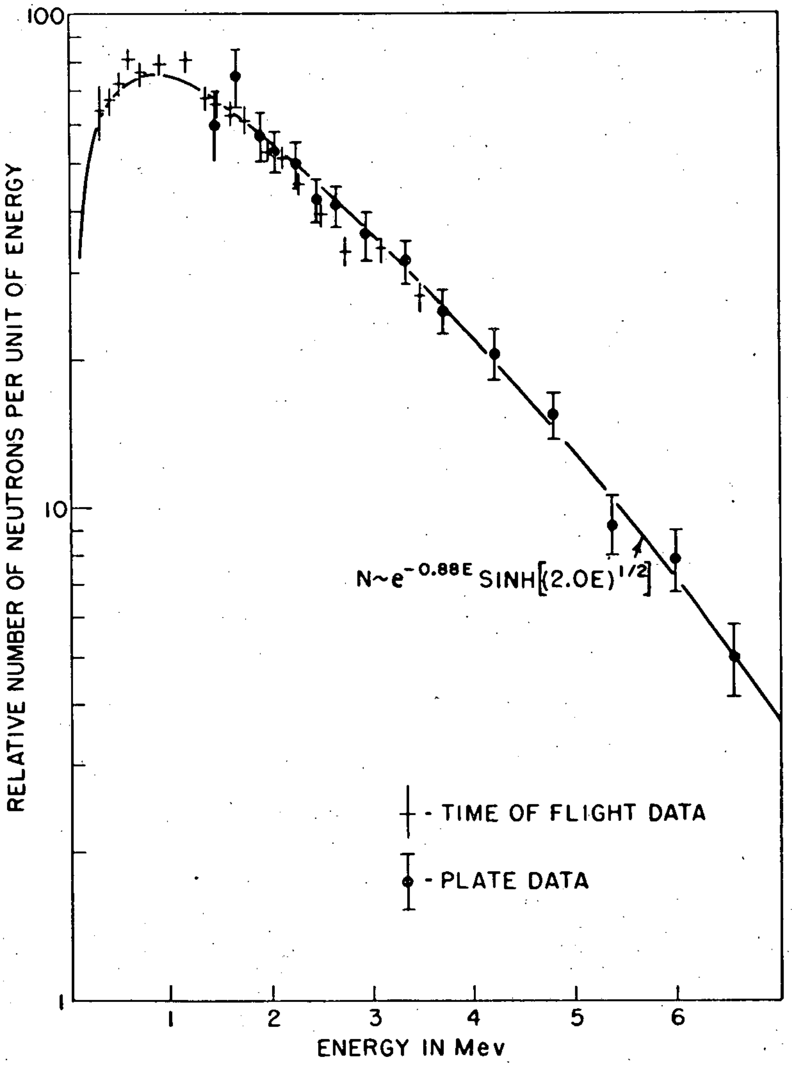

MU – 18904

Fig. 11.86. Energy spectrum of Cf^{252} fission neutrons as determined by SMITH, FIELDS, and ROBERTS.[394]

than the more approximate 2-component analyses mentioned above.

On the basis of this analysis, it appears that the result of the assumption of an evaporation spectra based on the WEISSKOPF statistical model for fission neutrons in the center-of-mass system leads to a spectrum which is essentially equivalent to a Maxwellian distribution (equation 11.49) in the laboratory system. Isotropic emission of neutrons in the center-of-mass system is assumed.

TERRELL'S [391] analysis implies that the average energy of the neutrons will be equal to the average energy per nucleon of the fission fragments (about 0.78 Mev) plus some quantity proportional to the average number of neutrons emitted. Specifically, TERRELL finds a good fit to many sets of data with the expression.

$$\underset{\text{(in Mev)}}{E_{\text{Average}}} \cong 0.78 + 0.621\,(\bar{\nu} + 1)^{1/2} \qquad (11.51)$$

The whole subject of the analysis of fission neutron spectra and of its meaning for neutron evaporation models and nuclear temperature parameters is well reviewed by TERRELL[391] in a paper which covers all pertinent work published by mid-1958.

If neutron emission is controlled by an evaporation process it seems logical to assume that neutron emission is isotropic in the center-of-mass system and this assumption is usually made in the absence of any clear evidence to the contrary. It is possible, however, that the deformation of the fragments or their other characteristics at the moment of scission will favor neutron emission in certain directions. HILL AND WHEELER [399], for example, suggest that there may be preferential emission forward and backward along the direction of the fragment motion. Hence, it is quite important that the actual angular distribution be firmly established.

One approach is to assume the validity of one of the evaporation model treatments, to assume some angular distribution, such as $1 + A_2 P_2 \cos \theta$, to calculate the corresponding neutron spectra in the laboratory system, and from the agreement or non-agreement of these spectra with the experimental data to set an upper limit to the amount of anisotropy. However, because of many complicating factors, it is not possible to prove anything very definite about anisotropy by this approach.

---

[399] D. L. Hill and J. A. Wheeler, Phys. Rev. 89, 1102 (1953)

Research groups in several laboratories[400-402] have devised apparatus which will permit a definitive answer on the center-of-mass anisotropy. In these experiments, the velocity and the direction of motion of neutrons and fragments are measured simultaneously so that neutron velocities relative to the fragment velocities and the angular distribution of neutrons in the reference system of the moving fragments can be calculated in a straightforward fashion. Final results from these experiments are not available as this is being written.

There are several published reports[396, 403,404] in which the angular distribution of the neutrons with respect to the fragment direction of motion in the laboratory system is measured. The dominant feature of the laboratory distribution is a strong peaking in the direction of the fragment emission caused by the center-of-mass motion. Let us consider briefly FRASER'S[396] experiment. In this study neutrons from the thermal neutron fission of U^{233}, U^{235} and Pu^{239} were measured. Collimated fission fragments were selected in energy in a gridded ionization chamber and coincident prompt neutrons in a given direction were counted by proton recoils in an electron collecting chamber filled with methane. By proper energy discrimination on the fragment pulses it was possible to study neutrons in correlation with the total distribution of fission fragment energies or with the light fragment distributions only. Significant differences were noted in the two cases. The results in the case of Pu^{239} are shown in Fig. 11.87. Neutron emission is strongly peaked in the direction of motion of the fragment. The angular distribution expressed as a ratio $N(0^o)/N(180^o)$ is about 70 percent greater when light fragments only are observed than when all fragments are observed. FRASER was able to accomodate his observed angular distributions to an evaporation model with isotropic emission of neutrons in the moving fragment system provided he assumed a 30 percent greater probability of emission of neutrons from the light fragment than from

---

400. H. Bowman and S. G. Thompson, unpublished results; preliminary experiment described in Paper P/652 Volume 15, Proceedings of the 2nd Int'l Conf. on Peaceful Uses of Atomic Energy, Geneva, 1958.

401. A. Smith, P. Fields, and R. Sjoblom, Bull. Amer. Phys. Soc. II, 31, 1959.

402. J. S. Fraser and J.C.D. Milton, Chalk River, unpublished

403. R.R. Wilson, Phys. Rev. 72, 189 (1947)

404. R. Ramanna and P.N. Rama Rao, Paper P/1633, p 361, Vol. 15, Proceedings of the 2nd Int'l United Nations Conference on the Peaceful Uses of Atomic Energy, Geneva, 1958.

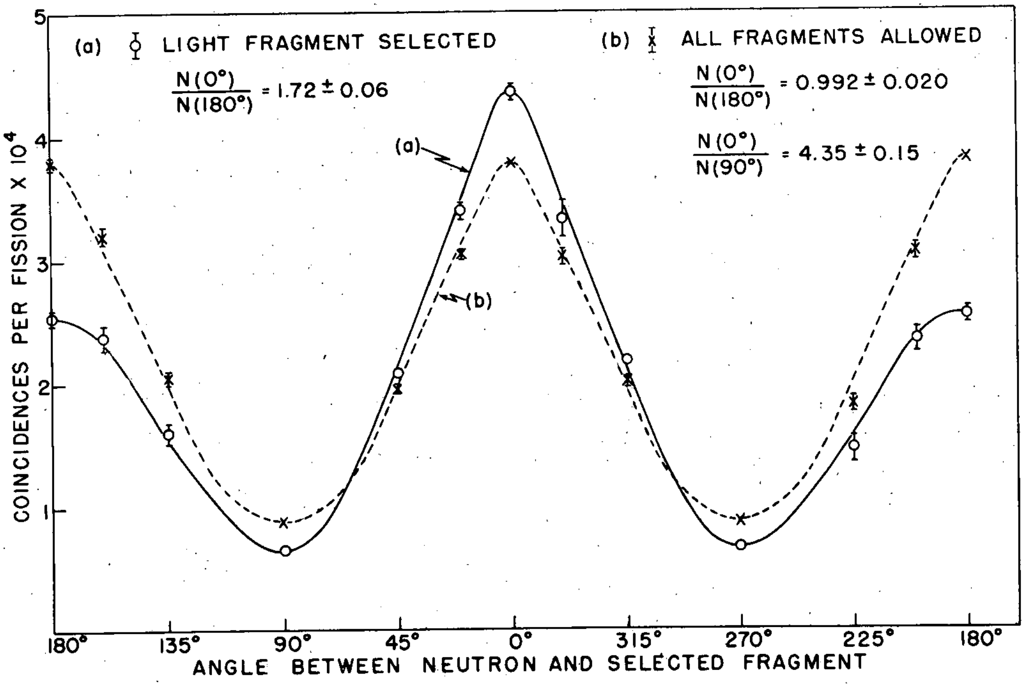

MU-18837

Fig. 11.87. Angular distribution of prompt neutrons from Pu^{239} induced to fission with thermal neutrons. See FRASER.396

the heavy. RAMANNA AND RAO[404] came to a similar conclusion. However, a later reanalysis by MILTON[405] of the data of both experiments using better data for the low energy neutron spectrum in the laboratory system led to the altered conclusion that both fragments emitted the same number of neutrons within 10 percent. Any conclusions on the relative rates of neutron emission from the fragments is indirect and sensitive to the neutron energy spectrum measurements.

For some experimental studies such as shielding studies, neutron dosimetry and biological hazard studies, it is convenient to have a laboratory source of neutrons with a neutron spectrum roughly approximating the U^{235} fission neutron spectrum. A mixture of polonium with selected amounts of boron, beryllium, fluorine and lithium will produce an (α,n) spectrum of the desired shape.[406] Such "mock fission" sources are available commercially.[407]

11.7.5 Theoretical Calculations of Prompt-Neutron Multiplicities.

The probability P_ν of emission of any given integral number ν of prompt neutrons from fission can be calculated from the distribution of excitation energy among the fission fragments if sufficiently accurate information can be obtained. LEACHMAN[408-409] has carried out such calculations based on simple neutron evaporation theory and the results are in good agreement with experiment. We shall outline LEACHMAN'S method.

LEACHMAN first writes down the mass equation of fission:

$$M\,(A\,\delta\,\,Z) + E_n + B = M(A^L\,\delta^L\,Z^L) + M(A^H\,\delta^H\,Z^H) + E_K + E_X$$

where

M = atomic mass

A = mass number

Z = nuclear charge

δ = even-odd parameter

E_n = energy of incident neutron

B = binding energy of neutron to target nucleus

E_K = total kinetic energy of fragments

E_X = total excitation energy of fragments

---

405. J.C.D. Milton and J.S. Fraser, private communication to author; see also footnote on page 540 of Terrell's article.[391]

406. See W. N. Hess, UCRL-3839 (1957); E. Tochilin and R.V. Alves, USNRDL-TR-201, March 1958 and Bull. Amer. Phys. Soc. II 2, 378 (1957).

407. Mound Laboratory, Monsanto Chemical Co., Miamisburg, Ohio

408. R. B. Leachman, Phys. Rev. 101, 1005 (1956).

409. R. B. Leachman, Paper P/592, p. 195, Vol. 2, Proceedings of the Int'l Conference on the Peaceful Uses of Atomic Energy, United Nations, N. Y., 1956.

The mass of the fissioning nucleus can be obtained from experimental mass determination or from minor extrapolations of experimental measurements. The masses of the primary fragments have to be estimated from some empirical mass equation. LEACHMAN based his estimates on the treatment of CORYELL[410]. No attempt was made to evaluate the masses of all the possible fragments but, to simplify the analyses, only three mass ratios, $R_A = A^H/A^L$, were considered. A^L and A^H refer to the mass number of the light and heavy fragments, respectively. For fission of U^{235} by neutrons the chosen ratios were 133/103, 141/95 and 149/87. Also only the most probable non-integer Z^L and Z^H values for each A^L and A^H were used. These most probable Z values were estimated from the equal charge displacement relations discussed in Section 11.5.

With these simplifications it was possible to calculate the sum of the kinetic and excitation energy, $E_K + E_X$, of the fragments properly weighted over the known distribution in fragment mass ratios. The next step was to calculate the distribution in E_X from the experimentally observed distribution in E_K. The raw data obtained in ionization chamber experiments of the type described in Section 11.6.1 cannot be used without some corrections for ionization defect and experimental dispersion. When these corrections were made by a suitable mathematical treatment of the data (not a simple matter) and the assumption was made that the distributions in E_X were independent and identical for the light and heavy fragments, the upper curve of Fig. 11.88 was obtained for the typical excitation energy distribution. The width of this curve per fragment is about 11 Mev. The width agrees well with the energy distribution for Zr^{97} fragments observed by COHEN[411]. The negative excitation energies implied by Fig. 11.88 have no physical significance but are retained because they have mathematical significance in computing the probability for emitting zero neutrons. The next step is to calculate the neutron emission probability. This is done by an evaporation calculation based on simple neutron emission concepts originally introduced by WEISSKOPF[412]. The expression, $N(E) \propto E \exp\left(\frac{-E}{T}\right)$, is used for neutron boil-off. In this equation N(E) is the emission probability for neutrons with energy E. The nuclear temperature, T, was taken to be 1.4 Mev.

---

410. C. D. Coryell, "Beta-Decay Energetics," Ann. Revs. of Nucl. Sci. 2, 305 (1953).

411. B. L. Cohen, Phys. Rev. 104, 1046 (1956)

412. J. M. Blatt and V. F. Weisskopf, "Theoretical Nuclear Physics," John Wiley and Sons, New York (1952).

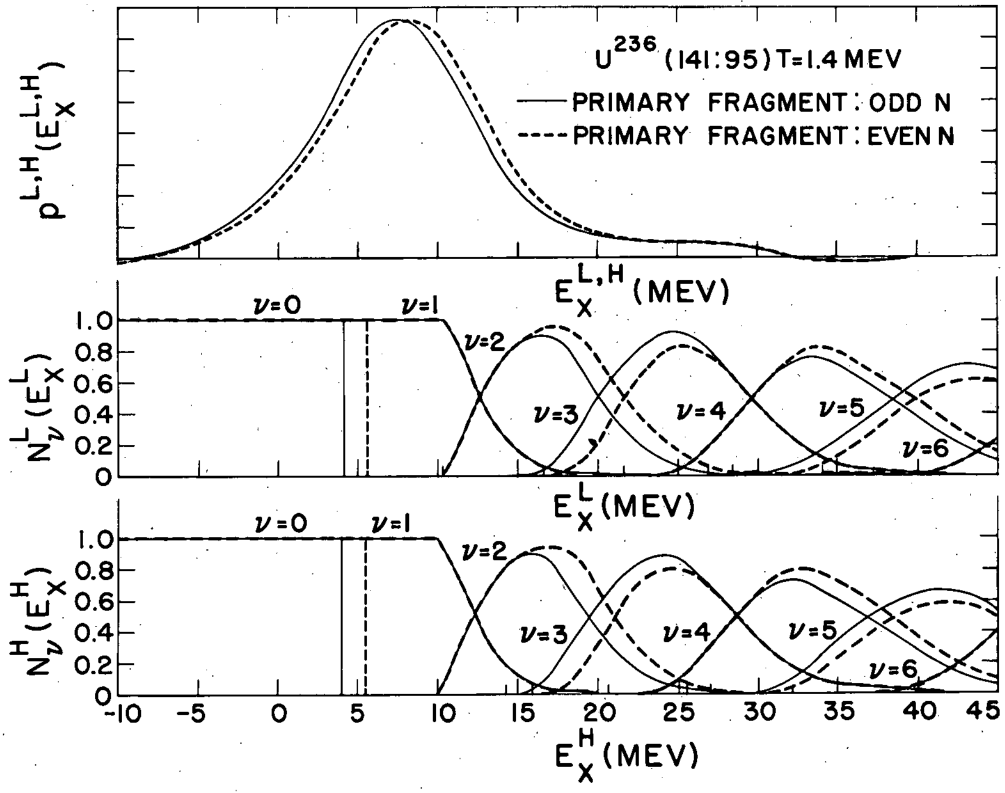

MU-18850

Fig. 11.88. LEACHMAN'S calculations of the distribution in fragment excitation energy (upper curve) and of neutron emission probability as a function of fragment excitation energies (lower curves) for the most probable mode of thermal fission of U^{235}. R. B. Leachman, Phys. Rev. 101, 1005 (1956). The abscissa scales for the three sets of curves are the same.

The curves in the lower part of the Fig. 11.88 are the neutron emission probabilities as a function of excitation energy for each fragment. It is assumed that a neutron is always emitted when emission is energetically possible. The binding energies of fission neutrons involved in these calculations are estimated from a mass surface of the nuclides based on CORYELL'S treatment of parameters.[410]

This combination of the excitation and neutron emission data of the type shown in Fig. 11.88 with proper weighting of the possible mass splits make it possible to calculate a distribution in the number of fission neutrons as shown in Fig. 11.89 for neutron induced fission and in Fig. 11.90 for spontaneous fission. LEACHMAN'S multiplicity distributions are shown as histograms and the measured distributions as solid circles. The agreement is considered to be quite satisfactory.

According to the assumptions of this treatment, neutron emission occurs to the complete exclusion of gamma ray emission when neutron emission is possible. Once the fragments are de-excited below the neutron binding energy of the least bound neutron, the residual energy is released in gamma radiation. As a by-product of the theory it is possible to calculate the average energy release in gamma radiation. This turns out to be 4.6 Mev per fission in the case of U^{235} which is difficult to reconcile with recent measurements of this quantity which are about twice that value. See Section 11.9. There is no satisfactory explanation of this discrepancy. MILTON[413] has suggested that gamma emission might be able to compete with neutron emission in the highly deformed fragment nuclei at the moment of scission.

LEACHMAN AND KAZEK[414] applied this theory of neutron emission to the type of experimental data discussed in Section 11.7.3 in which the neutron multiplicities were recorded simultaneously with the energy or velocity of both fission fragments. LEACHMAN AND KAZEK considered the case of the most probable mass ratio in the slow neutron fission of U^{235} and the spontaneous fission of Cf^{252} and for this mass ratio calculated $\bar{\nu}$ as a function of the total kinetic energy. In both cases the quantity $d\,\bar{\nu}/d\,E_K$ was linear. The results are shown in Table 11.36.

---

[413] J.C.D. Milton, Chalk River Laboratory report CRP-642-A, unpublished, 1956.

[414] R. B. Leachman and C. S. Kazek, Jr., "Neutron Emission from Fission Modes," Phys. Rev. 105, 1511 (1957).

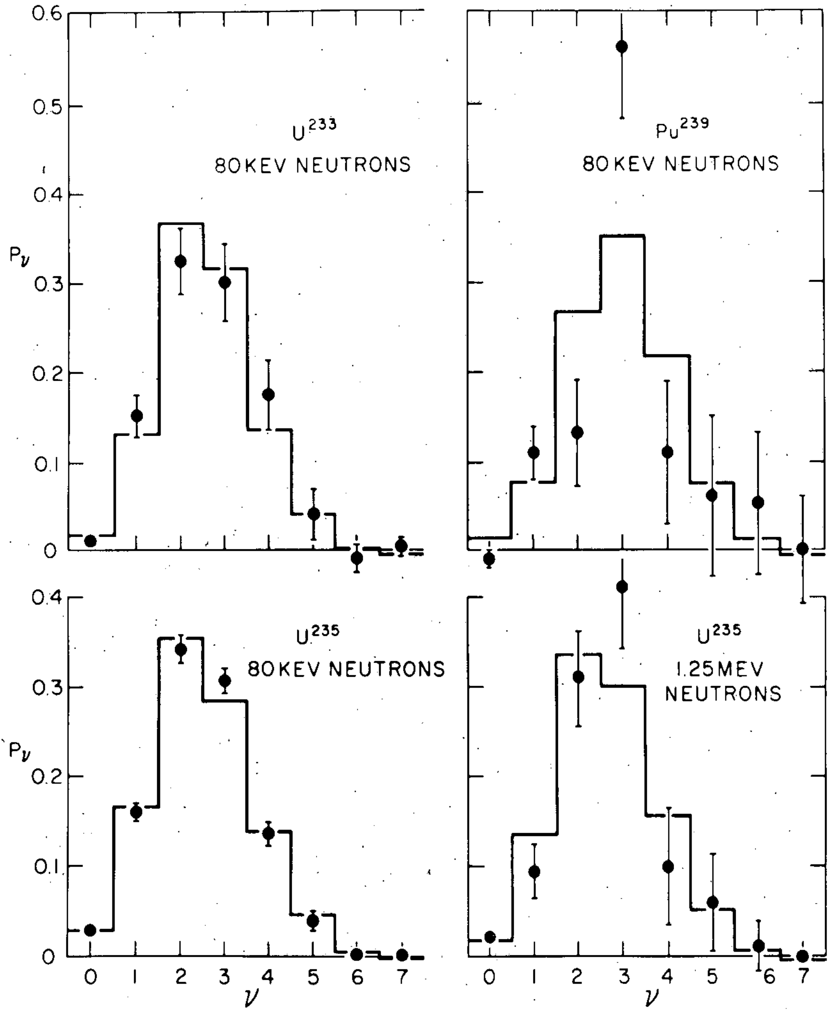

MU-18849

Fig. 11.89. Calculated and observed variations in ν for neutron-induced fission. The statistical uncertainties in the U^{233} and Pu^{239} data are considerably greater than those indicated for the U^{235} data. R. B. Leachman, Phys. Rev. 101, 1005 (1956).

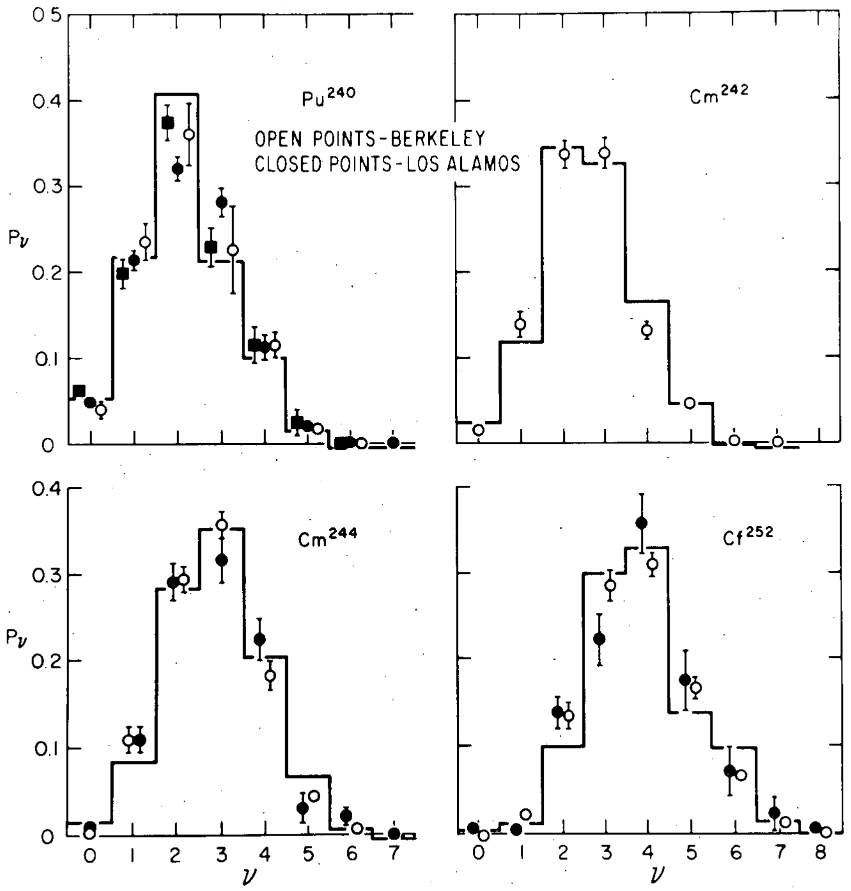

MU-18848

Fig. 11.90. Calculated and observed variations in ν for spontaneous fission. The histograms were calculated by LEACHMAN. The data are taken from Tables 11.31, 11.32 and 11.33.

Table 11.36 The variation of the average number of neutrons $\bar{\nu}$ with the kinetic energy E_K of the fragments as calculated by LEACHMAN AND KAZEK[414] for the most probable mass ratios R_A of fission. The "temperature" of neutron emission is given by T.

Fission case	R_A	T (Mev)	$d\bar{\nu}/dE_K$ (Mev^{-1})
U^{235}+ thermal neutrons	141/95	1.4	-0.121
		1.0	-0.130
Cf^{252}	145/107	1.4	-0.116

In the case of Cf^{252} the calculated value can be compared with the value of -0.143 ± 0.020 neutron fission^{-1} Mev^{-1} derived by STEIN AND WHETSTONE[415] from their experimental data. See Table 11.35 and discussion in Section 11.7.3.

The LEACHMAN method of calculation of neutron emission probabilities is rather complex and TERRELL[416] found it desirable to correlate the various sets of experimental data on neutron emission probabilities by means of a simpler calculation based on a minimum of parameters. In TERRELL'S treatment it is assumed (1) that neutrons will be emitted whenever this is energetically possible, (2) that the emission of any neutron from any fission fragment reduces the excitation of the fragment by a value which is nearly constant around an average value E_o, and (3) that the total excitation energy of the two primary fragments has a Gaussian distribution with rms deviation σE_o from the average excitation energy $\bar{E}$. E_o is of the order of 7 Mev and σ is of the order of 1. Since the excitation energy has a Gaussian distribution and each emitted neutron reduces the excitation energy by E_o the neutron emission probabilities also follow a Gaussian law. This conclusion is essentially independent of the manner in which the two fragments share the excitation and should also be true if a few neutrons are emitted before fission with about the same value of E_o. TERRELL derives the relationship

$$\sum_{n=0}^{\nu} P_n = (2\pi)^{-1/2} \int_{-\infty}^{(\nu-\bar{\nu} + 1/2+b)/\sigma} \exp(-t^2/2)dt \qquad (11.52)$$

in which P_n is the probability of observing n neutrons

$\bar{\nu}$ is the average number of neutrons

σ, as mentioned above, is the rms width of the total excitation in units of the average energy charge, E_o, per emitted neutron, and

b is a small adjustment ($b < 10^{-2}$).

This equation was applied to all experimental data on the probability distributions P_ν; namely, the data listed in Tables 11.31, 11.32 and 11.33. It was found that all data are reasonably well-represented by this distribution if the parameter σ was chosen $\cong$ 1.08. An exception was Cf^{252} which required a

---

415. W. E. Stein and S.L. Whetstone, Jr., Phys. Rev. 110, 476 (1958)
416. J. Terrell, Phys. Rev. 108, 783 (1957)

σ value of 1.21 ± 0.01. The closeness of the fit of the semi-empirical curve to the experimental data is shown in Fig. 11.91, taken from TERRELL'S paper.

With a σ value of 1.08 and a reasonable choice of 6.7 Mev for E_o, the rms width of most of the fragment excitation energy distributions is 7.2 Mev and the full width at half maximum is 17 Mev. The corresponding figures for the exceptional case of Cf^{252} ($\sigma = 1.21$) are 8.1 and 19 Mev. These values are in reasonably good agreement with the excitation energy distributions deduced from the experimental work on fragment kinetic energy described in Section 11.6.

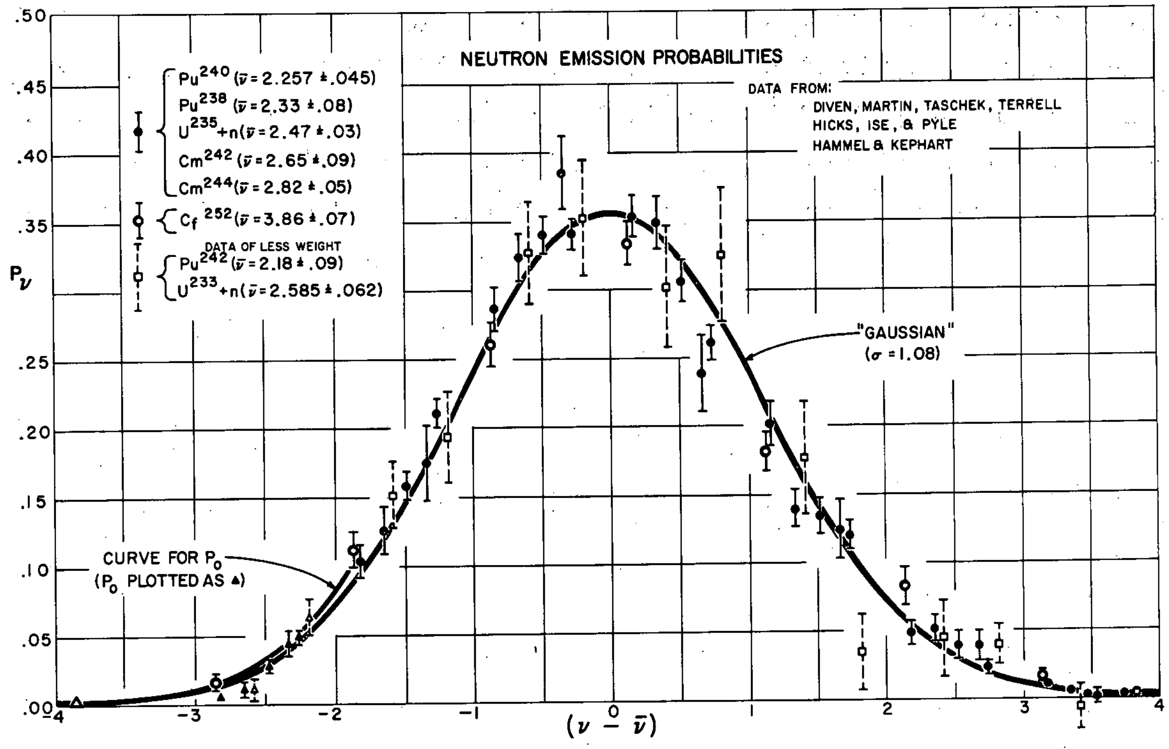

MU-18854

Fig. 11.91. Experimental non-cumulative neutron emission probabilities. Standard deviations are shown. The continuous curves are for the "Gaussian" distribution derived by TERRELL. Figure from reference 416.

11.8 DELAYED NEUTRONS IN FISSION

11.8.1 Introduction and Resume of Early Investigations. When U^{235} or some other heavy element nuclide is caused to fission, a neutron radioactivity may be observed. The total number of these "delayed" neutrons is of the order of 1% of the prompt neutrons. The "delayed" neutrons are actually emitted promptly from a highly-excited nuclide produced by the β decay of a precursor, whose β-decay half-life controls the rate of emission of neutrons. If chemical separation of fission products is made, the neutron radioactivity is separated chemically with the precursor.

Delayed neutrons play an important role in the control of reactors and this has stimulated an extensive study of their abundance and other characteristics. These studies can be divided into two groups. The most extensive studies have consisted of the examination of the gross neutron activity of activated samples of fissionable material not subjected to chemical processing. The second type of study consists of the chemical processing of fission products immediately after irradiation and the identification of dealyed-neutron periods in specific chemical fractions.

KEEPIN[417-419] has written excellent reviews on the subject of delayed neutrons and we follow his treatment in much of what follows.

Less than a month after the discovery of nuclear fission in 1939 Enrico Fermi[420] suggested that delayed neutrons might be emitted from fission fragments after these had undergone one or more beta transitions. This was made plausible by the theory of fission advanced by BOHR and WHEELER[421] and FRENKEL[422] because it could be shown that in certain cases the energy released

---

417. G. R. Keepin, "Delayed Neutrons — A Review as of October 1955", Los Alamos Scientific Laboratory Report, LA-1970, October 1955.

418. G. R. Keepin, "Delayed Neutrons" in Chapter 7 of Progress in Nuclear Energy, Series One, Physics and Mathematics, Volume 1, McGraw-Hill Book Co., New York, 1956.

419. G. R. Keepin and T. F. Wimett, Paper P/831, Volume 4, p. 162, Proceedings of the International Conference on the Peaceful Uses of Atomic Energy, United Nations, New York, 1956.

420. See L. Szilard and W. H. Zinn, Phys. Rev. 55, 799 (1939).

421. N. Bohr and J. A. Wheeler, Phys. Rev. 56, 426 (1939).

422. J. Frenkel, J. Phys. USSR 1, 125 (1939).

in beta decay could exceed the binding energy of a neutron in the daughter nucleus. Under these conditions a "delayed" neutron could be emitted with an observed period equal to that of the preceding beta-emitter by the process illustrated schematically in Fig. 11.92.

The role of delayed neutrons in the control of the nuclear chain reaction was first suggested in the literature by ZELDOWICH and HARITON.[423] More than a year before achievement of the first self-sustaining chain reaction FERMI[424] independently pointed out the importance of delayed neutrons in controlling the rate of fission in a chain-reacting assembly. When the multiplication constant k slightly exceeds unity the effect of the delayed neutrons is to make the rate of neutron increase much less (roughly a factor of 150 less) than it would have been had all the neutrons been released promptly. This greatly simplifies the problem of keeping the chain reaction under control. Hence, a knowledge of the effects of delayed neutrons is a matter of great practical importance in reactor design.

The first evidence for delayed emission of neutrons was reported by ROBERTS, MEYER, and WANG.[425] These "delayed" neutrons whose reported half life was 12.5 ± 3 sec., were believed either to be photoneutrons produced by the γ-activity of the fission fragments or to be emitted directly from one of the fission products. Subsequent yield measurements[426] quickly ruled out the first possibility; two months later the BOHR-WHEELER hypothesis[421] was advanced, thus providing a plausible mechanism for the experimental fact of delayed-neutron emission. Following this, other workers soon found more delayed-neutrons periods; BOOTH, DUNNING, and SLACK[427] found two periods of half life 45 seconds and 10-15 seconds with a total yield of ~0.02 delayed neutrons per fission. GIBBS and THOMSON[428] observed no periods of appreciable yield between 10^{-3} and 10^{-1} seconds. BRØSTROM, KOCH and LAURITSEN[429] found two periods with half lives of 12.3 and 0.1 - 0.3 seconds.

---

423. Zeldowich and Hariton, USPEKHI FIZ. NAUK 23, No. 4, 354 (1940).
424. E. Fermi in a letter to S.K. Allison, Oct. 1941; see A. H. Snell et al., Phys. Rev. 72, 545 (1947).
425. R. Roberts, R. Meyer and P. Wang, Phys. Rev. 55, 510 (1939).
426. R. Roberts, R. Meyer, L. Hafstad and L. Wang, Phys. Rev. 55, 664 (1939).
427. E. T. Booth, J. R. Dunning and F. G. Slack, Phys. Rev. 55, 876 (1939).
428. D. F. Gibbs and G. P. Thomson, Nature 144, 202 (1939).
429. K. J. Brøstrom, J. Koch, and T. Lauritsen, Nature 144, 830 (1939).

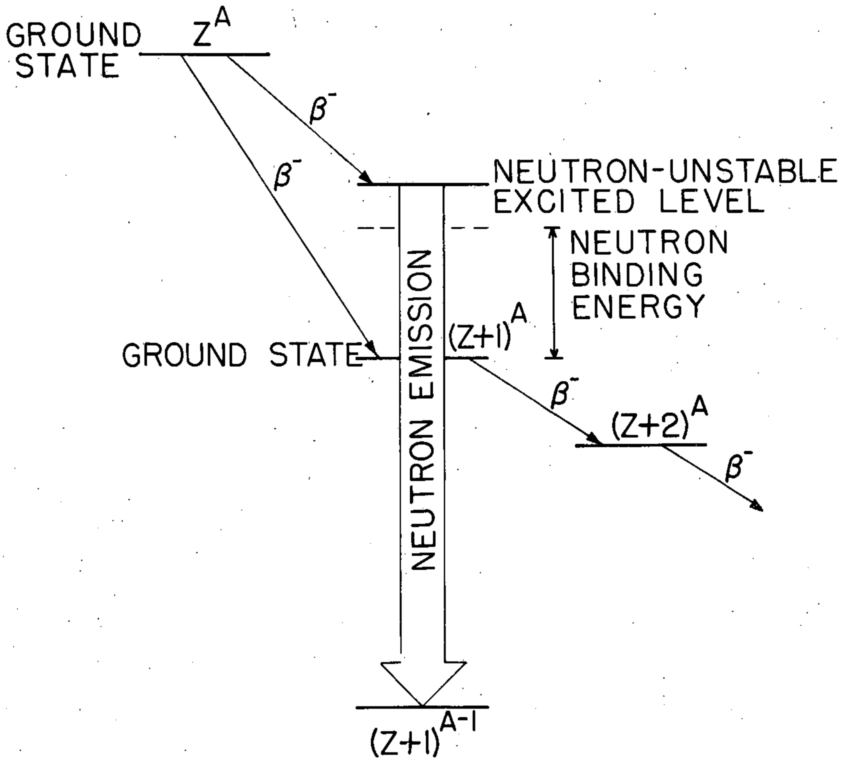
GROUND STATE
Z^A
β^-
β^-
NEUTRON-UNSTABLE EXCITED LEVEL
NEUTRON BINDING ENERGY
NEUTRON EMISSION
GROUND STATE
$(Z+1)^A$
β^-
$(Z+2)^A$
β^-
$(Z+1)^{A-1}$

MU-13463

Fig. 11.92. Schematic drawing of mechanism for slow neutron emission. Partial beta decay to excited levels in daughter may reach levels lying above the neutron binding energy. Partial beta decay to ground state results in conventional beta decay chain with no neutron emission.

The earliest detailed measurements on delayed neutrons from U^{235} fission were made in 1942 by SNELL and co-workers at Chicago.[430] A BF_3 counter surrounded by paraffin was used to monitor the decay of delayed-neutron activity from a 106-lb. block of U_3O_8 bombarded with Be + D neutrons. Five delayed-neutron periods (half lives) were found ranging from 0.4 sec. to 56 sec. The two longer periods were attributed to Br^{87} and I^{137} β-activities preceding neutron emission from excited states of Kr^{87} and Xe^{137}. REDMAN and SAXON[431] were the first to study delayed neutrons using a nuclear reactorn – the Argonne graphite pile. The Chicago and Argonne results showed significant disagreement only for the shorter periods.

With the higher neutron flux available at the Argonne heavy water pile (central flux $\sim 10^{11}$ neutrons/cm^2/sec.) and a newly-constructed rapid transfer system (for improved short period work), the delayed neutrons from U^{235} were studied again in 1945 by HUGHES, DABBS, CAHN, and HALL.[432] The decay of delayed neutrons from an irradiated sample of U^{235} (~89% isotopically enriched U_3O_8) was recorded on electrocardiograph tape, and then analyzed graphically into six periods. The results, given in Table 11.37 have served as a standard of comparison for all subsequent delayed-neutron studies on U^{235}, as well as the other fissionable isotopes. In 1945, DE HOFFMAN, FELD, and STEIN[433] utilized very short bursts of prompt neutrons from the "dragon" assembly (Los Alamos) to investigate delayed neutrons from U^{235}, particularly the shorter periods. They obtained five periods in substantial agreement with those of HUGHES et al., and reported indications of a sixth short-period group of 4 millisecond half-life and abundance ~2% that of the total delayed neutrons. Later studies on the contribution of "room-return" neutrons indicated that this observed 4 millisecond period could be accounted for by neutrons scattered back to the "dragon" assembly from surrounding walls and floor.

---

[430] A. H. Snell, V. A. Nedzel, H. W. Ibser, J. S. Levinger, R. G. Wilkinson, and M. B. Sampson, Phys. Rev. 72, 541 (1947).

[431] W. Redman and D. Saxon, Phys. Rev. 72, 570 (1947).

[432] D. J. Hughes, J. Dabbs, A. Cahn, and D. B.Hall, Phys. Rev. 73, 111 (1948).

[433] F. de Hoffman, B. T. Feld, and P. R. Stein, Phys. Rev. 74, 1330 (1948).

The six periods listed in Table 11.37 account for all the delayed neutrons in the fission of U^{235}. Although, as we shall see below, some of these delayed-neutron periods represent complex mixtures of activities with similar half-lives. These same periods with different abundances also account for the delayed neutrons observed in the fission of other heavy nuclides. Before summarizing later research on the well-established delayed-neutron periods, we wish to mention the extensive work which has been done to find whether other periods of shorter or longer half life are present in the delayed-neutron decay curves.

The first reported search for short delayed neutrons of very short periods was made by GIBBS and THOMSON[428] with modulated (D,D) neutrons on U_3O_8. As mentioned earlier, they found no delayed-neutron periods of appreciable abundance between 10^{-3} and 10^{-1} seconds. The work at Argonne (cf. Table 11.37) revealed a new short delayed-neutron period from U^{235} of half life 50 msec and relative abundance 0.033%. No period between 1 and 50 msec was found. These short-period activity studies were made with a thermal neutron shutter ("guillotine") to produce short irradiations at the Argonne heavy water pile. The short period ($t_{1/2}$ ~4 msec) from U^{235} reported by DE HOFFMAN,[433] has been discussed. BROLLEY et al.,[434] using a pulsed cyclotron beam to generate short neutron bursts, found no U^{235} fission product activity shorter than 0.43 sec. half life. Using a bare U^{235} critical assembly pulsed at intervals with an 11 Mev betatron BENDT and SCOTT[435] measured a short-period, delayed-neutron group of half life 150 ± 41 milliseconds and abundance 2.7 ± 0.7 percent. No shorter period was found. The authors discussed the hypothesis that this group of delayed neutrons follows the decay of Li^9, the latter being formed as a light fragment in ternary fission. However, COOK[436] finds that Be^7 is produced in less than one in about 10^7 fission; also FLYNN, GLENDENIN and STEINBERG[437] set a similar upper limit on the yield of Be^{10}. From this and other evidence, it is doubtful that the Li^9 assignment of this period can be correct.

---

[434] J. E. Brolley, D. H. Cooper, W. S. Hall, M. S. Livingston and L. K. Schlacks, Phys. Rev. 83, 990 (1951).

[435] P. J. Bendt and F. R. Scott, Phys. Rev. 97, 744 (1955).

[436] G. B. Cook, Nature 169, 622 (1952).

[437] Flynn, Glendenin and Steinberg, Phys. Rev. 101, 1492 (1956).

Table 11.37

Half lives and abundances of delayed neutrons from U^{235}*

Group index	Half life	Relative abundance
1	55.6 ± 0.2	0.034 ± 0.009
2	22.0 ± 0.2	0.220 ± 0.023
3	4.51 ± 0.1	0.282 ± 0.017
4	1.52 ± 0.05	0.319 ± 0.017
5	0.43 ± 0.05	0.112 ± 0.011
6	0.05 ± 0.02	0.033

Ratio of total delayed neutrons to total neutrons = 0.00755

---

*This is a widely quoted table from Hughes et al., (ref. 433); for a more recent table see Table 11.39.

Using modern high flux reactors as fission sources, it has been possible to look for delayed neutron periods appearing in low abundance with half lives of minutes or longer. No confirmed reports of any periods longer than the well-established 55 second activity have appeared. One experimental problem in the search for such activities is caused by the fact that hard-gamma radiation from some of the fission products can give an apparent delayed-neutron period by photodisintegration of the deuterium present in the moderating material or in the neutron detector.

11.8.2 Recent Results on Delayed-Neutron Periods and Their Abundances. In the summary reports of KEEPIN[417-419] there appears a complete tabulation of all determinations through 1956 of the delayed-neutron periods and abundances for U^{235} and for several other fissionable nuclides. We should like to report here only the work of KEEPIN, WIMETT and ZEIGLER[438] because it is more extensive than other published studies.[439] We shall describe this work briefly.

A bare U^{235} metal assembly at the Los Alamos Laboratory known as the "Godiva" reactor was used to provide a high flux of neutrons through small samples of fissile material centered in the reacting assembly.[440] Such samples could be irradiated for short bursts ("instantaneous exposure") or for long times ("infinite exposure") to emphasize the shorter-lived or longer-lived components, respectively, in the neutron decay curve. A pneumatic system rapidly transferred the sample of fissile material from the reactor assembly to a well-shielded neutron counter. The decay of the delayed-neutron activity was monitored by a multi-channel, recording, time-delay analyzer with 0.001, 0.01, 0.1, and 10 second channel widths following in automatic sequence; the number of channels of each width was variable, thus permitting selection of the most suitable channel-width distribution for a given decay curve. The decay curves which were obtained were composite curves rather difficult to resolve graphically with confidence. The authors programmed a least-squares analysis of the counting data on an IBM-704 digital computer. The three longer periods (τ_1 τ_2 τ_3) and their abundance ratios were calculated from the "infinite irradiation" data; the four shorter periods and their abundance ratios were calculated from the "instantaneous irradiation" data. The six relative abundances so obtained were then normalized to unity to give directly the fraction of delayed neutrons in each group. When total yield measurements were desired the number of fission events in the sources was determined by radiochemical isolation of Mo^{99} from the irradiated sample.

---

[438] G. R. Keepin, T. F. Wimett and R. K. Ziegler, Phys. Rev. 107, 1044 (1957); see also J. Nuclear Energy 6, 1 (1957).

[439] A rather similar study of delayed neutron periods and abundances for U^{233}, U^{235}, U^{238}, Pu^{239}, and Th^{232} caused to fission with the fast neutrons of the Zephyr assembly has been published by Smith, McVicar, Thorne and Rose, J. Nuclear Energy 4, 133 (1957).

[440] H. C. Paxton, "Critical Assemblies at Los Alamos", Nucleonics 13, 49 (1955); R. E. Peterson and G. A. Newby, Nuclear Sci. and Eng. 1, 112 (1956).

The Godiva central spectrum (for "fast" neutron irradiations) is a slightly degraded fission-neutron spectrum. When it was desired to study delayed neutrons from a sample caused to fission with thermal neutrons a "thermal" spectrum was obtained within an 8-inch cubic polyethylene block, cadmium-shielded and mounted near Godiva.

Fast-fission delayed neutron data taken with samples of U^{235}, U^{238}, U^{233}, Pu^{239}, Pu^{240} and Th^{232} are summarized in Table 11.38. Thermal-fission data are presented in Table 11.39. The absolute total yields of delayed neutrons per fission are given in Table 11.40. In all cases, the data were completely described by six neutron periods although there were slight differences in the values of the periods from one isotope to the next. The differences in relative and absolute abundances in different fissioning nuclei are reasonable on the basis of shifts in the mass and charge distribution of the fission products.

Differences in the periods reported in this work compared to the earlier work of HUGHES (Table 11.37) and others are attributed largely to (1) different amounts of data in the critical time interval 5 to 40 seconds and (2) or the different methods of analysis — least squares fit versus the more subjective graphical "exponential peeling" method.

It has been usual to assume that the six delayed-neutron periods which constantly recur in studies of the gross neutron radioactivity of most fissile heavy nuclei must be associated with just six beta active nuclides whose half lives are just the six half periods deduced from the analysis of the gross decay data. However, the radiochemical studies described in the next section show that the 22 second, the 6 second and the 2 second periods are complex and

Table 11.38

Fast-fission delayed-neutron data of Keepin, Wimett and Ziegler[a-e]

Group index i	Half-life T_i	Relative abundance a_i/a	Absolute group yield (%) (for pure isotope)
	U^{235}(99.9% 235; n/F = 0.0165 ± 0.0005)		
1	54.51 ± 0.94	0.038 ± 0.003	0.063 ± 0.005
2	21.84 ± 0.54	0.213 ± 0.005	0.351 ± 0.011
3	6.00 ± 0.17	0.188 ± 0.016	0.310 ± 0.028
4	2.23 ± 0.06	0.407 ± 0.007	0.672 ± 0.023
5	0.496 ± 0.029	0.128 ± 0.008	0.211 ± 0.015
6	0.179 ± 0.017	0.026 ± 0.003	0.043 ± 0.005
	U^{238}(99.98% 238; n/F = 0.0412 ± 0.0017)		
1	52.38 ± 1.29	0.013 ± 0.001	0.054 ± 0.005
2	21.58 ± 0.39	0.137 ± 0.002	0.564 ± 0.025
3	5.00 ± 0.19	0.162 ± 0.020	0.667 ± 0.087
4	1.93 ± 0.07	0.388 ± 0.012	1.599 ± 0.081
5	0.490 ± 0.023	0.225 ± 0.013	0.927 ± 0.060
6	0.172 ± 0.009	0.075 ± 0.005	0.309 ± 0.024
	U^{233}(100% 233; n/F = 0.0070 ± 0.0004)		
1	55.11 ± 1.86	0.086 ± 0.003	0.060 ± 0.003
2	20.74 ± 0.86	0.274 ± 0.005	0.192 ± 0.009
3	5.30 ± 0.19	0.227 ± 0.035	0.159 ± 0.025
4	2.29 ± 0.01	0.317 ± 0.011	0.222 ± 0.012
5	0.546 ± 0.108	0.073 ± 0.014	0.051 ± 0.010
6	0.221 ± 0.042	0.023 ± 0.007	0.016 ± 0.005
	Pu^{239}(99.8% 239; n/F = 0.0063 ± 0.0003)		
1	53.75 ± 0.95	0.038 ± 0.003	0.024 ± 0.002
2	22.29 ± 0.36	0.280 ± 0.004	0.176 ± 0.009
3	5.19 ± 0.12	0.216 ± 0.018	0.136 ± 0.013
4	2.09 ± 0.08	0.328 ± 0.010	0.207 ± 0.012
5	0.549 ± 0.049	0.103 ± 0.009	0.065 ± 0.007
6	0.216 ± 0.017	0.035 ± 0.005	0.022 ± 0.003
	Pu^{240}(81.5% 240; n/F = 0.0088 ± 0.0006)		
1	53.56 ± 1.21	0.028 ± 0.003	0.022 ± 0.003
2	22.14 ± 0.38	0.273 ± 0.004	0.238 ± 0.016
3	5.14 ± 0.42	0.192 ± 0.053	0.162 ± 0.044
4	2.08 ± 0.19	0.350 ± 0.020	0.315 ± 0.027
5	0.511 ± 0.077	0.128 ± 0.018	0.119 ± 0.018
6	0.172 ± 0.033	0.029 ± 0.006	0.024 ± 0.005

Table 11.38 (cont'd.)

Group index i	Half-life T_i	Relative abundance a_i/a	Absolute group yield (%) (for pure isotope)
	Th^{232}(100% 232; n/F = 0.0496 ± 0.0020)		
1	56.03 ± 0.95	0.034 ± 0.002	0.169 ± 0.012
2	20.75 ± 0.66	0.150 ± 0.005	0.744 ± 0.037
3	5.74 ± 0.24	0.155 ± 0.021	0.769 ± 0.108
4	2.16 ± 0.08	0.446 ± 0.015	2.212 ± 0.110
5	0.571± 0.042	0.172 ± 0.013	0.853 ± 0.073
6	0.211± 0.019	0.043 ± 0.006	0.213 ± 0.031

---

[a] Total data for each nuclide were obtained from 40 prompt-burst irradiations and 40 long irradiations with the exception of the U^{235} fast-fission data which were obtained from 80 prompt-burst irradiations and 80 long irradiations.

[b] Indicated for each nuclide (in parentheses) are: (1) isotopic purity of sample used for period and abundance measurements, and (2) n/F ≡ total absolute yield in delayed neutrons per fission; note that n/F values (and absolute group yields) have been corrected to 100% isotopic purity.

[c] Uncertainties indicated are calculated probable errors (from IBM-704 computer).

[d] T_1, T_2, and the ratio a_1/a_2 are taken from final long-irradiation data.

[e] $\Sigma a_i = a = n/F \equiv$ total delayed neutrons per fission. Abundance values reported include correction (< 3%) for detector response.

Table 11.39

Thermal fission delayed neutron data of Keepin, Wimett and Zeigler[a-e]

Group index i	Half-life, T_i	Relative abundance, a_i/a	Absolute group yield (%)
	U^{235}(99.9% 235; n/F = 0.0158 ± 0.0005)		
1	55.72 ± 1.28	0.033 ± 0.003	0.052 ± 0.005
2	22.72 ± 0.71	0.219 ± 0.009	0.346 ± 0.018
3	6.22 ± 0.23	0.196 ± 0.022	0.310 ± 0.036
4	2.30 ± 0.09	0.395 ± 0.011	0.624 ± 0.026
5	0.610 ± 0.083	0.115 ± 0.009	0.182 ± 0.015
6	0.230 ± 0.025	0.042 ± 0.008	0.066 ± 0.008
	Pu^{239}(99.8% 239; n/F = 0.0061 ± 0.0003)		
1	54.28 ± 2.34	0.035 ± 0.009	0.021 ± 0.006
2	23.04 ± 1.67	0.298 ± 0.035	0.182 ± 0.023
3	5.60 ± 0.40	0.211 ± 0.048	0.129 ± 0.030
4	2.13 ± 0.24	0.326 ± 0.033	0.199 ± 0.022
5	0.618 ± 0.213	0.086 ± 0.029	0.052 ± 0.018
6	0.257 ± 0.045	0.044 ± 0.016	0.027 ± 0.010
	U^{233}(100% 233; n/F = 0.0066 ± 0.0003)		
1	55.0 ± 0.54	0.086 ± 0.003	0.057 ± 0.003
2	20.57 ± 0.38	0.299 ± 0.004	0.197 ± 0.009
3	5.00 ± 0.21	0.252 ± 0.040	0.166 ± 0.027
4	2.13 ± 0.020	0.278 ± 0.020	0.184 ± 0.016
5	0.615 ± 0.242	0.051 ± 0.024	0.034 ± 0.016
6	0.277 ± 0.047	0.034 ± 0.014	0.022 ± 0.009

---

[a] Total data for each nuclide were obtained from 40 prompt-burst irradiations and 40 long irradiations.

[b] Indicated for each nuclide (in parentheses) are: (1) isotopic purity of sample used for period and abundance measurements, and (2) n/F ≡ total absolute yield in delayed neutrons per fission; note that n/F values (and absolute group yields) have been corrected to 100% isotopic purity.

[c] Uncertainties indicated are calculated probable errors (from IBM-704 computer).

[d] T_1, T_2, and the ratio a_1/a_2 are taken from final long-irradiation data.

[e] $\Sigma a_i = a = n/F \equiv$ total delayed neutrons per fission. Abundance values reported include correction ($< 3\%$) for detector response.

Table 11.40

Absolute yields of delayed neutrons

Fissile nuclide	Absolute yield (delayed neutrons/fission for pure isotope) Fast fission	Thermal fission
Pu^{239}	0.0063 ± 0.0003	0.0061 ± 0.0003
U^{233}	0.0070 ± 0.0004	0.0066 ± 0.0003
Pu^{240}	0.0088 ± 0.0006	-----
U^{235}	0.0165 ± 0.0005	0.0158 ± 0.0005
U^{238}	0.0412 ± 0.0017	-----
Th^{232}	0.0496 ± 0.0020	-----

that each contains at least one bromine and one iodine precursor activity. It is quite possible that the 0.5 and 0.2 second periods are also complex.

COX and co-workers[441] have investigated delayed neutrons in the spontaneous fission of Cf^{252}. A weightless source of Cf^{252} with a fission rate of 3.76×10^6 per minute was deposited upon a platinum planchette. A steel "catching" disk was placed 0.5 mm from this source to catch the fission fragments ejected from the source. After a preset collection time a pneumatic shuttle transferred the "catcher" to the center of a neutron detection system and the neutron emission rate was measured until the activity on the collection disk had decayed to a negligible amount. This process was repeated many times and the collection time was varied over a wide range in order to enhance particular delayed-neutron emitters.

The chief results are summarized in Table 11.41. The considerable difference between this table and Table 11.39 can be explained by a consideration of the differences in the distribution of fission fragments for Cf^{252} compared to U^{235}. The heavy fragments have rather similar distributions in mass and charge so that heavy fragment delayed-neutron precursors such as iodine isotopes should appear in both cases. On the other hand, the light fragment distribution of Cf^{252} is shifted to much heavier masses and to a region where delayed-neutron precursors are not expected on theoretical grounds. Hence, those activities such as Br^{87} and Br^{88} which contribute to the U^{235} delayed neutron decay curves are absent in the case of Cf^{252}.

Energy measurements have been made on the delayed neutron groups by several groups of investigators.[426,432,442,443,444] Some of the results on the mean energies are summarized in Table 11.42.

---

441. Cox, Fields, Friedman, Sjoblom and Smith, Phys. Rev. 112, 960 (1958).
442. Burgy, Pardue, Willar, and Wollan, Phys. Rev. 70, 104 (1946).
443. T. W. Bonner, S. J. Bame, Jr., and J. E. Evans, Phys. Rev. 101, 1514 (1956).
444. R. Batchelor and H. R. McK. Hyder, J. Nuclear Energy 3, 7 (1956).

Table 11.41

Delayed neutron periods in the spontaneous fission of Cf^{252}; from Cox and co-workers[441]

Group number	Half life (seconds)	Relative abundance	Absolute yield neutrons/fission (%)	Suggested precursors
1	20.0 ± 0.5	0.255 ± 0.01	0.22 ± 0.01	I^{137}Xe?Cs?Te?Sb?
2	2.0 ± 0.4	0.338 ± 0.046	0.29 ± 0.04	I^{139}Xe?Cs?Te?Sb?
3	0.5 ± 0.4	0.407 ± 0.12	0.35 ± 0.1	I^{140}Cs?Xe?
		Total	0.86 ± 0.1	

Table 11.42

Mean energies of the delayed neutron groups for U^{235}

Group index	$T_{1/2}$(sec)	Hughes[432] Argonne (kev)	Burgy[442] Oak Ridge (kev)	Batchelor[444] Harwell (kev)
1	54	250 ± 60	300 ± 60	250 ± 20
2	22	560 ± 60	670 ± 60	460 ± 10
3	5.9	430 ± 60	650 ± 100	405 ± 20
4	2.2	620 ± 60	910 ± 90	450 ± 20
5	0.46	420 ± 60	400 ± 70	---
6	0.13	---	---	---

11.8.3 Radiochemical Identification of Delayed-Neutron Precursors*. Radiochemical investigations have proved that at least three of the six well-established delayed-neutron periods are complex. From the work reported below, it is certain that there are at least nine distinct radioactivities which contribute to the gross neutron decay curves, and it is probable that there are other unresolved contributors. The chemical assignments are summarized in Table 11.43. The studies on which these assignments are based are outlined below.

The 54 Second and 22 Second Periods

In 1940 HAHN and STRASSMANN[445] chemically isolated several short-lived halogen activities from fission. Included among these were a 50 ± 9 second bromine activity and a 30 ± 6 second iodine activity. In later works,[446,447] masses of 87 and 137, respectively, were assigned to these activities. Independently, SNELL and co-workers[448] identified the 55 second delayed-neutron precursor as an isotope of bromine and the 22 second precursor as an isotope of iodine. Comparison with known Br and I β-emitters led to tentative identification of Br^{87} as the 55 second and I^{137} as the 22 second delayed-neutron precursors. Soon thereafter, SUGARMAN[449] established (a) the half life of Br^{87} as 56.1 ± 0.7 second in agreement with the (then) measured 55.6 ± 0.2 second delayed neutron period, and (b) the half life of I^{137} as 19.3 ± 0.5 second in substantial agreement with the 22.0 ± 0.2 second delayed neutron period.**

---

*A delayed neutron precursor is a fission product nuclide which β-decays to an excited state of a delayed neutron emitter.

**It may be pointed out that a real difference in delayed neutron periods and their corresponding radiochemically-determined periods may exist owing to (1) lengthening of the effective precursor period by "feed in" by cascade β emission from several members of the chain, and (2) contributions from other (presumably unknown) delayed neutron emitters of comparable period.

445. O. Hahn and F. Strassmann, Naturwiss. 28, 817 (1940).

446. H. J. Born and W. Seelmann-Eggeberg, Naturwiss. 31, 59 (1943); 31, 86 (1943).

447. V. Reizler, Naturwiss. 31, 326 (1943).

448. A. H. Snell, J. S. Levinger, E. P. Meiners, M. B. Sampson, and R. G. Wilkinson, Phys. Rev. 72, 545 (1947).

449. N. Sugarman, J. Chem. Phys. 17, 11 (1949).

Table 11.43

Assignment of delayed neutron precursors

Delayed neutron period	Delayed neutron precursor	Additional predicted precursors**
54 seconds	56.1 second Br^{87}	
22 seconds	24.2 second I^{137} plus 16.3 second Br^{88}	
6.0 seconds*	4.5 second Br^{89}(?) plus 5.6 second I^{138}	
2 seconds	1.6 second Br^{90}(?) plus 2.7 second I^{139}	Br^{91}, Cs^{144}
~0.5 seconds		I^{140}, Kr^{95}, Br^{92}
0.18 seconds		As^{87}, Rb^{97}

*This period has often been given as 4.5 seconds (See Table 11.37). This discrepancy is accounted for by difficulties in resolving the multicomponent neutron decay curves.

**After Keepin, Phys. Rev. 106, 1359 (1957); see also comments of R. B. Leachman in Geneva Conference Paper P/665, 1958.

STEHNEY and SUGARMAN[450] have measured the total fission yield of Br^{87} as 3.1 ± 0.1% and the energies of Br^{87} β-rays as 2.6 and 8 Mev. See Fig. 11.93. This establishes the neutron emitting levels in Kr^{87} at energies $\geq$ 5.4 Mev.

PERLOW and STEHNEY[451] identified a neutron period of 16.3 ± 0.8 seconds among the bromine fission products and assigned it to the precursor Br^{88}. This was the first identification of a precursor of odd-odd nuclear type. This 16.3 second activity contributes to the 22 second period but to a lesser extent than does 24 second I^{137}. KEEPIN, WIMETT and ZIEGLER,[438] for example, were not able to resolve a 15 second period from their decay curves of gross neutron activity.

The results of COX et al.[441] on the delayed-neutron periods in the spontaneous fission of Cf^{252} (give above in Table 11.41) indicate that there may be additional contributors to the 22 second group. In the case of Cf^{252} bromine isotopes cannot contribute to the delayed neutrons and one might expect the 24 second I^{137} to dominate completely. However, the measured period is 20 ± 0.5 seconds instead of 24 seconds indicating that one or more unidentified heavy-fragment precursors must contribute to the Cf^{252} 20-second group; these unidentified precursors may well be present also in U^{235} fission.

The 6 Second Period

A contributing precursor of the third delayed-neutron group (~6 second half life) has been shown[449] to follow the chemistry of bromine and to have a mass number in the range 89 to 91. Attempt to measure the half lives of Br^{89} and Br^{91} radiochemically — by extraction of the descendent Sr activity — were unsuccessful due to prohibitively low activity at the time of counting.[449]

Because of the difficulties in radiochemical identification of the 6 second and shorter periods, SUGARMAN[452] strove to place some limitations on the possible choices of mass number and element by means of a recoil technique. Previous work had shown (See Section 11.6.4) a regular variation of recoil range with the mass of the fission fragments, the range decreasing, as the mass

---

[450] A. F. Stehney and N. Sugarman, Phys. Rev. 89, 194 (1953).

[451] G. J. Perlow and A F. Stehney, Phys. Rev. 107, 776 (1957).

[452] N. Sugarman, J. Chem. Phys. 15, 544 (1947).

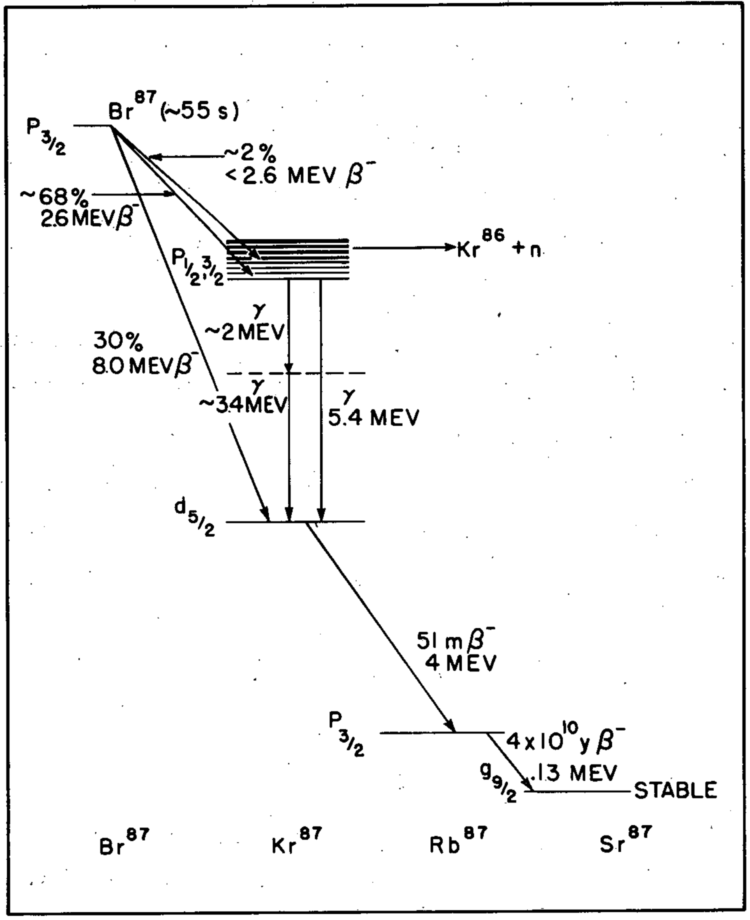
P3/2
Br87 (~55 s)
~2%
<2.6 MEV β−
~68%
2.6 MEV β−
P1/2, 3/2
Kr86 + n
γ
~2 MEV
30%
8.0 MEV β−
γ
~3.4 MEV
γ
5.4 MEV
d5/2
51 m β−
4 MEV
P3/2
4 x 10^10 y β−
.13 MEV
g9/2
STABLE
Br87
Kr87
Rb87
Sr87

MU-18980

Fig. 11.93. Schematic interpretation of delayed neutron emission in the case of the mass 87 fission chain. Figure prepared by KEEPIN.[417]

increases, as shown in Fig. 11.70. Thus the mass number of a fission product can be estimated by measuring the range and comparing it with ranges of fission products of known mass number. SUGARMAN[452] measured the amounts of the 4.5 second and 1.5 second delayed-neutron activity passing through various thicknesses of aluminum foil. He then used the recoil ranges of the 55.6-second and the 22-second activities as standards to compute a value of the ranges of the unknowns. He was able to state that a 4.5 second activity and the 1.5 second activity had mass number of 90 ± 10 and 129 ± 5 respectively. From a knowledge of the regularities in the mass yield curve of fission, the mass number ranges could be further reduced to 86-91 and 129-135 respectively. Using this as a guide, Sugarman showed that the 4.5 second activity accompanied the 55.6 second Br^{87} activity through radiochemical procedures specific for bromine. This established the identity of a main contributor to the 4-6 second delayed neutron group as bromine of mass number 86 to 91. Present evidence favors the assignment Br^{89}. PERLOW and STEHNEY[453] corroborate the existence of a bromine fission product delayed neutron precursor with a half life of 4.4 ± 0.5 seconds.

PERLOW and STEHNEY[453] also found an iodine activity which emitted neutrons with a 6.3 ± 0.7 second half life and attributed it to I^{138} which is known from other studies of its beta particle decay to have a half life of 5.9 seconds.

The 2 Second Period

PERLOW and STEHNEY[453] studied neutron radioactivity in bromine and iodine fractions isolated quickly after neutron irradiation of U^{235} and found a 1.6 ± 0.6 second neutron period in the bromine fraction and a 2.0 ± 0.5 second period in the iodine fraction. The bromine activity is tentatively assigned to Br^{90} while the iodine activity is to be identified with I^{139} whose half life has been determined radiochemically[449] to be 2.7 seconds.

---

[453] G. J. Perlow and A. F. Stehney, Phys. Rev. 113, 1269 (1959); see also Paper P/691, Volume 15, of Proceedings of the Second United Nations Conference on the Peaceful Uses of Atomic Energy, Geneva, 1958.

The 0.5 Second and 0.2 Second Periods

The identity of these delayed-neutron precursors has not been established because of experimental difficulties. KEEPIN'S suggestions of possible assignments are given in Table 11.43.

11.8.4 The Shell Model Interpretation of the Delayed Neutron Emitters. The BOHR-WHEELER mass equation makes it clear that beta emitters far removed from stability can have sufficiently great decay energies that neutron emission from excited levels of daughter products may be possible. However, this mass equation is not able to give correct assignments to the delayed neutron precursors observed in fission. The shell model can assist in making proper assignments and predictions through a consideration of the sharp drops in neutron binding energies which occur at the shell edges. Only the 50 and 82 neutron shells are of significance in this regard as they are the only neutron shells which occur in the regions of appreciable fission yield.

In the beginning it was usual to state that the delayed neutron precursors should have one or a few pairs of neutrons beyond a closed neutron configuration; these nuclides would be expected to decay by beta emission to excited states in odd-neutron nuclides, which because of their particularly low binding energies for the last neutron would exhibit the greatest probability for neutron emission. The known activities ${}^{52}\mathrm{Br}^{87}$, ${}^{(54)}_{35}\mathrm{Br}^{(89)}$, ${}^{84}_{53}\mathrm{I}^{137}$, and ${}^{86}_{53}\mathrm{I}^{139}$ fall in line with this view. However, it has come to be realized* that $E_\beta - B_n > 0$ is the real criterion for delayed neutron emission and that one must consider odd-odd nuclei with neutron numbers slightly higher than closed shells as equally probable candidates for delayed neutron precursors; this stems from the fact that the beta decay energy of odd-odd nuclei is greater than for odd-even nuclei. Hence it is not surprising that the odd-odd nuclei Br^{88} and I^{138} have also been identified among the fission product neutron activities.

Some authors[454,455] have carried thru semi-theoretical analyses of nuclear mass trends, neutron binding energies and the systematics of delayed neutron

---

[454] G. R. Keepin, Phys. Rev. 106, 1359 (1957).

[455] A. C. Pappas, Paper P/583, Volume 15, Proceedings of the Second United Nations International Conference on the Peaceful Uses of Atomic Energy, Geneva, 1958.

*See for example the discussion in reference 453.

emission probabilities in order to compile a list of possible contributors to the delayed-neutron emitters in fission.

It is noteworthy that other delayed neutron activities discovered in experiments unconnected with nuclear fission are explained by similar shell model considerations. N^{17} discovered by ALVAREZ[456] and Li^9 discovered by GARDNER, KNABLE and MOYER[457] are beta emitters producing a daughter nucleus with a weakly-bound neutron added to a particularly stable even-even configuration.

---

[456] L. W. Alvarez, Phys. Rev. 75, 1127 (1949).

[457] A. L. Gardner, N. Knable and B. J. Moyer, Phys. Rev. 83, 1054 (1951).

11.9 GAMMA RAYS IN FISSION

A knowledge of the prompt gamma rays accompanying the fission of a heavy nucleus should provide some very crucial tests for any detailed theory of the fission process. A knowledge of the prompt gamma spectrum is also of some importance in designing shielding for a reactor or other critical assembly.

Early studies of prompt gamma rays in the fission of U^{235} by DEUTSCH and ROTBLATT[458] and by KINSEY, HANNA and VAN PATTER[459] gave 4.6 Mev and 5.1 Mev respectively as the total release of energy in prompt gamma radiation per fission act. However, the later results of FRANCIS and GAMBLE[460] and of MAIENSCHEIN et al.[461] gave the considerably higher values of 7.46 and 8.0 Mev respectively. A very careful study of prompt gamma emission in U^{235} fission was reported by MAIENSCHEIN, PEELLE, ZOBEL and LOVE[462] at Geneva in 1958. The gamma-ray energy spectrometer was of the multiple-crystal scintillation type.[463] One sodium iodide (tl) crystal (the "center" crystal) absorbed the energy of electrons produced by gamma radiation incident upon it. Auxiliary crystals largely shielded from the U^{235} source detected secondary gamma rays from either the Compton or pair interaction processes in the center crystal. The two crystals were operated in coincidence. Experiments to determine the gamma ray spectrum in time coincidence with fission used for a source the U^{235} contained in an ionization chamber. The minimum response time of the fission-gamma coincidence system was about 2 x 10^{-8} seconds. The prompt gamma-spectrum observed by this technique is given in Fig. 11.94. The average energy is 7.2 ± 0.8 Mev.

These experimentalists also show gamma spectra for radiation emitted shortly after fission in delay periods ranging from 0.12 x 10^{-6} to 1.4 x 10^{-6}

---

458. M. Deutsch and H. Rotblatt, Atomic Energy Commission Declassified Report, AECD-3179 (1944).

459. Kinsey, Hanna and Van Patter, Can. J. Research 26A, 79 (1948).

460. J. Francis and R. Gamble, Oak Ridge National Laboratory Report, ORNL-1879 (unpublished).

461. F. Maienschein et al., Oak Ridge National Laboratory Report, ORNL-1879 (unpublished).

462. F. C. Maienschein, R. W. Peelle, W. Zobel and T. A. Love, Paper P/670, Proceedings of the Second United Nations Conference on the Peaceful Uses of Atomic Energy, Geneva, 1958.

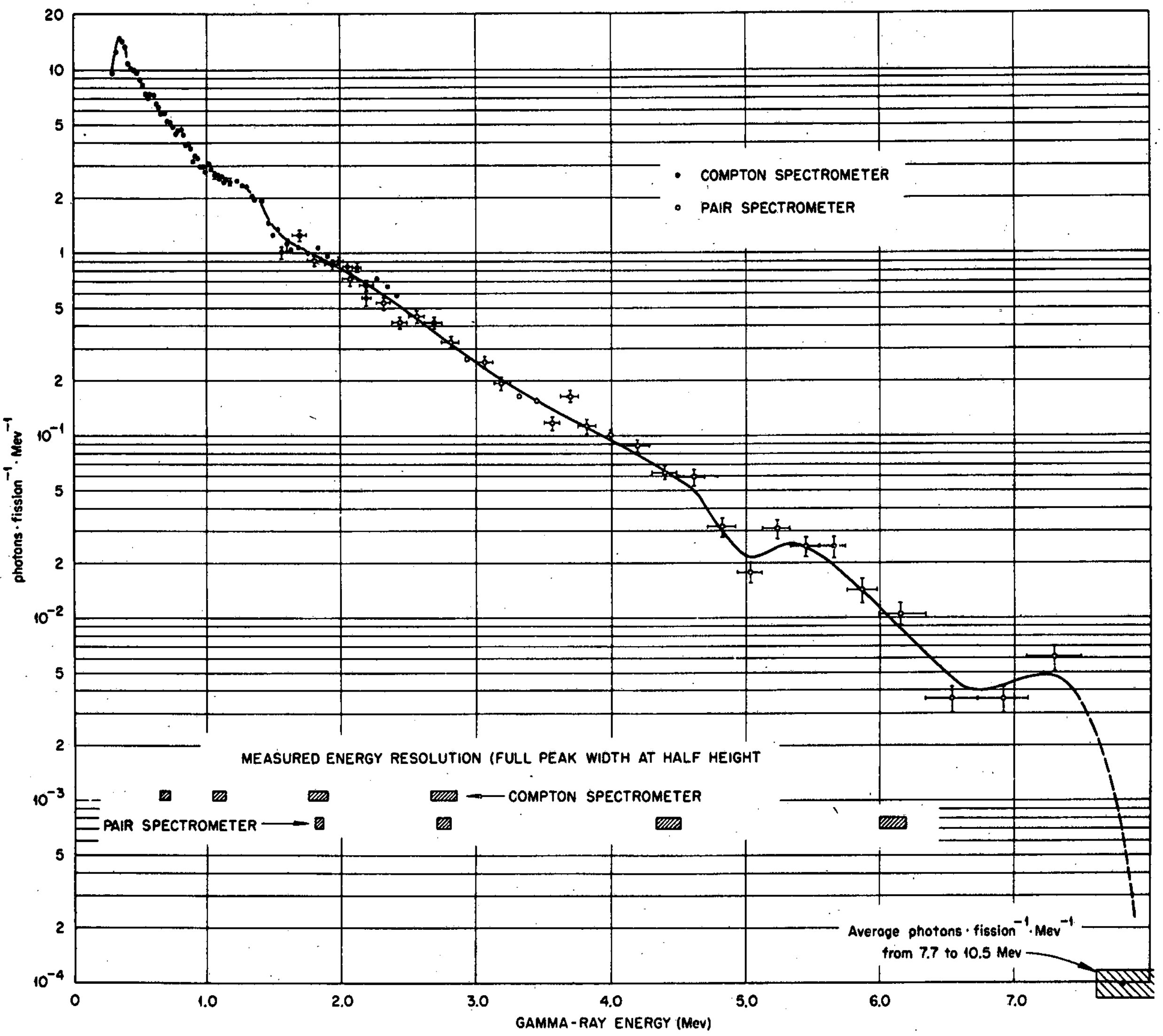

MUB-342

Fig. 11.94. The energy spectrum of gamma rays observed within 5×10^{-8} seconds of the fission of U^{235} (Maienschein et al.).[462] The ordinate errors shown were obtained from counting statistics, and the energy errors represent in each case the energy interval over which the results were averaged. The authors state that this plot represents, a preliminary analysis of the data and systematic errors as large as 15% may occur in some energy regions.

seconds. They also studied gamma rays emitted a few seconds to a few minutes after fission. The most surprising feature of these delayed spectra was that integral photon intensities as great as 5.7 percent of the prompt radiation were found for delay times in the microsecond range. Since nuclear beta decay is energetically forbidden for decay times as short as 10^{-3} seconds these measured gamma rays must be assumed to arise from isomeric transitions. SKLIAREVSKII[464] found that virtually all the gamma ray photons are emitted in a time interval 1/2 to 2-1/2 millimicroseconds after fission.

There are experimental difficulties connected with a study of U^{235} fission because of the neutron atmosphere required for the experiments. SMITH, FIELDS and FRIEDMAN[465] thought it desirable to study prompt gamma emission in the spontaneous fission of Cf^{252} where the experimental conditions are "clean" and there are no complicating backgrounds. Furthermore, since the characteristics of fission in Cf^{252} and U^{235} are very similar, as we have noted throughout this chapter, the release of gamma radiation might be expected to be similar in the two cases. BOWMAN and THOMPSON[466] carried out a similar study.

The measurements were made by coincidence techniques requiring the simultaneous response of fission fragment and gamma ray detectors. SMITH, FIELDS and FRIEDMAN[465] used a gas scintillator cell as a fission detector because of the speed of its response and single or multiple sodium iodide crystal detectors for the gamma rays. BOWMAN and THOMPSON[466] used an ionization chamber to detect fission fragments and a sodium iodide crystal to detect gamma rays. In both studies the measured gamma ray spectrum had to be corrected in a major way for the photoelectric efficiency of the crystal, Compton electron and pair production effects, etc.

---

463. For a discussion of a Compton spectrometer see R. Hofstadter and J. A. McIntyre, Phys. Rev. 78, 619 (1950) and T. H. Braid, Phys. Rev. 102, 1109 (1956). For a discussion of a pair spectrometer, see H. I. West, Phys. Rev. 101, 915 (1956).

464. V. V. Skliarevskii, D. E. Fomenko and E. P. Stepanov, JETP 32, 256 (1957); translation Soviet Physics JETP 5, 220 (1957).

465. A. B. Smith, P. R. Fields and A. M. Friedman, Phys. Rev. 104, 699 (1956).

466. H. R. Bowman and S. G. Thompson, University of California Radiation Laboratory Report, UCRL-5038, March, 1958; also published as Paper P/652 in Proceedings of the Second International Conference on the Peaceful Uses of Atomic Energy, Geneva, 1958.

Figure 11.95 taken from the paper of SMITH, FIELDS and FRIEDMAN[465] shows the corrected photon spectrum of Cf^{252} and compares it with the spectrum observed in the slow-neutron induced fission of U^{235}. The spectra are seen to be very similar. Some characteristics of the photon spectra are compared in Table 11.44.

SMITH, FIELDS and FRIEDMAN[465] also made some measurements of the gamma ray spectrum in coincidence with fragment pairs measured in a double ionization chamber. The photon spectrum was studied as a function of the mass ratio. The data were divided into three groups corresponding to symmetric mass division, the most probable mass division and the most asymmetric mass division. Within the 8% statistical accuracy of the measurement the results were identical.

MILTON and FRASER[467] combined gamma ray detection with simultaneous measurement of the velocities of both fragments in the spontaneous fission of Cf^{252}. The energy of the gamma rays was measured over the energy interval 300 kev-1.4 Mev. This spectrum changed slightly but significantly as a function of the mass ratio of the fragments but not significantly as a function of total kinetic energy of the fragments. The yield of gamma rays showed a pronounced dip in the region where one of the fragments is near the doubly magic nucleus Sn^{132}.

The magnitude of the total fragment excitation energy taken away by gamma emission is a puzzle. It is usually assumed that neutron emission will occur much more rapidly than gamma emission as long as the fission fragments retain sufficient energy to emit a neutron. The various neutron "boil-off" models such as those of LEACHMAN and KAZEK[468] or of TERRELL[469] would predict that about 4-5 Mev of excitation would be left after all possible neutrons had been emitted. This estimate is roughly half the observed total gamma ray energy.

The experimental results seem to lead to the conclusion that gamma-ray emission competes more successfully with neutron emission than present theory would predict; although this hypothesis is hard to reconcile with the spectral shape which shows that less than 2 percent of the photons have energies greater

---

[467] J. C. D. Milton and J. S. Fraser, Phys. Rev. 111, 877 (1958); also published as Paper P/200, Proceedings of the Second International Conference on the Peaceful Uses of Atomic Energy, Geneva, 1958.

[468] R. B. Leachman and C. S. Kazek, Phys. Rev. 105, 1511 (1957).

[469] J. Terrell, Phys. Rev. 113, 527 (1959).

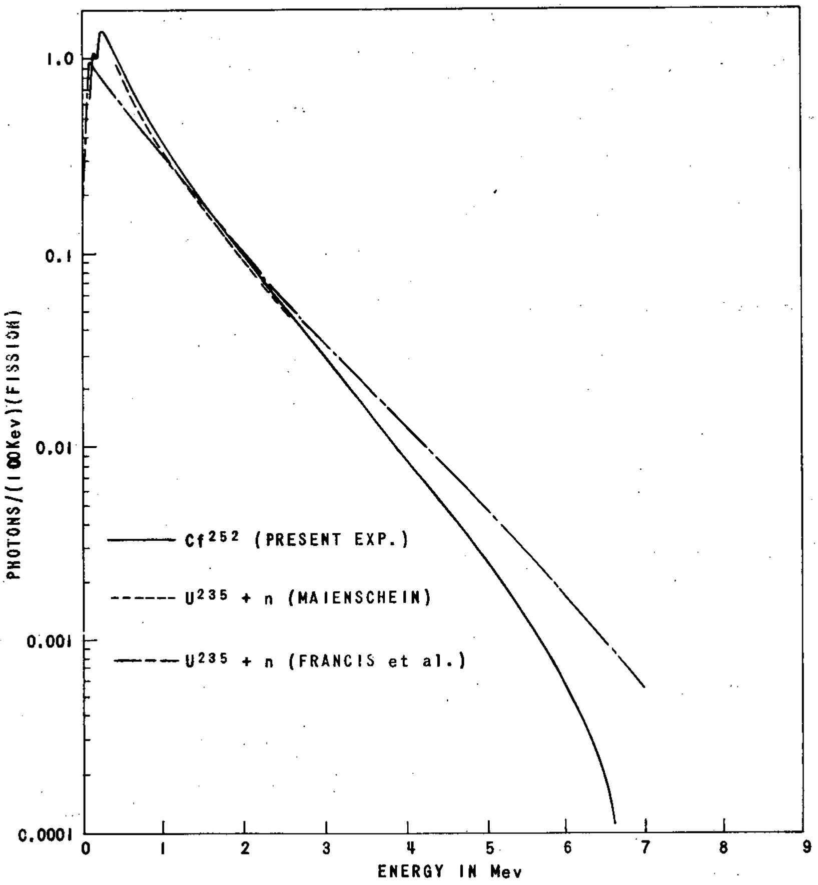

MU-18906

Fig. 11.95. Photon spectrum from the fission of Cf^{252} and U^{235} From Smith, Fields and Friedman.[465]

Table 11.44

Characteristics of prompt gamma rays emitted in fission

Fissioning isotope	Total photons per fission	Photons per fission (0.5-2.3 Mev)	Energy loss in photons per fission (0.5-2.3 Mev)	Total energy loss in photons	Ref.
U^{235}+n	7.4	---	---	7.2 Mev	462
Cf^{252}	10.3	5.0	5.2	8.2 Mev	465
Cf^{252}	10	---	---	9 Mev	466

than 2 Mev. TERRELL[469] states that it seems quite possible that the extremely high electromagnetic fields present during the acceleration of fission fragments to final velocity might induce gamma-ray emission in times of the order of 10^{-21} second. High nuclear distortions might also favor gamma emission, as suggested by MILTON.[470]

The multiplicity of the gamma rays also poses a theoretical problem.

PREVIOUS REVIEW ARTICLES ON LOW ENERGY FISSION

I. Halpern, "Nuclear Fission", Annual Review of Nuclear Science 9, 245 (1959).

Proceedings of a Symposium on the Physics of Fission, held at Chalk River, Ontario, May 14-18, 1956, Report CRP-642A, Atomic Energy of Canada Ltd., Chalk River, Ontario, 1956.

"Physics of Fission", a 1956 symposium published in Atomnaya Energ. Supplement 1. English translation available from Pergamon Press, New York, 1958 or from Consultants Bureau.

W. J. Whitehouse, Progress in Nuclear Physics 2, 120 (1952).

---

[470] J. C. D. Milton, unpublished suggestion, 1956.

Table 11.44

Characteristics of prompt gamma rays emitted in fission

Fissioning isotope	Total photons per fission	Photons per fission (0.5-2.3 Mev)	Energy loss in photons per fission (0.5-2.3 Mev)	Total energy loss in photons	Ref.
U^{235}+n	7.4	---	---	7.2 Mev	462
Cf^{252}	10.3	5.0	5.2	8.2 Mev	465
Cf^{252}	10	---	---	9 Mev	466

than 2 Mev. TERRELL[469] states that it seems quite possible that the extremely high electromagnetic fields present during the acceleration of fission fragments to final velocity might induce gamma-ray emission in times of the order of 10^{-21} second. High nuclear distortions might also favor gamma emission, as suggested by MILTON.[470]

The multiplicity of the gamma rays also poses a theoretical problem.

PREVIOUS REVIEW ARTICLES ON LOW ENERGY FISSION

I. Halpern, "Nuclear Fission", Annual Review of Nuclear Science 9, 245 (1959).

Proceedings of a Symposium on the Physics of Fission, held at Chalk River, Ontario, May 14-18, 1956, Report CRP-642A, Atomic Energy of Canada Ltd., Chalk River, Ontario, 1956.

"Physics of Fission", a 1956 symposium published in Atomnaya Energ. Supplement 1. English translation available from Pergamon Press, New York, 1958 or from Consultants Bureau.

W. J. Whitehouse, Progress in Nuclear Physics 2, 120 (1952).

---

[470] J. C. D. Milton, unpublished suggestion, 1956.

ACKNOWLEDGEMENTS

The author has been aided by many of his co-workers at the Lawrence Radiation Laboratory including J. A. Alexander, H. Bowman, S. G. Thompson, M. Michel, J. Niday, W. Nervik, M. L. Muga, and many others. He wishes to give special thanks to G. T. Seaborg for a critical reading of the entire manuscript and to W. J. Swiatecki for invaluable instruction in the liquid drop model. Many individuals from other laboratories have been most helpful in supplying figures from their own publications and in answering queries concerning important details. For these services thanks are extended to R. B. Leachman, E. P. Steinberg, J. S. Fraser, J. C. D. Milton, G. C. Hanna, H. G. Thode, R. H. Tomlinson, G. A. Cowan, L. M. Bollinger, P. Fields, C. B. Fulmer, S. Katcoff, V. L. Sailor, W. E. Stein, S. C. Whetstone, R. H. Stokes, J. Terrell, A. Turkevich, and A. C. Wahl. Mrs. Suzanne Vandenbosch helped greatly in the collection and organization of data. Invaluable assistance in typing of several versions of the manuscript and in the preparation of figures was given by Miss Yoshi Uchida, Mrs. Lilly Hirota and Miss Eileen Carson.

This report was prepared as an account of Government sponsored work. Neither the United States, nor the Commission, nor any person acting on behalf of the Commission:

A. Makes any warranty or representation, expressed or implied, with respect to the accuracy, completeness, or usefulness of the information contained in this report, or that the use of any information, apparatus, method, or process disclosed in this report may not infringe privately owned rights; or

B. Assumes any liabilities with respect to the use of, or for damages resulting from the use of any information, apparatus, method, or process disclosed in this report.

As used in the above, "person acting on behalf of the Commission" includes any employee or contractor of the Commission, or employee of such contractor, to the extent that such employee or contractor of the Commission, or employee of such contractor prepares, disseminates, or provides access to, any information pursuant to his employment or contract with the Commission, or his employment with such contractor.